Synthesis of (Nor)-Adamantane Derivatives via [1,2]-Alkyl Migration Reactions

Wissenschaftliche Arbeit zur Erlangung des Doktorgrades

der Naturwissenschaftlichen Fachbereiche

im Fachgebiet Organische Chemie

an der Justus-Liebig-Universität Gießen

vorgelegt von
Benjamin Zonker
aus Trier

Gießen 2021

Die vorliegende Arbeit wurde im Zeitraum von Januar 2017 bis Dezember 2020 am Institut für Organische Chemie der Justus-Liebig-Universität Gießen unter der direkten Betreuung von Privatdozent Mgr. Radim Hrdina, Ph.D. in Assoziation mit der Arbeitsgruppe von Prof. Dr. Peter R. Schreiner, Ph.D. angefertigt.

" The scientist's task is to find ways to try to disprove things that seem to make sense."

- Sir Terry Pratchett, OBE

Declaration in accordance §17 of the "Promotionsordnung"

I declare that I have completed this dissertation single-handedly without the unauthorized help of a second party and only with the assistance acknowledged therein. I have appropriately acknowledged and cited all text passages that are derived verbatim from or are based on the content of published work of others, and all information relating to verbal communications. I consent to the use of an anti-plagiarism software to check my thesis. I have abided by the principles of good scientific conduct laid down in the charter of the Justus Liebig University Giessen "Satzung der Justus-Liebig-Universität Gießen zur Sicherung guter wissenschaftlicher Praxis" in carrying out the investigations described in the dissertation.

Dekan: Prof. Dr. Thomas Wilke

1. Gutachter: Prof. Dr. Peter R. Schreiner, *Ph.D.*

2. Gutachter: PD Mgr. Radim Hrdina, *Ph.D.*

Abstract

In this thesis, selected results on the rearrangement between the noradamantane and the adamantane hydrocarbon cage are presented, as well as their application in organic synthesis. This reversible reaction proceeds through a *Wagner-Meerwein* rearrangement – a [1,2]-alkyl shift of a carbocation – either leading to the diamondoid structure of adamantane or the contracted derivative, depending on the structural elements surrounding the carbocation and the reaction conditions.

The rearrangement was used to synthesize 1,2-functionalized heterocyclic adamantylamines from noradamantane iminium triflates. In the classical *Wagner-Meerwein* reaction, the alkyl shift forms a tertiary from a secondary carbocation, following the way to the energetically more stable structure. When iminium salts are rearranged, the stability is inverted since the secondary carbocation is stabilized by its iminium ion resonance structure. High temperatures and a trapping nucleophile (*i.e.*, a Friedel-Crafts acceptor) are needed to push the equilibrium to the targeted adamantyl cage. Deeper investigations provided insight into the mechanism of the reaction, its difficulties, and its limits. Postfunctionalization of one of the target molecules showed the possibilities for further transformation of the compounds, demonstrating their potential use in medicinal research and synthetic or material chemistry.

In an additional publication, the procedure was reversed. Contrary to the previous protocol, the rearrangement starts at the adamantane structure and proceeds in the direction of the iminium salt. The reaction yielded the targeted noradamantane and ring-contracted diamantane derivatives – after hydrolysis of the iminium salt – with an adjacent carbaldehyde function. These compounds can be used as precursors for the above-mentioned iminium triflate rearrangements and thus increase the number of possible 1,2-functionalised adamantanes accessible through this route.

Zusammenfassung

In der vorliegenden Arbeit werden Forschungsergebnisse zur Umlagerung zwischen Noradamantan- und Adamantan-Kohlenwasserstoffkäfigen vorgestellt, sowie deren Anwendung in der organischen Synthese. Diese reversible Umlagerung gehört zu den *Wagner-Meerwein*-Umlagerungen, die – abhängig von den, das Carbokation umgebenden, Strukturelementen und Reaktionsbedingungen – entweder zur Diamantoidstruktur des Adamantans oder zum ringkontrahierten Derivat führt.

Die Umlagerung wurde genutzt, um aus Noradamantan-Iminiumtriflaten 1-2-funktionalisierte heterozyklische Adamantylamine zu synthetisieren. Die klassische *Wagner-Meerwein*-Reaktion beschreibt die Bildung eines tertiären, aus einem sekundären Carbokation. Bei der Umlagerung von Iminiumsalzen kehrt sich diese Richtung um, da das sekundäre Carbokation durch seine Iminium-Resonanzstruktur stabilisiert wird. Hohe Temperaturen und ein abfangendes Nukleophil (in diesem Fall ein Friedel-Crafts-Akzeptor) werden benötigt, um das Gleichgewicht hin zum angestrebten Adamantankäfig zu verschieben. Tiefergehende Untersuchungen lieferten Einblicke in den Mechanismus der Reaktion sowie ihre Grenzen. Gezielte Postfunktionalisierung eines der Zielmoleküle zeigte mögliche weitergehende Verwendungen als Substrate in der medizinischen Forschung sowie der synthetischen Chemie.

In einer weiteren Publikation wurde die Methode umgedreht. Im Gegensatz zum vorhergehenden Protokoll ist die Ausgangsverbindung ein Adamantanderivat und die Umlagerung läuft in Richtung des Iminiumsalzes ab. Die Reaktion lieferte die angestrebten Noradamantan- und ringkontrahierte Diamantanderivate – nach Hydrolyse des Iminiumsalzes – mit einer benachbarten Carbaldehydfunktion. Diese Verbindungen können als Vorstufen für die oben genannten Iminiumtriflat-Umlagerungen verwendet werden und vergrößern somit die, durch diese Route synthetisierbare Zahl an möglichen 1,2-funktionalisierten Adamantanen.

Table of Content

1 Introduction

1.1 [1,2]-Alkyl Migration Reactions

Rearrangement reactions have the ability to transform a simple precursor to a relatively complex target molecule in a single step and are often used as the key transformation in the preparation of synthetically interesting building blocks and biologically active compounds.[1] 1,2-Alkyl shifts are among the oldest known rearrangements.[2] Even though described for more than 100 years, some representatives are still of high interest, constantly developed and modern synthesis relies heavily on their use.[3] The ensuing chapters are intended to give a brief overview of the most common members of the 1,2-alkyl migration family.

1.1.1 Benzylic Acid Rearrangement

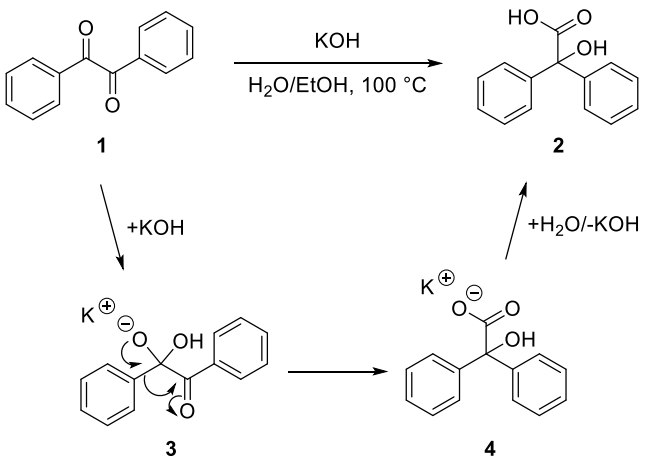

Scheme 1. Classical benzylic acid rearrangement described by Liebig.[2]

With the benzylic acid rearrangement, *Liebig* described the first rearrangement in organic synthesis in 1838.[2] He showed that α-diketones undergo a 1,2-rearrangement when treated with a strong base in aqueous conditions to yield α-hydroxycarboxylic acids (*Scheme 1*). The synthetic route for (-)-Isatisine (a natural compound commonly used in Chinese traditional medicine for viral diseases)[4] uses this rearrangement as a key step to form a complex ring system which is further transformed into the target molecule (*Scheme 2, page 2*).

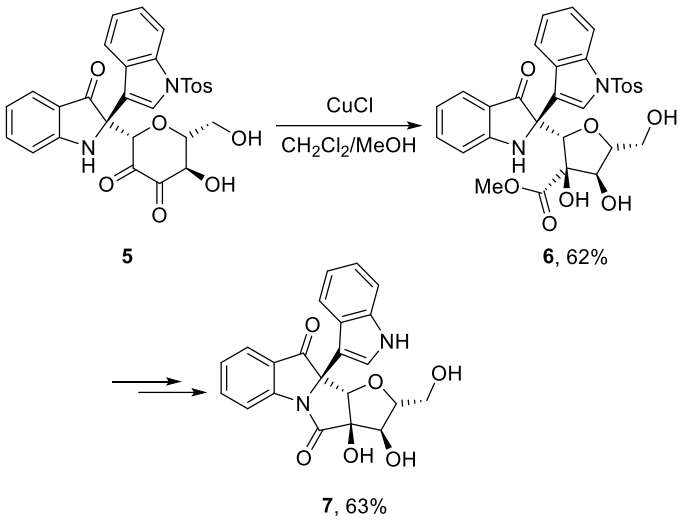

Scheme 2. Benzylic acid rearrangement in natural product synthesis.[4]

1.1.2 Wagner-Meerwein Rearrangement

The *Wagner-Meerwein* rearrangement was developed in parallel by *Georg Wagner*[5] and *Hans Meerwein*[6] in the late 19th and the early 20th century, respectively. Generally, the reaction proceeds *via* a 1,2-carbon atom migration, in which the formation of a more stable carbocation provides the driving force for this reaction (*Scheme 3*).[7] Examples of their usefulness are ever-present and growing in synthesis[3, 8] and in mechanistic investigations.[9]

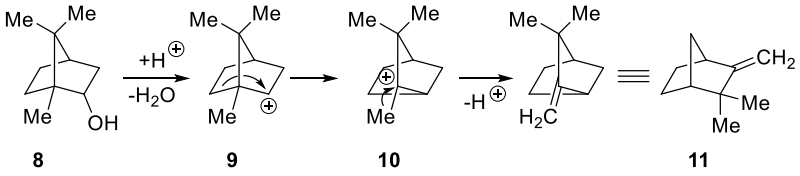

Scheme 3. 1,2-Alkyl migration reported by Meerwein.[6]

The formation of the accepting cation can be accomplished in many ways, *e.g.,* by dehydration[5, 10] or by halocyclization.[8, 11] Modern examples aim for migrations resulting in enantiomeric excess of a specific conformation, *e.g.,* using precatalyst **12** shown in *Figure 1*.[11]

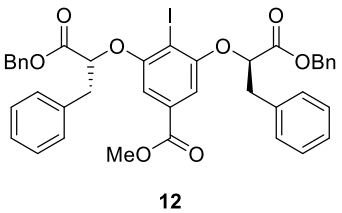

Figure 1. Chiral iodine precatalyst 12 for enantioselective Wager-Meerwein rearrangement.[11]

After *in situ* oxidation of the chiral iodine precatalyst with *m*CPBA, the resulting hypervalent iodine reagent catalyses aryl or alky migration (MG ≙ migrating group) in a *Wagner-Meerwein* fashion (*Scheme 4*), combined with a difluorination.

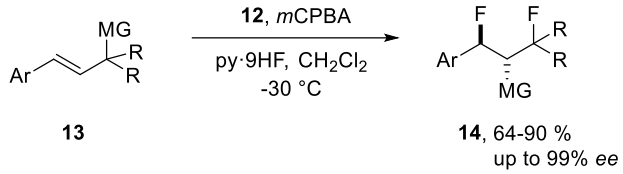

Scheme 4. Example of recent enantioselective Wagner-Meerwein reaction by Sharma et al.[11]

1.1.3 Pinacol-Type Rearrangements

The pinacol rearrangement joins the line of well-known and -established rearrangements developed in the last century.[12] The classical pinacol rearrangement starts with the dehydration of α–diol to form an α-hydroxy carbocation, which undergoes an alkyl migration to deliver the corresponding ketone (*Scheme 5*).

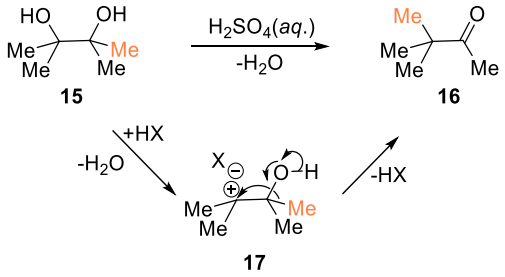

Scheme 5. Pinacol-pinacolone rearrangement with a simplified mechanism.[12-13]

The semi-pinacol rearrangement (*Figure 2*) is a modification of the classical rearrangement, in which the starting materials are not α-diols, but similar compounds, whose functional groups allow the formation of the electrophilic carbon centre by other means (*e.g.*, epoxide opening,[14] halogen abstraction,[15] electrophilic addition to a double bond,[16] *etc.*).

In this version of the rearrangement, the formed electrophilic centre is often a secondary carbon, instead of a tertiary one in the classical reaction.[13]

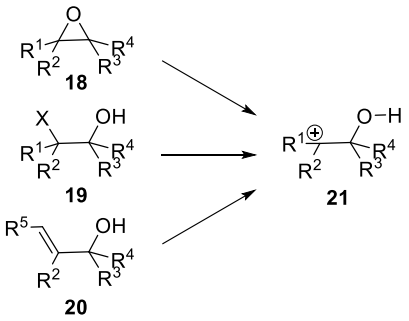

Figure 2. Examples of ways to form the electrophilic carbon centre in a semi-pinacol rearrangement in contrast to a pinacol rearrangement.[3]

Both variants of the pinacol-rearrangement are readily employed in the synthesis of interesting building blocks and natural products.[3, 13, 17] Stereo control is an essential feature in total synthesis of natural products. One possibility to achieve this in a pinacol rearrangement is by treating the starting material with a chiral *Brønsted* acid (*Scheme 6*). The depicted phosphoric acid **24** catalysis a broad range of substrates in very good to excellent yields with superb enantioselectivity.[18]

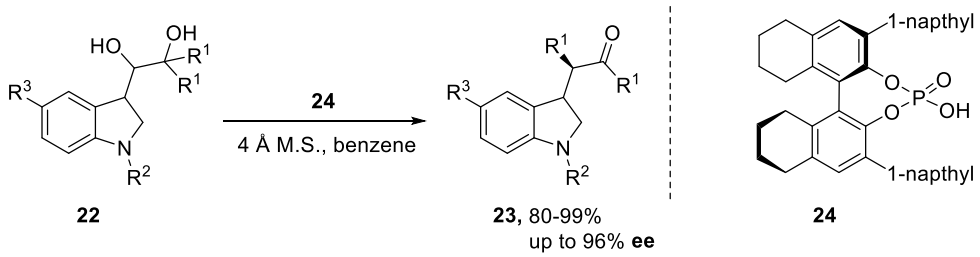

Scheme 6. Example of stereocontrol in pinacol rearrangements: Chiral phosphoric Brønsted acid catalysis.[18]

1.1.4 Tiffeneau-Demjanov Rearrangement

The *Tiffeneau-Demjanov* rearrangement is a special variant of the semi-pinacol rearrangement, in which an unstable diazonium ion is formed from a *β*-hydroxy amine (*Scheme 7*).[19] After the expulsion of dinitrogen, a carbocation is formed and the semi-pinacol rearrangement continues in the usual fashion (see *Chapter 1.1.3*).

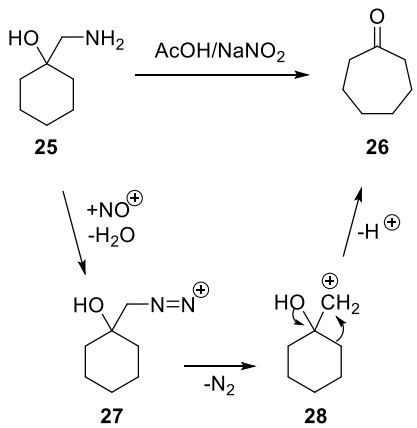

Scheme 7. Ring expansion as first described by Tiffeneau et al.[19-20]

While it is possible to use it in ring contraction reactions in very specific situations, its major use is ring expansion.[21] The ring expansion is easily controlled since the less substituted carbon generally migrates to the electrophilic centre.[21] This renders the protocol a very powerful tool, confirmed by its first use in natural product synthesis by *Goldberg* and *Monnier* in 1940, only a few years after its discovery.[20]

1.2 Adamantane – Versatile Compound in Medicinal Chemistry, Catalysis and Material Science

1.2.1 Background

29

Figure 3. Adamantane (tricyclo[3.3.1.1^{3,7}]decane).

First isolated and synthesized in the first half of the 20th century,[22] the success story of the smallest diamond (*Figure 3*) started properly after *Schleyer's Lewis* acid induced synthesis in 1957 made it available in yields that exceeded the earlier method.[23]

Since then the simple hydrocarbon cage is found in a wide range of drugs,[24] homogeneous and heterogeneous catalysts,[25] and other molecular systems, wherever enhanced lipophilicity or conformational rigidity is required.[26] In the following chapters, these roles and uses are portrayed, in order to illustrate their significance with a few selected examples.

1.2.2 Pharmaceuticals

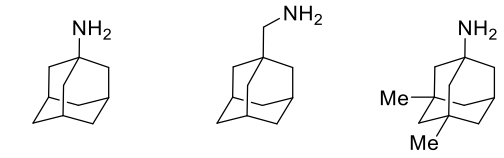

Figure 4. Simple adamantanes with biological activities used in medicinal treatments for influenza A[27] or Alzheimer's disease.[28]

Simple adamantylamines, like amantadine and its derivatives (*Figure 4*), are known for their anti-influenza A activity for over 50 years.[27] Tertiary functionalized amantadine (1-aminoadamanatane) was the first commercial drug with an adamantane skeleton.[24e] Since then, mechanistic inquiries helped to understand their method of operation[29] and new derivatives (*e.g.,* compounds shown in *Figure 5)* were developed to counter upcoming resistances.[30]

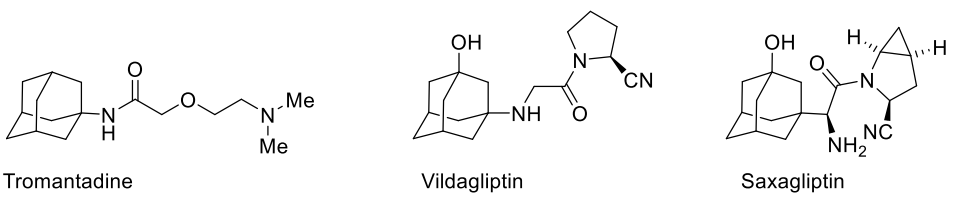

Figure 5. Drugs containing the adamantane scaffold, effective against various diseases e.g., type II diabetes[31] or herpes simplex.[32]

These more complex compounds show activity against diseases like type II diabetes[31] or herpes simplex.[32]

The adamantane cages can also be added as a lipophilicity modifier to bigger molecules or peptides. For instance, adamantane-capped photosensitizer **28** (*Figure 6*) is used to induce cell death after irradiation *via* singlet-oxygen generation in cancer cells.[33] Peptide *c(RGDyK)-Ad* (*Figure 7*) is a cell-penetrating peptide and acts as a delivery system of metallo-anticancer agents through self-assembled nanoparticle formation.[34]

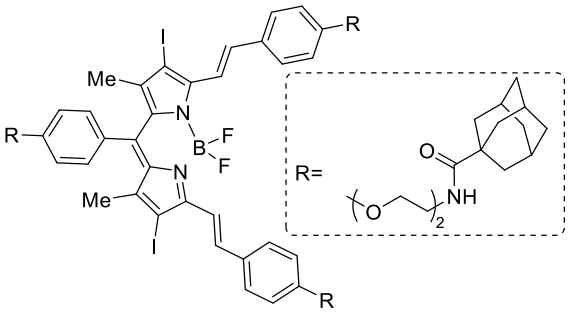

28

Figure 6. Adamantane-capped photosensitizer 28.[33]

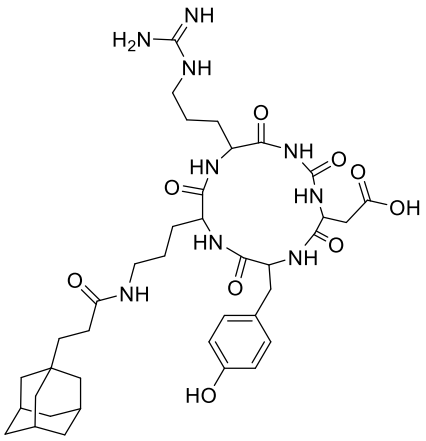

c(RGDyK)-Ad

Figure 7. The peptide c(RGDyK)-Ad is used as a drug-delivery system.[34]

For the synthesis of these kinds of medicinal compounds, functional groups at the adamantane moiety are crucial for connectivity to the target molecule.[35] In the shown compounds it is conspicuous that said functional groups are only on the 1- and 3-positions (tertiary carbon) in the adamantane structure which is most common in the early developed drugs and drug precursors, due to easier access provided by the inherent reactivity of its structure.[35] The introduction of a functional group selectively on the 2-position (secondary carbon) of the cage is still a challenge. Two major approaches are employed for the synthesis of 1,2-functionalized compounds: (i) intramolecular rearrangements of similar cages (compare *Chapter1.3.1*),[10a, 36] and (ii) directed C–H oxidation, using a formerly introduced directing group at the 1-position (*Scheme 8*).[35, 37]

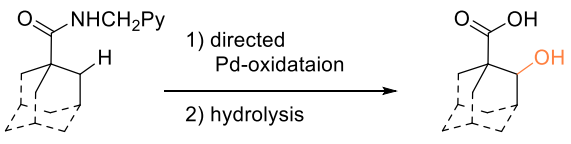

29 **30**, 12-85%

Scheme 8. Example for directed C-H activation at the adamantane scaffold by Larrosa et. al.[38]

1.2.3 Catalysts

Catalysts containing adamantanes structures are well distributed in the various sub-disciplines. The steric and electronic properties put the caged carbohydrate in key roles in the mechanism of many of these synthetic systems.[25]

Organometallic Catalysts

One important class of ligands containing adamantane are adamantylphosphines, since they provide high turnover numbers with low catalyst loadings.[25] As a direct consequence, many are commercially available.

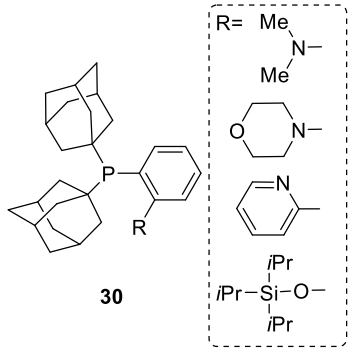

Figure 8. Commercially available adamantane containing ligands.

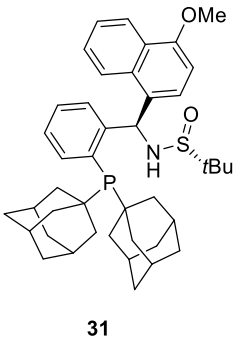

Figure 9. XiangPhos, a non-commercial ligand used in gold catalysis.[39]

As suitable representatives of these commercial phosphine ligands, *Figure 8* illustrates a specific group: the DalPhos ligands. Examples of their uses include palladium-catalysed aryl aminations,[40] etherification[41] and formation of indols.[42] An example of a non-commercial adamantylphosphine used as a ligand in transition metal catalysis is depicted in *Figure 9*.[39]

Zhang et al. reported in 2018 the intramolecular asymmetric cyclopropanation of 1,6-enynes in very high yields and superb enantiomeric excess, catalysed by a gold-XiangPhos complex (*Scheme 9*).

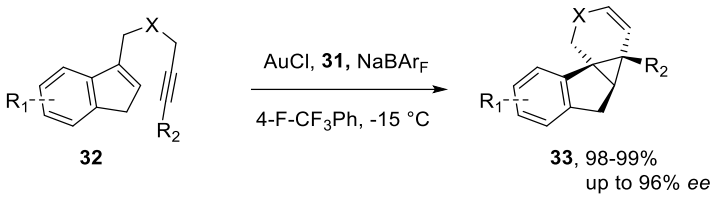

Scheme 9. Intramolecular asymmetric cyclopropanations catalysed by a gold-XiangPhos catalyst.[39]

Additionally, adamantyl ligands are used in dirhodium catalysed reactions. The dirhodium complex shown in *Figure* 10 has a chiral ligand incorporating an adamantane structure and is used to synthesize cyclic carbamates and aminoindanes in excellent yields and enantioselectivity.[43]

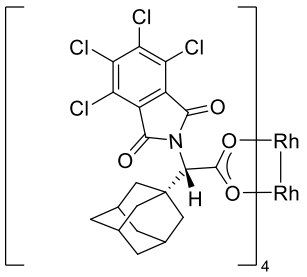

Figure 10. Chiral ligands containing adamantane for asymmetric C-H aminations.[43]

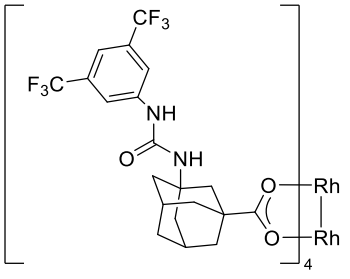

Figure 11. Bifunctional Rhodium catalyst 35 with an adamantane-containing ligand.[44]

The bifunctional catalyst co-developed by the *Hrdina* and *Schreiner* group in 2019 (*Figure 11*)[44], is applied in selective nitrenoid insertion into double bonds in conjugated systems. This newly developed system provides the possibility to overcome the intrinsic reactivity of the double bonds, leading to a 1:4 ratio of products contrary to a 2:1 ratio when standard ligands are used (*Scheme 10*).

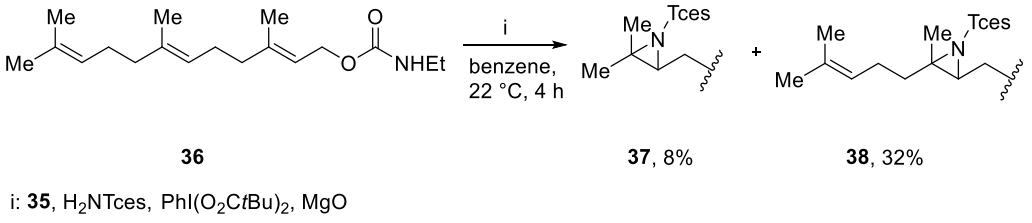

Scheme 10. Catalytic system developed by Berndt et al. using adamantane containing Rh-catalyst 35.[44]

Another strong feature of adamantane is its stabilizing effect, as shown by *Arduengo et al.* with the synthesis and description of 1,3-di-l-adamantylimidazol-2-ylidene (*Figure 12*), the first *N*-heterocyclic carbene (NHC) stable at room temperatures.[45]

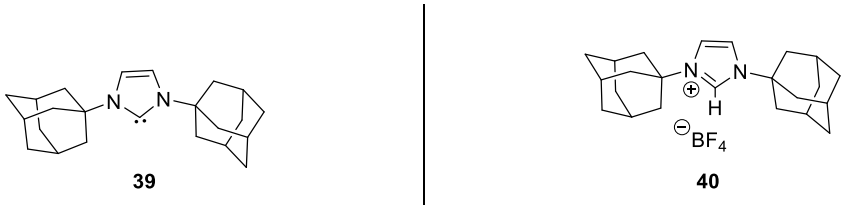

Figure 12. The Arduengo carbene (39, left), the first stable N-heterocyclic carbene (NHC) synthesized and fully described and its precursor, the BF_4-salt 40 (right).[45b]

Early on used as an organocatalyst,[46] adamantyl substituted NHCs are also versatile ligands in transition metal catalysis. Its first use as a palladium ligand for the *β*-alkynylation of aromatic amides was described by the *Yu* group in 2013 (*Scheme 11*).[47]

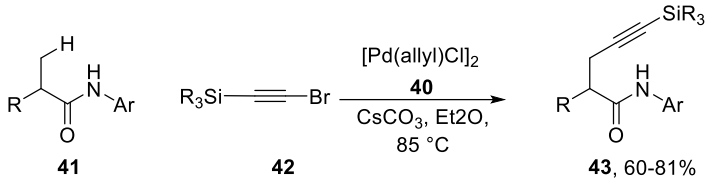

Scheme 11. Adamantyl-NHC as ligands in palladium catalysis.[47]

Concurrently, *Grubbs* group used an asymmetric adamantyl-NHC as a chelating ligand in ruthenium-catalysed ring-opening/cross-metathesis to synthesize compounds with up to 98% *Z*-configuration and good to very high enantioselectivity (*Scheme 12*).[48]

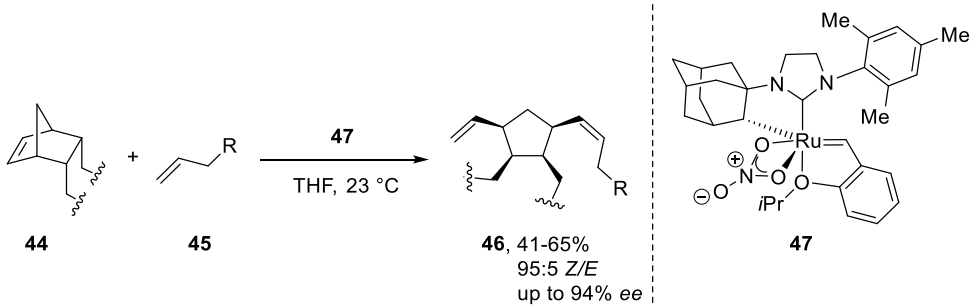

Scheme 12. Ruthenium catalysed ring-opening/cross-metathesis with an adamantyl-NHC chelating ligand developed by the Grubbs group.[48]

Organocatalysts

Since their development in the late 1990s and early 2000, thiourea catalysts play an important role in organocatalysis.[25, 49] Adamantane moieties are also found in thiourea catalysis, *e.g.*, bi-functional catalysts **48** and highly electrophile thiourea **49** (*Figure 13*), which are used to catalyse asymmetric vinylogous *Michael* additions,[50] or for the synthesis of precursors for α-amino-phosphonic acids, respectively.[51]

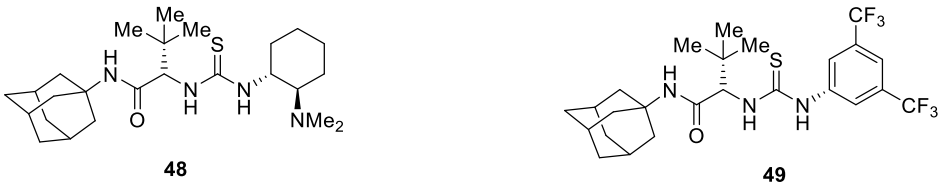

Figure 13. Thioureas containing adamantane moieties employed as organocatalysts.[50-51]

Even peptides can benefit from the higher lipophilicity gained by implementation of adamantane. Peptide **50** (*Figure 14*) is built from natural and non-natural amino acids and features an adamantane cage in its centre. The enhanced lipophilicity allows the use of non-polar solvents. Additionally, the rigidity introduced by the cage helps to prevent unwanted folding and therefore self-inactivation by the catalyst. This led to its activity in kinetic resolution of cyclic diols in good yields and excellent enantioselectivity.[52]

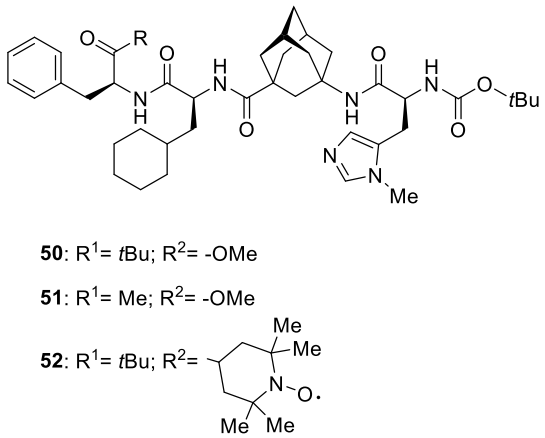

Figure 14. Peptides 50-52, used as asymmetric catalyst for kinetic resolution of cyclic diols.[52-53]

Further improvement of these peptides led to the development of multicatalysts **51**·H_2SO_4 (*Figure 14*) for the synthesis of *trans*-diols from alkenes and subsequent resolution thereof,[53a] and even a system for follow-up oxidation of the resolved diols (*Scheme 13*).[53b]

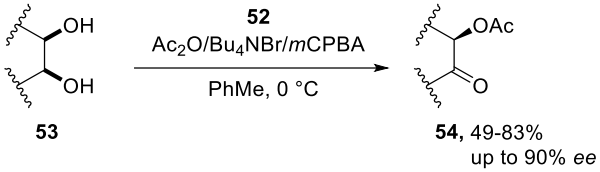

Scheme 13. Multicatalysis using an adamantyl peptide for resolution and oxidation of diols.[53b]

1.2.4 Material Science

The rigid diamondoid structure of adamantane is equally useful in surface-orientated systems like self-assembling molecular monolayers, which are of interest for electronic devices or molecular machines.[54]

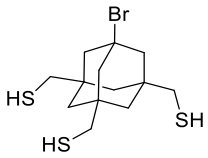

55

Figure 15. Tripod-like bromo adamantyl-thiol 55.[54]

The tripod-like adamantane compound **55** was examined as an anchor for self-assembled monolayers on gold surfaces (*Figure 15).*[54] Its three thiol-functions acts as the adsorption points to the surface layer, hence the comparison with a "tripod". The result was a better separation between the individual molecules in the monolayer (compared to less bulky molecules), thus erecting useful anchors and two-dimensional guiding structures for nanostructures on the gold surface.[55]

Because of their precisely defined geometrical shape, adamantane hydrazides (*Figure 16*) were chosen for combination with organo-functionalized Sn/S-clusters, resulting in diamondoid-decorated clusters.[56] Having an organic ligand outer layer allows additional optimization of the cluster for, *e.g.*, catalysis, gas storage, thermoelectric properties, *etc.*[56-57]

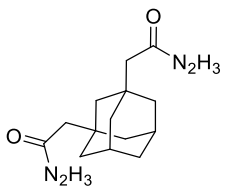

56

Figure 16. Adamantane hydrazine as an example of functionalized diamondoids used for modifying inorganic clusters.[56]

Porous organic polymers (POP) provide an interesting feature for uses in areas like gas storage[58] and heterogeneous catalysis.[59] Using polyfunctionalized adamantane as a base in these polymers delivers three-dimensional porous materials, which are robust and rigid.[60] *Totten* and co-workers envisioned that such an adamantyl-POP could have improved performance for degradation of toxic organophosphates. Actually, the adamantyl-POP showed a superior reactivity to its single-carbon-centred analogue (*Figure 17*)[61] and the authors attribute the enhanced activity to the much bigger surface area of the adamantane-based polymer.

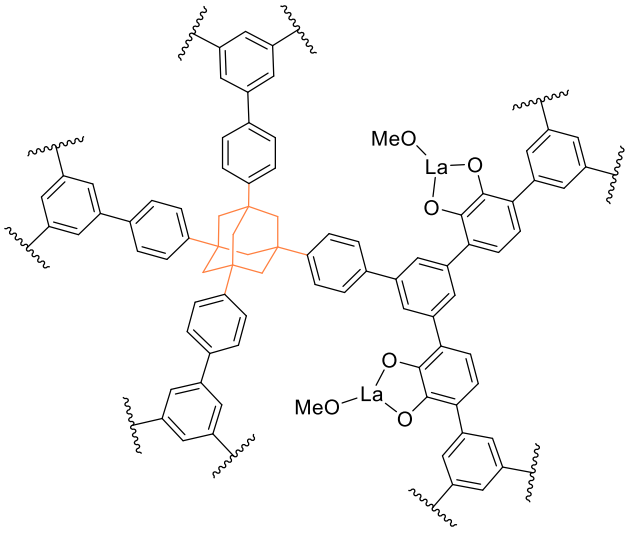

57

Figure 17. Adamantane-based 3D-POP developed as a catalyst by Totten et al.[61]

Similarly, an adamantane-based covalent organic framework (COF) shown in *Figure 18* was synthesized as a gas-adsorbent by *Trandafir et al.*[62] While able to adsorb large amounts of carbon dioxide, the authors describe an unexpected catalytic activity in hydrogenation reactions, which they assigned to residual palladium atoms from the employed cross-coupling reaction. Additional palladium nanoparticles enhanced this reactivity further and provided – in combination with the adamantyl polymer – a stable and easily recyclable catalyst.

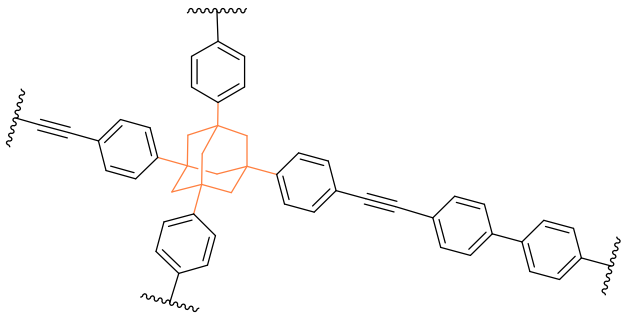

58

Figure 18. Adamantyl-COF able to store CO_2 and palladium nanoparticles for catalytic hydrogenation reactions.[62]

1.2.5 Noradamantane

59

Figure 19. Noradamantane (tricyclo[3.3.1.0^{3,7}]nonane).

Noradamantane (*Figure 19*) is a tricyclic cage compound resembling adamantane, but contracted at one bridge, resulting in two five- and one six-membered ring compared to the three six-membered rings in adamantane. Thence, still a bridgehead compound, it is not a part of the diamondoid group.[63] First synthesized *via* the same *Lewis* acid method as adamantane,[64] it is a well-known and -studied hydrocarbon.[64-65] Its properties and features are similar to these of adamantane described in the previous chapters. Especially its bioactivity – for instance in its anti-viral activity – is comparable in many cases, thus providing additional versatility in cases of upcoming and already existing resistances against established pharmaceuticals.[24e, 66]

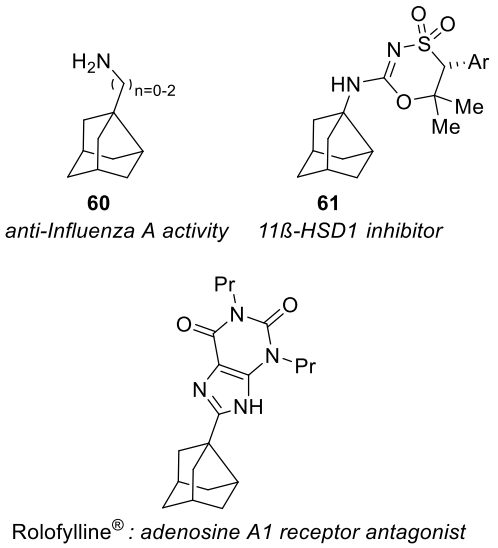

Figure 20. Biologically active compounds connected to a noradamantane skeleton.[66-67]

Figure 20 shows the mentioned influenza drugs as well as more complex bioactive compounds connected to the noradamantane skeleton.[67] Albeit its closeness in features and properties, its most uses are still as precursors for adamantane derivatives (see *Chapter 1.3.1*).[10a, 36e, 36f, 68]

1.2.6 Diamantane

As part of the diamondoid family, diamantane and adamantane derivatives share many properties and features. Diamondoids are hydrocarbon cage molecules, whose structures can be superimposed onto the diamond lattice (*Figure 21*).[69] While not as renowned as adamantane, the existing similarities lead to analogous fields of application, but also comparable obstacles. Functionalization at the desired positions can be hard to achieve,[70] and while much more lipophilic, its general solubility in a standard solvent is much lower than that of its smaller counterpart.[68a]

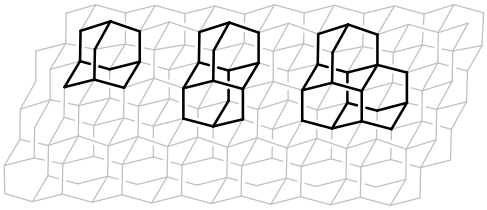

Figure 21. Section of a diamond lattice with examples of diamondoids highlighted in black (left to right: adamantane, diamantane, triamantane).[70a]

The application and uses are manyfold and, depending on the area of research, diamantanes can be both superior and inferior to the smaller diamondoid. Since the focus of this work is on adamantane, this introduction will only give a brief comparison of the two lowest diamondoids for the sake of completeness.

In catalysis, bulky diamantyl phosphine oxides (*Figure 22)* can be used as a preligand in transition metal catalysis (cp. *Figure 8, page 8*).

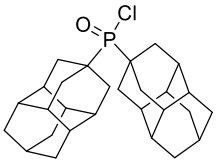

62

Figure 22 Bisdiamantanyl phosphine oxide, a preligand for transition metal catalysts.

One example of its use is portrayed in *Scheme 14*. Pd(II) complex **66** catalysis the enantioselective arylation of oxazolines with great success, enabling excellent C–H functionalization of aryl halides without the need to installed directing groups (cp. *Chapter 1.2.2*).[71]

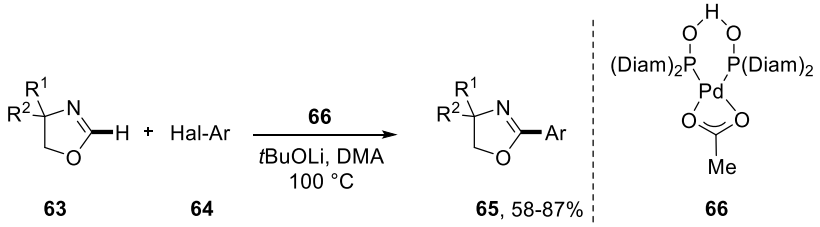

63 **64** **65**, 58-87% **66**

Scheme 14. Enantioselective arylation of oxazolines by Ghorai et al.[71]

Bioactivity against influenza A strains is an intensively studied feature of adamantane derivatives (compare *chapter 1.2.2*). While seemingly working *via* a different pathway than adamantanes, diamantane derivatives show similar antiviral properties.[72] Furthermore, 1,2-diaminodiamantane based platinum complex **67** (*Figure 23*) was recently discovered to show antiproliferative activity, outpacing similar anti-cancer medication (*i.e.,* cisplatin) in binding speed and potency.[73]

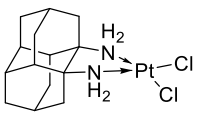

67

Figure 23. Diaplatin, an anti-cancer platinum complex by Bakhonsky et al.[73]

Similar to the adamantane thiols in self-assembled monolayers (SAM, cp. *Chapter 1.2.4*), diamantane thiols (*Figure 24*) are found to exhibit promising behaviour when assembled on gold surfaces.[74]

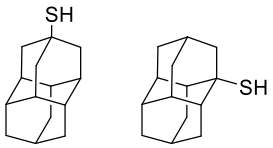

68 **69**

Figure 24. Thiols examined in self-assembled monolayers by Lopatina et al.[74]

Polymers based on diamantane monomers (*Figure 25*) show thermal stability significantly higher compared to polymers from smaller cages (*e.g.,* adamantane) or mono-cyclic compounds.[75]

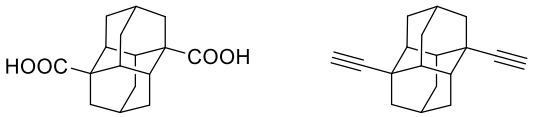

70 **71**

Figure 25. Examples compounds used as starting monomers for diamantane-based polymers.[75]

1.3 Rearrangements of (Nor)-Adamantanes

1.3.1 Functionalized Adamantanes – The Protoadamantane Route

Rearrangements to the adamantane framework from other tricyclic hydrocarbon cages like protoadamantane or noradamantane were discovered in the 1970s and 1980s, shortly after the very first syntheses of 1,2-functionalized adamantanes using directed oxidation of the secondary carbon in the bridgehead position.[35, 37g, 76] The protoadamantane-route was discovered by the *McKervey* group and the *Schleyer* group simultaneously in 1970 (*Scheme 15,* protoadamantane framework in orange).[36g, 77] These methods opened new possibilities for adamantane to many further transformations and reactions, and protoadamantane as a precursor for adamantane is still of interest and many examples are available from the recent reports.[15, 36b, 36c, 36h, 78]

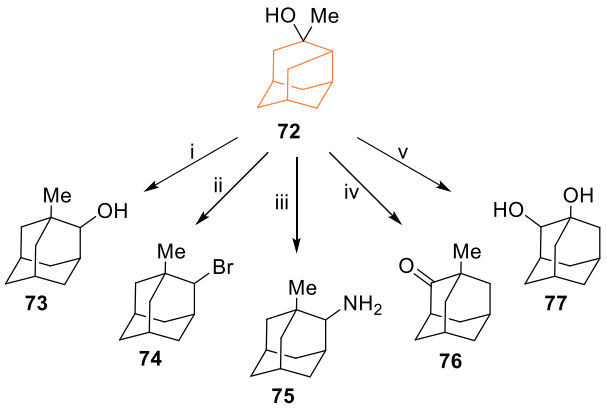

Scheme 15. Combination of the protoadamantane-routes to 1,2-functionalized adamantanes by the Schleyer (i-iv)[36g] and McKervy groups (v)[77]: i) HCl, acetone/water ii) HBr, ether iii) H_2SO_4, acetonitrile iv) CrO_3, H_2SO_4 acetone[36g] v) 1. CrO_3, H_2SO_4, acetone; 2. pTsOH, ethylene glycol, benzene; 3. $BF_3{\cdot}Et_2O$, acetic anhydride.

1.3.2 Functionalized Adamantanes – The Noradamantane Route

A second precursor for the adamantane framework – especially for 1,2-functionalized derivatives thereof – is noradamantane (*Figure 19, Chapter 1.2.5*). With the rearrangement of one carbon-carbon bond, it is only one step away from the strong diamondoid structure. Since the discovery of the method in the late 1980s, syntheses of adamantane derivatives from a noradamantane backbone using carbon migration are still commonplace in modern organic chemistry.[68d] The following examples of the noradamantyl-adamantanyl rearrangement belong to the *Wagner-Meerwein* family, meaning, though often formed in different ways, the electrophilic acceptor of the migrating bond is a carbocation in each case.[3] The reactions follow the same general process: Formation of the secondary carbocation, rearrangement to the more stable tertiary cation, followed by quenching of the reaction with suitable nucleophiles.

A very early method for the formation of the secondary carbocation is the acidic CO-insertion in noradamantane carboxaldehyde published by *Takeuchi* and colleagues in 1987.[36f] Followed by basic hydrolysis to cleave the formed ester, it eventually leads to 1,2-adamantanediol (*Scheme 16, **A***). The method is suitable for ring expansion in a wide variety of other cages, *e.g.,* norbornanes, camphor derivatives and adamantane itself. Similarly, noradamantyl phenyl ketone (**76**) is also amenable to undergo such a rearrangement after *in situ* reduction and successive iodination to yield 1,2-bisiodo adamantyl phenyls (*Scheme 16, **B***).[68b]

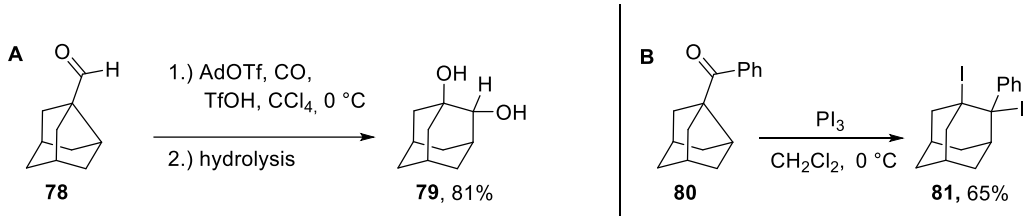

Scheme 16. A) Noradamantyl-adamantyl rearrangement to 1,2-diols by Takeuchi et al.[36f] B) Noradamantyl-adamantyl rearrangement by Okazaki et al. to 1,2-bisiodo adamantyl phenyls.[68b]

Acidic dehydration of tertiary noradamantyl alcohols leads to 2,2-dialkyl adamantanols (*Scheme 17, **A***).[36d] Combining this method with a subsequent *Ritter* reaction by adding nitriles to the reaction mixture, *Torres* and co-workers were able to synthesize 2,2-alkylated aminoadamantanes. Some compounds published therein show low micromolar activity against influenza virus strains and, more importantly, against amantadine-resistant strains (*Scheme 17, **B***).[10a]

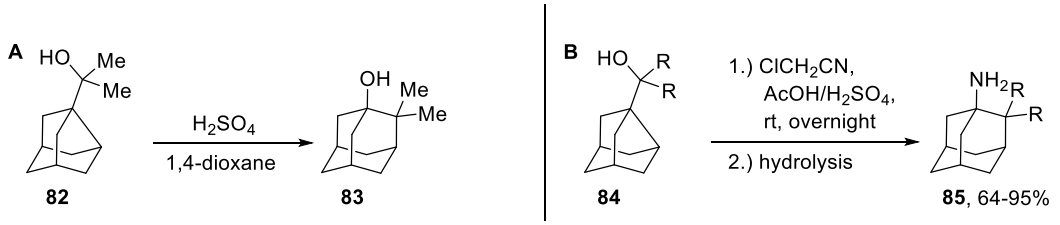

Scheme 17. A) Noradamantyl-adamantyl rearrangement to 2,2-dimethyl adamantanol by Stoelting et al.[36d] B) Amended version combined with Ritter reaction to 2,2-dialky aminoadamantanes by Torres et al.[10a]

1.4 Conclusion and Objective

In conclusion, adamantane is a most versatile compound found in a wide field of applications and uses. As shown by the examples given in this introduction, adamantane and its relatives proved to be valuable assets in pharmaceuticals (*Chapter 1.2.2*), synthesis (*Chapter 1.2.3*), and material science (*Chapter 1.2.4*). Features like their strong lipophilicity and their precisely defined geometry made it possible to improve existing compounds or find new structures with the desired properties. Nevertheless, pharmaceuticals which worked for decades might become obsolete through developed resistances, many synthetic challenges remain still unmet, and especially in these times of resource shortage and sustainability issues, innovations in the sector of material science are strongly needed. For adamantane to be useful in these challenges, it needs to be accessible.[24e, 35] Therefore, the key element of my doctoral work was to investigate the reversible *Wagner-Meerwein*-type rearrangement between the adamantane and the noradamantane structure (*Scheme 18)* for its uses in synthesis.

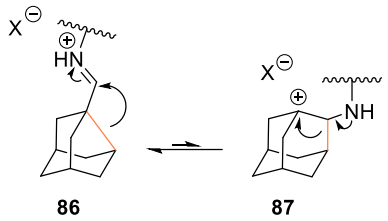

Scheme 18. General scheme of the investigated adamantane-noradamantane rearrangement.

The overall objective was to employ the *Brønsted* acid-induced rearrangement to synthesize new adamantane derivatives of interest, *e.g.*, 1,2-functionalized adamantanes. The following articles represent the mayor results of these studies.

1,2-Functionalized adamantylamines (including annulated adamantane heterocycles and non-cyclic amines; *Chapter 2*) were successfully synthesized from noradamantane iminium triflates. Further investigations led to undescribed noradamantane, new routes to known cage-compounds and ring-contracted diamantane derivatives (*Chapter 3*).

1.5 References

[1] D. Kamakura, H. Todoroki, D. Urabe, K. Hagiwara, M. Inoue, *Angew. Chem. Int. Ed.* **2020**, *59*, 479-486.
[2] J. Liebig, *Liebigs Ann. Pharm.* **1838**, *25*, 1-31.
[3] X.-M. Zhang, Y.-Q. Tu, F.-M. Zhang, Z.-H. Chen, S.-H. Wang, *Chem. Soc. Rev.* **2017**, *46*, 2272-2305.
[4] W. Wu, M. Xiao, J. Wang, Y. Li, Z. Xie, *Org. Lett.* **2012**, *14*, 1624-1627.
[5] G. Wagner, *J. Russ. Phys. Chem. Soc* **1899**, 690.
[6] H. Meerwein, *Justus Liebigs Ann. Chem.* **1914**, 129–175.
[7] (a)I. M. Tkachenko, P. A. Mankova, V. B. Rybakov, E. V. Golovin, Y. N. Klimochkin, *Org. Biomol. Chem.* **2020**; (b)L. Birladeanu, *J. Chem. Ed.* **2000**, *77*, 858; (c)K. i. Takeuchi, K. Ikai, M. Yoshida, A. Tsugeno, *Tetrahedron* **1988**, *44*, 5681-5694.
[8] F. Romanov-Michailidis, L. Guénée, A. Alexakis, *Angew. Chem. Int. Ed.* **2013**, *52*, 9266-9270.
[9] (a)R. Properzi, P. S. Kaib, M. Leutzsch, G. Pupo, R. Mitra, C. K. De, L. Song, P. R. Schreiner, B. List, *Nature Chemistry* **2020**, *12*, 1174-1179; (b)M. C. Reis, C. S. López, O. N. Faza, D. J. Tantillo, *Chem. Sci.* **2019**, *10*, 2159-2170; (c)D. J. Cram, *J. Am. Chem. Soc.* **1949**, *71*, 3863-3870.
[10] (a)E. Torres, R. Fernandez, S. Miquet, M. Font-Bardia, E. Vanderlinden, L. Naesens, S. Vazquez, *ACS Med. Chem. Lett.* **2012**, *3*, 1065-1069; (b)H. Meerwein, *Liebigs Ann. Chem.* **1914**, *405*, 129-175.
[11] H. A. Sharma, K. M. Mennie, E. E. Kwan, E. N. Jacobsen, *J. Am. Chem. Soc.* **2020**, *142*, 16090-16096.
[12] (a)G. A. Hill, E. W. Flosdorf, *Org. Synth.* **1925**, *5*, 91; (b)G. A. Hill, C. S. Spear, J. S. Lachowicz, *J. Am. Chem. Soc.* **1923**, *45*, 1557-1562.
[13] Z.-L. Song, C.-A. Fan, Y.-Q. Tu, *Chem. Rev.* **2011**, *111*, 7523-7556.
[14] B. Wang, Y. Q. Tu, *Acc. Chem. Res.* **2011**, *44*, 1207-1222.
[15] X. Wang, Y. Dong, E. L. Ezell, J. C. Garrison, J. K. Wood, J. P. Hagen, J. L. Vennerstrom, *Tetrahedron* **2017**, *73*, 2972-2976.
[16] S. E. Reisman, J. M. Ready, A. Hasuoka, C. J. Smith, J. L. Wood, *J. Am. Chem. Soc.* **2006**, *128*, 1448-1449.
[17] H. Wu, Q. Wang, J. Zhu, *J. Am. Chem. Soc.* **2019**, *141*, 11372-11377.
[18] T. Liang, Z. Zhang, J. C. Antilla, *Angew. Chem. Int. Ed.* **2010**, *49*, 9734-9736.
[19] M. Tiffeneau, P. Weill, B. Tchoubar, *C. R. Acad. Sci.* **1937**, *205*, 54-56.
[20] M. Goldberg, R. Monnier, *Helv. Chim. Acta* **1940**, *23*, 376-384.
[21] S. M. Kohlbacher, V.-S. Ionasz, L. Ielo, V. Pace, *Monatsh. Chem.* **2019**, 1-9.
[22] (a)V. Prelog, R. Seiwerth, *Ber. Dtsch. Chem. Ges. B* **1941**, *74b*, 1644-1648; (b)S. Landa, V. Machacek, *Collect. Czech. Chem. Commun* **1933**, *5*, 1-5.
[23] P. von R. Schleyer, *J. Am. Chem. Soc.* **1957**, *79*, 3292-3292.
[24] (a)L. C. Watkins, W. F. DeGrado, G. A. Voth, *J. Am. Chem. Soc.* **2020**, *142*, 17425-17433; (b)C. Tzitzoglaki, K. McGuire, P. Lagarias, A. Konstantinidi, A. Hoffmann, N. A. Fokina, C. Ma, I. P. Papanastasiou, P. R. Schreiner, S. Vázquez, *ACS Chem. Biol.* **2020**, *15*, 2331-2337; (c)T. P. Stockdale, C. M. Williams, *Chem. Soc. Rev.* **2015**, *44*, 7737-7763; (d)M. Côté, J. Misasi, T. Ren, A. Bruchez, K. Lee, C. M. Filone, L. Hensley, Q. Li, D. Ory, K. Chandran, J. Cunningham, *Nature* **2011**, *477*, 344-348; (e)L. Wanka, K. Iqbal, P. R. Schreiner, *Chem. Rev.* **2013**, *113*, 3516-3604; (f)R. C. Fort, P. v. R. Schleyer, *Chem. Rev.* **1964**, *64*, 277-300.
[25] K. A. Agnew-Francis, C. M. Williams, *Adv. Synth. Catal.* **2016**, *358*, 675-700.

[26] A. Štimac, M. Šekutor, K. Mlinarić-Majerski, L. Frkanec, R. Frkanec, *Molecules* **2017**, *22*, 297.
[27] (a)W. L. Davies, R. R. Grunert, R. F. Haff, J. W. McGahen, E. M. Neumayer, M. Paulshock, J. C. Watts, T. R. Wood, E. C. Hermann, C. E. Hoffmann, *Science* **1964**, *144*, 862-863; (b)G. Jackson, R. Muldoon, L. Akers, *Antimicrob. Agents Chemother.* **1963**, *161*, 703-707.
[28] S. K. Sonkusare, C. Kaul, P. Ramarao, *Pharmacol. Res.* **2005**, *51*, 1-17.
[29] (a)M. Lipsitch, J. B. Plotkin, L. Simonsen, B. Bloom, *Science* **2012**, *336*, 1529-1531; (b)G. Zoidis, N. Kolocouris, L. Naesens, E. De Clercq, *Bioorg. Med. Chem.* **2009**, *17*, 1534-1541; (c)P. Camps, M. D. Duque, S. Vázquez, L. Naesens, E. De Clercq, F. X. Sureda, M. López-Querol, A. Camins, M. Pallàs, S. R. Prathalingam, J. M. Kelly, V. Romerof, D. Ivorra, D. Cortés, *Bioorg. Med. Chem.* **2008**, *16*, 9925-9936; (d)E. De Clercq, *Nat. Rev. Drug Discov.* **2006**, *5*, 1015-1025.
[30] (a)V. Pardali, E. Giannakopoulou, A. Konstantinidi, A. Kolocouris, G. Zoidis, *Croatica Chemica Acta* **2019**, *92*, 1E-1E; (b)M. Hussain, H. D. Galvin, T. Y. Haw, A. N. Nutsford, M. Husain, *Infect. Drug. Resist.* **2017**, *10*, 121; (c)N. Y. Kuznetsov, R. M. Tikhov, I. A. Godovikov, M. G. Medvedev, K. A. Lyssenko, E. I. Burtseva, E. S. Kirillova, Y. N. Bubnov, *Org. Biomol. Chem.* **2017**, *15*, 3152-3157.
[31] L. P. H. Yang, *Drugs* **2012**, *72*, 229-248.
[32] G. May, D. Peteri, *Arzneimittel Forsch.* **1973**, *23*, 718-721.
[33] Q. Zhang, Y. Cai, X.-J. Wang, J.-L. Xu, Z. Ye, S. Wang, P. H. Seeberger, J. Yin, *ACS Applied Materials & Interfaces* **2016**, *8*, 33405-33411.
[34] S.-S. Xue, C.-P. Tan, M.-H. Chen, J.-J. Cao, D.-Y. Zhang, R.-R. Ye, L.-N. Ji, Z.-W. Mao, *Chem. Commun.* **2017**, *53*, 842-845.
[35] R. Hrdina, *Synthesis* **2019**, *51*, 629-642.
[36] (a)B. Zonker, E. Duman, H. Hausmann, J. Becker, R. Hrdina, *Org. Biomol. Chem.* **2020**, *18*, 4941-4945; (b)N. Cindro, I. Antol, K. Mlinarić-Majerski, I. Halasz, P. Wan, N. Basarić, *J. Org. Chem.* **2015**, *80*, 12420-12430; (c)N. Kolocouris, G. Zoidis, C. Fytas, *Synlett* **2007**, *2007*, 1063-1066; (d)D. Stoelting, V. Shiner Jr, *J. Am. Chem. Soc.* **1993**, *115*, 1695-1705; (e)Y. Ohga, K. I. Takeuchi, *J. Phys. Org. Chem.* **1993**, *6*, 293-301; (f)K. i. Takeuchi, I. Kitagawa, F. Akiyama, T. Shibata, M. Kato, K. Okamoto, *Synthesis* **1987**, *07*, 612-615; (g)P. V. Schleyer, D. Lenoir, R. Glaser, P. Mison, *J. Org. Chem.* **1971**, *36*, 1821-1826; (h)A. N. Abdel-Sayed, L. Bauer, *Tetrahedron* **1988**, *44*, 1873-1882.
[37] (a)M. Larrosa, Justus-Liebig-Universtität Gießen (Gießen), **2018**; (b)J. F. Hartwig, M. A. Larsen, *ACS Cent. Sci.* **2016**, *2*, 281-292; (c)J. F. Hartwig, *J. Am. Chem. Soc.* **2016**, *138*, 2-24; (d)J.-L. Pan, Q.-Z. Li, T.-Y. Zhang, S.-H. Hou, J.-C. Kang, S.-Y. Zhang, *Chem. Commun.* **2016**, *52*, 13151-13154; (e)R. Hrdina, F. M. Metz, M. Larrosa, J. P. Berndt, Y. Y. Zhygadlo, S. Becker, J. Becker, *Eur. J. Org. Chem.* **2015**, *2015*, 6231-6236; (f)J. J. Rohde, M. A. Pliushchev, B. K. Sorensen, D. Wodka, Q. Shuai, J. Wang, S. Fung, K. M. Monzon, W. J. Chiou, L. Pan, X. Deng, L. E. Chovan, A. Ramaiya, M. Mullally, R. F. Henry, D. F. Stolarik, H. M. Imade, K. C. Marsh, D. W. A. Beno, T. A. Fey, B. A. Droz, M. E. Brune, H. S. Camp, H. L. Sham, E. U. Frevert, P. B. Jacobson, J. T. Link, *J. Med. Chem.* **2007**, *50*, 149-164; (g)W. H. W. Lunn, W. D. Podmore, S. S. Szinai, *J. Chem. Soc.* **1968**, 1657-1660.
[38] M. Larrosa, B. Zonker, J. Volkmann, F. Wech, C. Logemann, H. Hausmann, R. Hrdina, *Chem. Eur. J.* **2018**, *24*, 6269-6276.
[39] P.-C. Zhang, Y. Wang, Z.-M. Zhang, J. Zhang, *Org. Lett.* **2018**, *20*, 7049-7052.

[40] (a)P. G. Alsabeh, R. J. Lundgren, R. McDonald, C. C. Johansson Seechurn, T. J. Colacot, M. Stradiotto, *Chem. Eur. J.* **2013**, *19*, 2131-2141; (b)R. J. Lundgren, B. D. Peters, P. G. Alsabeh, M. Stradiotto, *Angew. Chem. Int. Ed.* **2010**, *49*, 4071-4074; (c)K. D. Hesp, M. Stradiotto, *J. Am. Chem. Soc.* **2010**, *132*, 18026-18029.
[41] S. Gowrisankar, A. G. Sergeev, P. Anbarasan, A. Spannenberg, H. Neumann, M. Beller, *J. Am. Chem. Soc.* **2010**, *132*, 11592-11598.
[42] C. B. Lavery, R. McDonald, M. Stradiotto, *Chem. Commun.* **2012**, *48*, 7277-7279.
[43] R. P. Reddy, H. M. L. Davies, *Org. Lett.* **2006**, *8*, 5013-5016.
[44] J.-P. Berndt, Y. Radchenko, J. Becker, C. Logemann, D. R. Bhandari, R. Hrdina, P. R. Schreiner, *Chem. Sci.* **2019**, *10*, 3324-3329.
[45] (a)D. Enders, O. Niemeier, A. Henseler, *Chem. Rev.* **2007**, *107*, 5606-5655; (b)A. J. Arduengo, R. L. Harlow, M. Kline, *J. Am. Chem. Soc.* **1991**, *113*, 361-363.
[46] G. A. Grasa, R. M. Kissling, S. P. Nolan, *Org. Lett.* **2002**, *4*, 3583-3586.
[47] J. He, M. Wasa, K. S. L. Chan, J.-Q. Yu, *J. Am. Chem. Soc.* **2013**, *135*, 3387-3390.
[48] J. Hartung, R. H. Grubbs, *J. Am. Chem. Soc.* **2013**, *135*, 10183-10185.
[49] (a)P. R. Schreiner, A. Wittkopp, *Org. Lett.* **2002**, *4*, 217-220; (b)M. S. Sigman, E. N. Jacobsen, *J. Am. Chem. Soc.* **1998**, *120*, 4901-4902.
[50] M. S. Manna, S. Mukherjee, *Chem. Eur. J.* **2012**, *18*, 15277-15282.
[51] A. Ray Choudhury, S. Mukherjee, *Chem. Sci.* **2016**, *7*, 6940-6945.
[52] (a)C. E. Müller, D. Zell, R. Hrdina, R. C. Wende, L. Wanka, S. r. M. Schuler, P. R. Schreiner, *J. Org. Chem.* **2013**, *78*, 8465-8484; (b)C. E. Muller, L. Wanka, K. Jewell, P. R. Schreiner, *Angew. Chem. Int. Ed.* **2008**, *47*, 6180-6183.
[53] (a)R. Hrdina, C. E. Muller, R. C. Wende, L. Wanka, P. R. Schreiner, *Chem. Commun.* **2012**, *48*, 2498-2500; (b)C. E. Müller, R. Hrdina, R. C. Wende, P. R. Schreiner, *Chem. Eur. J.* **2011**, *17*, 6309-6314; (c)C. Hofmann, J. M. Schümann, P. R. Schreiner, *J. Org. Chem.* **2015**, *80*, 1972-1978.
[54] T. Kitagawa, Y. Idomoto, H. Matsubara, D. Hobara, T. Kakiuchi, T. Okazaki, K. Komatsu, *J. Org. Chem.* **2006**, *71*, 1362-1369.
[55] (a)M. Valášek, M. Lindner, M. Mayor, *Beilstein J. Nanotechnol.* **2016**, *7*, 374-405; (b)M. A. Karimi, S. G. Bahoosh, M. Valášek, M. Bürkle, M. Mayor, F. Pauly, E. Scheer, *Nanoscale* **2016**, *8*, 10582-10590.
[56] B. E. K. Barth, B. A. Tkachenko, J. P. Eußner, P. R. Schreiner, S. Dehnen, *Organometallics* **2014**, *33*, 1678-1688.
[57] H. Li, M. Eddaoudi, M. O'Keeffe, O. M. Yaghi, *Nature* **1999**, *402*, 276-279.
[58] B. G. Hauser, O. K. Farha, J. Exley, J. T. Hupp, *Chem. Mat.* **2013**, *25*, 12-16.
[59] Y. Zhang, Y. Zhang, Y. L. Sun, X. Du, J. Y. Shi, W. D. Wang, W. Wang, *Chem. Eur. J.* **2012**, *18*, 6328-6334.
[60] H. Nasrallah, J.-C. Hierso, *Chem. Mat.* **2018**, *31*, 619-642.
[61] R. K. Totten, M. H. Weston, J. K. Park, O. K. Farha, J. T. Hupp, S. T. Nguyen, *ACS Catalysis* **2013**, *3*, 1454-1459.
[62] M. M. Trandafir, L. Pop, N. D. Hădade, M. Florea, F. Neaţu, C. M. Teodorescu, B. Duraki, J. A. van Bokhoven, I. Grosu, V. I. Pârvulescu, H. Garcia, *Cat. Sci. Tech.* **2016**, *6*, 8344-8354.
[63] J. Dahl, S. Liu, R. Carlson, *Science* **2003**, *299*, 96-99.
[64] P. von Ragué Schleyer, E. Wiskott, *Tetrahedron Lett.* **1967**, *8*, 2845-2850.
[65] J. S. Wishnok, P. v. R. Schleyer, *Org. Prep. Proced. Int.* **1973**, *5*, 215-217.
[66] N. Moorthy, V. Poongavanam, V. Pratheepa, *Mini-Rev. Med. Chem.* **2014**, *14*, 819-830.

[67] (a)A. G. Moore, S. R. Schow, R. T. Lum, M. G. Nelson, C. R. Melville, *Synthesis* **1999**, *1999*, 1123-1126; (b)T. Boehme, K. Ritter, C. Engel, S. Guessregen, T. Haack, G. Tschank, Sanofi, **2012**.
[68] (a)B. Zonker, J. Becker, R. Hrdina, *Org. Biomol. Chem.* **2021**, *19*, 4027-4031; (b)T. Okazaki, K. Tokunaga, T. Kitagawa, K. i. Takeuchi, *Bull. Chem. Soc. Jpn.* **1999**, *72*, 549-561; (c)G. A. Olah, A. H. Wu, O. Farooq, *J. Org. Chem.* **1989**, *54*, 1452-1453; (d)J. J. Sosnowski, A. L. Rheingold, R. K. Murray, Jr., *J. Org. Chem.* **1985**, *50*, 3788.
[69] A. P. Marchand, *Science* **2003**, *299*, 52-53.
[70] (a)P. A. Gunchenko, L. V. Chernish, E. Y. Tikhonchuk, J. Becker, P. R. Schreiner, A. A. Fokin, *J. Org. Pharm. Chem.* **2020**, *18*, 16-22; (b)A. A. Fokin, A. E. Pashenko, V. V. Bakhonsky, T. S. Zhuk, L. V. Chernish, P. A. Gunchenko, A. O. Kushko, J. Becker, R. C. Wende, P. R. Schreiner, *Synthesis* **2017**, *49*, 2003-2008.
[71] D. Ghorai, V. Mueller, H. Keil, D. Stalke, G. Zanoni, B. A. Tkachenko, P. R. Schreiner, L. Ackermann, *Adv. Synth. Catal.* **2017**, *359*, 3137-3141.
[72] C. Tzitzoglaki, K. McGuire, P. Lagarias, A. Konstantinidi, A. Hoffmann, N. A. Fokina, C. Ma, I. P. Papanastasiou, P. R. Schreiner, S. Vazquez, M. Schmidtke, J. Wang, D. D. Busath, A. Kolocouris, *ACS Chem. Biol.* **2020**, *15*, 2331-2337.
[73] V. V. Bakhonsky, A. A. Pashenko, J. Becker, H. Hausmann, H. J. De Groot, H. S. Overkleeft, A. A. Fokin, P. R. Schreiner, *Dalton Trans.* **2020**, *49*, 14009-14016.
[74] Y. Y. Lopatina, V. I. Vorobyova, A. A. Fokin, P. R. Schreiner, A. A. Marchenko, T. S. Zhuk, *J. Phys. Chem. C* **2019**, *123*, 27477-27482.
[75] (a)A. A. Malik, T. G. Archibald, K. Baum, M. R. Unroe, *Macromolecules* **1991**, *24*, 5266-5268; (b)Y.-T. Chern, W.-L. Wang, *Macromolecules* **1995**, *28*, 5554-5560.
[76] (a)W. V. Curran, R. B. Angier, *Chem. Commun.* **1967**, *563*; (b)W. V. Curran, R. B. Angier, *J. Org. Chem.* **1969**, *34*, 3668-3670.
[77] B. D. Cuddy, D. Grant, M. A. McKervey, *J. Chem. Soc. C* **1971**, 3173-3179.
[78] (a)I. Papanastasiou, A. Tsotinis, N. Kolocouris, S. R. Prathalingam, J. M. Kelly, *J. Med. Chem.* **2008**, *51*, 1496-1500; (b)K. Mlinarić-Majerski, G. Kragol, T. Š. Ramljak, *Synlett* **2008**, *2008*, 405-409.

2 [1,2]-Rearrangement of iminium salts provides access to heterocycles with adamantane scaffold

2.1 Abstract

We describe a *Brønsted* acid-catalysed cascade reaction consisting of a *Wagner–Meerwein* rearrangement and a subsequent intra- or intermolecular Friedel–Crafts reaction leading to adamantane based heterocycles. In contrast to the reported W.-M. rearrangements, in this case an iminium moiety serves as the acceptor of a migrating nucleophilic alkyl group in a [1,2]-alkyl shift.

Published as: B. Zonker, E. Duman, H. Hausmann, J. Becker and R. Hrdina, *Org. Biomol. Chem.* **2020**, *18*, 4941-4945.

Organic & Biomolecular Chemistry

ROYAL SOCIETY OF CHEMISTRY

COMMUNICATION

View Article Online
View Journal | View Issue

Cite this: *Org. Biomol. Chem.*, 2020, **18**, 4941

Received 3rd June 2020,
Accepted 22nd June 2020

DOI: 10.1039/d0ob01156h

rsc.li/obc

[1,2]-Rearrangement of iminium salts provides access to heterocycles with adamantane scaffold†

Benjamin Zonker, [a] Ediz Duman,[a] Heike Hausmann,[a] Jonathan Becker[b] and Radim Hrdina *[a]

We describe a Brønsted acid-catalysed cascade reaction consisting of a Wagner–Meerwein rearrangement and a subsequent intra- or intermolecular Friedel–Crafts reaction leading to adamantane-based heterocycles. In contrast to the reported W.–M. rearrangements, in this case an *iminium moiety* serves as the acceptor of a migrating nucleophilic alkyl group in a [1,2]-alkyl shift.

The adamantane scaffold is commonly used in drug design[1] and catalyst development[2] to modulate the lipophilicity[3] of the final compound or to introduce rigidity[4] into the system. Properties and reactivity of the adamantane framework single its derivatives out as a special class of aliphatic compounds. Especially the synthesis of 1,2-disubstituted derivatives of such bridgehead compounds is rather challenging.[5]

We report a new method for the preparation of adamantane annulated aza-heterocycles employing a Brønsted acid catalysed C–C bond cleavage and C–C bond formation in a cascade.[6] The Wagner–Meerwein rearrangement belongs to one of the first reactions described in organic chemistry.[7] For more than hundred years, this reaction was utilised to prepare densely functionalised products based on intramolecular nucleophilic [1,2]-alkyl,[8] -aryl[9] or -hydride[10] shifts. The acceptor of the migrating group in the molecule is typically a carbocation[11] or less frequently, a heteroatom stabilised carbenium ion.[12] The cascade reaction described herein involves an intramolecular nucleophilic [1,2]-alkyl shift, for the first time reported with an *iminium* group[13] as acceptor. The resulting carbocation is trapped by a subsequent intramolecular electrophilic aromatic substitution (Friedel–Crafts reaction[14]) to form aza-heterocycles[3,15] or *prim*-/*sec*-/*tert*-amines in case of the intermolecular variant (Fig. 1). This sequence of reactions is described on noradamantane derived iminium salts (Scheme 1),[16] whose properties allow this cascade reaction to proceed. These properties are following: first, the carbon of the iminium group is sterically shielded, which does not allow the electrophilic aromatic substitution to proceed at this point (Pictet–Spengler reaction[17]); second, the counterion is a non-nucleophilic anion;[18] third, the generated carbocation as a result of the [1,2]-alkyl shift is a bridgehead cation,[19] that means the reverse shift of the hydride is not possible, nor is the formation of an aziridinium ion (due to geometric constraint).[20] The reaction is catalysed by Brønsted acids (HA). Their role is not the activation of the starting material, the iminium salt for the W.–M. rearrangement step, but the protonation of the reactive intermediate and thus disabling the reverse reaction to the thermodynamically more stable starting material. The catalyst is regenerated by the following Friedel–Crafts reaction (Fig. 1).

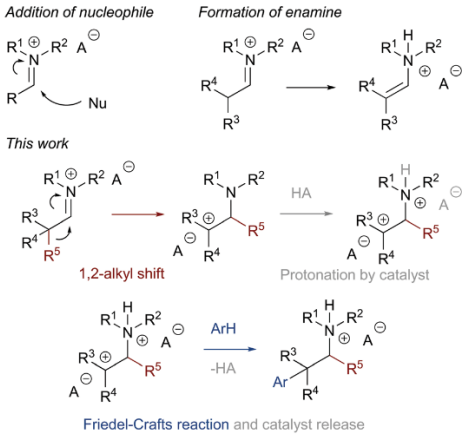

Fig. 1 Reactivity of iminium group: selected cases and new mode.

[a]*Institute of Organic Chemistry, Justus-Liebig University, Heinrich-Buff-Ring 17, 35392 Giessen, Germany. E-mail: radim.hrdina@org.chemie.uni-giessen.de*
[b]*Institute of Inorganic and Analytical Chemistry, Justus-Liebig University, Heinrich-Buff-Ring 17, 35392 Giessen, Germany*

† Electronic supplementary information (ESI) available. CCDC 2000166–2000167. For ESI and crystallographic data in CIF or other electronic format see DOI: 10.1039/d0ob01156h

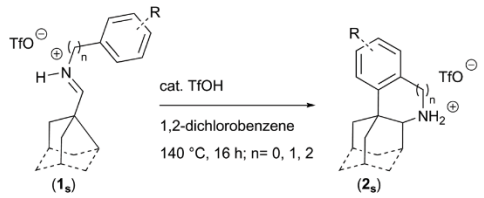

Scheme 1 Nucleophilic [1,2]-alkyl shift followed by intramolecular Friedel–Crafts reaction: cascade reaction from $\mathbf{1}_s$ to aza-heterocycles $\mathbf{2}_s$; ($\mathbf{1e}_s$: n = 1, R = H).

Noradamantane imine **1e** was chosen as a starting material to test the cascade reaction, to optimise the reaction conditions, to facilitate the reaction protocol and to shed light on the reaction mechanism (Scheme 1).

Compound **1e** was prepared by the condensation reaction of noradamantane-3-carbaldehyde with benzylamine.[21] The initial tests were done with 2 equivalents of Brønsted acid *versus* 1 equivalent of starting imine **1e** (to avoid side reactions the condensation step was separated from the cascade). The cascade reaction proceeds only when acids with non-nucleophilic anions (*p*-TsOH, TfOH) are applied. Triflic acid provides the highest conversion and was further used. The reaction at 140 °C is completed within hours. Replacement of TfOH by Cu $(OTf)_2$ does not provide any product. The amount of Brønsted acid can be reduced to a catalytic amount *versus* the iminium salt $\mathbf{1e}_s$ providing similar conversions. Isolated salt $\mathbf{1e}_s$ exposed just to 1,2-dichlorobenzene (nonpolar solvent) at 140 °C for 16 h does not undergo the cascade reaction (only traces of product $\mathbf{2e}_s$ were observed). Addition of catalytic amounts of triflic acid to the solution of iminium salt $\mathbf{1e}_s$ initiated the reaction. The scope of the reaction was tested with noradamantane imines **1** derived from substituted anilines, benzylamines and phenylethylamines (Fig. 2). Formation of five-, six- and seven-membered cyclic derivatives **2** was observed. The reaction with imines derived from 3-phenylpropylamine did not lead to the eight-membered rings under these conditions. The reaction was also tested on substituted noradamantane derivatives(**1l**, **1m**)[22] to demonstrate that both precursors of **1** (aldehyde and amine) can be varied.

In the next step, we focused on the intermolecular variant of the cascade reaction (Scheme 2). Here, the substrate for the electrophilic aromatic substitution reaction was used either as a solvent, or in excess (10 equivalents *versus* the iminium salt $\mathbf{3}_s$) in 1,2-dichlorobenzene. We chose *o*-xylene to prepare primary and secondary amines (**4a–c**), and pyrene to prepare tertiary amines (**4d**) as selected examples from the several possibilities this method enables. Compound **4c** was synthesised to show that even sterically demanding amines[23] can be employed in this reaction.

Oxidation of a secondary amine to the imine opens the pathway to various further post-functionalisations (*e.g.* addition of nucleophile, hydrolysis).

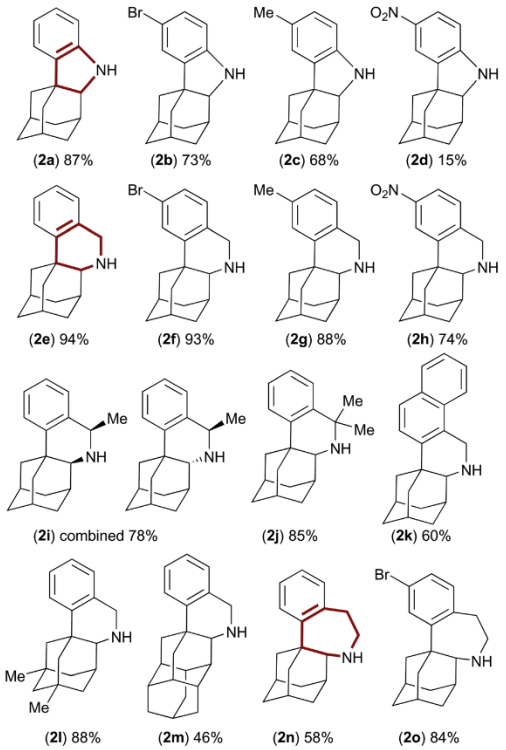

Fig. 2 Substrate scope for nucleophilic [1,2]-alkyl shift followed by intramolecular Friedel–Crafts reaction. Yields of isolated products **2** (as free bases) are stated.

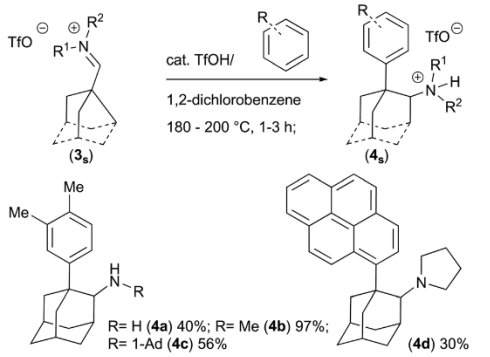

Scheme 2 Nucleophilic [1,2]-alkyl shift followed by intermolecular Friedel–Crafts reaction: cascade reaction from $\mathbf{3}_s$ to amines $\mathbf{4}_s$. Yields of isolated products **4** (as free bases) are stated.

We were surprised to observe the high conversion of amine **2a** to strained imine **5** using iodine as an oxidant[24] (Scheme 3A). To demonstrate the applicability of derivatives

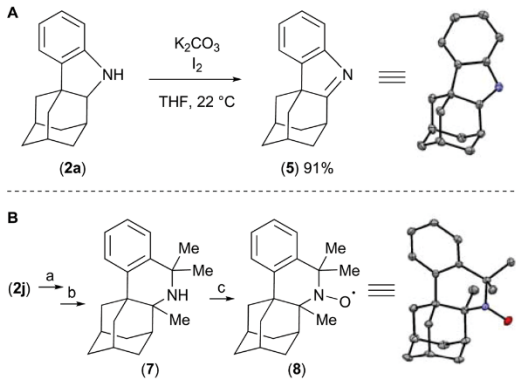

a) I_2, K_2CO_3,THF, 22 °C; (**6**) 84%
b) $BF_3{\cdot}Et_2O$, MeLi, PhMe/THF, -78 °C to 22 °C; (**7**) 81%
c) $Na_2WO_4{\cdot}2H_2O$, H_2O_2·urea, MeOH, 22 °C; (**8**) 76%

Scheme 3 Post-functionalisation reactions, A: synthesis of highly strained imine **5** (X-ray analysis structure of compound **5** depicted); B: facile and modular synthesis of nitroxyl radical derivative **8** (X-ray analysis structure of compound **8** depicted).

made by our new method, we prepared nitroxyl (TEMPO)[25] derivative **8** in just three steps from starting material **2j** (Scheme 3B). The crucial step was the alkylation of sterically shielded imine **6** towards intermediate **7**. This compound is an interesting example of a *piperidine* derivative, where all carbons in the ring contain *C*-substituents and no hydrogen.

Next, we focused on the mechanism of this new cascade reaction (Scheme 4). Thermodynamic stabilities of intermediates were estimated using computational studies. First we compared the relative stability of iminium ion $\mathbf{1e_s}^+$ *versus* reactive intermediate carbocation $\mathbf{10}^+$ using DFT method (Fig. 3). To

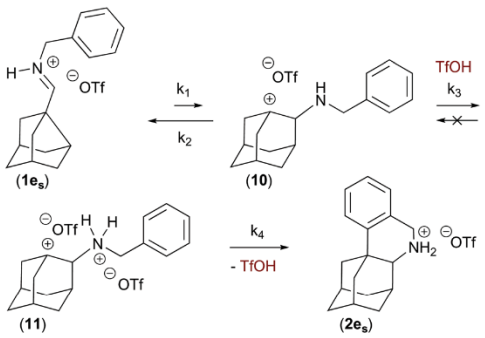

Scheme 4 The proposed mechanistic model with relative kinetic rate constants to determine the role of the Brønsted acid catalyst (TfOH), which is trapping of the intermediate **10**. The cascade is described as a sequence of a non-catalysed [1,2]-alkyl shift, protonation of the amino group in the molecule **10** to **11** and final Friedel–Crafts reaction towards the product $\mathbf{2e_s}$.

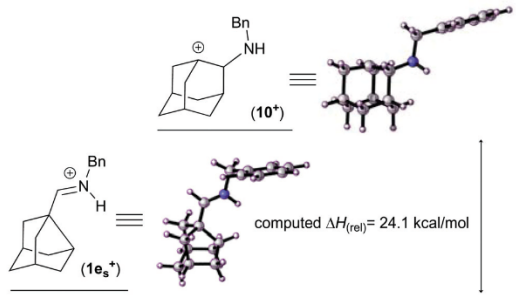

Fig. 3 Relative stability of intermediate $\mathbf{10}^+$ *versus* starting material $\mathbf{1e_s}^+$ using DFT method B3LYP/6-311G(d,p).

estimate the contribution of the benzylamine group on the stability of the carbocation in $\mathbf{10}^+$ we computed the isodesmic reaction, which showed that the effect of the neighbouring group has a stabilising effect (ΔH = 3.5 kcal mol^{-1}, ESI page 175, Scheme 6†). The ΔH difference between $\mathbf{1e_s}^+$ and $\mathbf{10}^+$ is only 24.1 kcal mol^{-1} considering the high stability of iminium ions.[26] To the rather low difference in enthalpy contribute two effects: strain in the noradamantane cage[27] and stability of the 1-adamantyl cation.[28]

For analysis of the individual reactions of the cascade, we prepared reactive intermediates **10** and **11** *in situ* from designed precursors. First we studied the Friedel–Crafts reaction of the cascade and generated **11** from compound $\mathbf{12_s}$ (Scheme 5A). Starting the reaction cascade from this point revealed that the reaction barrier of the Friedel–Crafts reaction is lower than it is for the [1,2]-alkyl shift (the cascade reaction does not proceed at 80 °C, see Table 1).

Then we studied the reversibility of the alkyl shift. Intermediate **10** was generated from precursor **13** using AgOTf (Scheme 5B). Upon addition of the silver triflate to a solution of **13** at 25 °C immediate precipitation of AgBr was observed and subsequent formation of iminium salt $\mathbf{1e_s}$ was detected using NMR spectroscopy and high resolution mass spectrometry.

In contrast, intermediate **11** generated from **14** did not undergo the rearrangement reaction to iminium salt $\mathbf{1e_s}$ upon stirring for 1 h at 25 °C (Scheme 5B).

Additionally, we focused on the trapping of intermediate **10** using the Ritter reaction (Scheme 5C).[29] Aromatic nitrile **17** was chosen as the trapping agent of adamantyl cation $\mathbf{10}^+$ in the thermal rearrangement of starting material $\mathbf{1e_s}$ to generate the intermediate nitrilium salt. The amino group – formed as a result of the rearrangement – serves as a nucleophile in the final ring-closing reaction. Formation of product **15** was observed, indicating that the [1,2]-alkyl shift of $\mathbf{1e_s}$ does not require any additional activation by Brønsted acid. The reaction was repeated with starting material $\mathbf{3b_s}$ to yield product **16** (for ^{1}H NMR spectra of reaction mixtures see ESI page 153†).

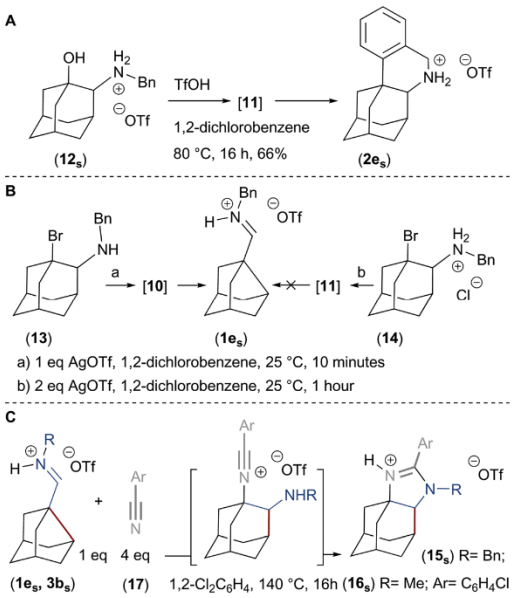

Scheme 5 Mechanistic investigations. A: Generation of intermediate **11** from precursor $\mathbf{12_s}$ and subsequent Friedel–Crafts reaction to the product $\mathbf{2e_s}$ at 80 °C. B: Reversibility of the [1,2]-alkyl shift; reactive intermediate **10** generated from bromo-precursor **13**, reactive intermediate **11** generated from compound **14**. C: Trapping of the intermediate **10** by nitrile **17** in ring-closing reaction.

Table 1 Screening of Brønsted acids and reaction conditions.[a] Nucleophilic [1,2]-alkyl shift followed by intramolecular Friedel–Crafts reaction: cascade reaction from $\mathbf{1e_s}$ to aza-heterocycles $\mathbf{2e_s}$

Brønsted acid (HA)	Equiv. of HA	Temperature in °C	Conversion in %[b]
CF_3COOH	2	140	0
$(RO)_2POOH$[c]	2	140	0
HCl	2	140	0
p-TsOH	2	140	60
TfOH	**2**	**140**	**96**
TfOH	2	120	81
TfOH	2	100	17
TfOH	2	80	0
TfOH	1.1	140	92
TfOH	1.0	140	Traces
$Cu(OTf)_2$	2	140	0[d]

[a] Reaction time 16 h; solvent: 1,2-dichlorobenzene or 1,2,4-trichlorobenzene, concentration of **1e** (0.4 M). [b] Determined by ^{1}H-NMR analysis. [c] 1,1′-Binaphthalene-2,2′-diyl phosphoric acid. [d] HA replaced by Lewis acid.

Finally, we performed a kinetic study (for the model see ESI page 155†) varying the amounts and concentrations of catalyst (TfOH) *versus* starting iminium salt $\mathbf{1_s}$ and confirmed that the first step of the reaction is reversible non-catalysed, the second step is the diffusion-controlled protonation of intermediate **10**, disabling the reverse reaction to iminium $\mathbf{1_s}$ and enabling the last step, the Friedel–Crafts reaction of **11** to product $\mathbf{2_s}$; rate constants (Scheme 4) were ordered as follows $k_3 > k_2 > k_4 > k_1$.

To conclude, we have developed and described a new cascade reaction based on a nucleophilic [1,2]-alkyl shift of iminium triflate salts followed by an electrophilic aromatic substitution reaction towards new adamantane based heterocycles and amines.

Conflicts of interest

There are no conflicts to declare.

Acknowledgements

This work was supported by the DFG (HR 97/1-1). The authors would like to thank members of the Institute of Organic Chemistry JLU Giessen for their generous and continuous support. Dr. Artur Mardyukov for DFT analysis, Ing. Josef Jeřábek for the computational solution of differential equations in kinetic model, Dr. Mahesh Vishe for manuscript reading and language corrections and Prof. Pavel Kočovský for fruitful discussions.

Notes and references

1 (*a*) A. Štimac, M. Šekutor, K. Mlinarić-Majerski, L. Frkanec and R. Frkanec, *Molecules*, 2017, **22**, 297; (*b*) E. De Clercq, *Nat. Rev. Drug Discovery*, 2006, **5**, 1015–1025; (*c*) T. P. Stockdale and C. M. Williams, *Chem. Soc. Rev.*, 2015, **44**, 7737–7763; (*d*) R. Hrdina, F. M. Metz, M. Larrosa, J.-P. Berndt, Y. Y. Zhygadlo, S. Becker and J. Becker, *Eur. J. Org. Chem.*, 2015, **28**, 6231–6236.
2 K. A. Agnew-Francis and C. M. Williams, *Adv. Synth. Catal.*, 2016, **358**, 675–700.
3 L. Wanka, K. Iqbal and P. R. Schreiner, *Chem. Rev.*, 2013, **113**, 3516–3604.
4 Y. Zhou, A. D. Brittain, D. Kong, M. Xiao, Y. Meng and L. Sun, *J. Mater. Chem. C*, 2015, **3**, 6947–6961.
5 R. Hrdina, *Synthesis*, 2019, **51**, 629–642.
6 C. Grondal, M. Jeanty and D. Enders, *Nat. Chem.*, 2010, **2**, 167–178.
7 (*a*) G. Wagner, *J. Russ. Phys. Chem. Soc.*, 1899, 690; (*b*) H. Meerwein, *Liebigs Ann. Chem.*, 1914, **405**, 129–175; (*c*) L. Birladeanu, *J. Chem. Educ.*, 2000, **77**, 858–863; (*d*) X.-M. Zhang, Y.-Q. Tu, F.-M. Zhang, Z.-H. Chen and S.-H. Wang, *Chem. Soc. Rev.*, 2017, **46**, 2272–2305; (*e*) G. Frenking, *Tetrahedron*, 1984, **40**, 377–379.
8 (*a*) D. Kamakura, H. Todoroki, D. Urabe, K. Hagiwara and M. Inoue, *Angew. Chem., Int. Ed.*, 2020, **59**, 479–486; (*b*) Y. Wang, B. Chen, X. He and J. Gui, *J. Am. Chem. Soc.*, 2020, **142**, 5007–5012; (*c*) S. Zhou, K. Xia, X. Leng and A. Li, *J. Am. Chem. Soc.*, 2019, **141**, 13718–13723; (*d*) M. C. Reis, C. S. López, O. N. Faza and D. J. Tantillo, *Chem. Sci.*, 2019,

10, 2159–2170; (*e*) H. Wu, B. Yang, L. Zhu, R. Lu, G. Li and H. Lu, *Org. Lett.*, 2016, **18**, 5804–5807; (*f*) F. Romanov-Michailidis, L. Guénée and A. Alexakis, *Angew. Chem., Int. Ed.*, 2013, **52**, 9266–9270; (*g*) F. Romanov-Michailidis, L. Guénée and A. Alexakis, *Org. Lett.*, 2013, **15**, 5890–5893.

9 D. J. Cram, *J. Am. Chem. Soc.*, 1949, **71**, 3863–3870.

10 G. Mladenova, L. Chen, C. F. Rodriquez, K. M. Siu, L. J. Johnston, A. C. Hopkinson and E. Lee-Ruff, *J. Org. Chem.*, 2001, **66**, 1109–1114.

11 (*a*) H. J. Schneider, *J. Phys. Org. Chem.*, 2018, **31**, e3846; (*b*) R. Properzi, P. S. Kaib, M. Leutzsch, G. Pupo, R. Mitra, C. K. De, P. R. Schreiner and B. List, *ChemRxiv*, 2019, **1**, DOI: 10.26434/chemrxiv.10887914.v1.

12 (*a*) K. Takeuchi, K. Ikai, M. Yoshida and A. Tsugeno, *Tetrahedron*, 1988, **44**, 5681–5694; (*b*) I. M. Tkachenko, P. A. Mankova, V. B. Rybakov, E. V. Golovin and Y. N. Klimochkin, *Org. Biomol. Chem.*, 2020, **18**, 465–478.

13 G. Tennant, Imines, Nitrones, Nitriles and Isocyanides, in *Comprehensive Organic Chemistry*, ed. D. Barton and W. D. Ollis, Pergamon Press, Oxford, 1979, pp. 387–389.

14 (*a*) M. Schmid, A. S. Grossmann, K. Wurst and T. Magauer, *J. Am. Chem. Soc.*, 2018, **140**, 8444–8447; (*b*) M. Rueping and B. J. Nachtsheim, *Beilstein J. Org. Chem.*, 2010, **6**, 6.

15 V. Pardali, E. Giannakopoulou, A. Konstantinidi, A. Kolocouris and G. Zoidis, *Croat. Chem. Acta*, 2019, **92**, 211–228.

16 E. Torres, R. Fernandez, S. Miquet, M. Font-Bardia, E. Vanderlinden, L. Naesens and S. Vazquez, *ACS Med. Chem. Lett.*, 2012, **3**, 1065–1069.

17 J. Seayad, A. M. Seayad and B. List, *J. Am. Chem. Soc.*, 2006, **128**, 1086–1087.

18 H. L. Goering and R. W. Thies, *J. Am. Chem. Soc.*, 1968, **90**, 2968–2970.

19 J. Y. Mak, R. H. Pouwer and C. M. Williams, *Angew. Chem., Int. Ed.*, 2014, **53**, 13664–13688.

20 R. Hrdina, M. Larrosa and C. Logemann, *J. Org. Chem.*, 2017, **82**, 4891–4899.

21 R. Y. Liu, Y. Yang and S. L. Buchwald, *Angew. Chem., Int. Ed.*, 2016, **55**, 14077–14080.

22 M. A. Gunawan, J.-C. Hierso, D. Poinsot, A. A. Fokin, N. A. Fokina, B. A. Tkachenko and P. R. Schreiner, *New J. Chem.*, 2014, **38**, 28–41.

23 (*a*) K. Muratov, O. I. Afanasyev, E. Kuchuk, S. Runikhina and D. Chusov, *Eur. J. Org. Chem.*, 2019, 6557–6560; (*b*) K. Banert, M. Heck, A. Ihle, J. Kronawitt, T. Pester and T. Shoker, *J. Org. Chem.*, 2018, **83**, 5138–5148; (*c*) N. A. Fokina, B. A. Tkachenko, A. Merz, M. Serafin, J. E. P. Dahl, R. M. K. Carlson, A. A. Fokin and P. R. Schreiner, *Eur. J. Org. Chem.*, 2007, 4738–4745; (*d*) Y. Ganga-Sah, D. B. Leznoff and A. J. Bennet, *J. Org. Chem.*, 2019, **84**, 15276–15282.

24 M. Dobler, H.-J. Borschberg and R. Azerad, *Tetrahedron: Asymmetry*, 1995, **6**, 213–220.

25 S. Wertz and A. Studer, *Green Chem.*, 2013, **15**, 3116–3134.

26 H. Grützmacher and C. M. Marchand, *Coord. Chem. Rev.*, 1997, **163**, 287–344.

27 E. M. Engler, J. D. Andose and P. v. R. Schleyer, *J. Am. Chem. Soc.*, 1973, 805–8025.

28 P. v. R. Schleyer, R. C. Fort, W. E. Watts, M. B. Comisarow and G. A. Olah, *J. Am. Chem. Soc.*, 1964, 4195–4197.

29 For review on the synthesis of heterocycles using Ritter reaction see: J. Bolsakova and A. Jirgensons, *Chem. Heterocycl. Compd.*, 2017, **53**, 1167–1177.

Supporting Information

[1,2]-Rearrangement of Iminium Salts Provides Access to Heterocycles with Adamantane Scaffold

Benjamin Zonker,[a] Ediz Duman,[a] Heike Hausmann,[a] Jonathan Becker[b] and Radim Hrdina*[a]

1. General information

NMR spectra were recorded on 200, 400 or 600 MHz machine at RT (25 °C) unless otherwise stated. ^{1}H-NMR chemical shifts are given in ppm relative to Me_4Si with the solvent resonance used as the internal standard ($CDCl_3$ δ = 7.26 ppm). ^{13}C-NMR (60, 101 or 150 MHz) chemical shifts are given in ppm relative to Me_4Si with the solvent resonance used as the internal standard ($CDCl_3$ = 77.16 ppm). IR spectra were recorded using an ATR sampler and are reported in wave numbers (cm^{-1}). HPLC analysis and semi-preparative separation was performed using Eurospher C18H reverse phase columns. Detection was performed using UV detector at 254 nm. Retention times (t_r) are given in minutes (min). Melting points (m.p.) were measured in open capillary tubes and are uncorrected. All reactions involving air sensitive compounds were carried out under dry and inert atmosphere (N_2 or argon) by means of an inert gas/vacuum double manifold line and standard Schlenk techniques. Flash column chromatography was performed with silicagel 60 as stationary phase. High resolution mass spectra were recorded with Brucker Micro TOF LC.

2. Experimental procedures

2.1 Preparation of starting materials

2.1.1 3-Noradamantane-methanol (9)

Under inert atmosphere, a suspension of $LiAlH_4$ (1.3 g, 2.2 eq., 34 mmol) in dry THF (25 mL) was cooled to 0 °C and 3-noradamantylcarboxylic acid (2.6 g, 1 eq., 16 mmol) in THF (25 mL) was added *via* syringe over 12 minutes. The mixture was allowed to warm to 22 °C while stirring overnight. Then the reaction was cooled to 0 °C and quenched with EtOAc (50 mL), followed by water (60 mL). The phases were separated, the aqueous phase was extracted with of EtOAc (50 mL), the combined organic phases were washed with water and brine, separated and dried over Na_2SO_4 (anhydrous). After filtration the solvent was evaporated to give the crude residue, which was purified by flash column chromatography on silica gel (mobile phase: 7-10% EtOAc in *n*-hexane) to give the desired product as an off-white solid in 88% yield (2.1 g, 13.8 mmol).

R_f (silica gel; EtOAc:n-hexane 1:4): 0.2.

^{1}H NMR: (400 MHz, $CDCl_3$): δ/ppm = 1.49 (s, 1H), 1.57-1.63 (m, 8H), 1.66-1.72 (m, 2H), 2.08-2.12 (m, 1H), 2.24 (m, 2H), 3.63 (s, 2H).

Spectrum in accordance with literature: S. R. Hare, M. Orman, F. Dewan, E. Dalchand, C. Buzard, S. Ahmed, J. C. Tolentino, U. Sethi, K. Terlizzi, C. Houferak, A. M. Stein, A. Stedronsky, D. M. Thamattoor, D. J. Tantillo, D. C. Merrer, *J. Org. Chem.,* 2015, **80**, 5049-5065.

2.1.2 3-Noradamantanecarbaldehyde (26)

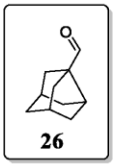

26

Under inert atmosphere, 3-noradamantane-methanol **9** (2.7 g, 1.0 eq., 17.9 mmol) was dissolved in dichloromethane (35 mL) and pyridinium chlorochromate (5.0 g, 1.3 eq., 23.3 mmol) was added portion wise over 10 minutes. The mixture was stirred at 22 °C overnight. Diisopropylether (150 mL) was added and stirred for 10 minutes. The mixture was filtered through a celite/silica pad and the resulting filtrate was evaporated to give the desired product as a white solid in a yield of 86% (2.3 g, 15.4 mmol).

R_f (silica gel; EtOAc:*n*-hexane 1:9): 0.4.

^{1}H NMR (400 MHz, $CDCl_3$) δ/ppm = 1.61-1.62 (m, 2H), 1.64 (m, 2H), 1.66-1.67 (m, 2H), 1.70-1.74 (m, 2H), 2.00-2.03 (m, 2H), 2.35 (m, 2H), 2.58 (m, 1H), 9.73 (s, 1H).

Spectrum in accordance with literature: B. L. Adams and P. Kovacic, *J. Am. Chem. Soc*., 1975, **97**, 2829-2835.

2.1.3 Precursor 18 for synthesis of compound 1l

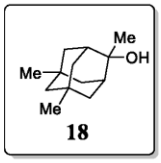

18

Under inert atmosphere, 5,7-dimethyladamantan-2-one[1] (500 mg, 1 eq., 2.8 mmol) was dissolved in dry THF (2 mL) and cooled to 0 °C. MeMgBr in diethyltether (1.5 mL, 3M, 1.4 eq., 3.9 mmol) was added carefully and the reaction was allowed to warm to 22 °C over 2 hours. After cooling to 0 °C, the reaction was quenched with saturated NH_4Cl solution. The aqueous phase was extracted with EtOAc (3x, 30 mL). The combined organic phases were washed with water and brine, dried over Na_2SO_4 (anhydrous), filtered and evaporated *in vacuo* to give 560 mg of yellowish oil as crude residue. Purification by flash column chromatography on silica gel (mobile phase: 5% EtOAc in *n*-hexane) gave a white solid in 93% yield (508 mg, 2.62 mmol).

R_f (silica gel; EtOAc:*n*-hexane 1:9): 0.1.

m.p. (cryst. from EtOAc): 49.6-51.0 °C.

^{1}H NMR (400 MHz, $CDCl_3$): δ/ppm = 0.80 (s, 3H), 0.80 (s, 3H), 1.11 (m, 1H), 1.15 (m, 3H), 1.28-1.33 (m, 6H), 1.57-1.60, (m, 2H) 1.69 (m, 2H), 1.87-1.90 (m, 2H).

^{13}C NMR (101 MHz, $CDCl_3$): δ/ppm = 27.1 (CH_3), 29.7 (C), 30.1 (CH_3), 30.4 (CH_3), 30.4 (C), 39.3 ($2CH_2$), 40.2 (2CH), 41.4 ($2CH_2$), 52.3 (CH_2), 73.1 (C).

IR (neat): $\tilde{\nu}$ /cm^{-1} = 3383, 2913, 2887, 1697, 1454, 1370, 1356, 1174, 1111, 1085, 1035, 354, 907, 882, 620.

HRMS: m/z = 217.1566 ($[M+Na]^+$; calculated for $C_{13}H_{22}NaO^+$ m/z = 217.1563).

[1]Synthesis according to literature procedure: M. Wijtmans, D. Verzijl, C. M. E.van Dam, L. Bosch, M. J. Smit, R. Leurs, I. J. P. de Esch, *Biorg. Med. Chem. Lett*., 2009, 2252-2257.

2.1.4 Precursor 19 for synthesis of compound 1l

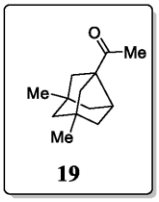

19

Alcohol **18** (530 mg, 1 eq., 2.73 mmol) was dissolved in acetic acid (0.5 mL) and 1,2-dichloroethane (2 mL). The solution was added dropwise to 5% NaOCl (8 mL, *aq.*) at 0 °C. After 5 h the phases were separated, the aqueous phase was extracted with dichloromethane, the combined organic phases were washed with water, dried with brine and Na_2SO_4 (anhydrous). After filtration, the dichloromethane was removed *via* rotary evaporation, 1,2-dichloroethane (2-3 mL) was added and the solution was heated to reflux overnight. The reaction mixture was evaporated to dryness, the resulting yellowish solution was dissolved in MeOH (6 mL), KOH (0.6 g, 3.7 eq., 10.0 mmol) was added and the solution was heated to reflux for 4 hours. The reaction was quenched with water and extracted with *n*-hexane (3x). The organic phases were dried with brine and Na_2SO_4 (anhydrous). After filtration, the solvent was evaporated *in vacuo*. The resulting liquid was purified with flash chromatography on silica gel (mobile phase: 10% EtOAc in *n*-hexane) to give a clear liquid in 55% yield (290 mg, 1.50 mmol).

R_f (silica gel; EtOAc:*n*-hexane 1:9): 0.3.

^{1}H NMR (400 MHz, $CDCl_3$): δ/ppm = 1.00 (s, 6H) 1.28-1.33 (m, 2H), 1.40-1.43 (m, 4H), 1.56-1.61 (m, 2H), 1.77-1.80 (m, 2H), 2.13 (s, 3H), 2.61-2.64 (m, 1H).

^{13}C NMR (101 MHz, $CDCl_3$): δ/ppm = 24.6 ($2CH_3$), 26.5 (CH), 41.9 (2C), 43.8 (CH_3), 49.2 (CH_2), 49.3 ($2CH_2$), 52.0 ($2CH_2$), 63.7 (C), 212.2 (C).

IR (neat): $\tilde{\nu}$ /cm^{-1} = 2946, 2853, 1697, 1457, 1355, 1218, 1158, 948, 913, 889, 599.

HRMS: m/z = 215.1408 ($[M+H]^+$; calculated for $C_{13}H_{20}NaO^+$ m/z = 215.1406).

2.1.5 Precursor 20 for synthesis of compound 1l

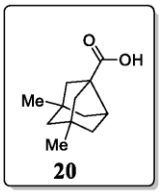

20

Bromine (0.5 mL, 5.3 eq., 9.7 mol) was dissolved at 0-5°C in a solution of NaOH (1.0 g, 13.7 eq., 25.0 mmol) in water (7.2 mL) and dioxane (1.5 mL). To the magnetically stirred solution, ketone **19** (350 mg, 1.0 eq., 1.8 mmol) was added dropwise at 3-5°C. The reaction was allowed to warm to 22 °C overnight. The mixture was acidified with conc. hydrochloric acid and extracted three times with ether. Afterwards the ether portion was extracted with 2M aqueous NaOH (2x) and the basic aqueous layer was acidified with hydrochloric acid. The organic material was extracted with *n*-hexane (3-4x), the extract was dried over Na_2SO_4 (anhydrous) and evaporated to dryness to give a white solid in 70% yield (246 mg, 1.27 mmol).

R_f (silica gel; EtOAc:*n*-hexane 3:7): 0.1.

m.p. (cryst. from $CDCl_3$): 94.0-95.9 °C.

^{1}H NMR (400 MHz, $CDCl_3$): δ/ppm = 1.00 (s, 6H), 1.28-1.31 (m, 2H), 1.37-1.40 (m, 2H), 1.46-1.50 (m, 2H), 1.62-1.66 (m, 2H), 1.88-1.91 (m, 2H), 2.69-2.72 (m, 1H).

^{13}C NMR (101 MHz, $CDCl_3$): δ/ppm = 24.5 ($2CH_3$), 41.9 (2C), 46.0 (CH), 49.0 (CH_2), 49.2 ($2CH_2$), 52.2 ($2CH_2$), 55.5 (C), 184.2 (C).

IR (neat): $\tilde{\nu}$/cm^{-1} =2947, 2864, 1691, 1457, 1415, 1375, 1312, 1271, 1227, 1174, 938, 909, 733.

HRMS: m/z = 217.1197 ([M+Na]$^+$; calculated for $C_{12}H_{18}NaO_2^+$ m/z = 217.1199).

2.1.6 Precursor 21 for synthesis of compound 1l

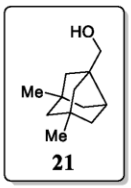

21

Under inert atmosphere, a suspension of $LiAlH_4$ (115 mg, 2.8 eq., 3.03 mmol) in dry THF (5 mL) was cooled to 0 °C and acid **20** (210 mg, 1 eq., 1.08 mmol) in THF (5 mL) was added *via* syringe dropwise. The mixture was stirred for 3 h while warming to 22 °C. The reaction was cooled to 0 °C and quenched with EtOAc and water until no more gas evolution was observed. The phases were separated, the aqueous phase was extracted with EtOAc (3x20 mL), the combined organic phases were washed with water and brine, and dried over Na_2SO_4 (anhydrous). After filtration, the solvent was evaporated to give the desired product as a slightly yellow liquid in 92% yield (179 mg, 1.0 mmol).

R_f (silica gel; EtOAc:*n*-hexane 1:9):0.2.

^{1}H NMR (400 MHz, $CDCl_3$): δ/ppm = 0.97 (s, 6H), 1.24-1.28 (m, 5H), 1.40-1.43 (m, 5H), 1.50-1.54 (m, 2H), 2.10-2.13 (m, 1H), 3.58 (s, 2H).

^{13}C NMR (101 MHz, $CDCl_3$): δ/ppm = 25.0 ($2CH_3$), 41.6 (2C), 42.4 (CH), 49.7 ($2CH_2$), 49.8 (CH_2), 51.7 ($2CH_2$), 53.1 (C), 69.1 (CH_2).

IR (neat): $\tilde{\nu}$/cm^{-1} = 3348, 2943, 2859, 1457, 1373, 1340, 1121, 1102, 1044, 1024, 952, 933, 660, 614.

HRMS: m/z = 203.1409 ($[M+Na]^+$; calculated for $C_{12}H_{20}NaO^+$ m/z = 203.1406).

2.1.7 Precursor 22 for synthesis of compound 1l

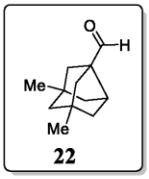

22

Alcohol **21** (2.7 g, 1.0 eq., 17.9 mmol) was dissolved in dichloromethane (35 mL) and pyridinium chlorochromate (5.0 g, 1.3 eq., 23.3 mmol) was added portion wise over 10 minutes. The mixture was stirred at 22 °C overnight. Diisopropylether (150 mL) was added and stirred for 10 minutes. The black mixture was filtered through a celite/silica pad and the resulting filtrate was evaporated to give a white solid in a yield of 86% (2.3 g, 15.4 mmol).

R_f (silica gel; EtOAc:*n*-hexane 1:9): 0.4.

m.p. (cryst. from EtOAc): 72.0-73.6 °C

^{1}H NMR (400 MHz, $CDCl_3$): δ/ppm = 1.02 (s, 6H), 1.29-1.35 (m, 4H), 1.42-1.45 (m, 2H), 1.54-1.59 (m, 2H), 1.81-1.84 (m, 2H), 2.56-2.60 (m, 1H), 9.67 (s, 1H).
^{13}C NMR (101 MHz, $CDCl_3$): δ/ppm = 24.5 ($2CH_3$), 42.0 (2C), 43.4 (CH), 49.1 ($2CH_2$), 49.2 ($2CH_2$), 49.6 (CH_2), 62.3 (C), 204.7 (C).

IR (neat): $\tilde{\nu}$/cm^{-1} = 2894, 2840, 1700, 1453, 1374, 1355, 1159, 1120, 1066, 963, 850.

HRMS: m/z = 201.1251 ($[M+Na]^+$; calculated for $C_{12}H_{18}NaO^+$ m/z = 201.1250).

2.1.8 Precursor 23 for synthesis of compound 1m

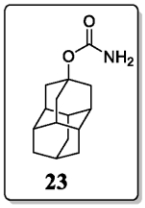

23

4-Hydroxydiamantane[2] (500 mg, 1 eq., 2.5 mmol) was dissolved in dry dichloromethane (8 mL) and cooled to 0 °C. Trichloroacetylisocyanate (343 µL, 1.2 eq., 2.9 mmol) was added and the reaction mixture was stirred at 22 °C for 2 hours. The solvent was removed *in vacuo* and the residue was dissolved in MeOH (15 mL) and treated with a saturated potassium carbonate solution (25 mL). The reaction mixture was stirred at 50°C for 24 hours after which the MeOH was removed *in vacuo*. The white precipitate was filtered and washed with water and dried to give clear colourless crystals in a yield of 87% (540 mg, 2.2 mmol).

R_f (silica gel; MeOH:CH_2CL_2 1:9): 0.6.

m.p. (cryst. from): 196.4-197.7 °C.

^{1}H NMR (400 MHz, CD_2Cl_2) δ/ppm = 1.74 (m, 10H), 1.95 (m, 3H), 2.05 (m, 6H), 4.52 (bs, 2H).

^{13}C NMR (101 MHz, CD_2Cl_2): δ/ppm = 26.3 (CH), 37.2 (3CH), 37.7 ($3CH_2$), 40.4 (3CH), 42.4 ($3CH_2$), 79.1 (C), 156.5 (C).

IR (neat): $\tilde{\nu}$/cm^{-1} 3508, 3446, 3313, 2877, 2847, 1713, 1603, 1448, 1374, 1332, 1284, 1246, 1131, 1085, 1045, 984, 889, 880, 801, 784, 741, 704, 617, 540, 503, 452.

HRMS: m/z = 270.1461 ($[M+Na]^+$; calculated for $C_{15}H_{21}NNaO_2^+$ m/z = 270.1465).

[2]Synthesis according to literature procedure: N. A. Fokina, B. A. Tkachenko, A. Merz, M. Serafin, J. E. P. Dahl, R. M. K. Carlson, A. A. Fokin, P. R. Schreiner, *Eur. J. Org Chem.,* 2007, 4738-4745.

2.1.9 Precursor 24 for synthesis of compound 1m

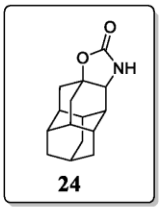

24

Carbamate **23** (494 mg, 1 eq., 2 mmol) was dissolved in dry 1,2-dichloroethane (12 mL) and iodobenzene diacetate (850 mg, 1.3 eq., 2.6 mmol), MgO (200 mg, 2.5 eq., 5 mmol) and rhodium diacetate dimer (9 mg, 0.03 eq., 0.05 mmol) were added. The reaction mixture was heated to 70 °C for 18 h, filtered and the solvent was removed *in vacuo*. Flash column chromatography on silica gel (mobile phase: 33% EtOAc in *n*-hexane) gave a colourless solid in a yield of 60% (300 mg, 1.2 mmol).

R_f (silica gel; MeOH:CH_2CL_2 1:9): 0.6.

m.p. (cryst. from EtOAc): 199.0-202.0 °C.

^{1}H NMR (400 MHz, CD_2Cl_2) δ/ppm = 1.68-1.84 (m, 10H), 1.92-2.04 (m, 4H), 2.09-2.15 (m, 3H), 3.56 (m, 1H), 5.24 (bs, 1H).

^{13}C NMR (101 MHz, CD_2Cl_2) δ = 26.5 (CH), 31.1 (CH), 36.4 (CH_2), 37.2 (CH_2), 37.3 (CH), 37.6 (CH), 37.6 (CH_2), 37.9 (CH_2), 38.9 (CH), 40.5 (CH&CH_2), 40.8 (CH), 65.4 (CH), 80.3 (C), 161.4 (C).

IR (neat): $\tilde{\nu}$/cm^{-1} = 3235, 2879, 1743, 1630, 1461, 1439, 1369, 1323, 1304, 1291, 1266, 1241, 121, 1188, 1123, 1093, 1075, 1041, 1013, 971, 950, 932, 899, 824, 779, 765, 123, 697, 664, 615, 570, 546, 472.

HRMS: m/z =268.1305 ([M+Na]$^+$; calculated for $C_{15}H_{19}NNaO_2^+$ m/z =268.1308).

2.1.10 Precursor 25 for synthesis of compound 1m

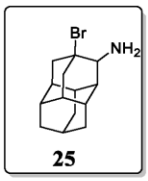

25

Precusor **24** (350 mg, 1 eq., 1.4 mmol) and KBr (340 mg, 2. eq., 2.8 mmol) were suspended in dry dichloromethane (5 mL), and TfOH (1070 mg, 4 eq., 5.7 mmol) was added dropwise to the reaction mixture at 22 °C. The reaction mixture was heated to 40 °C for 18 h. The reaction mixture was quenched and neutralized using a 10% NaOH (*aq.*). The product was extracted using EtOAc, the combined organic phases were washed with water and brine, dried over Na_2SO_4 (anhydrous) and solvent was evaporated *in vacuo*. Flash column chromatography on silica gel (mobile phase: 5% MeOH (1% NH_3 (*aq.*)) in CH_2Cl_2) gave a colourless non-crystalline solid in a yield of 66 % (265 mg, 0.9 mmol).

R$_f$ (silica gel; MeOH (1% NH_3 *aq.*):CH_2CL_2 5:95): 0.4.

^{1}H NMR (400 MHz, $CDCl_3$): δ/ppm = 1.62-1.72 (m, 6H), 1.79-1.88 (m, 7H), 2.00-2.08 (m, 3H), 2.35 (dt, *J* = 12.5, 3.0 Hz, 1H), 2.45 (dd, *J* = 12.5, 3.0 Hz, 1H), 2.62 (dt, *J* = 12.5, 3.0 Hz, 1H), 3.14 (m, 1H).

^{13}C NMR (101 MHz, $CDCl_3$): δ/ppm = 26.0 (CH), 29.7 (CH), 36.2 (CH), 36.7 (CH_2), 36.9 ($2CH_2$), 37.6 (CH), 41.2 (CH), 41.4 (CH), 42.9 (CH_2), 46.1 (CH), 49.7 (CH_2), 62.8 (CH), 74.7 (C).

IR (neat): $\tilde{\nu}$/cm^{-1} = 2901, 2849, 1634, 1459, 1440, 1316, 1243, 1065, 1028, 961, 814, 789, 698, 654, 638, 533, 509.

HRMS: m/z = 282.0849 ($[M+H]^+$; calculated for $C_{14}H_{21}BrN^+$ m/z = 282.0852).

2.2 NMR spectra of starting materials

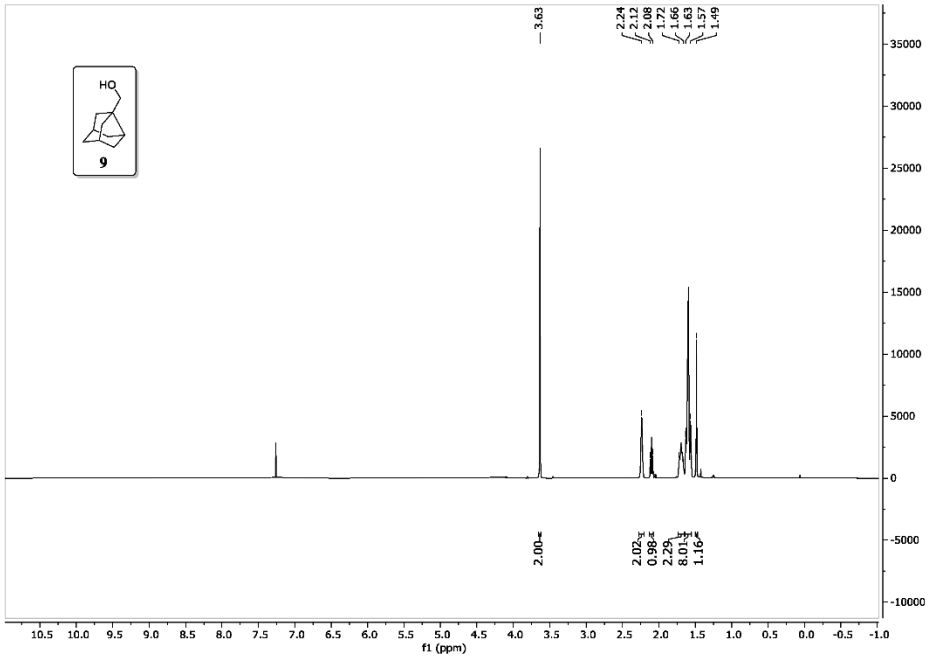
HO
9
3.63
2.24
2.12
2.08
1.72
1.66
1.63
1.57
1.49
2.00
2.02
0.98
2.29
8.01
1.16
f1 (ppm)

S17

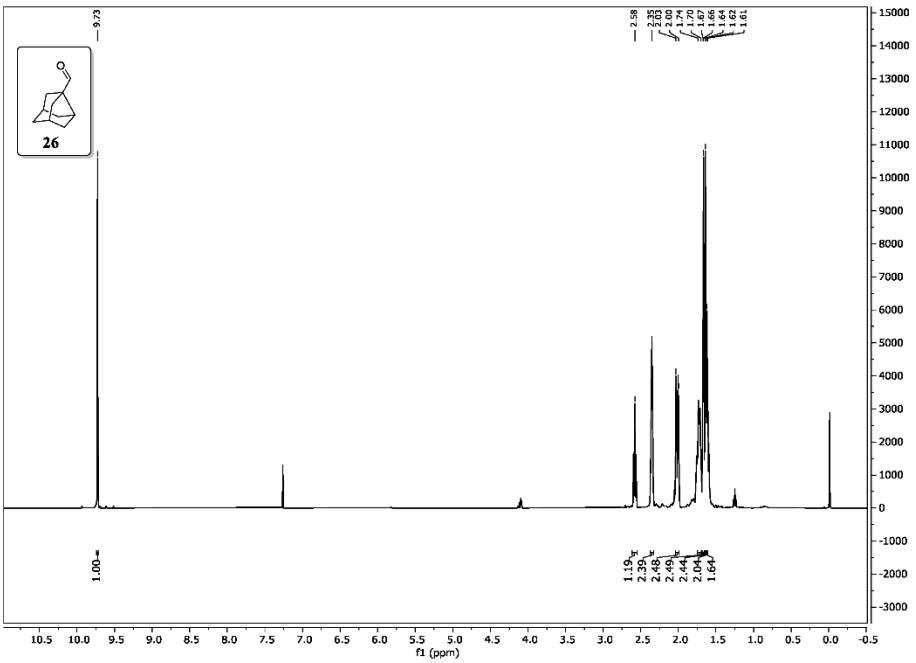
O
26
9.73
2.58
2.35
2.30
2.00
1.74
1.70
1.67
1.66
1.64
1.62
1.61
1.00
1.19
2.39
2.48
2.49
2.44
2.04
1.64
f1 (ppm)

S18

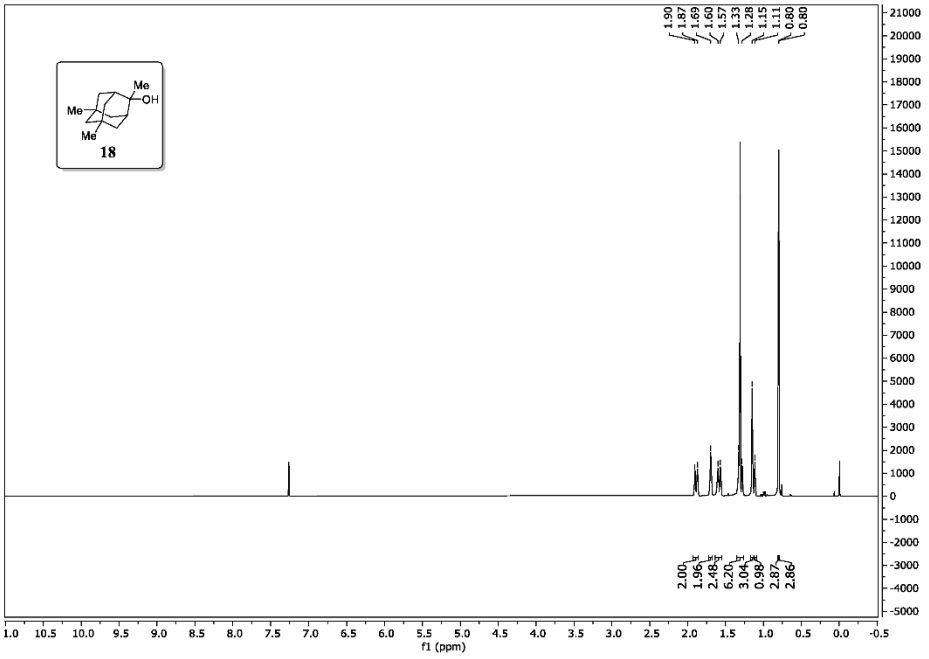
Me
OH
Me
Me
18
1.90
1.87
1.69
1.60
1.57
1.33
1.28
1.15
1.11
0.80
0.80
2.00
1.96
2.48
6.20
3.04
0.98
2.87
2.86
f1 (ppm)

S19

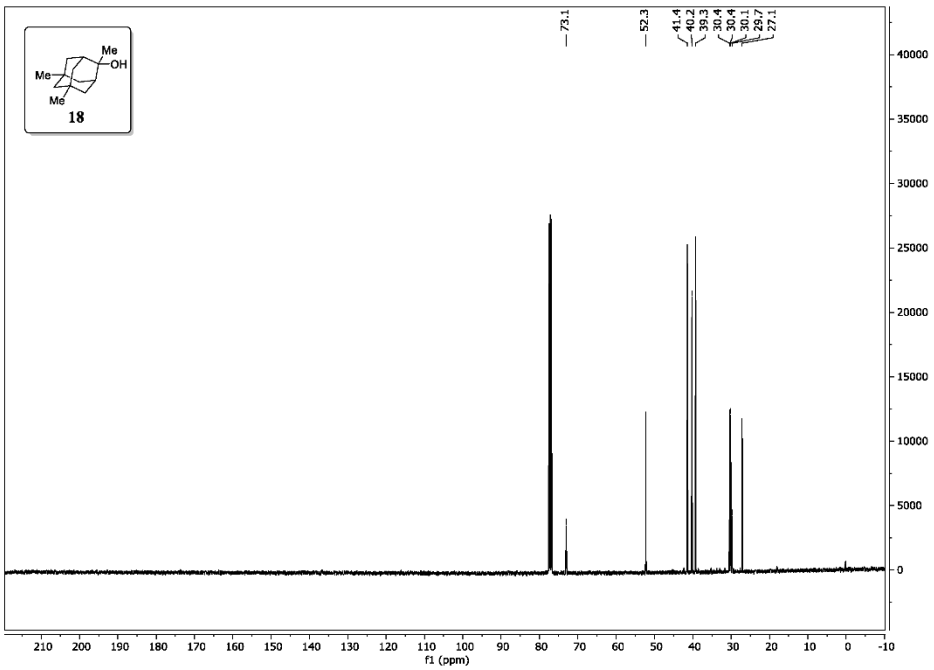
Me
OH
Me
Me
18
73.1
52.3
41.4
40.2
39.3
30.4
30.4
30.1
29.7
27.1
f1 (ppm)

S20

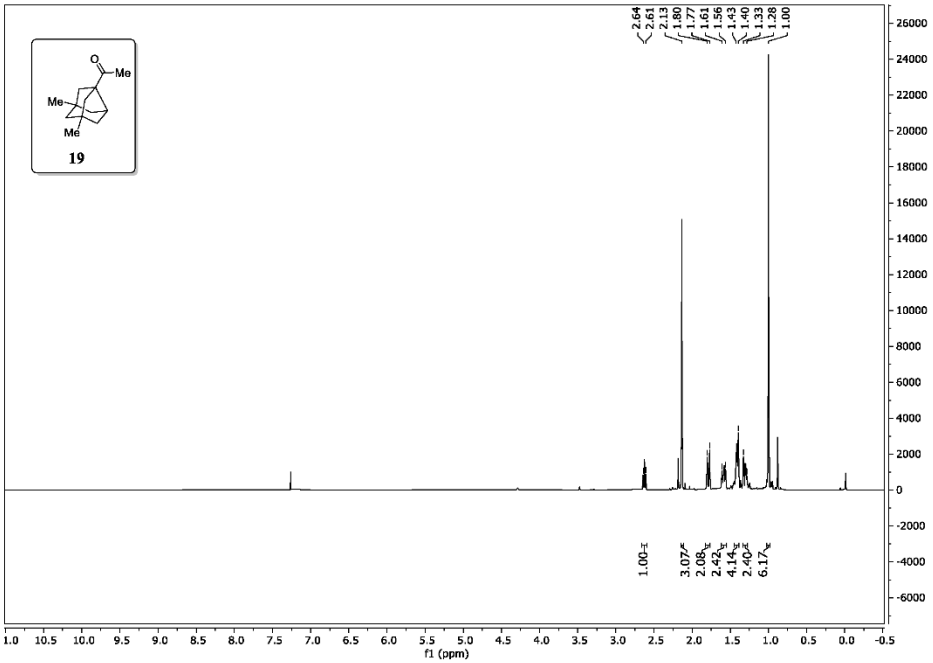
2.64
2.61
2.13
1.80
1.77
1.61
1.56
1.43
1.40
1.33
1.28
1.00
Me
Me
Me
19
1.00
3.07
2.08
2.42
4.14
2.40
6.17
f1 (ppm)

S21

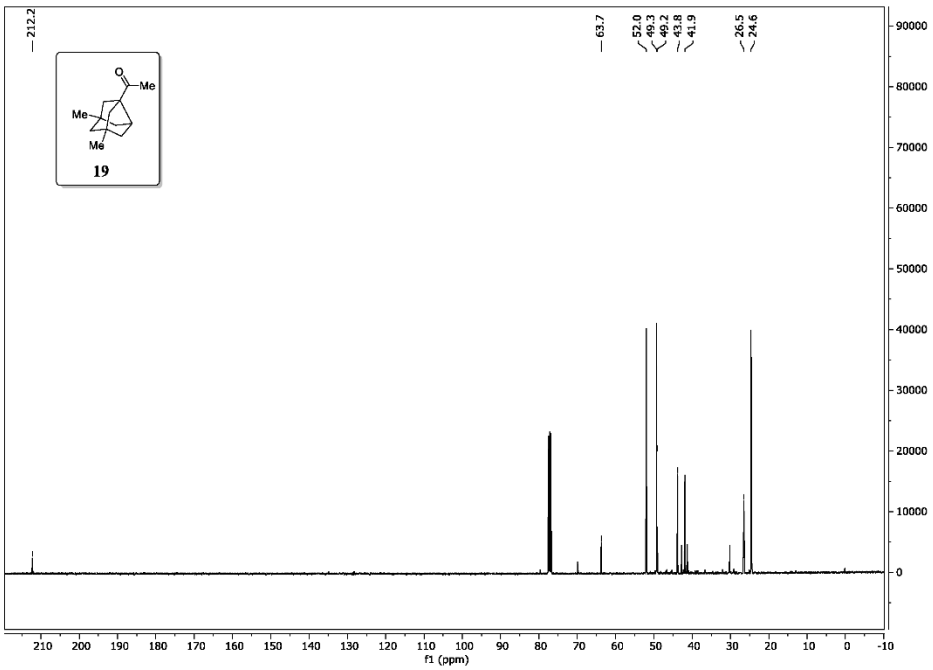
212.2
63.7
52.0
49.3
49.2
43.8
41.9
26.5
24.6
Me
Me
Me
19
f1 (ppm)

S22

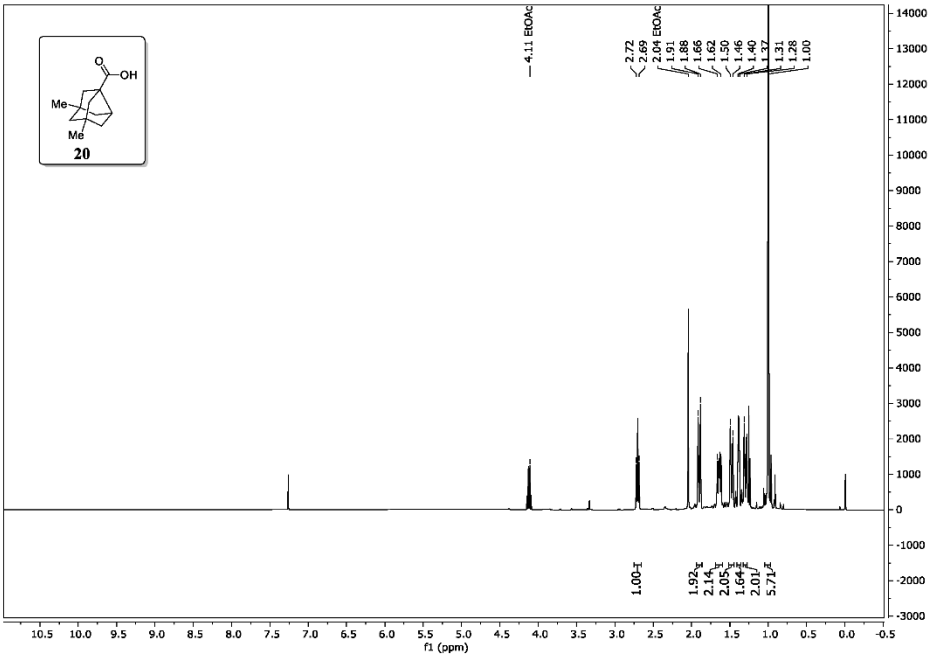
4.11 EtOAc
2.72
2.69
2.04 EtOAc
1.91
1.88
1.66
1.62
1.50
1.46
1.40
1.37
1.31
1.28
1.00
OH
Me
Me
20
1.00
1.92
2.14
2.05
1.64
2.01
5.71
f1 (ppm)

S23

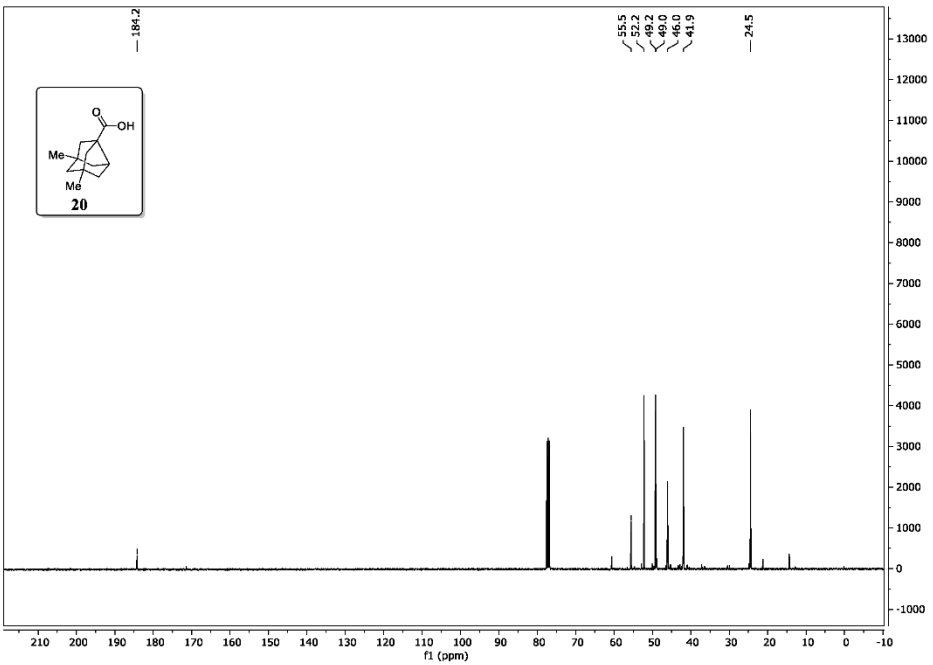
184.2
55.5
52.2
49.2
49.0
46.0
41.9
24.5
OH
Me
Me
20
f1 (ppm)

S24

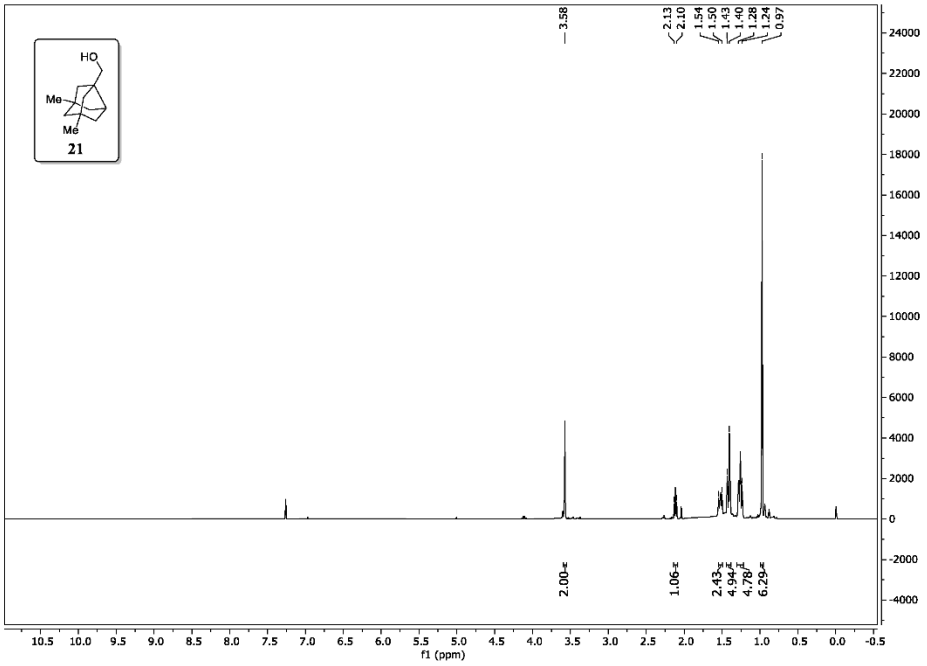
HO
Me
Me
21
3.58
2.13
2.10
1.54
1.50
1.43
1.40
1.28
1.24
0.97
2.00
1.06
2.43
4.94
4.78
6.29
f1 (ppm)

S25

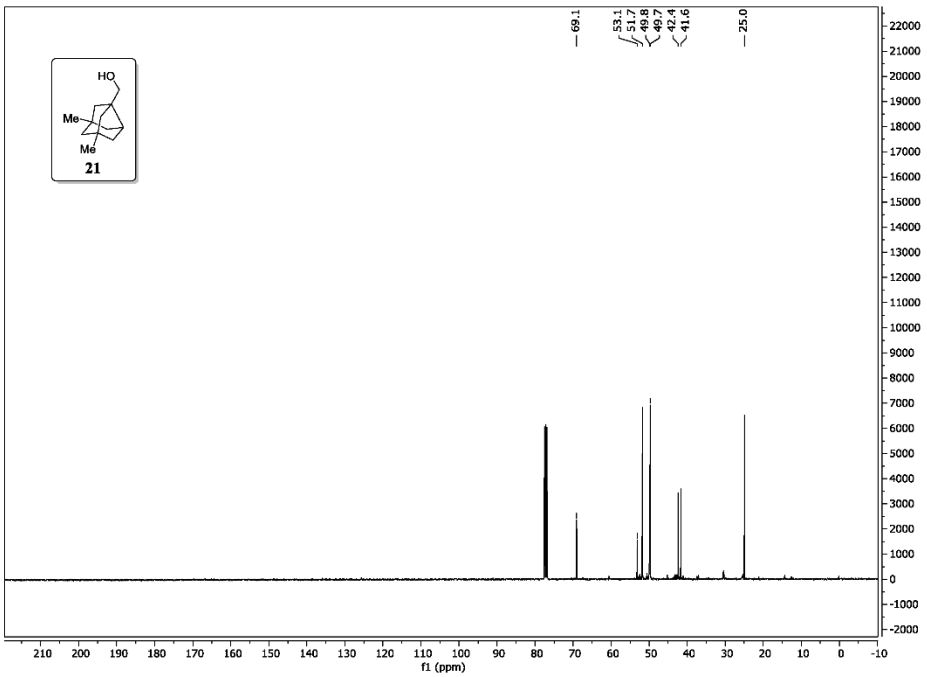
HO
Me
Me
21
69.1
53.1
51.7
49.8
49.7
42.4
41.6
25.0
f1 (ppm)

S26

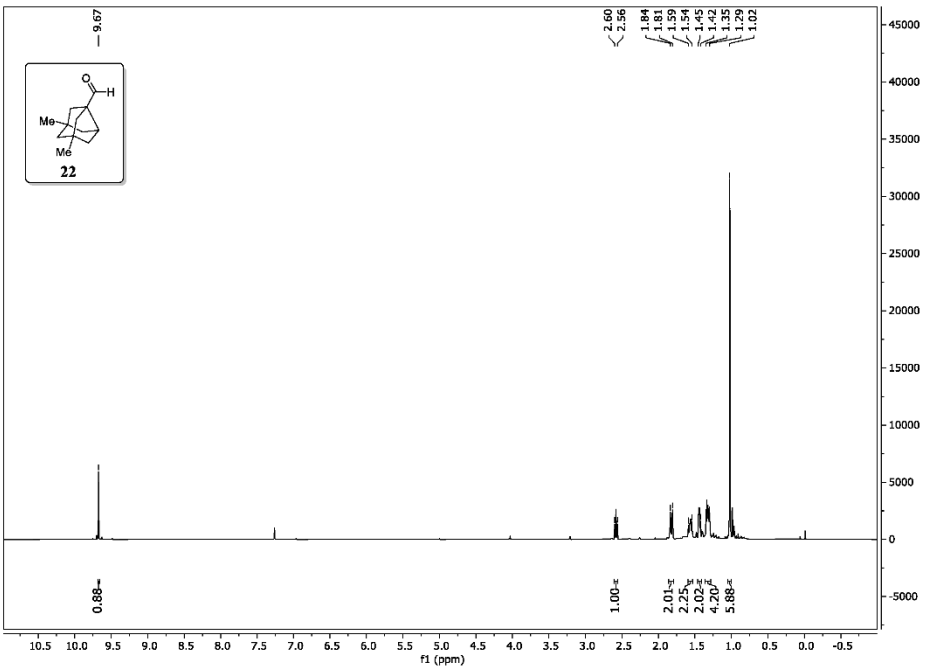
9.67
2.60
2.56
1.84
1.81
1.59
1.54
1.45
1.42
1.35
1.29
1.02
O
H
Me
Me
22
0.88
1.00
2.01
2.25
2.02
4.20
5.88
f1 (ppm)

S27

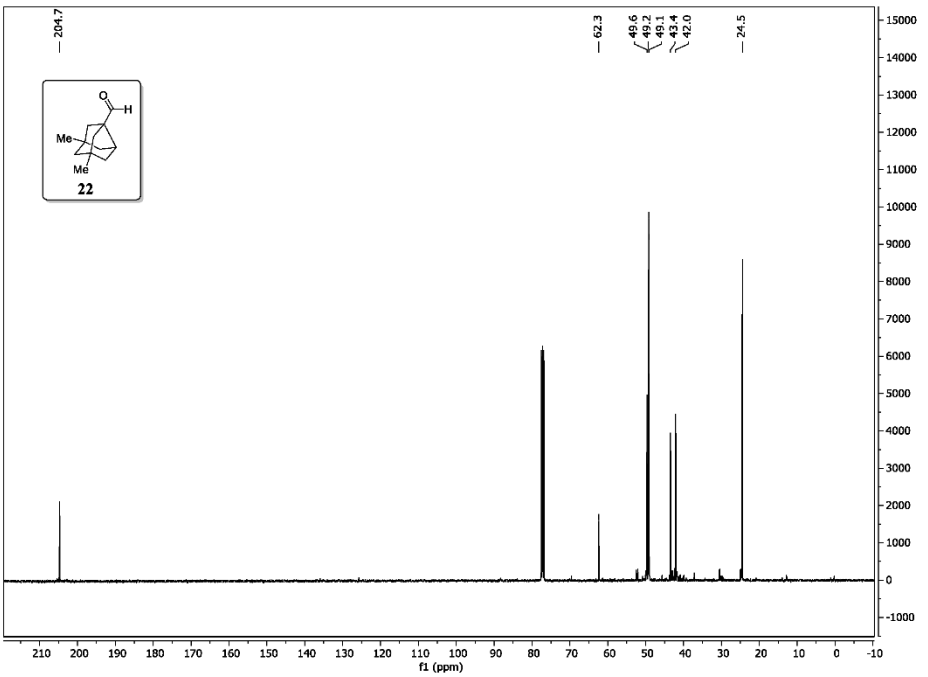
204.7
62.3
49.6
49.2
49.1
43.4
42.0
24.5
O
H
Me
Me
22
f1 (ppm)

S28

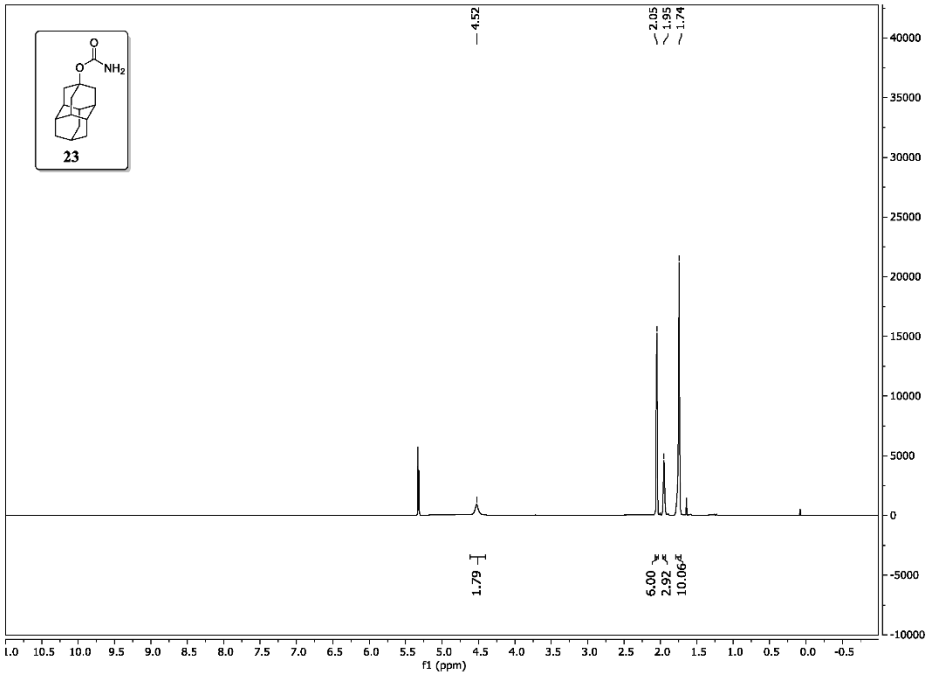
4.52
2.05
1.95
1.74
23
1.79
6.00
2.92
10.06
f1 (ppm)

S29

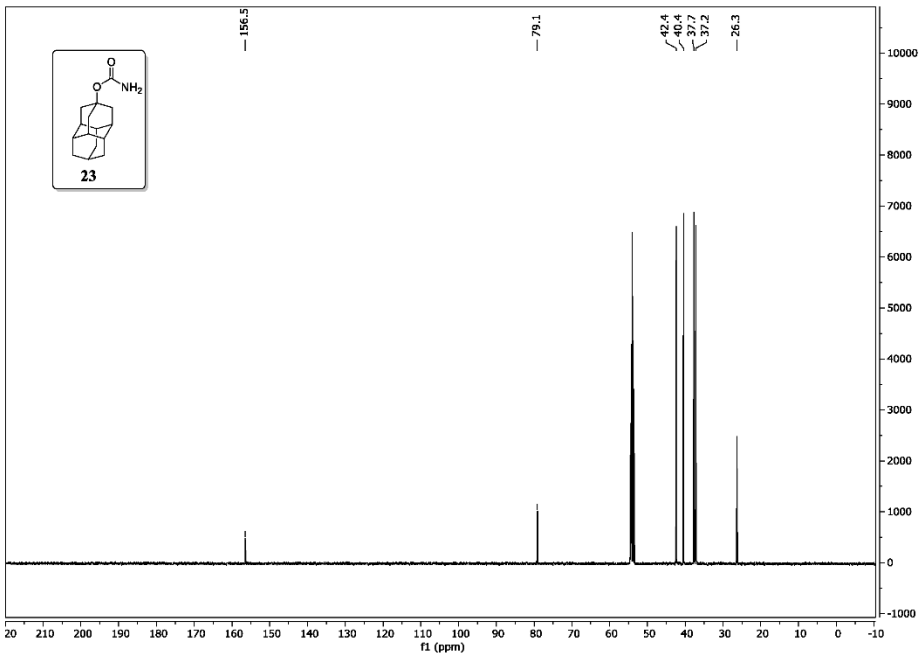
156.5
79.1
42.4
40.4
37.7
37.2
26.3
23
f1 (ppm)

S30

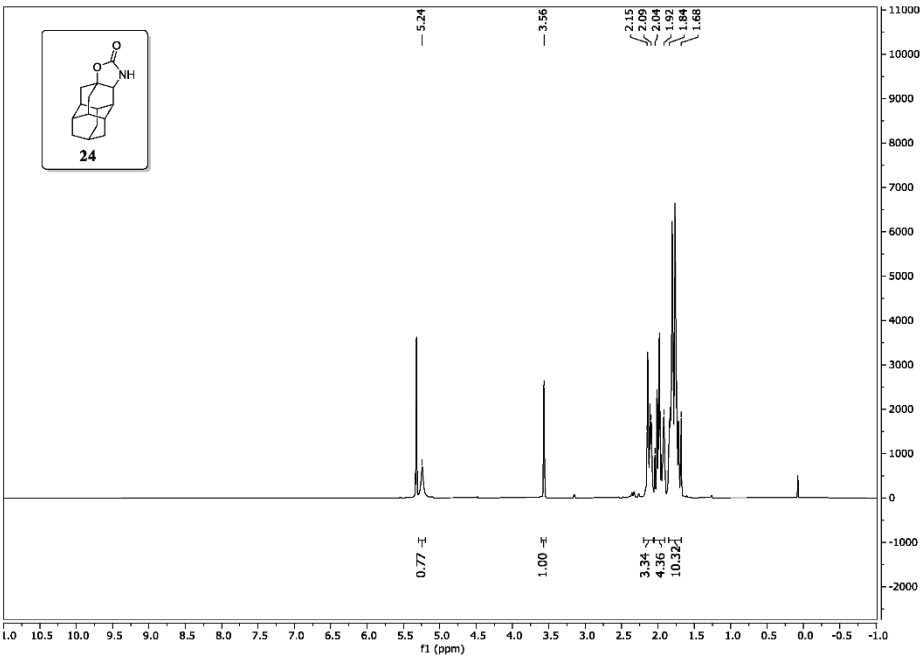
24
5.24
3.56
2.15
2.09
2.04
1.92
1.84
1.68
0.77
1.00
3.34
4.36
10.32
f1 (ppm)

S31

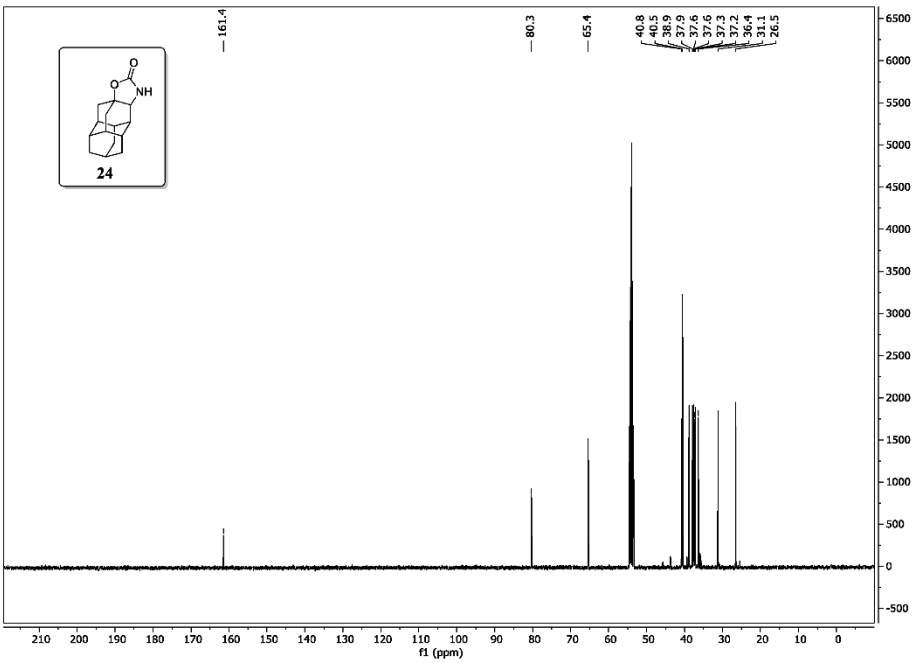
24
161.4
80.3
65.4
40.8
40.5
38.9
37.9
37.6
37.6
37.3
37.2
36.4
31.1
26.5
f1 (ppm)

S32

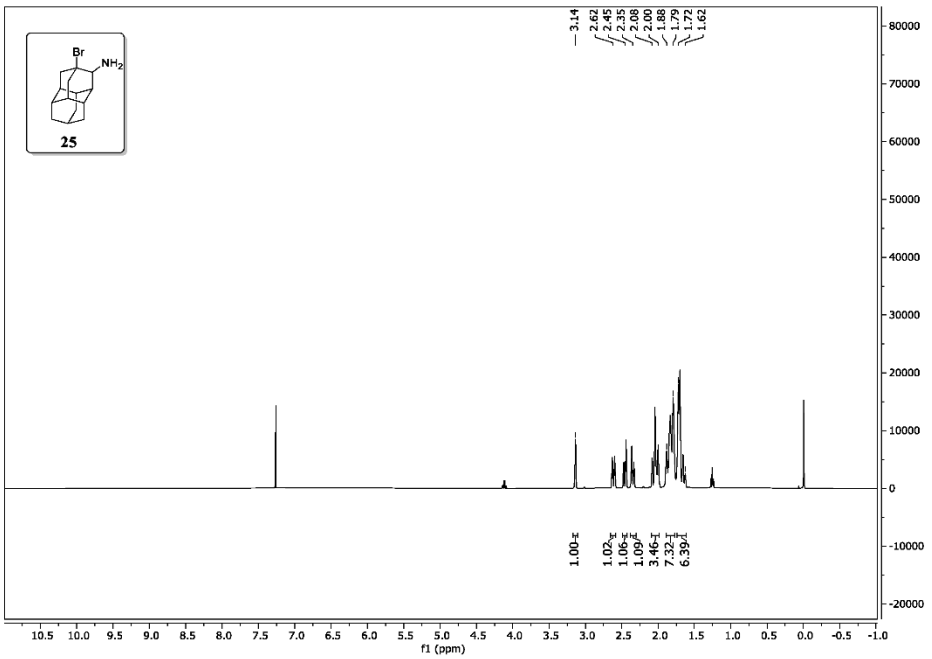
Br
NH2
25
3.14
2.62
2.45
2.35
2.08
2.00
1.88
1.79
1.72
1.62
1.00
1.02
1.06
1.09
3.46
7.32
6.39
f1 (ppm)

S33

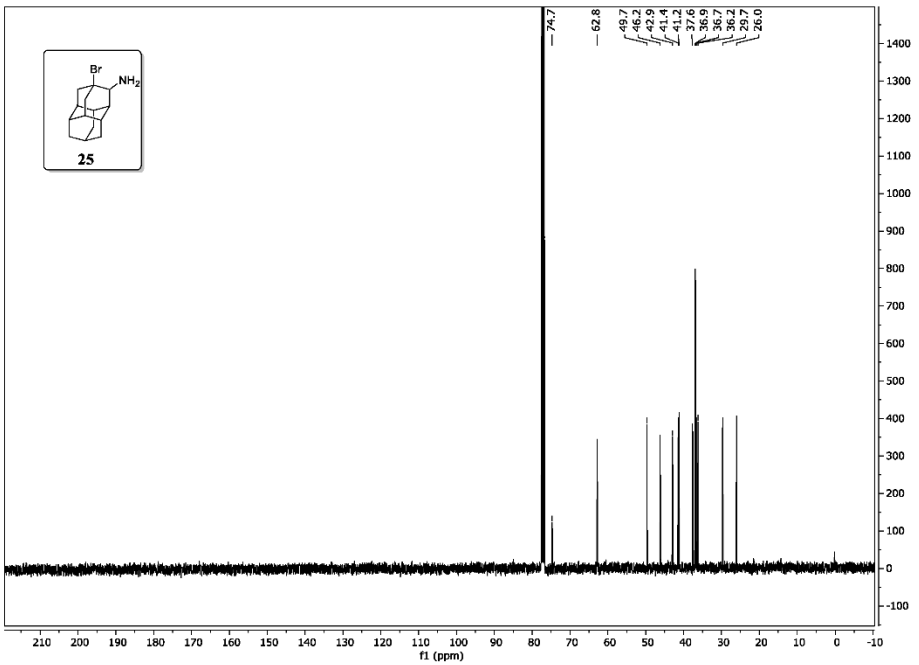
Br
NH2
25
74.7
62.8
49.7
46.2
42.9
41.4
41.2
37.6
36.9
36.7
36.2
29.7
26.0
f1 (ppm)

S34

2.3 Synthesis of imines **1a-o**, **3a-c**, salt $\mathbf{1e_s}$ and $\mathbf{3d_s}$

2.3.1 General procedure A for synthesis of 1a-1o and 3a-3d

Under inert atmosphere, 1.0 equivalent of corresponding aldehyde and 7 equivalents of Na_2SO_4 (anhydrous) were suspended in dry CH_2Cl_2 (4 mL per 1mmol of aldehyde), 1.1-1.7 equivalents of corresponding amine were added and the suspension was stirred at 22 °C overnight. The reaction mixture was filtered through a glass frit and the solvent and the excess of amine was evaporated in *vacuo*. The product was used in the next step without further purification.

2.3.2 Synthesis of imine 1a

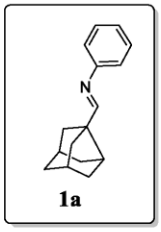

1a

Compound **1a** was synthesized according to *general procedure A* (1.7 eq. of amine) and was used in the next step without further purification.

^{1}H NMR: (400 MHz, $CDCl_3$): δ 1.63-1.71 (m, 4H), 1.77-1.86 (m, 4H), 2.06-2.09 (m, 2H), 2.36 (m, 2H), 2.50-2.54 (m, 1H), 7.03-7.05 (m, 2H), 7.14-7.18 (m, 1H), 7.30-7.34 (m, 2H), 7.95 (s, 1H).

2.3.3 Synthesis of imine 1b

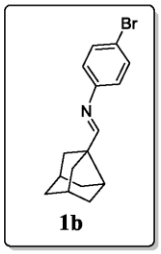

1b

Compound **1b** was synthesized according to *general procedure A* (1.2 eq. of amine) and was used in the next step without further purification.

^{1}H NMR (400 MHz, $CDCl_3$): δ/ppm = 1.59-1.85 (m, 10H), 2.03-2.06 (m, 2H), 2.35 (m, 2H), 2.49-2.52 (m, 1H), 6.89-6.93 (m, 2H), 7.41-7.44 (m, 2H), 7.92 (s, 1H).

2.3.4 Synthesis of imine 1c

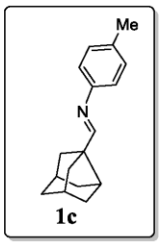

1c

Compound **1c** was synthesized according to *general procedure A* (1.2 eq. of amine) and was used in the next step without further purification.

^{1}H NMR (200 MHz, $CDCl_3$): δ/ppm = 1.63-1.88 (m, 8H), 2.05-2.10 (m, 2H), 2.34 (m, 5H), 2.48-2.53 (m, 1H), 6.94-6.98 (m, 2H), 7.11-7.15 (m, 2H), 7.95 (s, 1H).

2.3.5 Synthesis of imine 1d

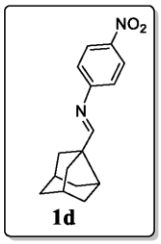

1d

Compound **1d** was synthesized according to *general procedure A* (1.2 eq. of amine) and was used in the next step without further purification.

^{1}H NMR (200 MHz, $CDCl_3$): δ/ppm = 1.61-1.79 (m, 8H), 1.99-2.05 (m, 2H), 2.36 (m, 2H), 2.55-2.61 (m, 1H), 6.60-6.64 (m, 2H), 8.04-8.08 (m, 2H), 9.73 (s, 1H).

2.3.6 Synthesis of imine 1e

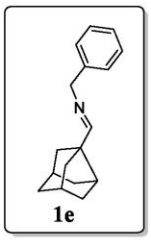

1e

Compound **1e** was synthesized according to *general procedure A* (1.7 eq. of amine) and was used in the next step without further purification.

^{1}H NMR (400 MHz, $CDCl_3$): δ/ppm = 1.61-1.66 (m, 4H), 1.71-1.80 (m, 4H), 1.97-1.99 (m, 2H), 2.30 (m, 2H), 2.42 (m, 1H), 4.62 (s, 2H), 7.23-7.26 (m, 3H), 7.30-7.34 (m, 2H), 7.90 (s, 1H).

2.3.7 Synthesis of imine 1f

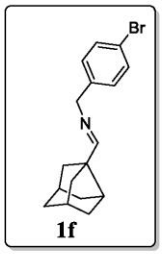

1f

Compound **1f** was synthesized according to *general procedure A* (1.2 eq. of amine) and was used in the next step without further purification.

^{1}H NMR (400MHZ, $CDCl_3$): δ/ppm = 1.61-1.80 (m, 8H) 1.95-1.98 (m, 2H), 2.30 (m, 2H), 2.39-2.43 (m, 1H), 4.54 (s, 2H), 7.11-7.13 (m, 2H), 7.41-7.43 (m, 2H), 7.89 (s, 1H).

2.3.8 Synthesis of imine 1g

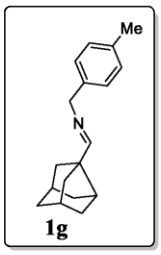

Compound **1g** was synthesized according to general procedure A (1.5 eq. of amine) and was used in the next step without further purification.

^{1}H NMR (400MHZ, $CDCl_3$): δ/ppm = 1.61-1.81 (m, 8H), 1.96-1.99 (m, 2H), 2.30 (m, 2H), 2.33 (s, 3H), 2.40-2.43 (m, 1H), 4.58 (s, 2H), 7.11-7.16 (m, 4H), 7.88 (s, 1H).

2.3.9 Synthesis of imine 1h

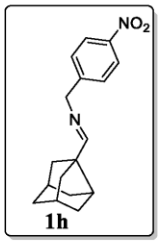

Compound **1h** was synthesized according to *general procedure A* (1.2 eq. of amine as hydrochloride) and was used in the next step without further purification.

^{1}H NMR (400MHZ, $CDCl_3$): δ/ppm = 1.62-1.68 (m, 4H), 1.73-1.80 (m, 4H), 1.98-2.01 (m, 2H), 2.32 (m, 2H), 2.43-.2.46 (m, 1H), 4.70 (s, 2H), 7.44-7.46 (m, 2H), 7.98 (s, 1H), 8.17-8.19 (m, 2H).

2.3.10 Synthesis of imine 1i

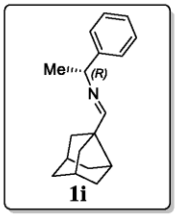

1i

Compound **1i** was synthesized according to *general procedure A* (1.1 eq. of amine) and was used in the next step without further purification.

^{1}H NMR (600 MHz, $CDCl_3$): δ/ppm = 1.48 (d, J = 6.7 Hz, 3H), 1.59-1.82 (m, 8H), 1.97 (m, 2H), 2.29 (m, 2H), 2.38 (m, 1H), 4.33 (q, J = 6.7 Hz, 1H), 7.21-7.23 (m, 1H), 7.30-7.36 (m, 4H), 7.87 (s, 1H).

2.3.11 Synthesis of imine 1j

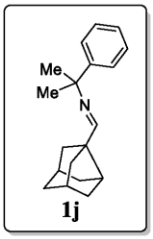

1j

Compound **1j** was synthesized according to *general procedure A* (1.2 eq. of amine) and was used in the next step without further purification.

^{1}H NMR (400 MHz, $CDCl_3$) δ/ppm = 1.51 (s, 6H), 1.59-1.79 (m, 9H), 1.95-1.98 (m, 2H), 2.29 (m, 2H), 2.32-2.36 (m, 1H), 7.18-7.21 (m, 1H), 7.29-7.32 (m, 2H), 7.36-7.38 (m, 2H), 7.72 (s, 1H).

2.3.12 Synthesis of imine 1k

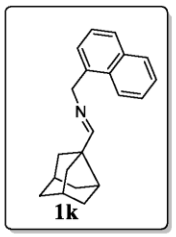

Compound **1k** was synthesized according to *general procedure A* (1.1 eq. of amine) and was used in the next step without further purification.

^{1}H NMR (400 MHz, $CDCl_3$): δ/ppm = 1.61-1.80 (m, 8H), 1.98-2.01 (m, 2H), 2.30 (m, 2H), 2.39-2.42 (m, 1H), 5.08 (s, 2H), 7.41-7.53 (m, 3H), 7.76-7.78 (m, 1H), 7.85- 7.88 (m, 1H), 7.93 (m, 1H), 8.01-8.03 (m, 1H).

2.3.13 Synthesis of imine 1l

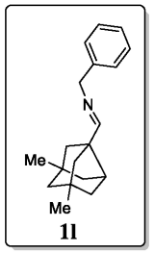

Compound **1l** was synthesized according to *general procedure A* (1.7 eq. of amine) and was used in the next step without further purification.

^{1}H NMR (400 MHz, $CDCl_3$): δ/ppm = 1.02 (s, 6H), 1.29-1.33 (m, 2H), 1.41 (m, 1H), 1.44 (m, 3H), 1.60-1.65 (m, 2H), 1.80-1.82 (m, 2H), 2.43-2.46 (m, 1H), 4.61 (s, 2H), 7.22-7.27 (m, 3H), 7.31-7.35 (m, 2H), 7.87 (s, 1H).

2.3.14 Synthesis of iminium $1m_s$

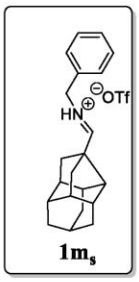

$1m_s$

1-Bromo-2-aminodiamantane **25** (238 mg,1. eq., 0.8 mmol) was dissolved in dry THF (1.7 mL) and K_2CO_3 (140 mg, 1.2 eq., 1.0 mmol) and benzyl bromide (159 mg, 1.1 eq., 0.9 mmol) were added and heated to 50 °C overnight. The reaction was quenched with water and extracted with EtOAc (2x). The combined organic phases were dried over Na_2SO_4 (anhydrous), filtered and the solvent was removed *in vacuo*. 90 mg of the crude mixture were dissolved in dry 1,2-dichlorobenzene (2.4 mL) and silver triflate (68 mg, 1.1 eq., 0.3 mmol) was added while stirring. Immediate precipitation of a white solid was observed. After 30 min, the mixture was filtered, washed with dichloromethane, the solvent was evaporated *in vacuo.* The crude residue was used in the next step without further purification.

^{1}H NMR (400 MHz, CDCl3): δ/ppm = 1.72-2.01 (m, 13H), 2.10 (m, 1H), 2.16 (m, 2H), 2.46 (m,1H), 4.99 (d, *J* = 4.3 Hz, 2H) 7.37-7.40 (m, 2H), 7.45-7.48 (m, 3H), 8.02 (d, *J* = 4.3 Hz, 1H), 12.52 (bs, 1H).

2.3.15 Synthesis of imine 1n

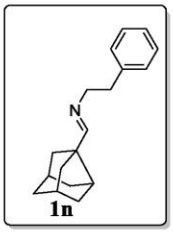

1n

Compound **1n** was synthesized according to *general procedure A* (1.2 eq. of amine) and was used in the next step without further purification.

^{1}H NMR: (400 MHz, $CDCl_3$): δ/ppm = 1.55-1.65 (m, 7H), 1.68-1.72 (m, 2H), 1.82-1.85(m, 2H), 2.16-2.20 (m, 1H), 2.26 (m, 2H), 2.91 (t, *J* = 7.1 Hz, 2H), 3.64 (t, *J* = 7.1 Hz, 2H), 7.14-7.19 (m, 2H), 7.24-7.28 (m, 2H), 7.49 (s, 1H).

2.3.16 Synthesis of imine 1o

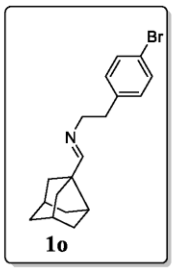

1o

Compound **1o** was synthesized according to *general procedure A* (1.2 eq. of amine) and was used in the next step without further purification.

^{1}H NMR (400 MHz, $CDCl_3$): δ/ppm = 1.57-1.72(m, 8H), 1.82-1.85 (m, 2H), 2.18-2.21 (m, 1H), 2.26 (m, 2H), 3.60 (td, *J* = 7.0, 1.0 Hz, 1H), 2.86 (t, *J* = 7.0 Hz, 1H), 7.00-7.04 (m, 2H), 7.36-7.39 (m, 2H), 7.50 (s, 1H).

2.3.17 Synthesis of imine 3a

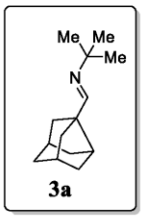

3a

Compound **3a** was synthesized according to *general procedure A* (1.7 eq. of amine) and was used in the next step without further purification.

^{1}H NMR (400 MHz, $CDCl_3$): δ/ppm = 1.16 (s, 9H), 1.57-1.68 (m, 9H), 1.73-1.79 (m, 2H), 1.87-1.91 (m, 2H), 2.27 (m, 1H), 7.71 (s, 1H).

2.3.18 Synthesis of imine 3b

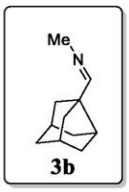

3b

Compound **3b** was synthesized according to *general procedure A* (1.7 eq. of amine) and was used in the next step without further purification.

^{1}H NMR (400 MHz, $CDCl_3$): δ/ppm = 1.59-1.68 (m, 7H), 1.73-1.78 (m, 2H), 1.89-1.91 (m, 2H), 2.28 (m, 2H), 2.36 (m, 2H), 3.28(s, 1H), 7.77(s, 1H).

2.3.19 Synthesis of imine 3c

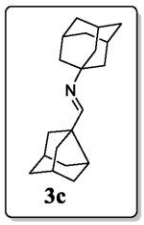

3c

Compound **3c** was synthesized according to *general procedure A* (1.1 eq. of amine) and was used in the next step without further purification.

^{1}H NMR (200 MHz, $CDCl_3$): δ/ppm = 1.56-1.68 (m, 20H), 1.87-1.92 (m, 2H), 2.10 (m, 3H), 2.26-2.28 (m, 3H), 7.72 (s, 1H).

2.3.20 Synthesis of iminium $3d_s$

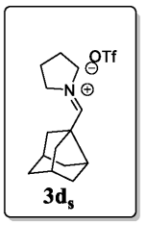

Under inert atmosphere, aldehyde **9** (150 mg, 1.eq., 1 mmol), KCN (77 mg, 1.2 eq., 1.2 mmol), $MgSO_4$ (240 mg, 2 eq., 2 mmol) and pyrrolidinum triflate (265 mg, 1.2 eq., 1.2 mmol) were suspended in dry THF (10 mL) and heated to reflux for two days. The reaction was filtered, quenched with water (20 mL), extracted with CH_2Cl_2 (2x 10 mL), washed with brine, dried over Na_2SO_4 (anhydrous), filtered and the solvent was evaporated *in vacuo*. The crude residue was then dissolved in CH_2Cl_2 (10 mL, extra dry) and treated with AgOTf (230 mg, 1 eq., 1 mmol) and stirred at 22 °C for 1 hour. The reaction mixture was filtered, washed with dry CH_2Cl_2 and the solvent was removed *in vacuo* and the crude residue was used in the next step without further purification.

^{1}H NMR (400 MHz, $CDCl_3$): δ/ppm 1.60-2.23 (m, 12), 2.37 (m, 2H), 2.86 (m, 1H), 3.38 (m, 2H), 3.53 (m, 1H), 3.99 (m, 2H), 4.25 (m, 2H), 8.60 (s, 1H).

2.3.21 Synthesis of iminium $1e_s$

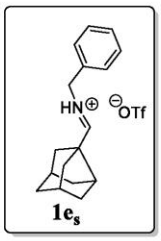

$1e_s$

Imine **1s** was dissolved in dry dichloromethane (500µL/100mg), and 1.05 eq. of triflic acid were added at 0 °C. After the solution homogenized it was overlaid with dry diethyl ether (1-2 mL/100mg) and the target salt was precipitated overnight under nitrogen atmosphere. After washing with dry ethyl ether the salt was obtained as clear colourless crystals in a yield of 80%.

^{1}H NMR (400 MHz, CD_2Cl_2): δ/ppm = 1.58-1.69 (m, 4H), 1.80-1.86 (m, 4H), 2.00-2.03 (m, 2H), 2.40 (m, 2H), 2.72 (m, 1H), 4.99 (m, 2H), 7.38-7.43 (m, 5H), 8.52 (d, *J* = 17.5 Hz, 1H), 12.15 (m, 1H).

^{13}C NMR (101 MHz, $CDCl_3$): δ/ppm = 34.17 (CH_2), 37.54 (2CH), 43.39 ($2CH_2$), 45.48 ($2CH_2$), 46.21 (CH), 55.00 (C), 56.39 (CH_2), 129.58 (2CH), 129.70 (2CH), 129.79 (CH), 131.54 (C), 186.44 (CH).

IR (neat): $\tilde{\nu}$/cm^{-1} = 3065, 2934, 2874, 1686, 1458, 1278, 1223, 1166, 1025, 965, 754, 695, 635, 599, 573, 514, 487, 466.

HRMS: m/z = 240.1751 ($[M+H]^+$; calculated for $C_{17}H_{22}N^+$ m/z =240.1747).

2.4 NMR spectra of imines **1a-o**, **3a-c**, salt $\mathbf{1e_s}$ and $\mathbf{3d_s}$

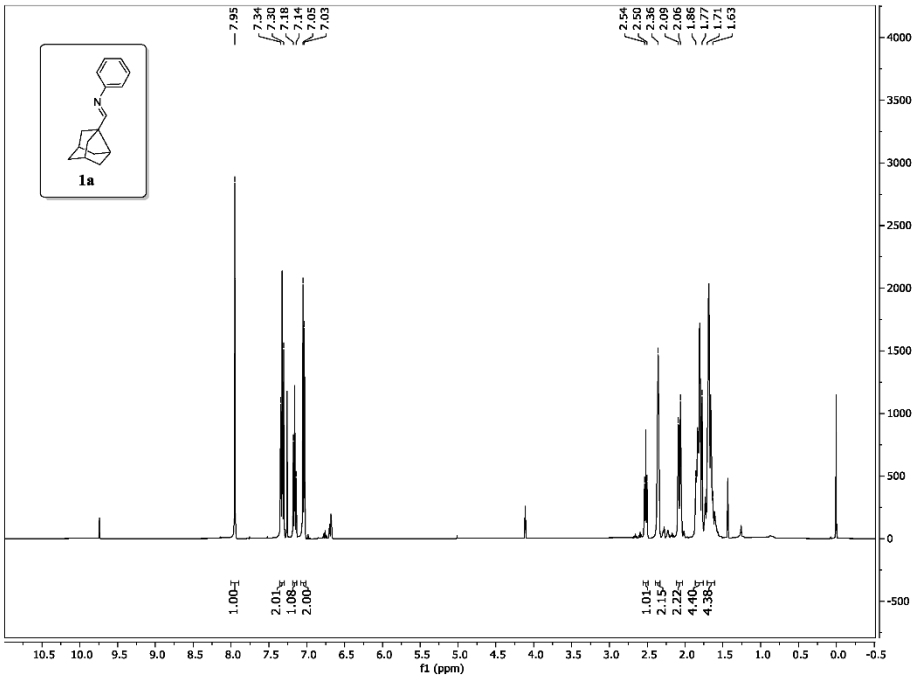
7.95
7.34
7.30
7.18
7.14
7.05
7.03
2.54
2.50
2.35
2.08
2.06
1.86
1.77
1.71
1.63
1a
1.00
2.01
1.08
2.00
1.01
2.15
2.22
4.40
4.38
f1 (ppm)

S47

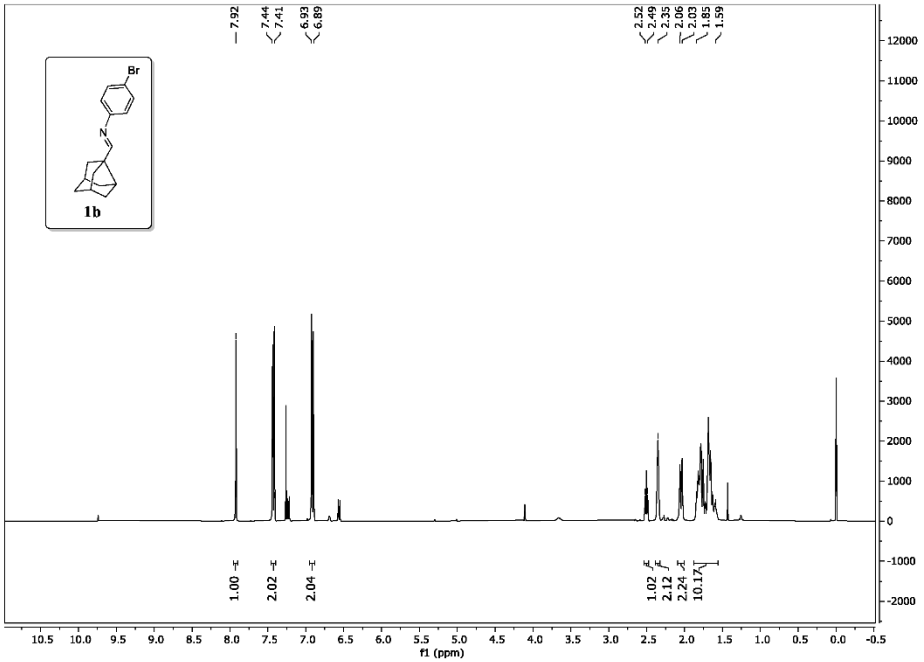
7.92
7.44
7.41
6.93
6.89
2.52
2.49
2.35
2.06
2.03
1.85
1.59
Br
1b
1.00
2.02
2.04
1.02
2.12
2.24
10.17
f1 (ppm)

S48

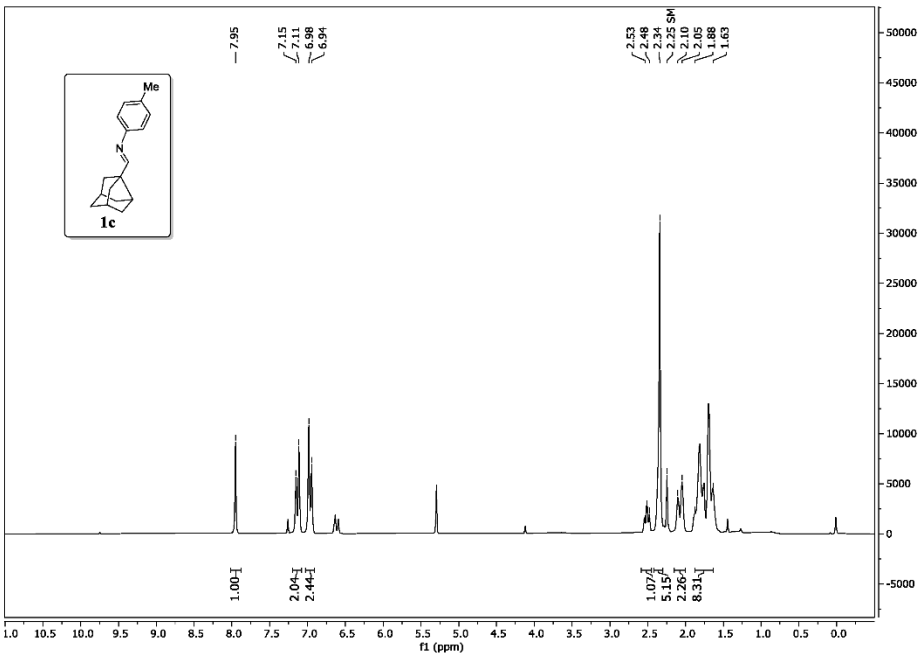
7.95
7.15
7.11
6.98
6.94
2.53
2.48
2.34
2.25 SM
2.10
2.05
1.88
1.63
Me
1c
1.00
2.04
2.44
1.07
5.15
2.26
8.31
f1 (ppm)

S49

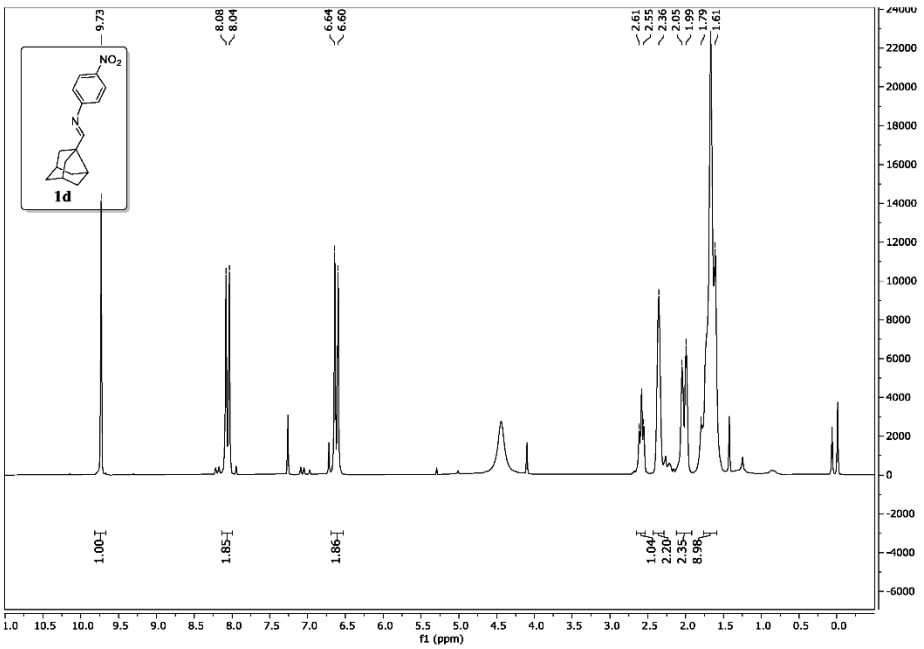
9.73
8.08
8.04
6.64
6.60
2.61
2.55
2.36
2.05
1.99
1.79
1.61
NO2
1d
1.00
1.85
1.86
1.04
2.20
2.35
8.98
f1 (ppm)

S50

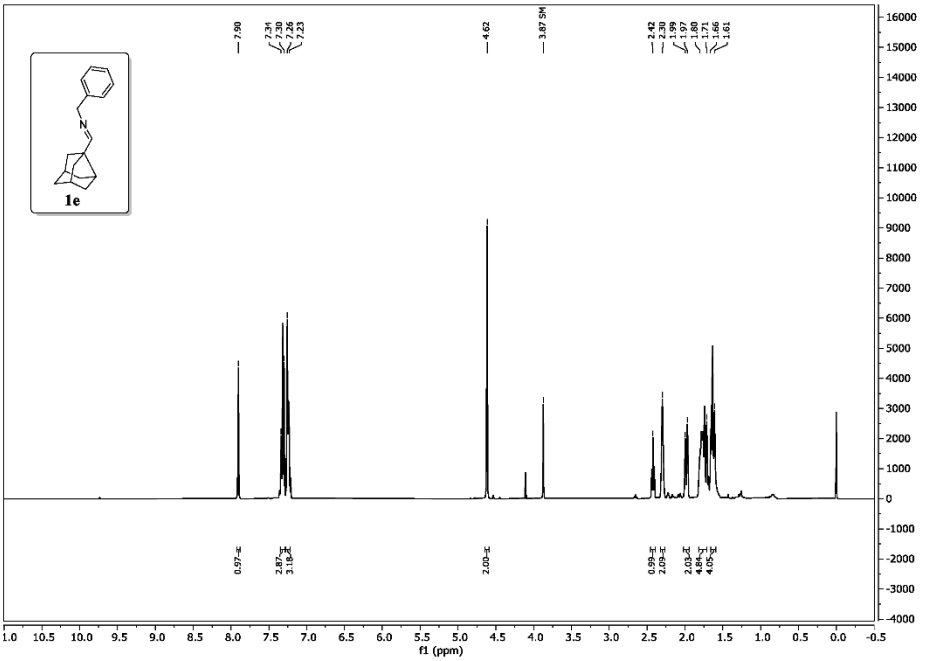
7.90
7.34
7.30
7.26
7.23
4.62
3.87 SM
2.42
2.39
1.99
1.97
1.80
1.71
1.66
1.61
1e
f1 (ppm)

S51

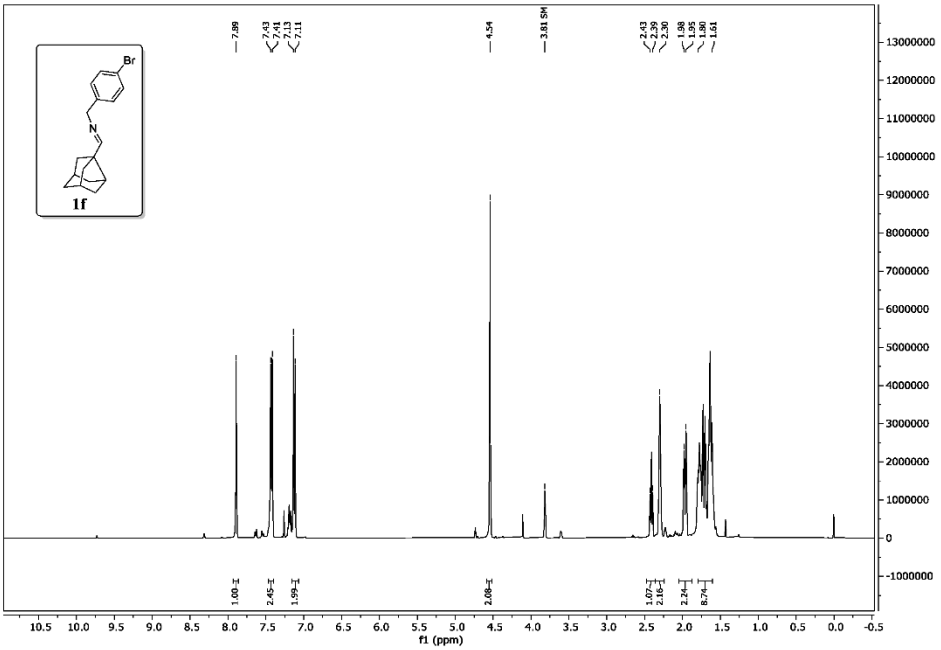
7.99
7.43
7.41
7.13
7.11
4.54
3.81 SM
2.43
2.39
2.36
1.98
1.95
1.90
1.61
Br
1f
f1 (ppm)

S52

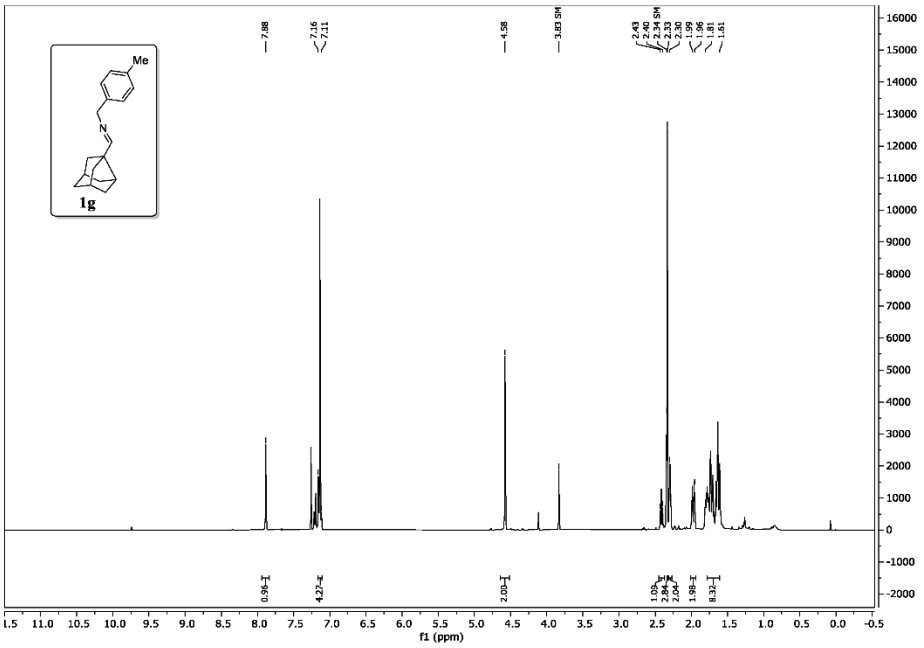
Me
1g
7.88
7.16
7.11
4.58
3.83 SM
2.43
2.40
2.34 SM
2.33
2.30
1.99
1.96
1.81
1.61
f1 (ppm)

S53

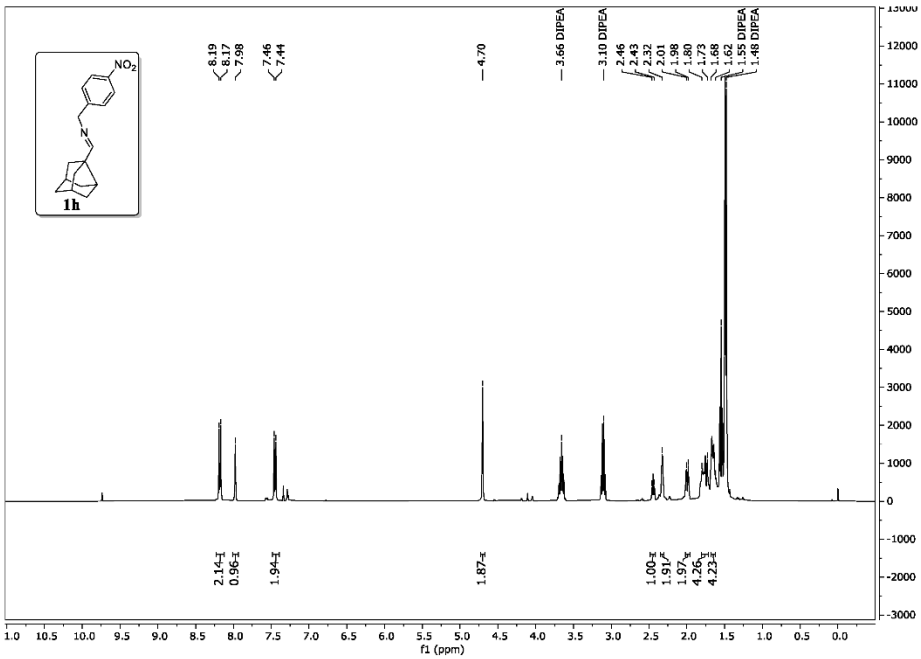
NO2
1h
8.19
8.17
7.98
7.46
7.44
4.70
3.66 DIPEA
3.10 DIPEA
2.46
2.43
2.32
2.01
1.98
1.80
1.73
1.68
1.62
1.55 DIPEA
1.48 DIPEA
f1 (ppm)

S54

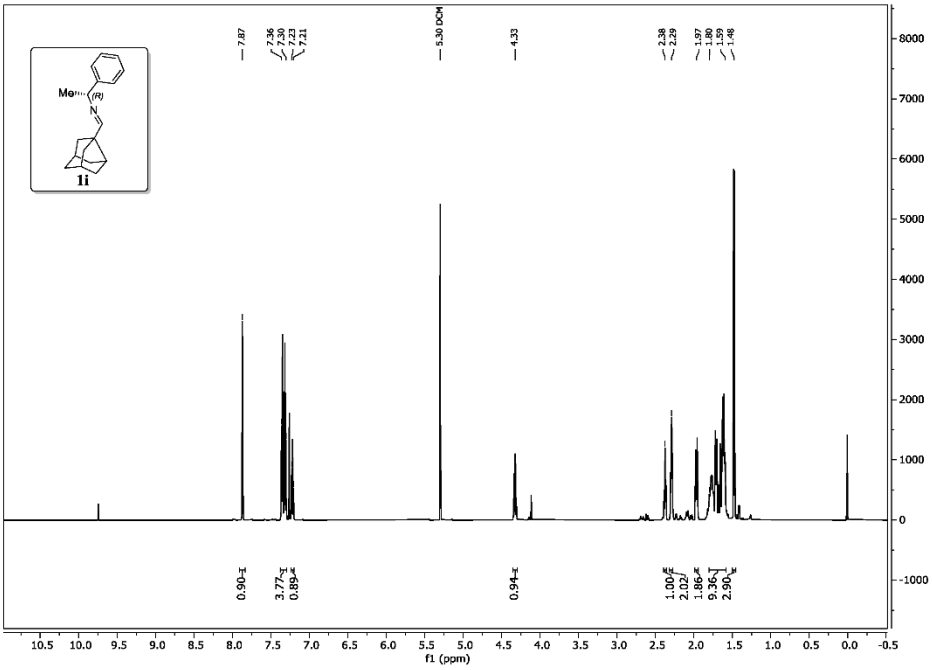
1i
7.87
7.36
7.30
7.23
7.21
5.30 DCM
4.33
2.38
2.29
1.97
1.80
1.59
1.48
f1 (ppm)

S55

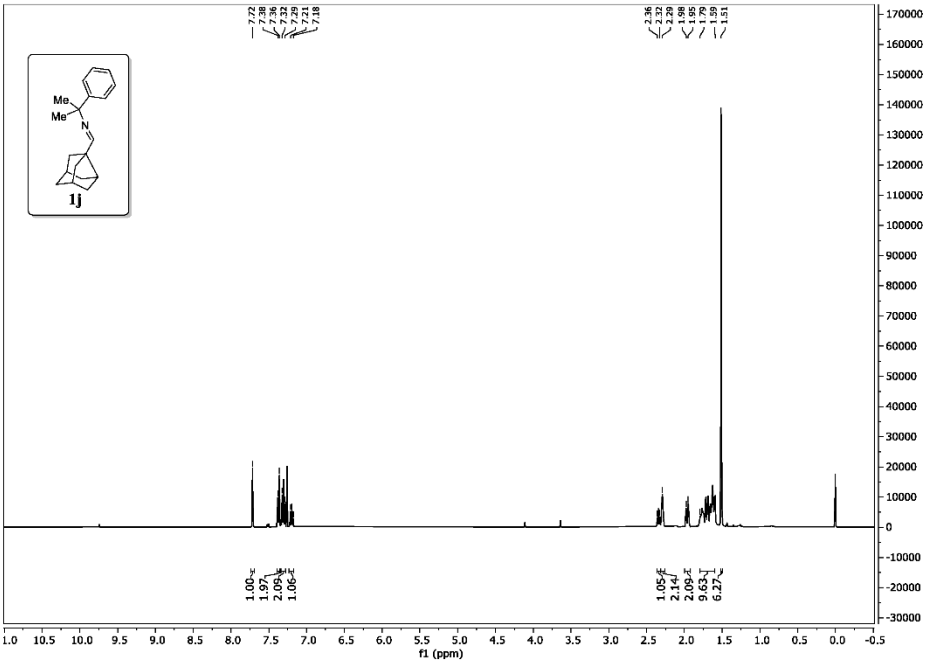
1j
7.72
7.38
7.36
7.33
7.29
7.21
7.18
2.36
2.32
2.29
1.98
1.95
1.79
1.59
1.51
f1 (ppm)

S56

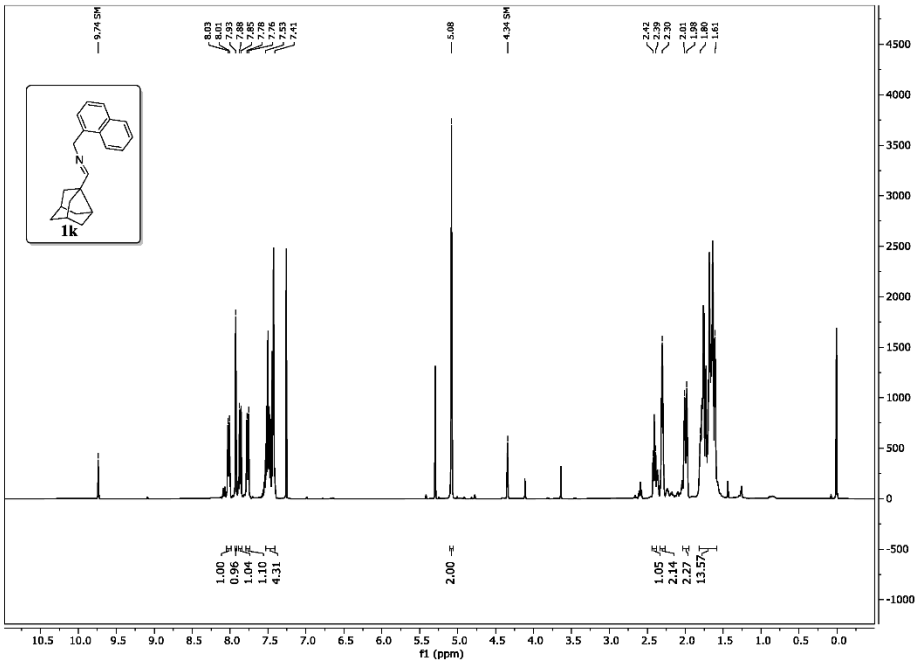
9.74 SM
8.03
8.01
7.93
7.88
7.85
7.78
7.76
7.53
7.41
5.08
4.34 SM
2.42
2.39
2.30
2.01
1.98
1.80
1.61
1k
1.00
0.96
1.04
1.10
4.31
2.00
1.05
2.14
2.27
13.57
f1 (ppm)

S57

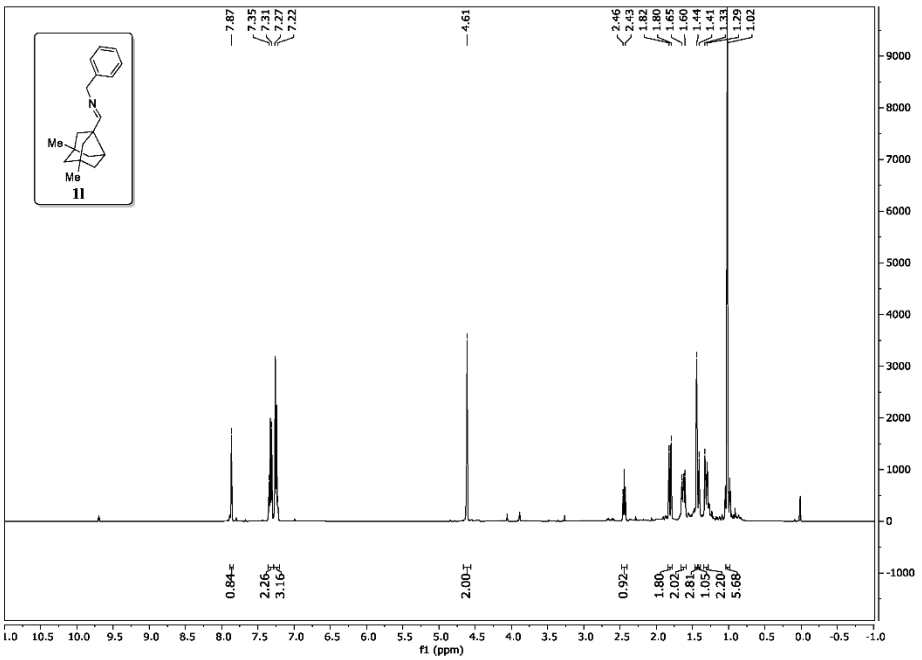
7.87
7.35
7.31
7.27
7.22
4.61
2.46
2.43
1.82
1.80
1.65
1.60
1.44
1.41
1.33
1.29
1.02
Me
Me
1l
0.84
2.26
3.16
2.00
0.92
1.80
2.02
2.81
1.05
2.20
5.68
f1 (ppm)

S58

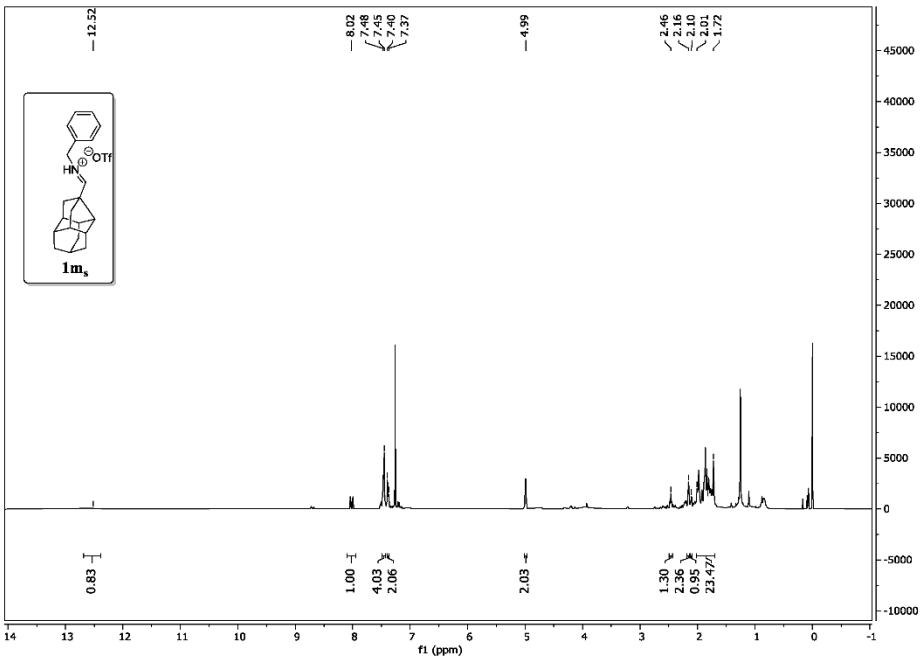
12.52
8.02
7.48
7.45
7.40
7.37
4.99
2.46
2.16
2.10
2.01
1.72
OTf
HN
1m_s
0.83
1.00
4.03
2.06
2.03
1.30
2.36
0.95
23.47
f1 (ppm)

S59

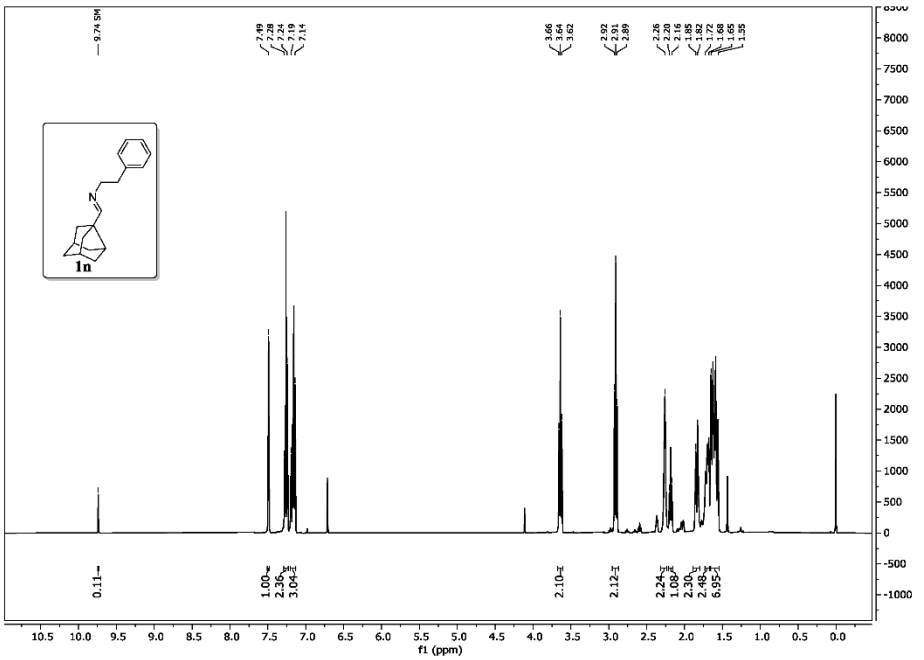
9.74 SM
7.49
7.28
7.24
7.19
7.14
3.66
3.64
3.62
2.92
2.91
2.89
2.26
2.20
1.95
1.85
1.82
1.72
1.68
1.65
1.55
N
1n
0.11
1.00
2.36
3.04
2.10
2.12
2.24
1.08
2.30
2.48
6.95
f1 (ppm)

S60

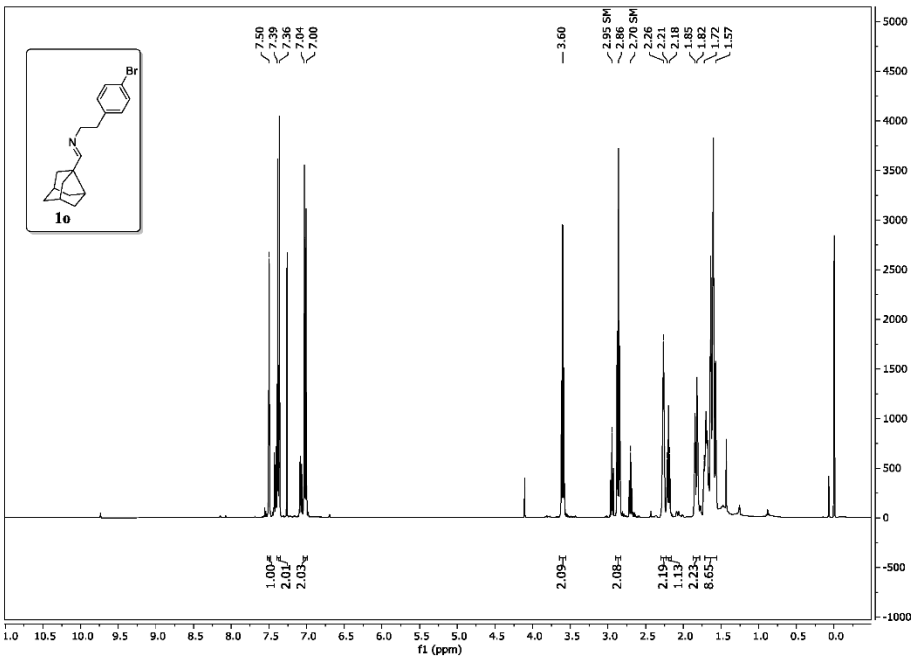
7.50
7.39
7.36
7.04
7.00
3.60
2.95 SM
2.86
2.70 SM
2.26
2.21
2.18
1.85
1.82
1.72
1.57
Br
N
1o
1.00
2.01
2.03
2.09
2.08
2.19
1.13
2.23
8.65
f1 (ppm)

S61

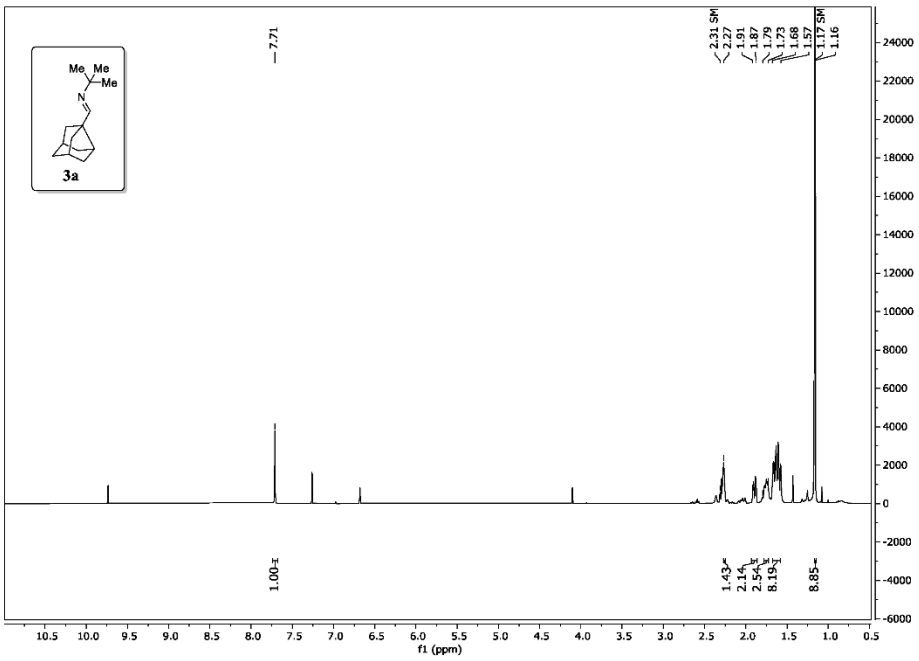
7.71
2.31 SM
2.27
1.91
1.87
1.79
1.73
1.68
1.57
1.17 SM
1.16
Me
Me
Me
N
3a
1.00
1.43
2.14
2.54
8.19
8.85
f1 (ppm)

S62

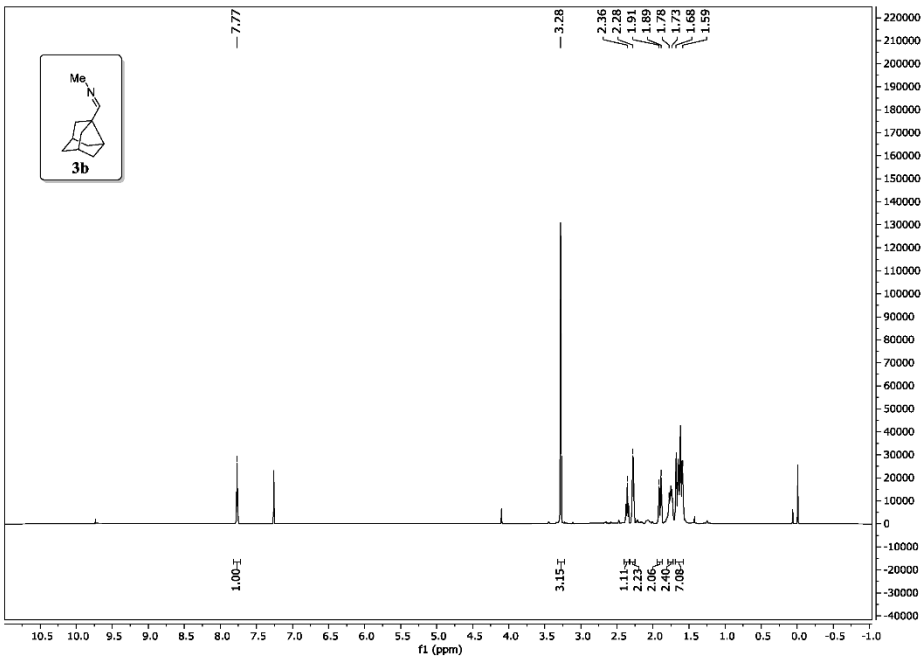
7.77
3.28
2.36
2.28
1.91
1.89
1.78
1.73
1.68
1.59
Me
N
3b
1.00
3.15
1.11
2.23
2.06
2.40
7.08
f1 (ppm)

S63

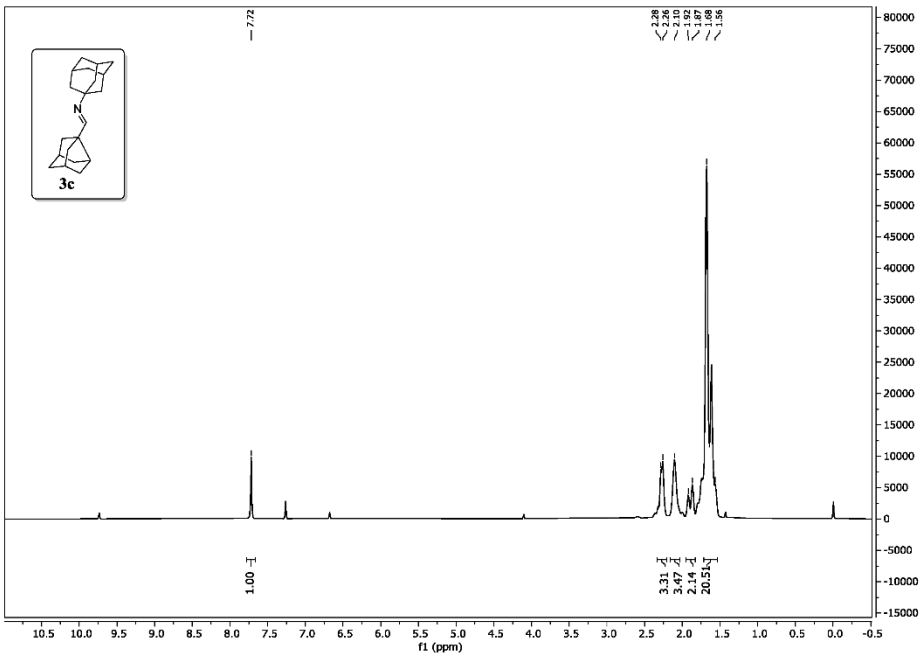
7.72
2.28
2.26
2.10
1.92
1.87
1.68
1.56
N
3c
1.00
3.31
3.47
2.14
20.51
f1 (ppm)

S64

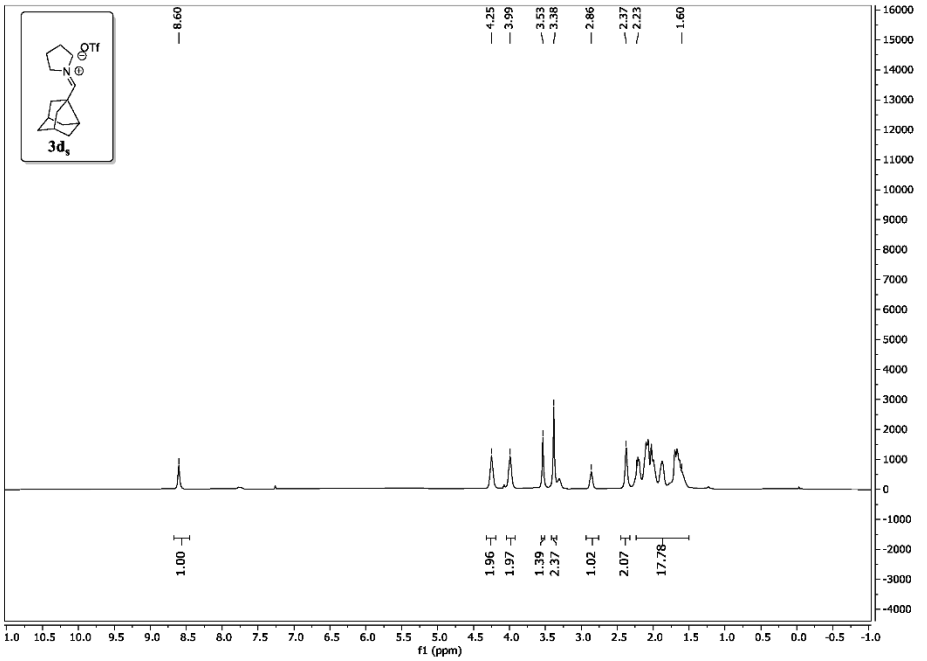
8.60
4.25
3.99
3.53
3.38
2.86
2.37
2.23
1.60
OTf
3ds
1.00
1.96
1.97
1.39
2.37
1.02
2.07
17.78
f1 (ppm)

S65

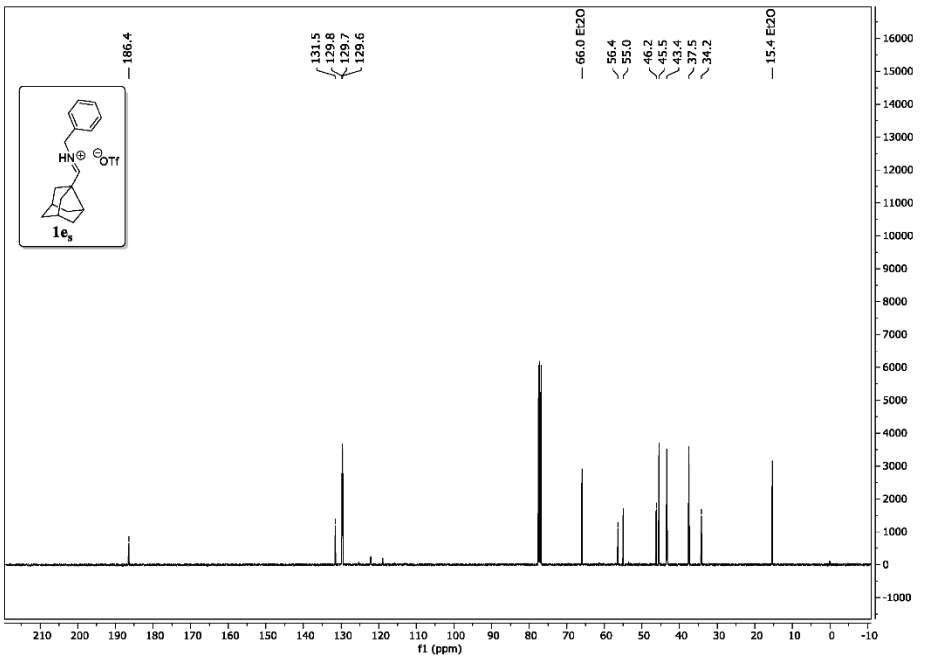
186.4
131.5
129.8
129.7
129.6
66.0 Et2O
56.4
55.0
46.2
45.5
43.4
37.5
34.2
15.4 Et2O
HN
OTf
1es
f1 (ppm)

S66

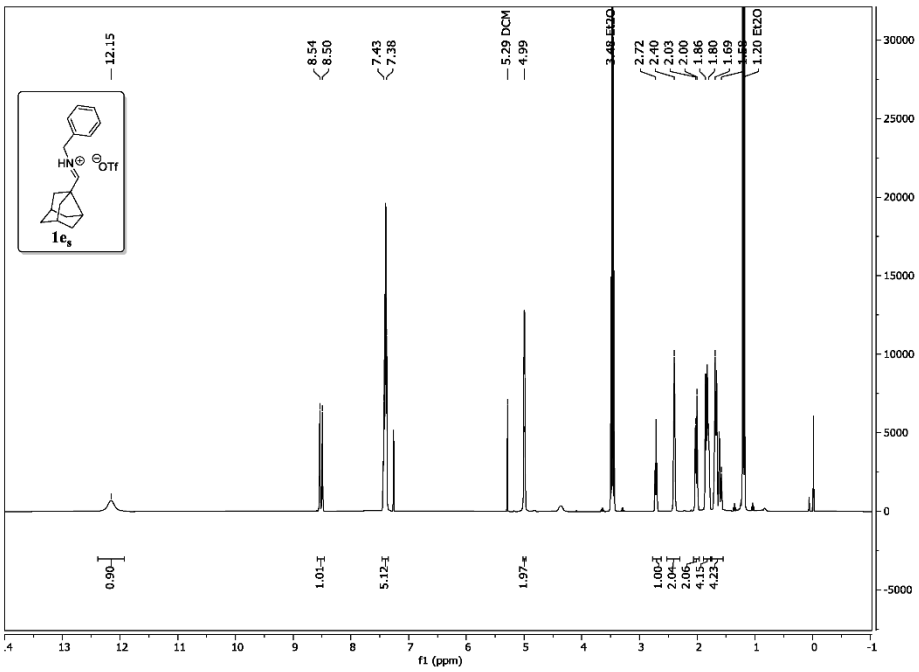
12.15
8.54
8.50
7.43
7.38
5.29 DCM
4.99
3.48 Et2O
2.72
2.40
2.03
2.00
1.86
1.80
1.69
1.20 Et2O
HN
OTf
1e8
0.90
1.01
5.12
1.97
1.00
2.04
2.06
4.15
4.23
f1 (ppm)

S67

2.5 Syntheses and description of compounds **2a-o** and **4a-d**

2.5.1 Optimization of reaction conditions

Table 1 shows the result of the reaction optimization. Under inert atmosphere, 1.0 equivalent of imine **1e** was dissolved in 1,2,4-trichlorobenzene or 1,2-dichlorobenzene (0.4 M) and stated equivalents of Brønsted acid were added. In one case, $Cu(OTf)_2$ was used instead of Brønsted acid (entry 11). The reaction vessel was transferred into a preheated oil bath at the given temperature and stirred overnight (16 h). After cooling down, the reaction mixture was diluted with EtOAc (~10 mL/mL solvent), washed with 2M NaOH (*aq.*), water and brine, dried over Na_2SO_4 (anhydrous), filtered and evaporated *in vacuo*. The crude residue was analysed *via* ^{1}H NMR analysis. For the reaction with 1 eq. of triflic acid (entry 11) the iminium salt **1e$_S$** was prepared (*chapter 2.3.20*), dissolved in deuterated solvent (1,4-dichlorobenzene-*d*$_4$) and heated under inert atmosphere overnight (16 h). After cooling to room temperature, the ^{1}H NMR spectrum of the reaction mixture was directly measured.

Table 1. Screening of Brønsted acids and reaction conditions

Entry	Brønsted acid (HA)	Equiv. of HA	Temperature in °C	Conversion in %[b]
1	CF_3COOH	2	140	0
2	*rac*-1,1'-Binaphthalene-2,2'-diyl phosphoric acid[l]	2	140	0
3	HCl	2	140	0
4	*p*-TsOH	2	140	60
5	**TfOH**	**2**	**140**	**96**
6	TfOH	2	120	81
7	TfOH	2	100	17
8	TfOH	2	80	0
9	TfOH	1.1	140	92
10	TfOH	1.0	140	traces
11	$Cu(OTf)_2$	2	140	0

2.5.2 General procedure B

Under inert atmosphere, 1.0 equivalent of imine **1** or **3** (general scale: 100 mg) was dissolved in 1,2,4-trichlorobenzene or 1,2-dichlorobenzene (0.4 M) and 2.0 equivalents of triflic acid were added. The reaction vessel was transferred into a preheated oil bath at 140 °C and stirred overnight. After cooling down, the reaction mixture was diluted with EtOAc (~10 mL/mL solvent), washed with 2M NaOH (*aq.*), water and brine, dried over Na_2SO_4 (anhydrous), filtered and evaporated *in vacuo*. If needed the crude residue was purified *via* flash column chromatography on silica gel (mobile phase: MeOH (1% NH_3 (*aq.*)) in CH_2Cl_2).

2.5.3 General procedure C

Under inert atmosphere, 1.0 equivalent of imine **3** (general scale: 100 mg) was dissolved in the corresponding solvent/reagent (0.2 M) and 2.0 equivalents of triflic acid were added. The reaction vessel was transferred into the microwave and heated with 300 W at 200 °C for 2.5 h. After cooling down, the reaction mixture was diluted with EtOAc (~10 mL/mL solvent), washed with 2M NaOH (*aq.*), water and brine, dried over Na_2SO_4 (anhydrous), filtered and evaporated *in vacuo*. If needed the crude residue was purified *via* flash column chromatography on silica gel (mobile phase: MeOH (1% NH_3 (*aq.*)) in CH_2Cl_2).

2.5.4 Synthesis of cyclic amine 2a

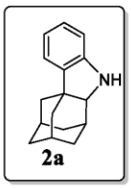

Compound **2a** was synthesized according to *general procedure B* to give a clear liquid in a yield of 87%.

R_f (silica gel; EtOAc:*c*-hexane 1:9):0.2.

^{1}H NMR (400 MHz, $CDCl_3$): δ/ppm = 1.39-1.44 (m, 1H), 1.64-1.69 (m, 1H), 1.73-1.81 (m, 4H), 1.87-1.90 (m, 3H), 2.08-2.12 (m, 2H), 2.20-2.28 (m, 2H), 3.41 (m, 1H), 3.89 (s, 1H), 6.75-6.79 (m, 2H), 6.99-7.06 (m, 2H).

^{13}C NMR (101 MHz, $CDCl_3$): δ/ppm = 27.5 (CH), 29.2 (CH), 30.4 (CH_2), 31.2 (CH), 37.4 (CH_2), 37.4 (CH_2), 38.6 (CH_2), 39.1 (CH_2), 42.4 (C), 71.6 (CH), 111.2 (CH), 119.3 (CH), 121.0 (CH), 126.9 (CH), 139.8 (C), 150.5 (C).

IR (neat): $\tilde{\nu}$ /cm^{-1} = 2901, 2848, 1609, 1587, 1476, 1459, 1385, 1331, 1235, 1194, 1102, 1078, 1013, 775, 738, 694, 669, 643, 582, 549, 462.

HRMS: m/z = 226.1591 ([M+H]$^+$; calculated for $C_{16}H_{20}N^+$ m/z = 226.1590).

2.5.5 Synthesis of cyclic amine 2b

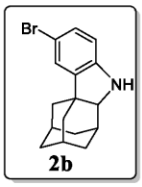

Compound **2b** was synthesized according to *general procedure B* to give an off-white solid in a yield of 73%.

R_f (silica gel; MeOH (1% NH_3 *aq.*):CH_2CL_2 5:95): 0.8.

m.p. (cryst. from): 129.2-130.3 °C.

^{1}H NMR (400 MHz, $CDCl_3$): 1.39 (m, 1H), 1.65 (m, 1H), 1.70-1.78 (m, 4H), 1.82-1.89 (m, 3H), 2.04-2.11 (m, 2H), 2.17-2.21 (m, 2H), 3.39 (m, 1H), 3.88 (bs, 1H), 6.62 (d, *J* = 8.2 Hz, 1H), 7.07 (d, *J* = 2.0 Hz, 1H), 7.12 (dd, *J* = 8.2, 2.0 Hz, 1H).

^{13}C NMR (101 MHz, $CDCl_3$): δ/ppm = 27.4 (CH), 29.1 (CH), 30.2 (CH_2), 31.0 (CH), 37.2 (CH_2), 37.3 (CH_2), 38.4 (CH_2), 39.0 (CH_2), 42.8 (C), 71.8 (CH), 111.1 (C), 112.5 (CH), 124.4 (CH), 129.4 (C), 142.0 (C), 149.6 (C).

IR (neat): $\tilde{\nu}$/cm^{-1} = 3353, 2909, 2847, 1601, 1463, 1446, 1420, 1385, 1333, 1301, 1275, 1233, 1190, 1077, 1055, 1026, 807, 755, 642, 611, 535, 489, 457, 445.

HRMS: m/z = 304.0695 ([M+H]$^+$; calculated for $C_{16}H_{19}BrN^+$ m/z =304.0696).

2.5.6 Synthesis of cyclic amine 2c

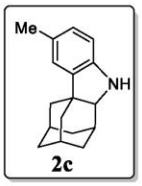

2c

Compound **2c** was synthesized according to *general procedure B* to give an off-white solid in a yield of 68%.

R_f (silica gel; EtOAc:*n*-hexane 1:9): 0.3.

m.p. (cryst. from CH_2Cl_2): 115.3-115.9 °C.

^{1}H NMR (400 MHz, $CDCl_3$): δ/ppm = 1.40 (m, 1H), 1.65 (m, 1H), 1.72-1.80 (m, 4H), 1.86-1.89 (m, 2H), 2.07-2.10 (m, 2H), 2.18 (m, 1H), 2.23 (m, 1H), 2.27 (m, 3H), 3.38 (m, 1H), 3.77 (bs, 1H), 6.68-6.70 (m, 2H), 6.82-6.86 (m, 2H).

^{13}C NMR (101 MHz, $CDCl_3$): δ/ppm = 21.1 (CH), 27.5 (CH), 29.2 (CH), 30.4 (CH_2), 31.2 (CH), 37.4(CH_2), 37.5(CH_2), 38.7(CH_2), 39.2(CH_2), 42.4(C), 71.8 (CH), 111.1 (CH), 121.9 (CH), 127.2 (CH), 128.6 (C), 140.1 (C), 148.1 (C).

IR (neat): $\tilde{\nu}$/cm^{-1} = 3350, 2903, 2845, 1615, 1483, 1450, 1386, 1331, 1303, 1290, 1232, 1193, 1174, 1109, 1078, 1030, 852, 828, 805, 755, 687, 637, 537, 537, 508, 471, 458, 445.

HRMS: m/z = 240.1744 ([M+H]$^+$; calculated for $C_{17}H_{22}N^+$ m/z = 240.1747).

2.5.7 Synthesis of cyclic amine 2d

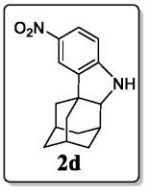

2d

Compound **2d** was synthesized according to *general procedure B* to give a yellow solid in a yield of 15%.

Rf (silica gel; MeOH (1% NH_3 *aq.*):CH_2CL_2 5:95): 0.6.

m.p. (cryst. from $CDCl_3$): 93.2-95.0 °C.

^{1}H NMR (400 MHz, $CDCl_3$): δ/ppm = 1.43 (m, 1H), 1.70-1.77 (m, 5H), 1.88-1.91 (m, 3H), 2.01 (m, 1H), 2.14 (m, 1H), 2.23-2.30 (m, 2H), 3.54 (m, 1H), 4.57 (bs, 1H), 6.67 (d, *J* = 8.7 Hz, 1H), 7.84 (d, *J* = 2.3 Hz, 1H), 8.02 (dd, *J* = 8.7, 2.3 Hz, 1H).

^{13}C NMR (101 MHz, $CDCl_3$): δ/ppm = 27.1 (CH), 29.0 (CH), 30.1 (CH_2), 30.7 (CH), 37.0 (CH_2), 37.1 (CH_2), 38.0 (CH_2), 39.2 (CH_2), 42.4 (C), 72.0 (CH), 109.2 (CH), 117.7 (CH), 125.2 (CH), 139.7 (C), 140.4 (C), 156.6 (C).

IR (neat): $\tilde{\nu}$ /cm^{-1} = 3350, 2914, 2850, 1611, 1480, 1439, 1341, 1306, 1292, 1271, 1196, 1165, 1147, 1099, 1074, 1022, 926, 889, 814, 757, 738, 605, 556, 540, 461.

HRMS: m/z = 293.1263 ($[M+H]^+$; calculated for $C_{16}H_{19}N_2O_2^+$ m/z = 293.1260).

2.5.8 Synthesis of cyclic amine 2e

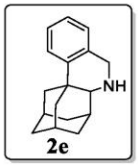

2e

Compound **2e** was synthesized according to *general procedure B* to give an off-white solid in a yield of 94%.

^{1}H NMR (400 MHz, $CDCl_3$): δ/ppm = 1.56-1.64 (m, 3H), 1.79 (m, 3H), 1.83-1.97 (m, 5H), 2.05-2.11 (m, 2H), 2.89 (m, 1H), 4.09 (d, *J* = 16.2 Hz, 1H), 4.23 (d, *J* = 16.2 Hz, 1H). 6.99 (m, 1H), 7.10 (m, 1H), 7.17 (m, 1H), 7.28 (m, 1H).

Spectrum in accordance with literature: I. Papanastasiou, A. Tsotinis, N. Kolocouris, S. P. Nikas, A. Vamvakides, *Med. Chem. Res*., 2014, **23**, 1966-1975.

2.5.9 Synthesis of cyclic amine 2f

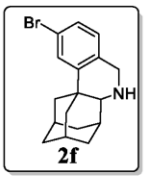

2f

Compound **2f** was synthesized according to *general procedure B* to give an off-white solid in a yield of 93%.

R_f (silica gel; NEt_3:MeOH:CH_2CL_2 1:10:89): 0.5.

m.p. (cryst. from): 92.0-94.0 °C.

^{1}H NMR (400 MHz, $CDCl_3$): δ/ppm 1.54-1.57 (m, 1H), 1.59-1.63 (m, 1H), 1.75-1.97 (m, 9H), 2.04 (m, 1H), 2.11 (m, 1H), 2.29 (dt, *J* = 12.5, 2.5 Hz, 1H), 2.84 (s, 1H), 4.13 (d, *J* = 16.2 Hz, 1H), 4.03 (d, *J* = 16.2 Hz, 1H), 6.86 (m, 1H), 7.21 (m, 1H), 7.38 (m, 1H).

^{13}C NMR (101 MHz, $CDCl_3$): δ/ppm = 28.5 (CH), 28.9 (CH), 30.6 (CH_2), 34.0 (CH), 36.0 (C), 37.2 (CH_2), 37.5 (CH_2), 40.6 (CH_2), 41.2 (CH_2), 49.2(CH_2), 62.1 (CH), 120.0 (C), 127.8 (CH), 128.2 (CH), 128.6 (CH), 133.7 (C), 147.0 (C).

IR (neat): $\tilde{\nu}$/cm^{-1} = 3311, 3081, 3031, 2903, 2848, 1677, 1587, 1563, 1458, 1439, 1400, 1337, 1317, 1290, 1253, 1197, 1155, 1123, 1101, 1085, 1054, 1030, 996, 981, 956, 913, 883, 799, 723, 704, 665.

HRMS: m/z =318.0851 ($[M+H]^+$; calculated for $C_{17}H_{21}BrN^+$ m/z =318.0852).

2.5.10 Synthesis of cyclic amine 2g

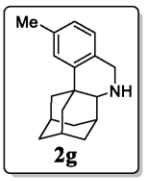

Compound **2g** was synthesized according to *general procedure B* to give a yellowish non-crystalline solid in a yield of 88%.

R_f (silica gel; EtOAc:*n*-hexane 1:4): 0.2.

^{1}H NMR (400 MHz, $CDCl_3$): δ/ppm 1.57-1.63 (m, 3H), 1.80-2.11 (m, 10H), 2.31 (s, 3H), 2.36-2.39 (m, 1H), 2.88 (s, 1H), 4.19 (d, *J* = 16.0 Hz, 1H), 4.06 (d, *J* = 16.0 Hz, 1H), 6.88-6.95 (m, 2H), 7.09 (s, 1H).

^{13}C NMR (101 MHz, $CDCl_3$): δ/ppm = 20.3 (CH_3), 27.5 (CH), 28.0 (CH), 28.0 (CH_2), 33.1 (CH), 34.6 (CH_2), 36.3(CH_2), 36.7 (CH_2), 39.7 (CH_2), 40.3 (C), 48.3 (CH_2), 61.4 (CH), 124.4 (CH), 124.9 (CH), 125.4 (CH), 130.6 (C), 134.6 (C), 143.4 (C)

IR (neat): $\tilde{\nu}$ /cm^{-1} = 3231, 3009, 2902, 2847, 1613, 1500, 1446, 1344, 1308, 1259, 1229, 1155, 1126, 1098, 1086, 1033, 993, 954, 875, 851, 801.

HRMS: m/z =254.1907 ([M+H]$^+$; calculated for $C_{18}H_{24}N^+$ m/z =254.1903).

2.5.11 Synthesis of cyclic amine 2h

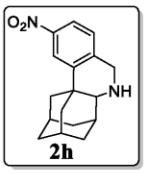

Compound **2h** was synthesized according to *general procedure B* to give a yellowish solid in a yield of 74%.

R_f (silica gel; NEt_3:MeOH:CH_2CL_2 1:10:89): 0.5.

m.p. (cryst. from): 116.0-117.0 °C.

^{1}H NMR (400 MHz, $CDCl_3$): δ/ppm 1.57-1.65 (m, 3H) 1.81 (m, 3H), 1.89-2.00 (m, 4H), 2.07-2.16 (m, 3H), 2.40 (dt, *J* = 12.4, 2.5 Hz, 1H), 2.89 (m, 1H), 4.19 (d, *J* = 17.2 Hz, 1H), 4.27 (d, *J* = 17.2 Hz, 1H), 7.13 (d, *J* = 8.5 Hz, 1H), 7.94 (dd, *J* = 8.5, 2.3 Hz, 1H), 8.15 (d, *J* = 2.3 Hz, 1H).

^{13}C NMR (101 MHz, $CDCl_3$): δ/ppm =28.4 (CH), 28.8 (CH), 30.5 (CH_2), 33.7 (CH), 36.3 (C), 37.0 (CH_2), 37.3 (CH_2), 40.4 (CH_2), 41.2 (CH_2), 49.5 (CH_2), 61.9 (CH), 120.6(CH), 123.7 (CH), 127.1 (CH), 142.4 (C), 145.4 (C), 144.9 (C)

IR (neat): $\tilde{\nu}$ /cm^{-1} =3323, 2888, 2850, 1582, 1515, 1445, 1342, 1317, 1288, 1254, 1229, 1198, 1122, 1097, 1086, 1072, 1028, 1003, 987, 969, 956, 911, 898, 885, 852, 842, 822, 789, 773, 736, 709, 659.

HRMS: m/z = 285.1602 ([M+H]$^+$; calculated for $C_{17}H_{21}N_2O_2^+$ m/z =285.1598)

2.5.12 Synthesis of cyclic amine 2i

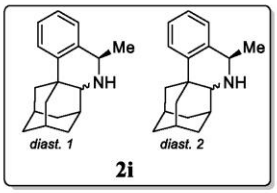

2i

Compound **2i** was synthesized according to *general procedure B* to give a high viscous liquid in a yield of 78% as a mixture of two diastereomers. Diastereomer 1 was isolated by HPLC (semipreparative column C18H, mobile phase 75% MeCN, 25% H_2O, 0.3 CV/min, diastereomer 2: t_r = 12.9 min; diastereomer 1: t_r = 15.9 min) and fully described. Absolute configuration of diastereomers was not assigned.

R_f (silica gel; EtOAc:*n*-hexane 2:3): 0.2.

diastereomer 1
^{1}H NMR (400 MHz, $CDCl_3$): δ/ppm = 1.52 (d, *J* = 6.6 Hz, 3H), 1.57-1.62 (m, 3H), 1.79-1.82 (m, 3H), 1.87 (m, 1H), 1.94-1.98 (m, 3H), 2.09-2.13 (m, 2H), 2.37 (dt, *J* = 12.5, 2.6 Hz, 1H), 2.94 (m, 1H), 4.27 (q, *J* = 6.6 Hz, 1H), 7.15-7.20 (m, 3H), 7.28 (m, 1H).

diastereomer 2
^{1}H NMR (400 MHz, $CDCl_3$): δ/ppm = 1.51 (d, *J* = 7.0 Hz, 3H), 1.55-1.63 (m, 3H), 1.79 (m, 2H), 1.83-1.91 (m, 5H), 2.02 (m, 1H), 2.12 (m, 1H), 2.38 (dt, *J* = 12.5, 2.4 Hz, 1H), 3.11 (m, 1H), 4.28 (q, *J* = 7.0 Hz, 1H), 7.05 (m, 1H), 7.10-7.18 (m, 2H), 7.28 (m, 1H).

diastereomer 1
^{13}C NMR (101 MHz, $CDCl_3$): δ/ppm = 23.0 (CH_3), 28.5 (CH), 29.1 (CH), 30.6 (CH_2), 33.5 (CH), 35.9 (C), 37.4 (CH_2), 37.7 (CH_2), 41.0 (CH_2), 41.6 (CH_2), 53.3 (CH), 61.6 (CH), 125.0 (CH), 125.8 (CH), 125.8 (CH), 126.6 (CH), 139.6 (C), 144.7 (C).

diastereomer 2
^{13}C NMR (101 MHz, $CDCl_3$): δ/ppm = 24.3, (CH_3) 28.6 (CH), 29.1 (CH), 30.8 (CH_2), 33.9 (CH), 36.2 (C), 37.5 (CH_2), 37.8 (CH_2), 40.8 (CH_2), 41.1 (CH_2), 51.7 (CH), 55.4 (CH), 124.9 (CH), 125.7 (CH), 126.3 (CH), 127.4 (CH) 143.9 (C), 144.7 (C).

IR (neat): $\tilde{\nu}$/cm^{-1} = 2903, 2849, 1631, 1487, 1447, 1371, 1343, 1256, 1209, 1135, 1103, 1040, 1023, 971, 749, 697, 652, 625, 559, 525, 501.

HRMS: m/z = 254.1904 ([M+H]$^+$; calculated for $C_{18}H_{24}N^+$ m/z = 254.1903).

2.5.13 Synthesis of cyclic amine 2j

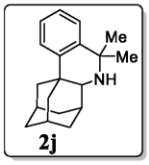

2j

Compound **2j** was synthesized according to *general procedure B* to non-crystalline solid in a yield of 85%.

R$_f$ (silica gel; MeOH (1% NH_3 *aq.*):CH_2Cl_2 1:33): 0.4.

^{1}H NMR (400 MHz, $CDCl_3$): δ/ppm = 1.49 (s, 3H), 1.51 (s, 3H), 1.54-1.60 (m, 3H), 1.79-1.85 (m, 4H), 1.88-1.92 (m, 4H), 2.00-2.03 (m, 1H), 2.10-2.11 (m, 1H), 2.37-2.41 (m, 1H), 3.02 (m, 1H), 7.14-7.16 (m, 2H), 7.20-7.22 (m, 1H), 7.27-7.28 (m, 1H).

^{13}C NMR (101 MHz, $CDCl_3$): δ/ppm = 28.6 (CH_3), 29.2 (CH_3), 30.7 (CH_2), 31.5 (CH), 33.0 (CH), 34.0 (CH), 36.2 (C), 37.6 (CH_2), 37.9 (CH_2), 41.0 (CH_2), 41.1 (CH_2), 54.1 (C), 56.5 (CH), 124.8 (CH), 125.7 (CH), 126.1 (CH), 126.5 (CH), 143.6 (C), 144.2 (C).

IR (neat): $\tilde{\nu}$/cm^{-1} = 2901, 2848, 1739, 1485, 1444, 1358, 1240, 1202, 1124, 1024, 750, 694, 646, 589, 529.

HRMS: m/z =268.2062 ([M+H]$^+$; calculated for $C_{19}H_{26}N^+$ m/z =268.2060).

2.5.14 Synthesis of cyclic amine 2k

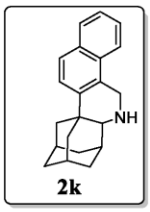

2k

Compound **2k** was synthesized according to *general procedure B* to give an off-white solid in a yield of 60%.

R_f (silica gel; MeOH (1% NH_3 *aq.*):CH_2CL_2 1:33): 0.6.

m.p. (cryst. from EtOAc): 70.2-71.9 °C.

^{1}H NMR (400 MHz, $CDCl_3$): δ/ppm = 1.60-1.67 (m, 2H), 1.75-1.78 (m, 1H), 1.84-1.87 (m, 3H), 1.90-2.00 (m, 4H), 2.06-2.15 (m, 3H), 2.47 (dt, *J* = 12.4, 2.5 Hz, 1H), 2.98 (s, 1H), 4.52 (d, *J* = 16.4 Hz, 1H), 4.64 (d, *J* = 16.5 Hz, 1H), 7.42-7.51 (m, 3H), 7.70 (m, 1H), 7.78-7.84 (m, 2H).

^{13}C NMR (101 MHz, $CDCl_3$): δ/ppm = 28.6 (CH), 29.2 (CH), 31.0 (CH_2), 34.1 (CH), 36.0 (C), 37.5 (CH_2), 37.8 (CH_2), 40.7 (CH_2), 41.0 (CH_2), 47.2 (CH_2), 62.2 (CH), 122.4 (CH), 123.4 (CH), 125.2 (CH), 126.2 (CH), 126.7 (CH), 128.5 (CH), 129.4 (C), 130.6 (C), 131.7 (C), 141.8 (C).

IR (neat): $\tilde{\nu}$ /cm^{-1} = 2902, 2846, 1596, 1510, 1447, 1266, 1135, 1064, 1007, 858, 802, 742, 691, 644, 646, 621, 547, 523.

HRMS: m/z = 290.1906 ($[M+H]^+$; calculated for $C_{21}H_{24}N^+$ m/z = 290.1903).

2.5.15 Synthesis of cyclic amine 2l

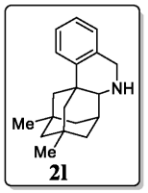

2l

Compound **2l** was synthesized according to *general procedure B* to give a clear liquid in a yield of 88%.

R_f (silica gel; MeOH (1% NH_3 *aq.*):CH_2CL_2 1:33): 0.2.

^{1}H NMR (400 MHz, $CDCl_3$): δ/ppm = 0.82 (s, 3H), 0.92 (s, 3H), 1.17-1.23 (m, 2H), 1.27 (m, 2H), 1.32-1.36 (m, 1H), 1.44-1.45 (m, 1H), 1.47-1.48 (m, 1H), 1.52-1.55 (m, 1H), 1.58-1.62 (m, 1H), 1.75-1.78 (m, 2H), 1.92-1.96 (m, 1H), 2.02-2.04 (m, 1H), 2.75 (m, 1H), 4.21 (d, *J* = 16.0 Hz, 1H), 4.08 (d, *J* = 16.1 Hz, 1H), 6.98-7.00 (m, 1H), 7.08-7.12 (m, 1H), 7.14-7.18 (m, 1H), 7.25-7.26 (m, 1H).

^{13}C NMR (101 MHz, $CDCl_3$): δ/ppm = 30.3 (CH_3), 30.5 (CH_3), 31.5 (C), 32.1 (C), 35.4 (CH), 37.1 (C), 37.2 (CH_2), 43.8 (CH_2), 47.1 (CH_2), 48.0 (CH_2), 49.8 (CH_2), 51.6 (CH_2), 61.5 (CH), 125.0 (CH), 125.7 (CH), 126.2 (CH), 126.4 (CH), 134.9 (C), 144.2 (C).

IR (neat): $\tilde{\nu}$ /cm^{-1} = 2946, 2864, 1714, 1458, 1375, 1313, 1258, 1166, 1092, 995, 730, 618.

HRMS: m/z = 268.2058 ($[M+H]^+$; calculated for $C_{19}H_{26}N^+$ m/z = 268.2060).

2.5.16 Synthesis of cyclic amine 2m

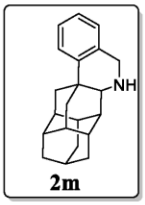

2m

Compound **2m** was synthesized according to *general procedure B* to give a non-crystalline solid in a yield of 46%.

R_f (silica gel; EtOAc:*n*-hexane 2:3): 0.2.

^{1}H NMR (400 MHz, $CDCl_3$): δ/ppm = 1.57-1.62 (m, 2H), 1.74-1.83 (m, 10H), 1.93-1.95 (m, 3H), 2.07 (m, 1H), 2.33 (m, 1H), 2.46 (bs, 1H), 2.85 (m, 1H), 4.10 (d, *J* = 16.2 Hz, 1H), 4.22 (d, *J* = 16.2 Hz, 1H), 6.99 (m, 1H), 7.11 (m, 1H), 7.18 (m, 1H), 7.31 (m, 1H).

^{13}C NMR (101 MHz, $CDCl_3$): δ/ppm = 26.2 (CH), 31.1 (CH), 33.6 (C), 37.1 (CH_2), 37.1 (CH), 37.4 (CH_2), 37.6 (CH_2&CH), 37.9 (CH), 38.2 (CH), 41.4 (CH_2), 42.4 (CH_2), 42.7 (CH), 49.0 (CH_2), 63.2 (CH), 125.2 (CH), 125.8 (CH), 126.1 (CH), 126.5 (CH), 133.8 (C), 143.6 (C).

IR (neat): $\tilde{\nu}$ /cm^{-1} = 3262, 3056, 2873, 2847, 1487, 1439, 1374, 1344, 1313, 1264, 1191, 1116, 1105, 1082, 1062, 1037, 985, 969, 932, 916, 905, 894, 870, 837, 753, 732, 707, 679, 659, 643, 612, 545, 531, 517, 497, 458, 445.

HRMS: m/z = 292.2062 ($[M+H]^+$; calculated for $C_{21}H_{26}N^+$ m/z = 292.2060).

2.5.17 Synthesis of cyclic amine 2n

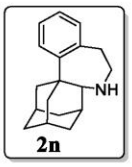

2n

Compound **2n** was synthesized according to *general procedure B* to give an off-white solid in a yield of 58%.

R_f (silica gel; MeOH (1% NH_3 *aq.*):CH_2CL_2 2:98): 0.2.

m.p. (cryst. from CH_2Cl_2): 145.7-146.3 °C.

^{1}H NMR (400 MHz, $CDCl_3$): δ/ppm 1.54-1.57 (m, 1H), 1.78-2.01 (m, 10H), 2.10-2.17 (m, 2H), 2.68 (dt, *J* = 15.2, 3.7 Hz, 1H), 2.91 (bs, 1H), 3.26-3.30 (m, 2H), 3.46-3.54 (m, 2H), 7.01 (m, 1H), 7.07 (m, 1H), 7.20 (m, 1H), 7.43 (m, 1H).

^{13}C NMR (101 MHz, $CDCl_3$): δ/ppm = 28.6(CH), 28.8(CH), 31.3(CH_2), 35.7(CH), 35.8(CH_2), 37.3(CH_2), 37.9(CH_2), 39.1(CH_2), 45.1(C), 45.6(CH_2), 47.6 (CH_2), 59.5 (CH), 126.2 (CH), 126.9 (CH), 128.5 (CH), 131.4 (CH), 138.0 (C), 146.8 (C).

IR (neat): $\tilde{\nu}$/cm^{-1} = 2904, 2847, 1487, 1451, 1342, 1305, 1253, 1156, 1140, 1105, 1060, 1028, 966, 748, 716, 669, 627, 471.

HRMS: m/z =254.1906 ($[M+H]^+$; calculated for $C_{18}H_{24}N^+$ m/z = 254.1903).

2.5.18 Synthesis of cyclic amine 2o

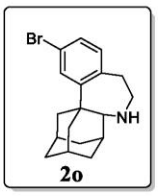

2o

Compound **2o** was synthesized according to *general procedure B* to give an off-white solid in a yield of 84%.

R_f (silica gel; MeOH (1% NH_3 *aq.*):CH_2CL_2 2:98): 0.2.

m.p. (cryst. from CH_2Cl_2): 134.6-136.1 °C.

^{1}H NMR (400 MHz, $CDCl_3$): δ/ppm 1.51-1.54 (m, 1H), 1.78-2.17 (m, 13H), 2.65 (dt, *J* = 15.1, 3.8 Hz, 1H) 3.19-3.23 (m, 2H), 3.35-3.43 (m, 2H), 6.87 (m, 1H), 7.18 (m, 1H), 7.52 (m, 1H).

^{13}C NMR (101 MHz, $CDCl_3$): δ/ppm = 28.5 (CH), 28.6 (CH), 31.1 (CH_2), 35.9 (CH), 36.0 (CH_2), 37.1 (CH_2), 37.7 (CH_2), 38.8 (CH_2), 45.1 (CH_2), 45.4 (CH_2), 47.4 (CH_2), 59.1 (CH), 120.7 (C), 128.9 (CH), 131.5 (CH), 132.9 (CH), 137.5 (C),149.5 (C).

IR (neat): $\tilde{\nu}$ /cm^{-1} = 2910, 2850, 1585, 1556, 1483, 1452, 1440, 1391, 1186, 1158, 1143, 1100, 1028, 1006, 989, 966, 878, 810, 792, 721, 671, 621, 575, 472.

HRMS: m/z = 332.1007 ([M+H]$^+$; calculated for $C_{18}H_{23}BrN^+$ m/z = 332.1009).

2.5.19 Synthesis of amine 4a

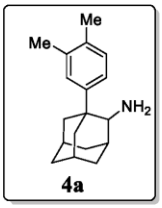

4a

Compound **4a** was synthesized according to *general procedure C* to give an off-white solid in a yield of 40%.

R$_f$ (silica gel; MeOH (1% NH_3 *aq.*):CH_2CL_2 3:97): 0.2.

m.p. (cryst. from EtOAc): 93.2-94.4 °C.

^{1}H NMR (400 MHz, $CDCl_3$): δ/ppm = 1.55 (m, 1H), 1.65-1.68 (m, 3H), 1.74-1.79 (m, 2H), 1.91 (m, 2H), 1.95-2.09 (m, 5H), 2.24 (s, 3H), 2.27 (s, 3H), 2.32 (m, 1H), 3.21 (m, 1H), 7.05-7.12 (m, 3H).

^{13}C NMR (101 MHz, $CDCl_3$): δ/ppm = 19.3 (CH_3), 20.1 (CH_3), 28.3 (CH), 28.8 (CH), 30.1 (CH_2), 33.7 (CH_2), 34.6 (CH), 37.2 (CH_2), 37.9 (CH_2), 40.4 (C), 45.0 (CH_2), 59.2 (CH), 123.0 (CH), 126.9 (CH), 129.7 (CH), 134.1 (C), 136.4 (C), 145.4 (C).

IR (neat): $\tilde{\nu}$ /cm^{-1} = 2908, 2852, 1706, 1505, 1449, 1383, 1259, 1176, 1112, 1092, 1061, 1031, 879, 813, 798, 716, 596, 439.

HRMS: m/z =256.2061 ([M+H]$^+$; calculated for $C_{18}H_{26}N^+$ m/z =256.2060).

2.5.20 Synthesis of amine 4b

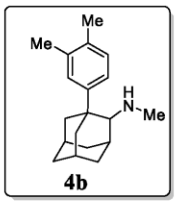

4b

Compound **4b** was synthesized according to *general procedure C* to give an off-white solid in a yield of 97%.

R_f (silica gel; MeOH (1% NH_3 *aq.*):CH_2CL_2 1:99): 0.1.

m.p. (cryst. from EtOAc): 76.6-78.0 °C.

^{1}H NMR (400 MHz, $CDCl_3$): δ/ppm = 1.47 (m, 1H), 1.58-1.68 (m, 2H), 1.72-1.77 (m, 2H), 1.85 (m, 1H), 1.93-2.00 (m, 2H), 2.06-2.09 (m, 4H), 2.16 (s, 3H), 2.25 (d, *J* = 10.2 Hz, 6H), 2.45 (m, 1H), 2.80 (m, 1H), 7.09-7.12 (m, 3H).

^{13}C NMR (101 MHz, $CDCl_3$): δ/ppm = 19.4 (CH_3), 20.2 (CH_3), 28.5 (CH), 29.1 (CH), 29.8 (CH), 30.2 (CH_2), 34.6 (CH_3), 35.0 (CH_2), 37.3 (CH_2), 37.4 (CH_2), 40.2 (C), 45.7 (CH_2), 68.2 (CH), 123.0 (CH), 126.9 (CH), 129.8 (CH), 134.2 (C), 136.4 (C), 145.6 (C).

IR (neat): $\tilde{\nu}$ /cm^{-1} = 3333, 2899, 2845, 2782, 1612, 1573, 1505, 1476, 1446, 1360, 1346, 1151, 1129, 1102, 1065, 1024, 998, 969, 897, 882, 823, 808, 782, 741, 721, 658, 598, 533, 514, 442.

HRMS: m/z = 270.2218 ($[M+H]^+$; calculated for $C_{19}H_{28}N^+$ m/z =270.2216).

2.5.21 Synthesis of amine 4c

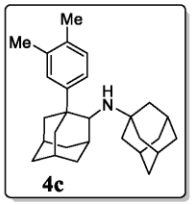

4c

Compound **4c** was synthesized according to *general procedure C* to give a white solid in a yield of 56%.

R_f (silica gel; MeOH (1% NH_3 *aq.*):CH_2CL_2 3:97): 0.4.

m.p. (cryst. from $CDCl_3$): 190.3-191.4 °C.

^{1}H NMR (400 MHz, $CDCl_3$): δ/ppm = 1.10-1.13 (m, 3H), 1.34-1.37 (m, 3H), 1.41-1.47 (m, 4H), 1.51-1.54 (m, 3H), 1.61-1.64 (m, 3H), 1.72-1.75 (m, 1H), 1.88 (m, 6H), 1.95 (m, 1H), 2.03 (m, 1H), 2.15-2.18 (m, 1H), 2.23 (s, 3H), 2.25 (s, 3H), 2.29-2.38 (m, 2H), 3.10 (m, 1H), 7.04-7.07 (m, 2H), 7.11 (m, 1H).

^{13}C NMR (101 MHz, $CDCl_3$): δ/ppm = 19.4 (CH3), 20.1 (CH3), 28.4 (CH), 28.8 (CH), 29.9 (3CH), 30.5 (CH2), 35.1 (CH2), 35.5 (CH), 36.9 (3CH2), 37.3 (CH2), 37.4 (CH2), 40.3 (C), 43.9 (3CH2), 45.8 (CH2), 50.4 (C), 58.2 (CH), 123.5 (CH), 127.6 (CH), 129.3 (CH), 133.8 (C), 135.8 (C), 145.8 (C).

IR (neat): $\tilde{\nu}$ /cm^{-1} =2899, 2846, 1503, 1446, 1354, 1307, 1147, 1099, 991, 882, 808, 714, 656, 588, 527, 441.

HRMS: m/z = 390.3159 ([M+H]$^+$; calculated for $C_{28}H_{39}N^+$ m/z = 390.3156).

2.5.22 Synthesis of salt 4d$_s$

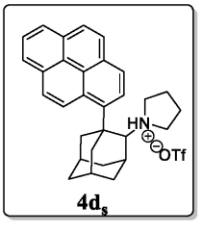

4d$_s$

Compound **4d$_s$** was synthesized according to *general procedure B*, with slight modification. Only 0.3 mL of 1,2-dichlorobenzene were used to solve the starting materials, and 572 mg (10 eq., 2.8 mmol) of pyrene (10 eq.) were added to the reaction mixture. The temperature was raised to 200 °C. After 3 h, the solvent was evaporated and the crude residue was purified by flash column chromatography on silica gel (mobile phase: 10% MeOH in CH_2CL_2) to give the triflic acid salt as white solid in a yield of 30% (62 mg, 0.1 mmol).

R$_f$ (silica gel; MeOH:CH_2CL_2 1:9): 0.4.

m.p. (cryst. from $CDCl_3$): 301.2-302.4 °C.

^{1}H NMR (400 MHz, $CDCl_3$): δ/ppm = 1.58 (m, 2H), 1.71-1.91 (m, 7H), 2.20-2.25 (m, 4H), 2.33-2.42 (m, 2H), 2.54-2.62 (m, 2H), 2.92 (m, 1H), 3.31 (m, 1H), 3.42 (m, 1H), 3.85 (m, 1H), 4.69 (m, 1H), 8.02-8.09 (m, 3H), 8.14-8.31 (m, 6H), 8.61 (m, 1H).

^{13}C NMR (101 MHz, CD_2Cl_2): δ/ppm = 20.9 (CH_2), 22.9 (CH_2), 27.7 (CH), 28.0 (CH), 29.6 (CH_2), 31.8 (CH), 36.5 (CH_2), 36.6 (CH_2), 37.9 (CH_2), 42.7 (C), 45.0 (CH_2), 54.4 (CH_2), 55.8 (CH_2), 74.2 (CH_2), 124.1 (CH), 125.2 (CH), 125.2 (CH), 125.3 (CH), 125.9 (CH), 126.0 (C), 126.2 (CH), 126.3 (CH), 127.4 (CH), 127.6 (CH), 127.7 (CH), 128.9 (C), 129.9 (C), 131.0 (C), 131.5 (C), 139.0 (C).

IR (neat): $\tilde{\nu}$ /cm^{-1} = 3047, 2915, 1602, 1459, 1414, 1282, 1238, 1222, 1156, 1028, 848, 758, 726, 684, 636, 573, 516.

HRMS: m/z =406.2544 ($[M+H]^+$; calculated for $C_{30}H_{32}N^+$ m/z =406.2529).

2.6 NMR spectra of compounds **2a-o** and **4a-d**

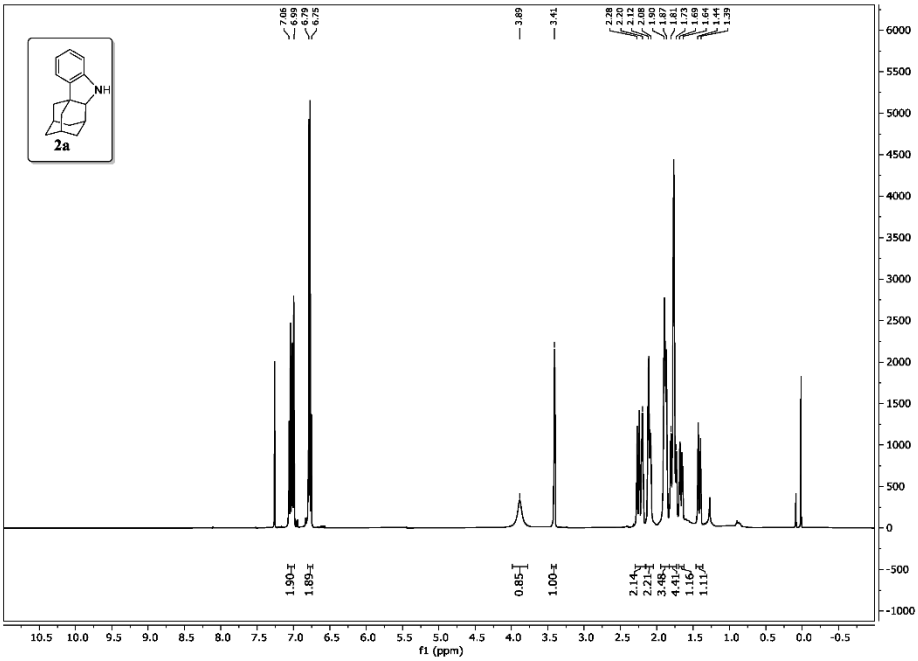
2a
NH
7.06
6.99
6.79
6.75
3.89
3.41
2.28
2.20
2.12
2.08
1.90
1.87
1.81
1.73
1.69
1.64
1.44
1.39
1.90
1.89
0.85
1.00
2.14
2.21
3.48
4.41
1.16
1.11
f1 (ppm)

S85

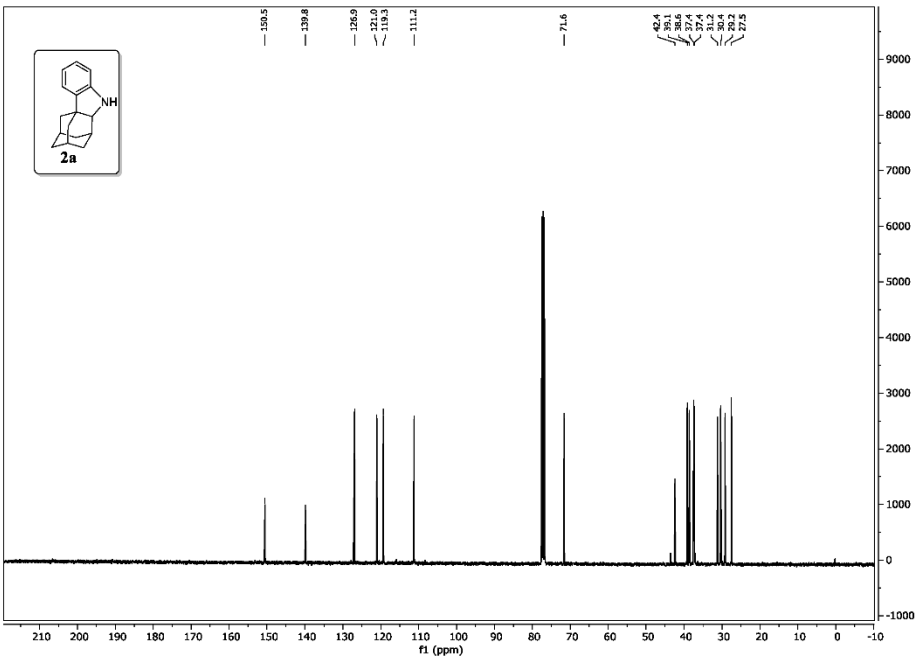
2a
NH
150.5
139.8
126.9
121.0
119.3
111.2
71.6
42.4
39.1
38.6
37.7
37.4
31.2
30.4
28.2
27.5
f1 (ppm)

S86

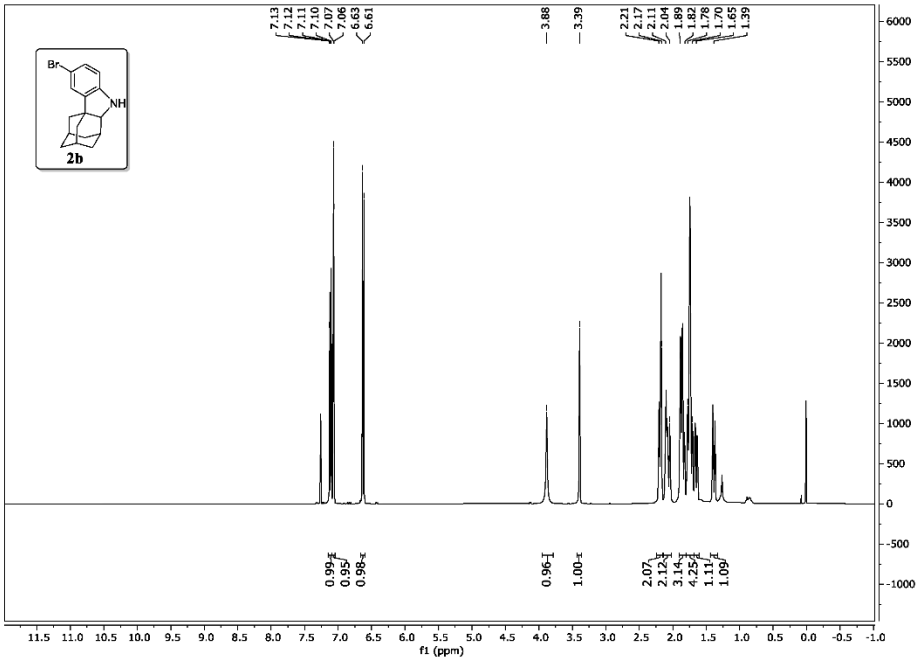
7.13
7.12
7.11
7.10
7.07
7.06
6.63
6.61
3.88
3.39
2.21
2.17
2.11
2.04
1.89
1.82
1.78
1.70
1.65
1.39
Br
NH
2b
0.99
0.95
0.98
0.96
1.00
2.07
2.12
3.14
4.25
1.11
1.09
f1 (ppm)

S87

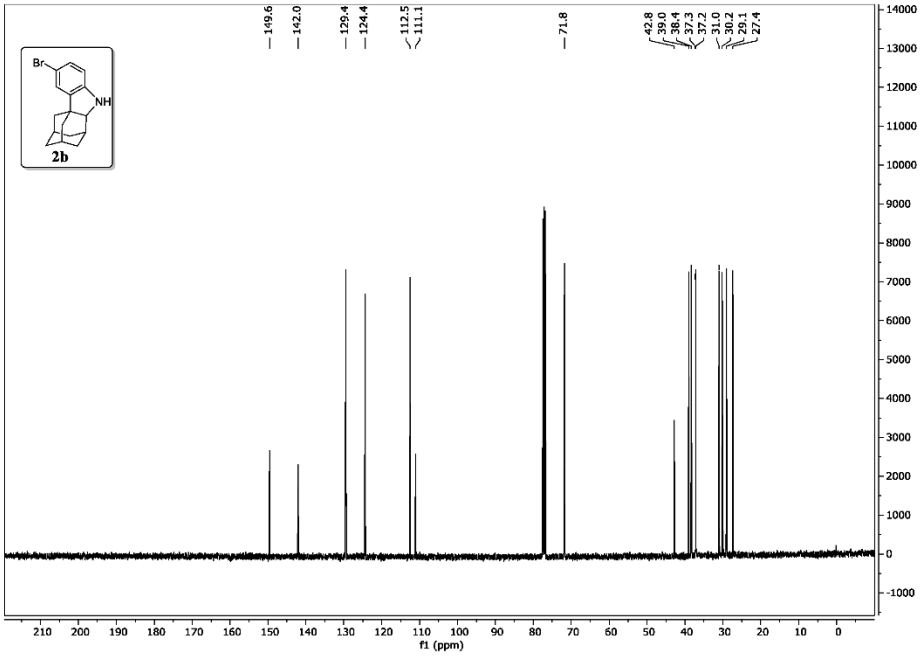
149.6
142.0
129.4
124.4
112.5
111.1
71.8
42.8
39.0
38.4
37.3
37.2
31.0
30.2
29.1
27.4
Br
NH
2b
f1 (ppm)

S88

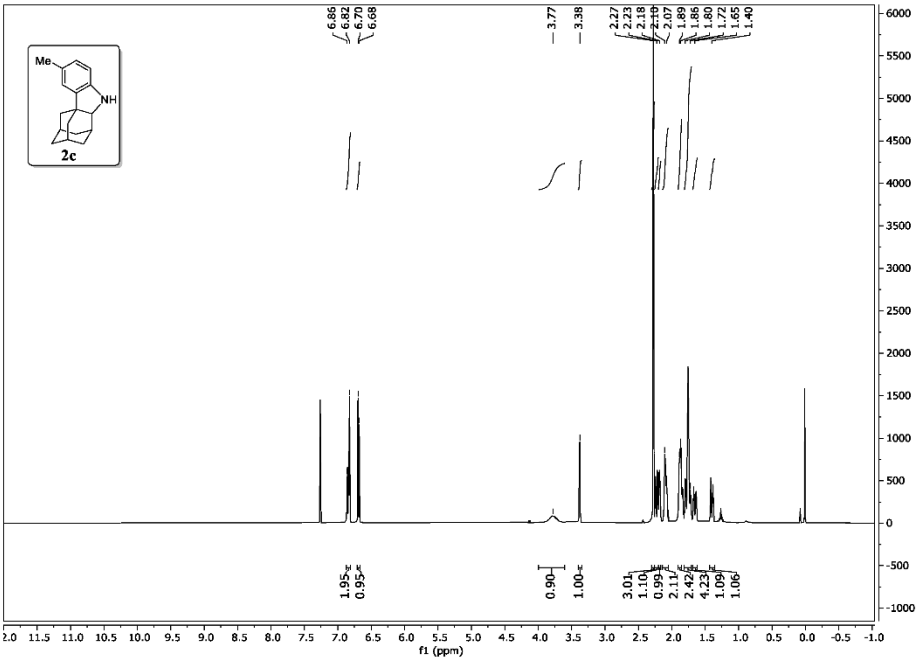
6.86
6.82
6.70
6.68
3.77
3.38
2.27
2.23
2.18
2.10
2.07
1.89
1.86
1.80
1.72
1.65
1.40
Me
NH
2c
1.95
0.95
0.90
1.00
3.01
1.10
0.99
2.11
2.42
4.23
1.09
1.06
f1 (ppm)

S89

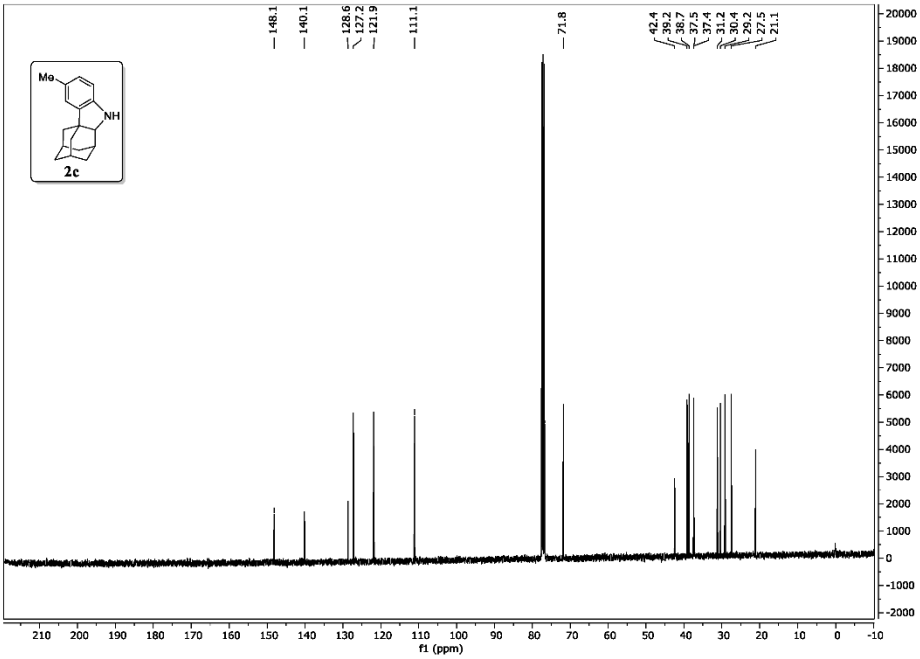
148.1
140.1
128.6
127.2
121.9
111.1
71.8
42.4
39.2
38.7
37.5
37.4
31.2
30.4
29.2
27.5
21.1
Me
NH
2c
f1 (ppm)

S90

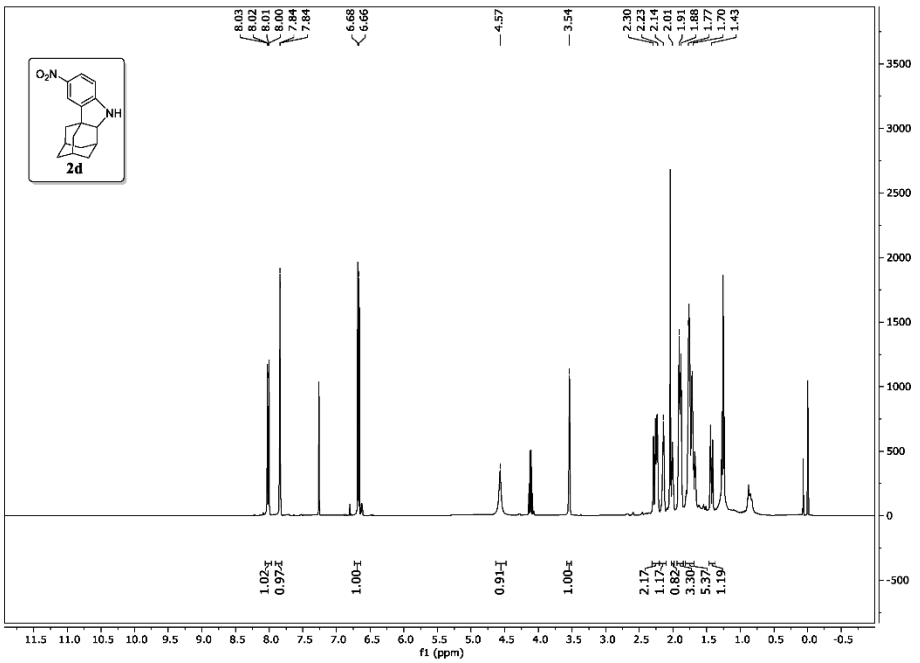
8.03
8.02
8.01
8.00
7.84
7.84
6.68
6.66
4.57
3.54
2.30
2.23
2.14
2.01
1.91
1.88
1.77
1.70
1.43
2d
1.02
0.97
1.00
0.91
1.00
2.17
1.17
0.82
3.30
5.37
1.19
f1 (ppm)

S91

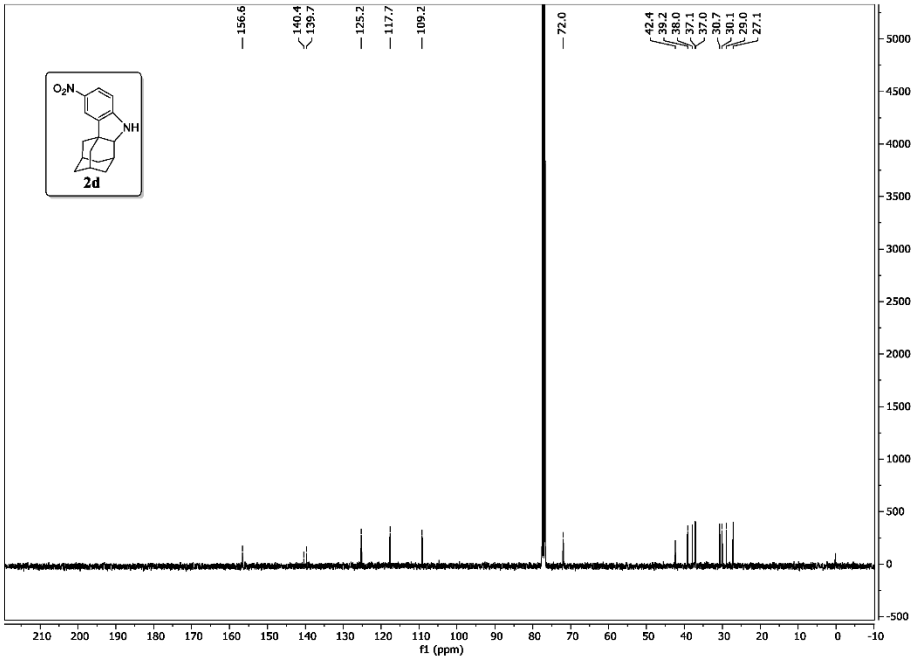
156.6
140.4
139.7
125.2
117.7
109.2
72.0
42.4
39.2
38.0
37.1
37.0
30.7
30.1
29.0
27.1
2d
f1 (ppm)

S92

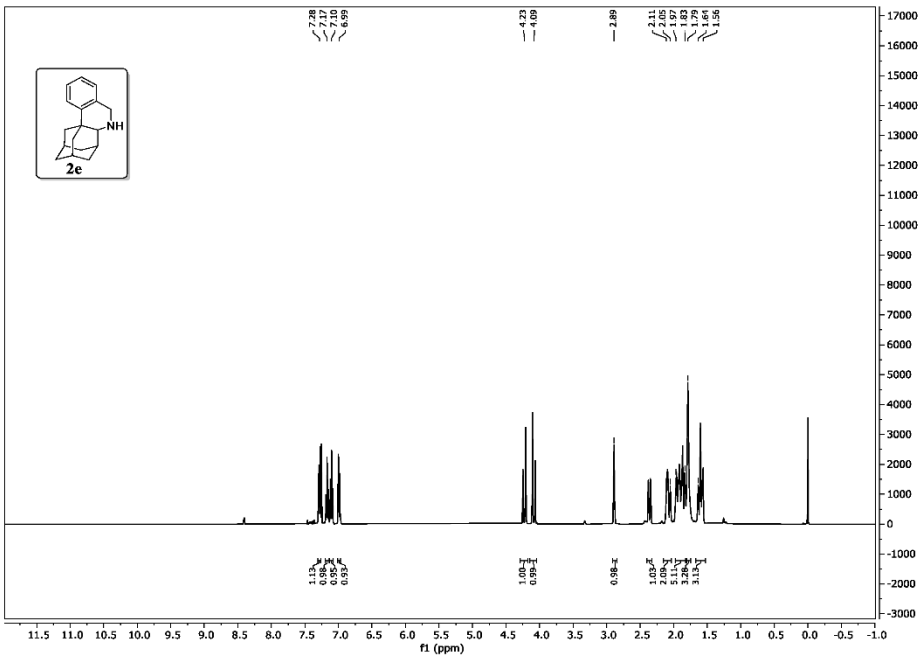

S93

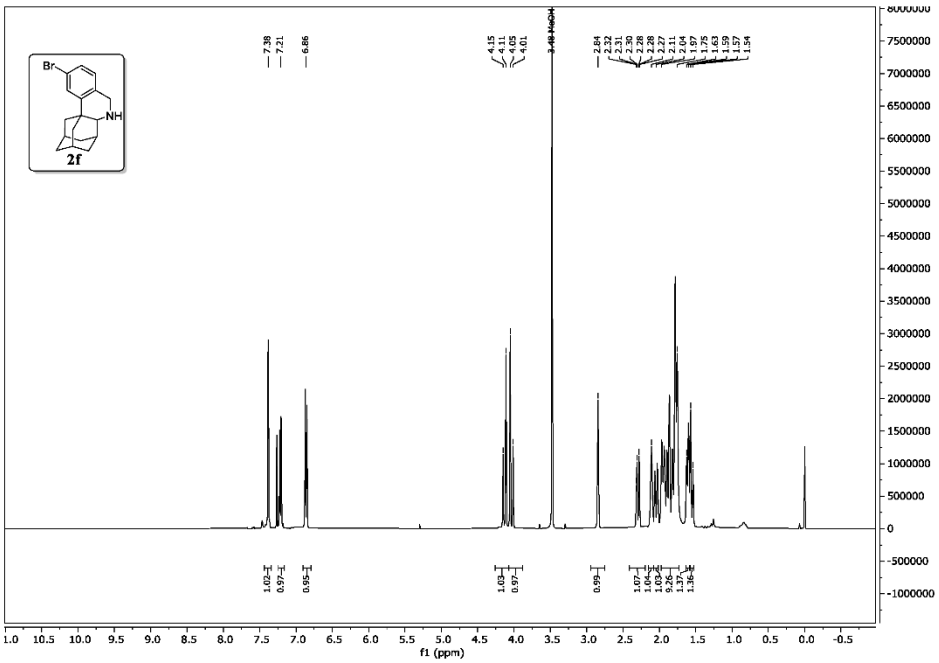

S94

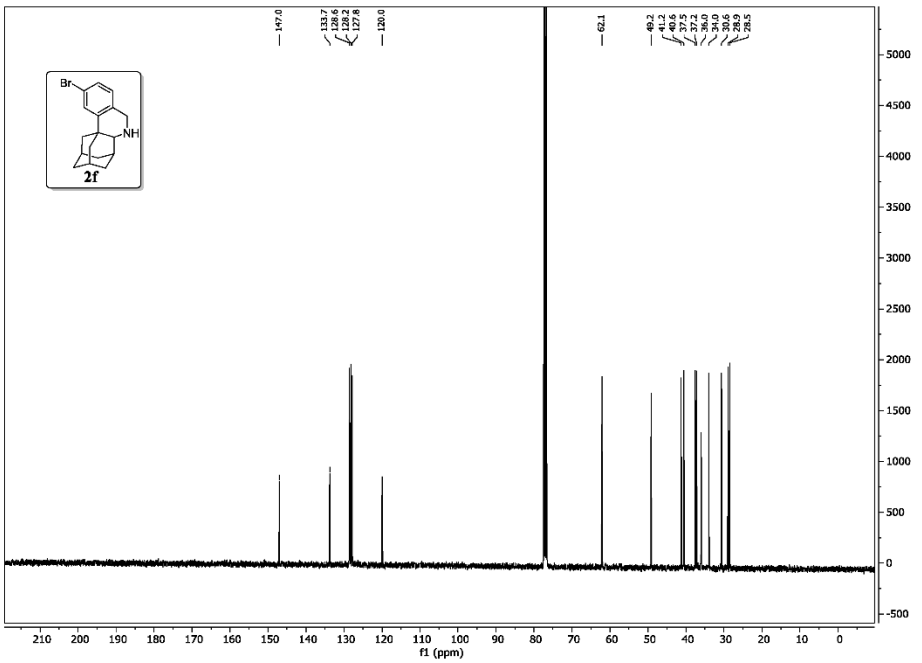
Br
NH
2f
147.0
133.7
128.6
128.2
127.8
120.0
62.1
49.2
41.2
40.6
37.5
37.4
36.0
34.0
30.6
28.9
28.5
f1 (ppm)

S95

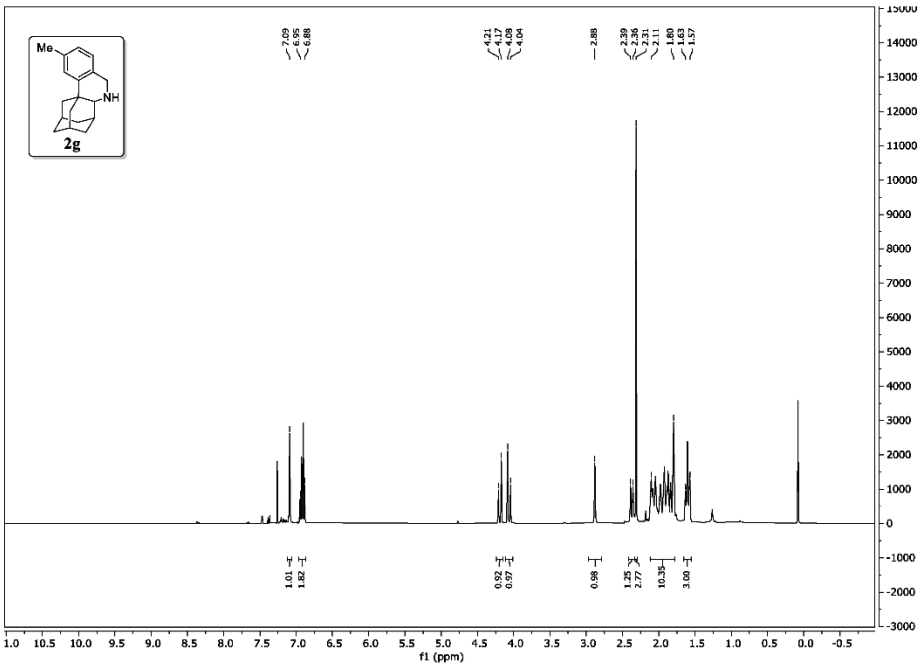
Me
NH
2g
7.09
6.95
6.88
4.21
4.17
4.08
4.04
2.88
2.39
2.36
2.31
2.11
1.60
1.45
1.57
1.01
1.82
0.92
0.97
0.98
1.26
2.77
10.38
3.00
f1 (ppm)

S96

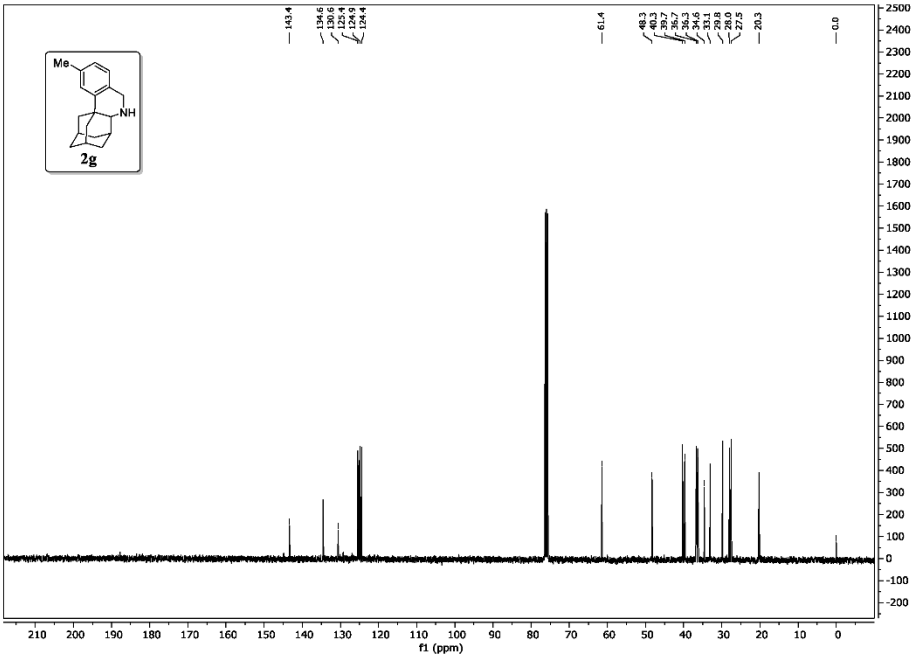
Me
NH
2g
143.4
134.6
130.6
125.4
124.9
124.4
61.4
48.3
40.3
39.7
36.7
36.3
34.6
33.1
29.8
28.0
27.5
20.3
0.0
f1 (ppm)

S97

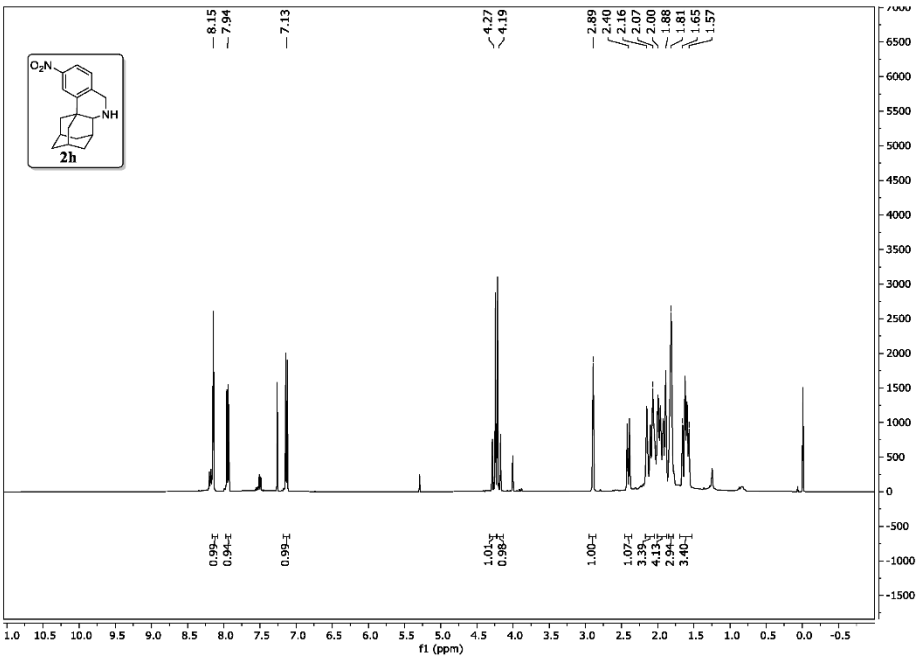
O2N
NH
2h
8.15
7.94
7.13
4.27
4.19
2.89
2.40
2.16
2.07
2.00
1.88
1.81
1.65
1.57
0.99
0.94
0.99
1.01
0.98
1.00
1.07
3.39
4.13
2.94
3.40
f1 (ppm)

S98

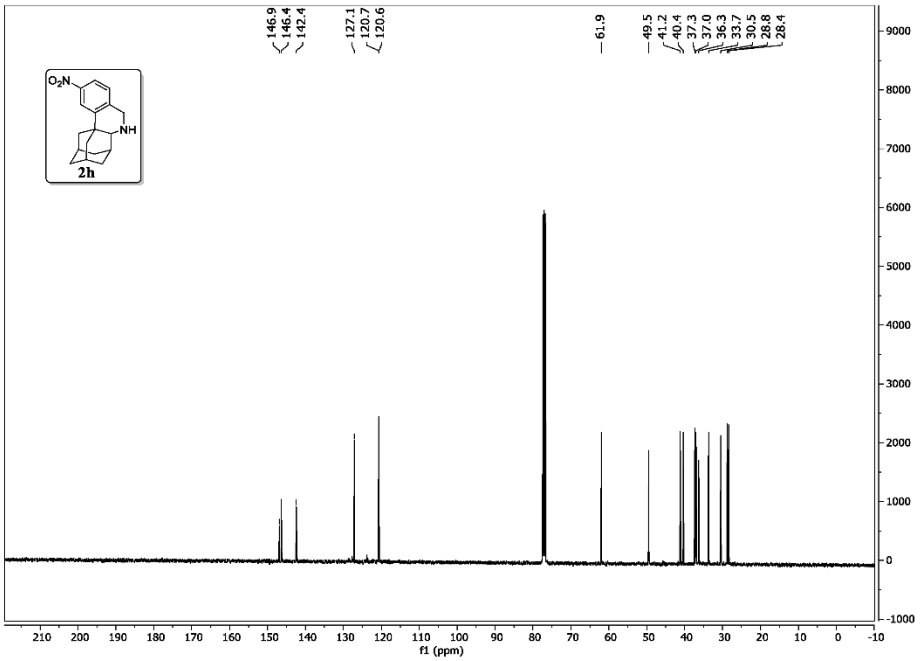

S99

diastereomer 1

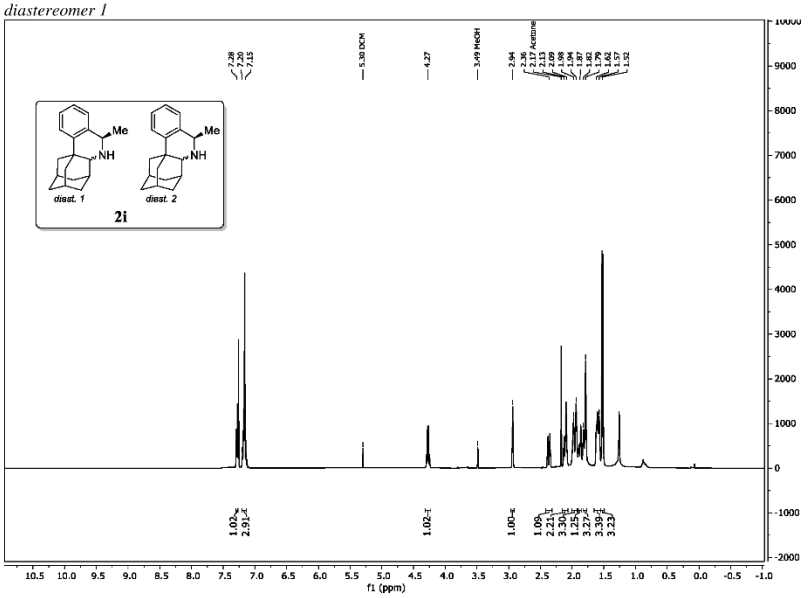

S100

diastereomer 2

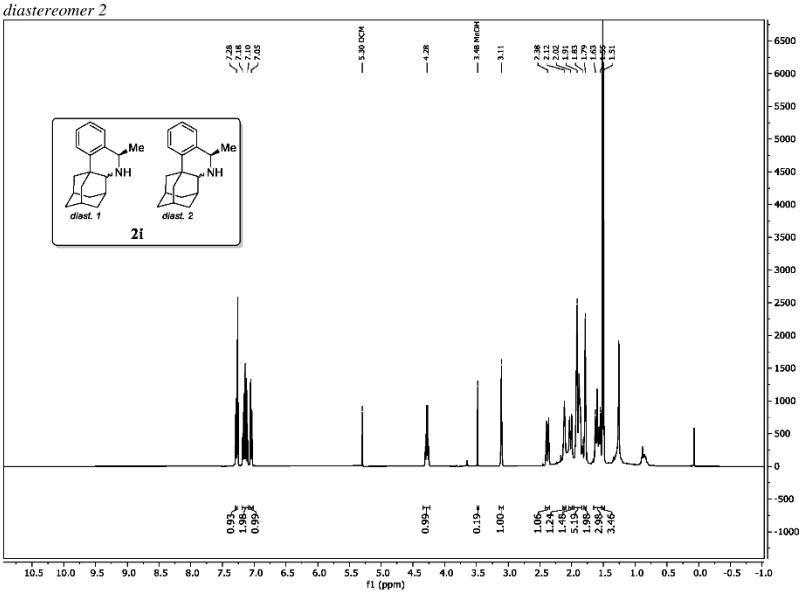

S101

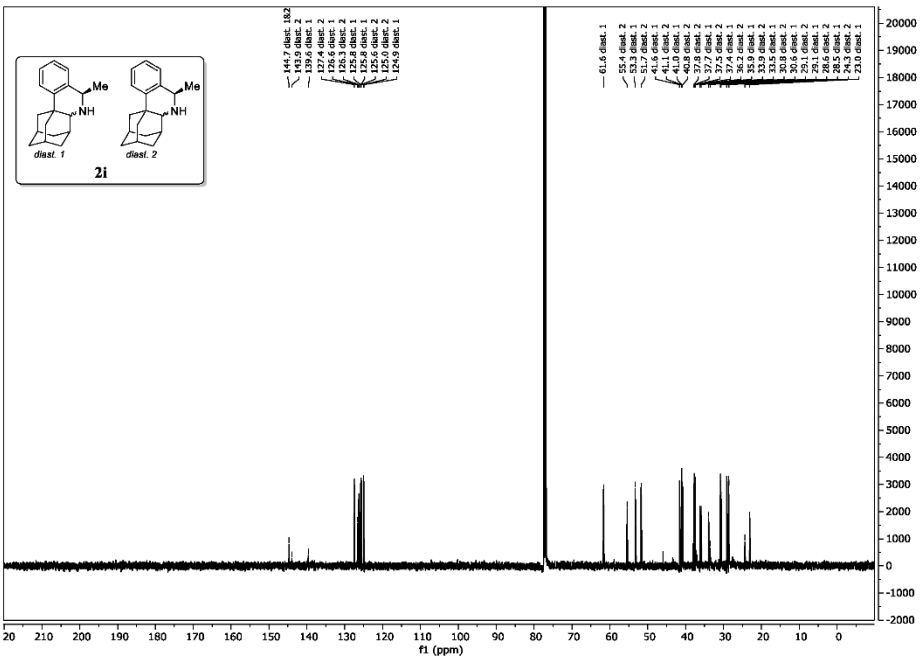

S102

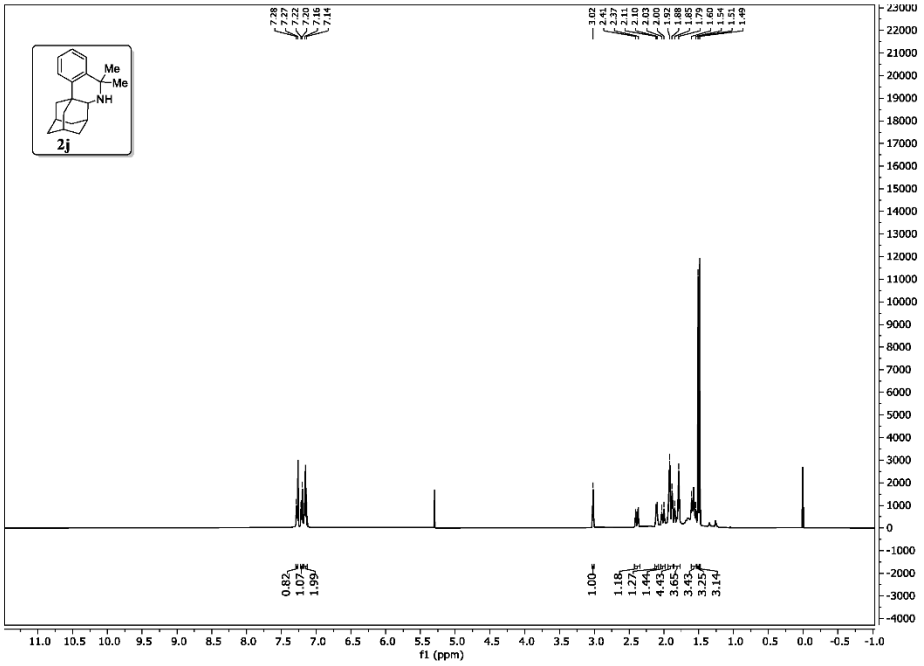

S103

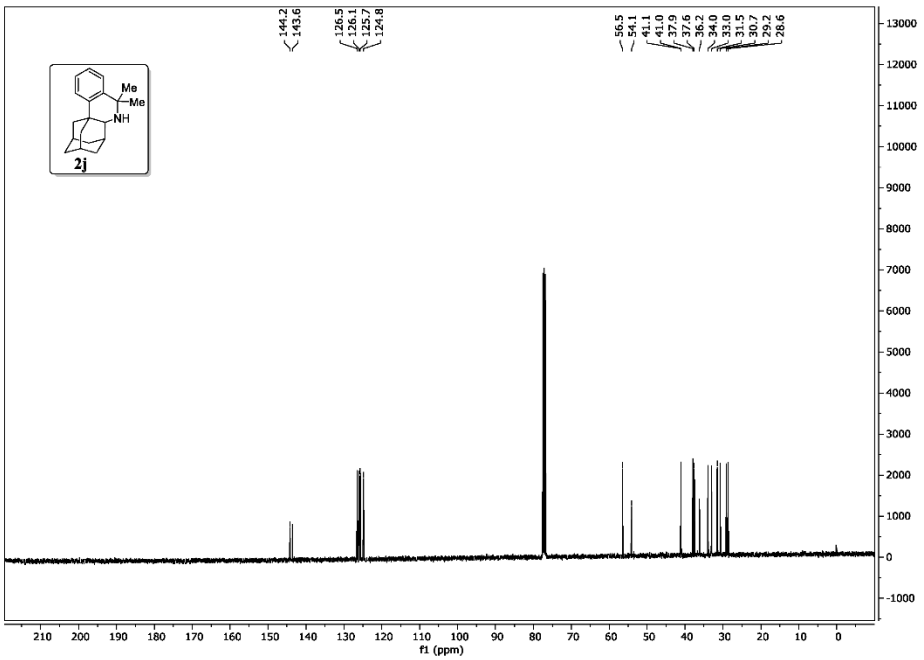

S104

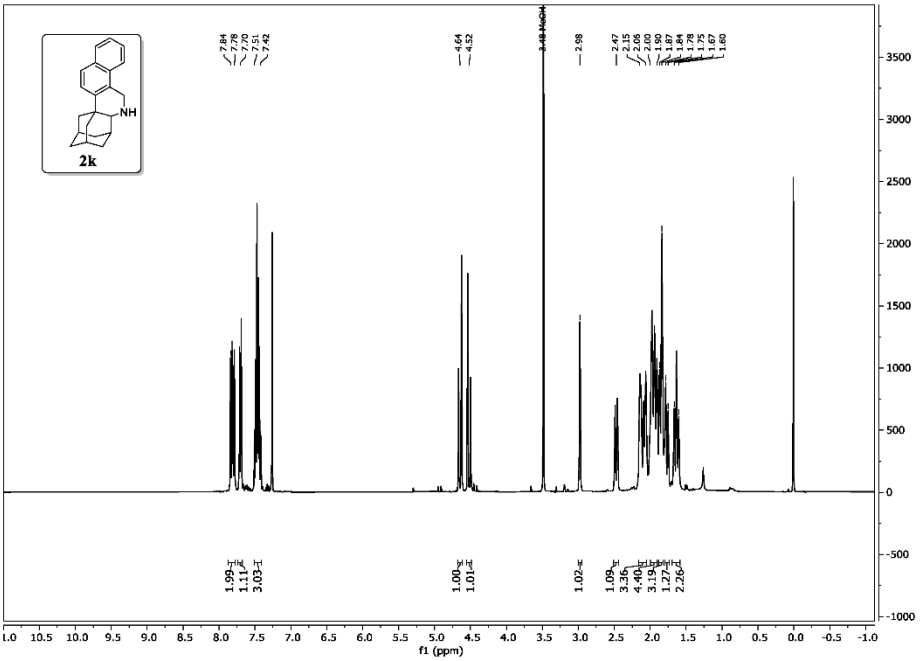
2k
NH
7.84
7.78
7.70
7.51
7.42
4.64
4.52
3.48 H2O/H
2.98
2.47
2.15
2.06
2.00
1.90
1.87
1.84
1.78
1.75
1.67
1.60
1.99
1.11
3.03
1.00
1.01
1.02
1.09
3.36
4.40
3.19
1.27
2.26
f1 (ppm)

S105

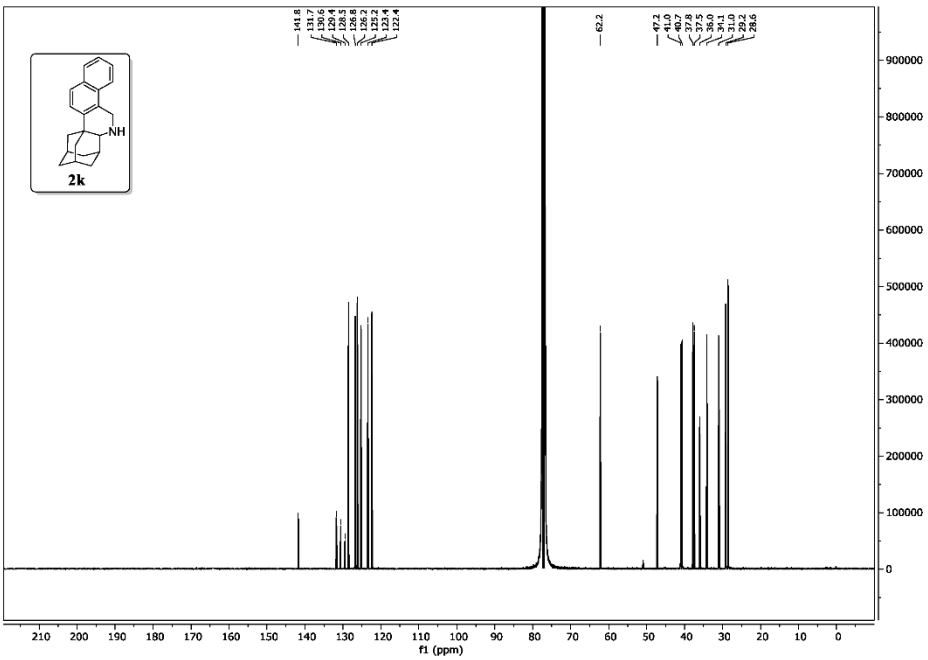
2k
NH
141.8
131.7
130.6
129.4
128.5
126.8
126.2
125.2
123.4
122.4
62.2
47.2
41.0
40.7
39.8
37.5
36.0
34.1
31.0
29.2
28.6
f1 (ppm)

S106

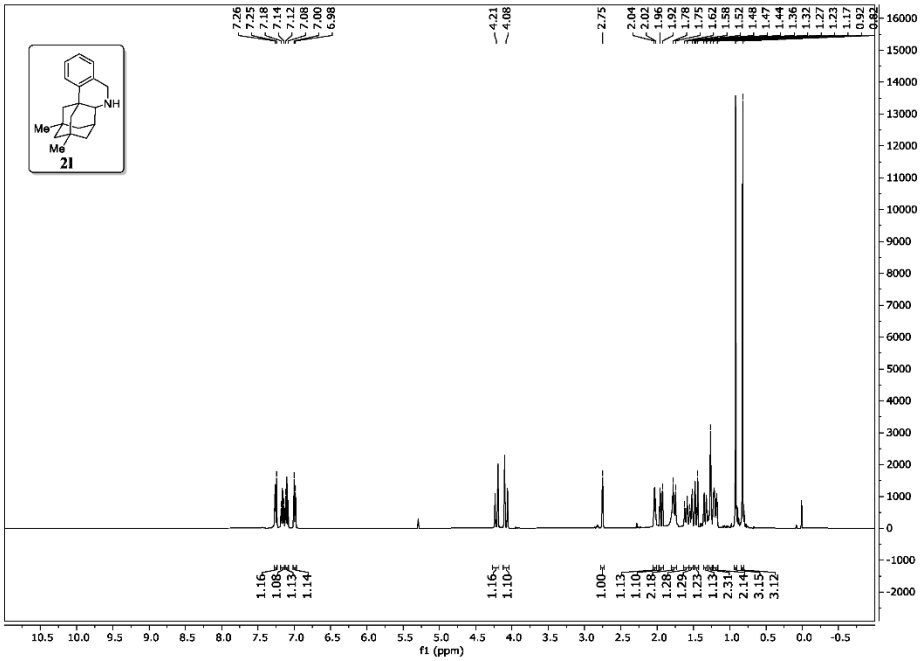
7.26
7.25
7.18
7.14
7.13
7.08
7.00
6.98
4.21
4.08
2.75
2.04
2.02
1.96
1.92
1.78
1.75
1.62
1.58
1.52
1.51
1.48
1.47
1.44
1.36
1.32
1.27
1.23
1.17
0.92
0.82
NH
Me
Me
2l
1.16
1.08
1.13
1.14
1.16
1.10
1.00
1.13
1.10
2.18
1.28
1.29
1.23
1.13
2.31
2.14
3.15
3.12
f1 (ppm)

S107

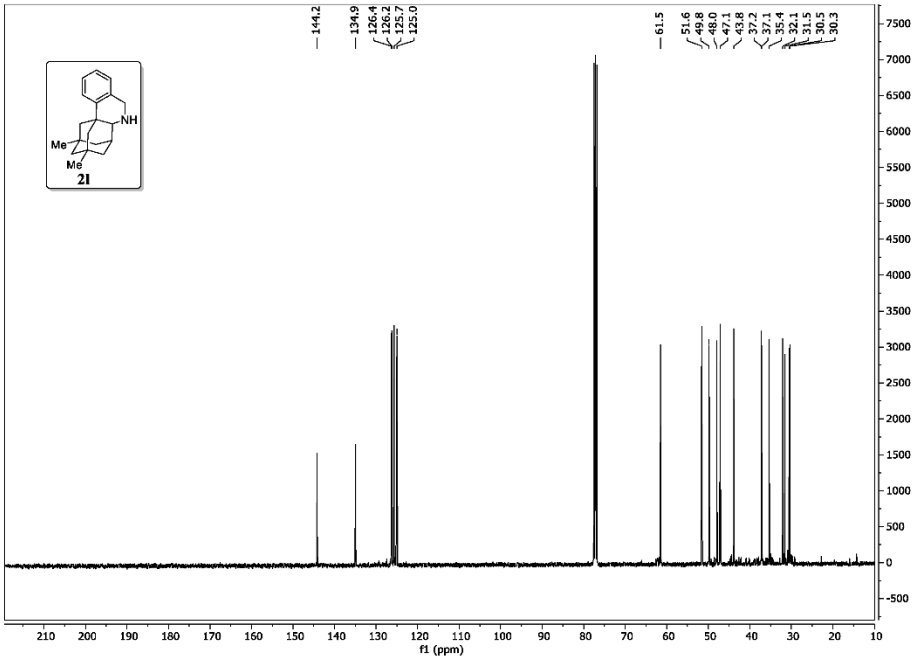
144.2
134.9
126.4
126.2
125.7
125.0
61.5
51.6
49.8
48.0
47.1
43.8
37.2
37.1
35.4
32.1
31.5
30.5
30.3
NH
Me
Me
2l
f1 (ppm)

S108

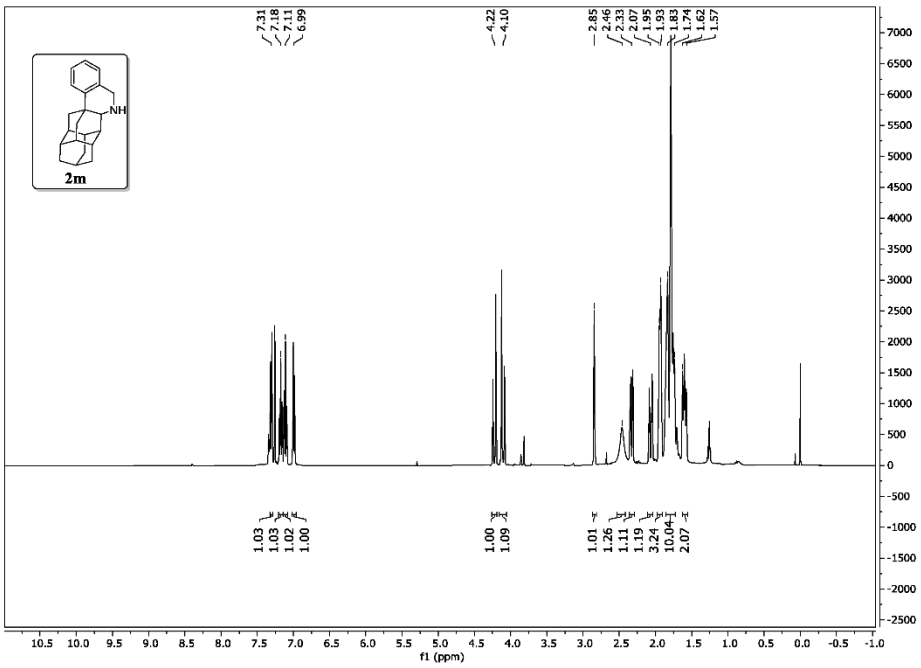
7.31
7.18
7.11
6.99
4.22
4.10
2.85
2.46
2.33
2.07
1.95
1.93
1.83
1.74
1.62
1.57
NH
2m
1.03
1.03
1.02
1.00
1.00
1.09
1.01
1.26
1.11
1.19
3.24
10.04
2.07
f1 (ppm)

S109

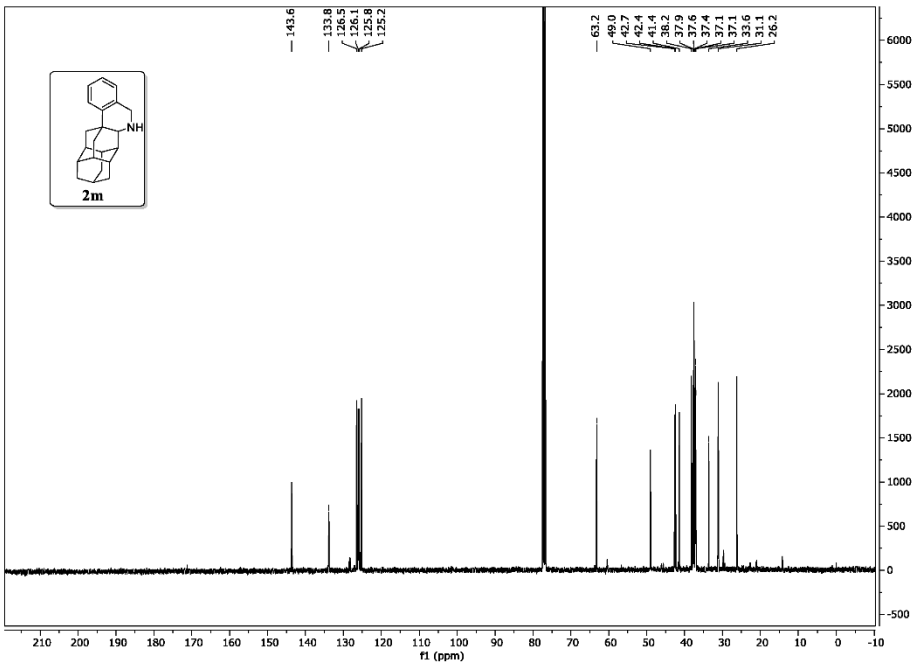
143.6
133.8
126.5
126.1
125.8
125.2
63.2
49.0
42.7
42.4
41.4
38.2
37.9
37.6
37.4
37.1
33.6
31.1
26.2
NH
2m
f1 (ppm)

S110

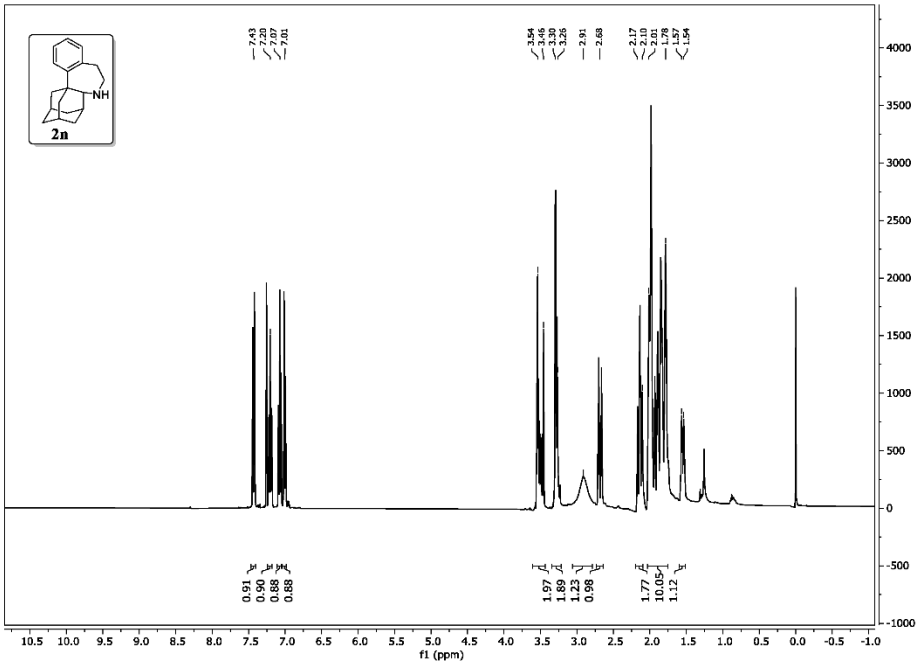
2n
NH
7.43
7.39
7.07
7.01
3.54
3.46
3.30
3.26
2.91
2.68
2.17
2.10
2.01
1.78
1.57
1.54
0.91
0.90
0.88
0.88
1.97
1.89
1.23
0.98
1.77
10.05
1.12
f1 (ppm)

S111

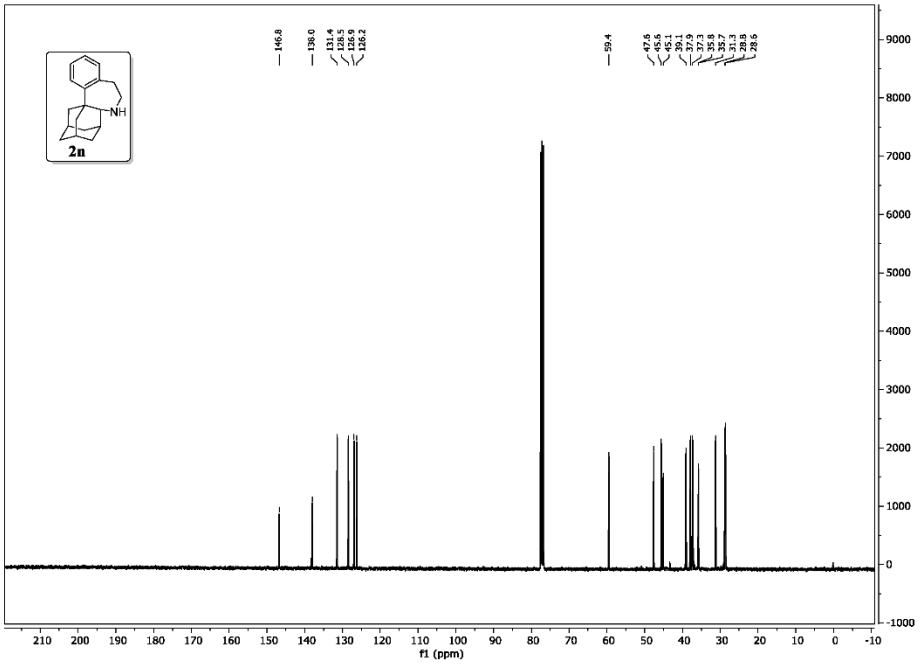
2n
NH
146.8
138.0
131.4
128.5
126.9
126.2
59.4
47.6
45.6
45.1
39.1
37.9
37.3
35.8
35.7
31.3
28.8
28.6
f1 (ppm)

S112

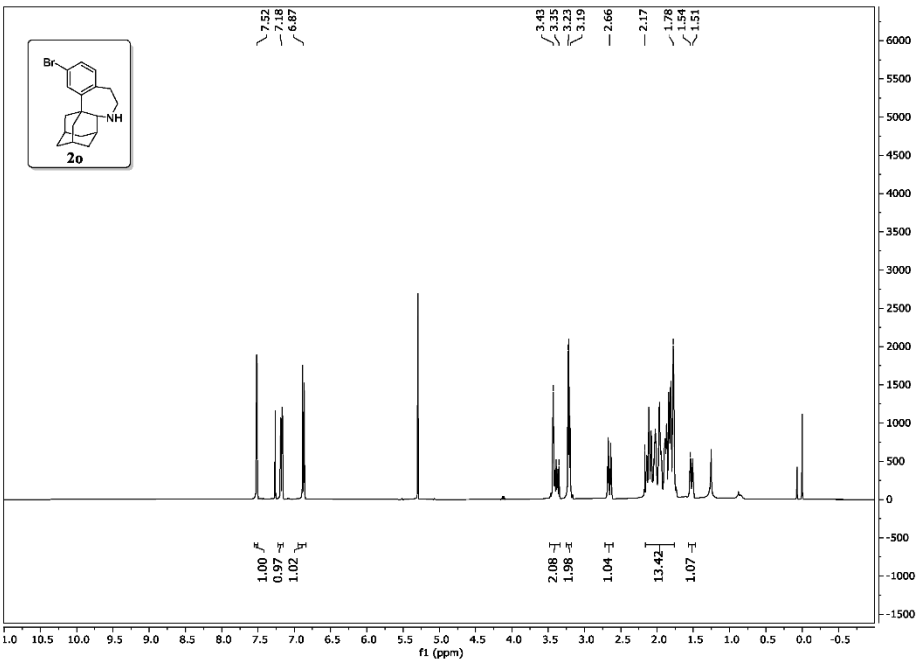
7.52
7.18
6.87
3.43
3.35
3.23
3.19
2.66
2.17
1.78
1.54
1.51
1.00
0.97
1.02
2.08
1.98
1.04
13.42
1.07
Br
NH
2o
f1 (ppm)

S113

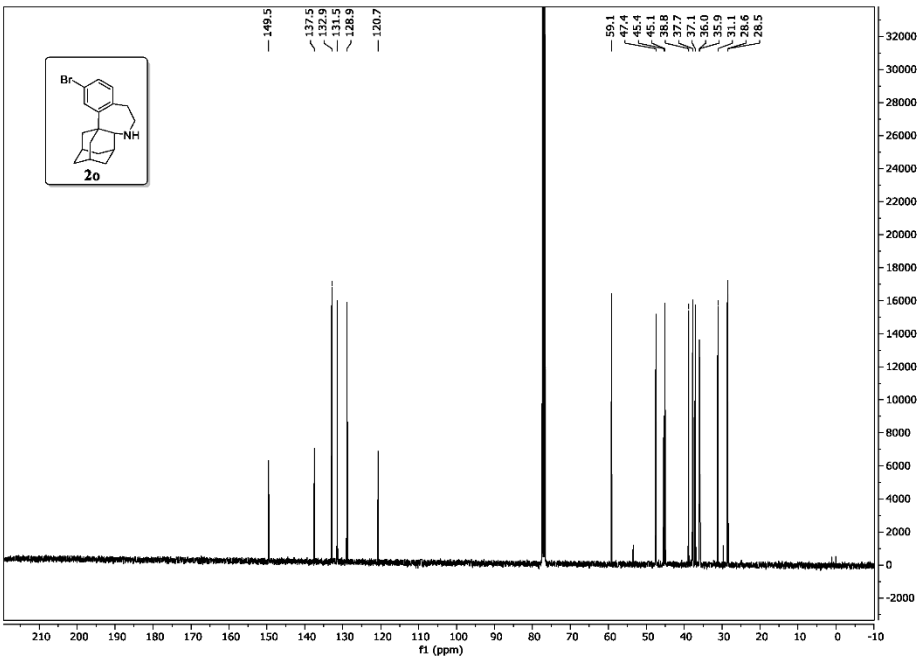
149.5
137.5
132.9
131.5
128.9
120.7
59.1
47.4
45.4
45.1
38.8
37.7
37.1
36.0
35.9
31.1
28.6
28.5
Br
NH
2o
f1 (ppm)

S114

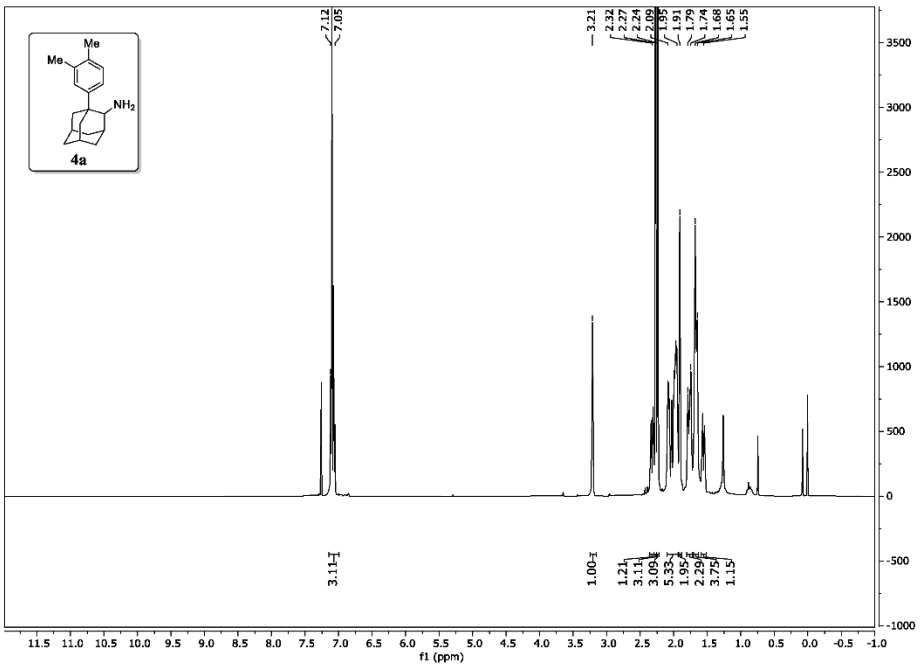
Me
Me
NH2
4a
7.12
7.05
3.21
2.32
2.27
2.24
2.09
1.95
1.91
1.79
1.74
1.68
1.65
1.55
3.11
1.00
1.21
3.11
3.09
5.32
1.95
2.29
3.75
1.15
f1 (ppm)

S115

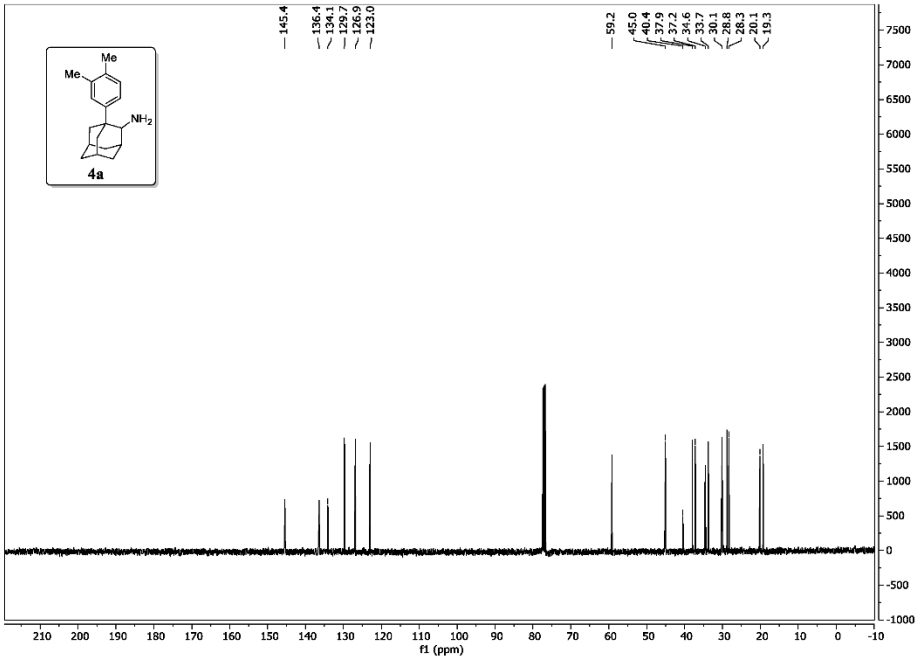
Me
Me
NH2
4a
145.4
136.4
134.1
129.7
126.9
123.0
59.2
45.0
40.4
37.9
37.2
34.6
33.7
30.1
28.8
28.3
20.1
19.3
f1 (ppm)

S116

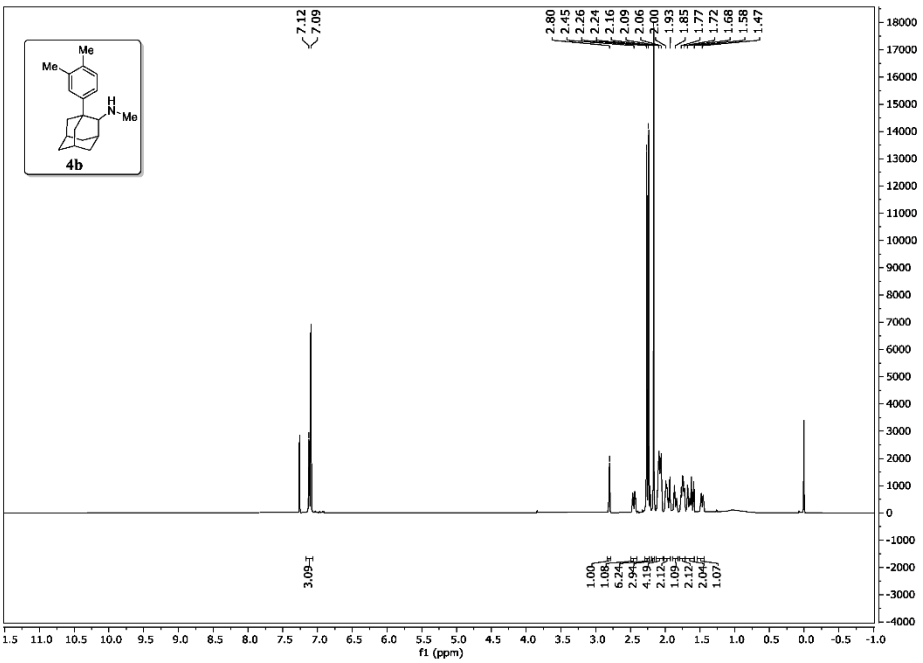
7.12
7.09
2.80
2.45
2.26
2.24
2.16
2.09
2.06
2.00
1.93
1.85
1.77
1.72
1.68
1.58
1.47
Me
Me
H
N
Me
4b
3.09
1.00
1.08
6.24
2.94
4.19
2.12
1.09
2.12
2.04
1.07
f1 (ppm)

S117

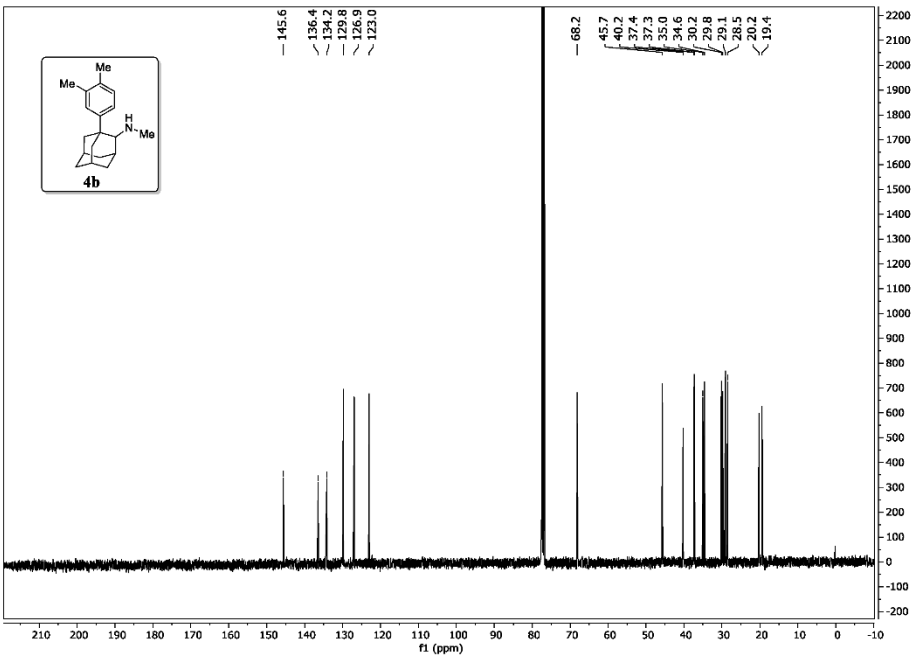
145.6
136.4
134.2
129.8
126.9
123.0
68.2
45.7
40.2
37.4
37.3
35.0
34.6
30.2
29.8
29.1
28.5
20.2
19.4
Me
Me
H
N
Me
4b
f1 (ppm)

S118

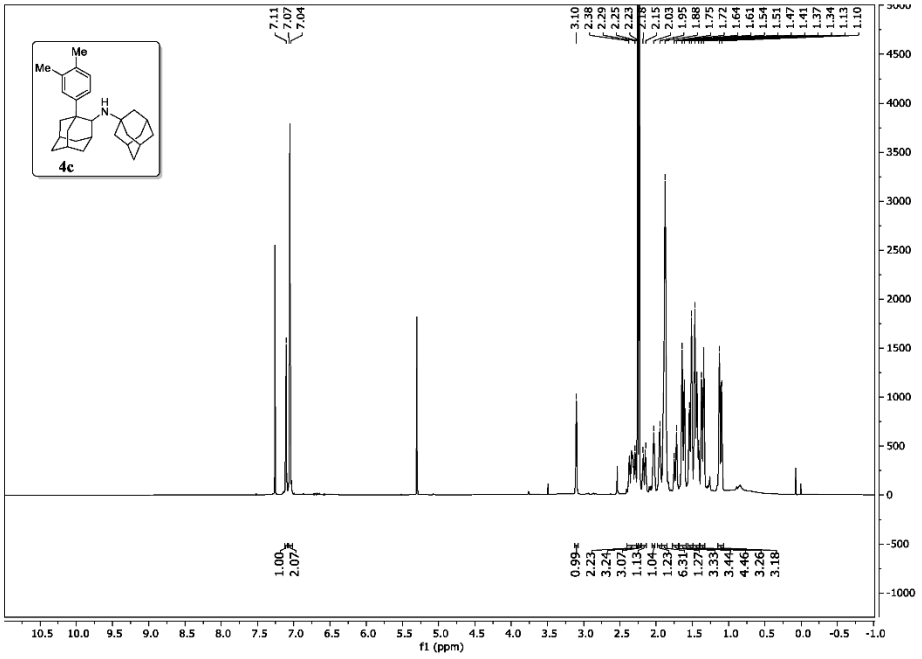

S119

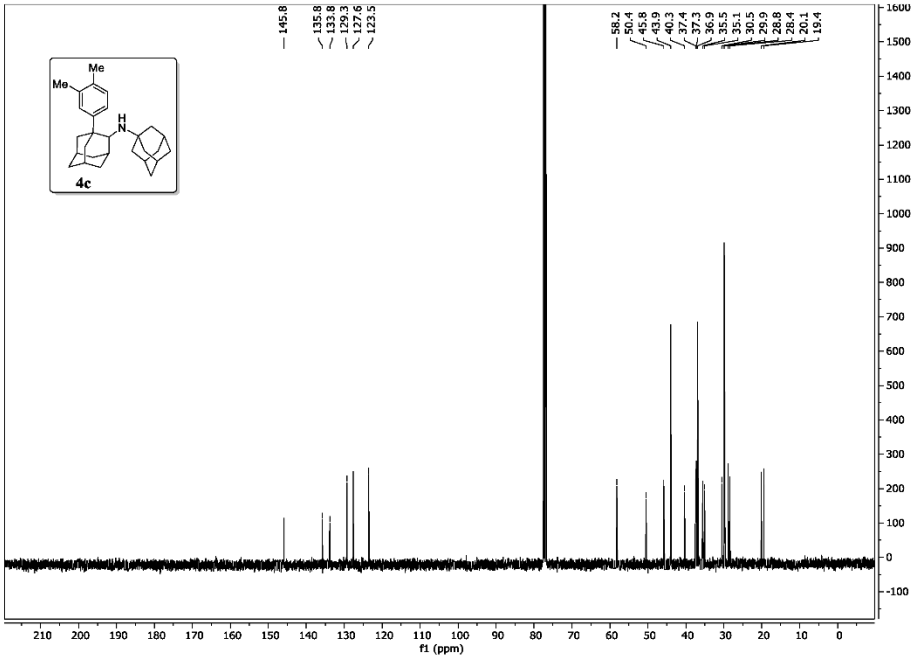

S120

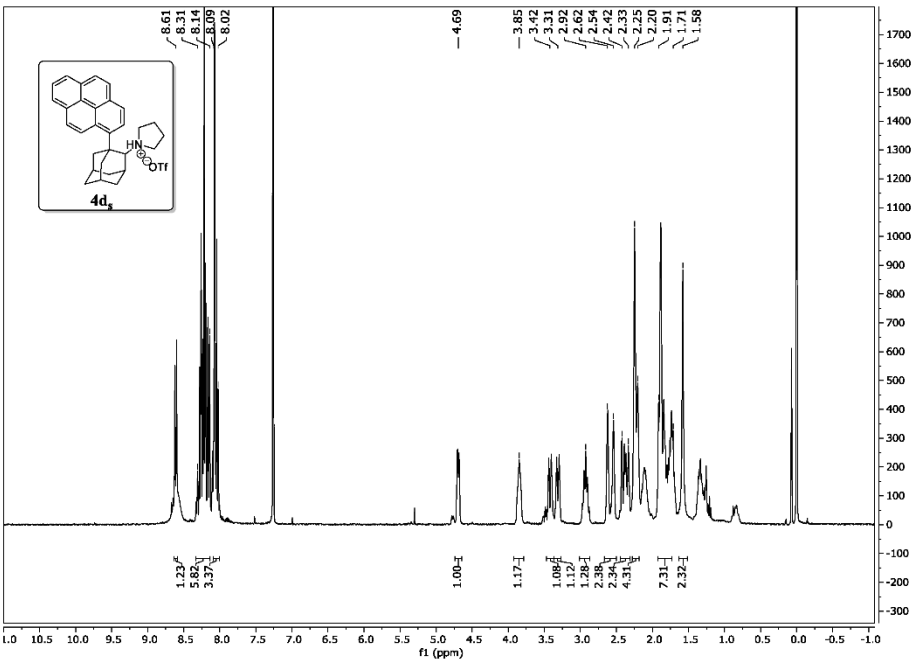
8.61
8.31
8.14
8.09
8.02
4.69
3.85
3.42
3.31
2.92
2.62
2.54
2.42
2.33
2.25
2.20
1.91
1.71
1.58
1.23
5.82
3.37
1.00
1.17
1.08
1.12
1.28
2.38
2.34
4.31
7.31
2.32
HN
OTf
4d5
f1 (ppm)

S121

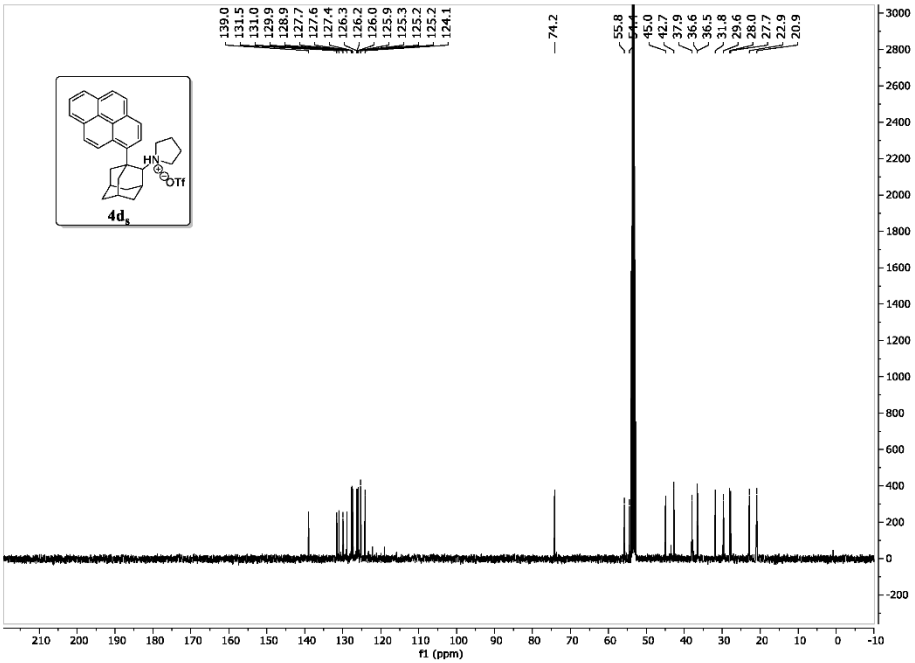
139.0
131.5
131.0
129.9
128.9
127.7
127.6
127.4
126.3
126.2
126.0
125.9
125.3
125.2
125.2
124.1
74.2
55.8
54.4
45.0
42.7
37.9
36.6
36.5
31.8
29.6
28.0
27.7
22.9
20.9
HN
OTf
4d5
f1 (ppm)

S122

2.7 Post-functionalization reactions

2.7.1 Synthesis of imine derivative 5

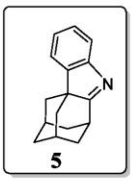

5

Under inert atmosphere, amine **2a** (160 mg, 1 eq., 0.71 mmol) was dissolved in dry THF (50 mL) and K_2CO_3 (490 mg, 5 eq., 3.56 mmol) and I_2 (1090 mg, 6 eq., 4.27 mmol) were added simultaneously. The mixture was stirred for 8 minutes, poured into 1N $Na_2S_2O_3$ (105 mL, *aq.*) and extracted with CH_2CL_2 (3x70 mL). The organic phases were combined, washed with brine and dried over Na_2SO_4 (anhydrous). After filtration the solvent was evaporated *in vacuo* to give the crude residue (170 mg) which was purified *via* flash column chromatography on silica gel (mobile phase: 10% acetone in *n*-hexane) to give the desired product as an off-white solid in 91% yield (146 mg, 0.64 mmol).

R_f (silica gel; acetone:*n*-hexane 1:9): 0.1.

m.p. (cryst. from EtOAc): 98.2-98.9 °C.

1H NMR (400 MHz, CDCl3): δ/ppm = 1.39-1.42 (m, 2H), 1.82-1.85 (m, 2H), 1.96 (m, 2H), 2.15-2.19 (m, 4H), 2.38-2.41 (m, 2H), 3.24 (m, 1H), 7.16-7.20 (m, 1H), 7.32-7.35 (m, 2H), 7.63-7.65 (m, 1H).

^{13}C NMR (101 MHz, $CDCl_3$): δ/ppm = 28.2 (2CH), 35.8 (CH_2), 36.9 (CH), 39.2 ($2CH_2$), 42.7 ($2CH_2$), 54.2 (C), 120.5 (CH), 121.7(CH), 124.4(CH), 127.7(CH), 145.2 (C), 155.8 (C), 192.5 (C).

IR (neat): $\tilde{\nu}$ /cm^{-1} =2916, 2849, 1587, 1448, 1200, 1184, 1077, 1009, 950, 885, 774, 751, 476.

HRMS: m/z = 224.1440 ($[M+H]^+$; calculated for $C_{16}H_{18}N^+$ m/z =224.1434).

2.7.2 Synthesis of imine derivative 6

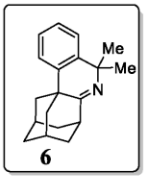

6

Under inert atmosphere, amine **2j** (680 mg, 1 eq., 2.55 mmol) was dissolved in dry THF (180 mL) and K_2CO_3 (1750 mg, 5 eq., 12.7 mmol) and I_2 (3880 mg, 6 eq., 15.3 mmol) were added simultaneously. The mixture was stirred for 8 minutes, poured into 1N $Na_2S_2O_3$ (360 mL, *aq.*) and extracted with CH_2CL_2 (3x200 mL). The organic phases were combined, washed with brine and dried over Na_2SO_4 (anhydrous). After filtration the solvent was evaporated *in vacuo* to give the crude residue (720 mg) which was purified *via* flash column chromatography on silica gel (mobile phase: 10% acetone in *n*-hexane) to give the desired product as an off-white solid in 84% yield (565 mg, 2.13 mmol).

R_f (silica gel; acetone:*n*-hexane 1:9): 0.2.

m.p. (cryst. from EtOAc): 100.2-100.7 °C.

^{1}H NMR (400 MHz, $CDCl_3$): δ/ppm = 1.54 (s, 6H), 1.81-1.84 (m, 2H), 1.95-2.00 (m, 6H), 2.16-2.20 (m, 3H), 2.23 (m, 1H), 2.68 (m, 1H), 7.20-7.24 (m, 2H), 7.29-7.33 (m, 1H).

^{13}C NMR (101 MHz, $CDCl_3$): δ/ppm = 29.0 ($2CH_3$), 33.9 (2CH), 36.1 (CH_2), 38.6 ($2CH_2$), 38.8 (C), 43.1 (CH), 46.7 ($2CH_2$), 56.5 (C), 124.6 (CH), 125.6 (CH), 126.6 (CH), 137.7 (C), 140.2 (C), 171.9 (C).

IR (neat): $\tilde{\nu}$ /cm^{-1} = 2981, 2910, 2850, 1674, 1489, 1446, 1354, 1260, 1142, 1078, 1045, 1025, 365, 907, 751, 730, 657, 625, 568, 529.

HRMS: m/z = 266.1907 ($[M+H]^+$; calculated for $C_{19}H_{24}N^+$ m/z = 266.1903).

2.7.3 Synthesis of piperidine derivative 7

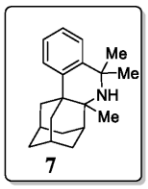

7

Under inert atmosphere, $BF_3 \cdot Et_2O$ (140 µl, 2 eq., 1.13 mmol) was dissolved in dry toluene (100 mL) and dry THF (40 mL). The solution was cooled to -78 °C. Imine **6** (150 mg, 1 eq., 0.57 mmol) was dissolved in dry THF (10 mL) and added. The mixture was stirred for 5 min at -78 °C. MeLi (1060 µl, 3 eq., 1.70 mmol) was added dropwise, and the mixture was slowly allowed to heat to room temperature (22 °C) overnight. The reaction was quenched with 20% NaOH (50 mL, *aq.*) and after separation of the phases, the aqueous phase was extracted with Et_2O (2x 70 mL). The combined organic phases were washed with brine and dried over Na_2SO_4 (anhydrous). After filtration the solvent was evaporated in vacuo to give the crude residue (200 mg) as a yellowish oil, which was purified *via* flash column chromatography on silica gel (mobile phase: 1% EtOAc in *c*-hexane.) to give the desired product as an off-white solid in 81% yield (129 mg, 0.46 mmol).

R_f (silica gel; EtOAc:*c*-hexane 1:99): 0.5.

m.p. (cryst. from $CDCl_3$): 79.6-80.8 °C.

^{1}H NMR (400 MHz, $CDCl_3$): δ/ppm = 1.20 (s, 3H), 1.50 (m, 1H), 1.61 (s, 3H), 1.69 (s, 3H), 1.75-1.80 (m, 3H), 1.85 (m, 1H), 1.95-2.00 (m, 3H), 2.15-2.30 (m, 4H), 2.34 (m, 1H), 7.24-7.34 (m, 4H).

^{13}C NMR (101 MHz, $CDCl_3$): δ/ppm = 23.0 (CH_3), 28.8 (CH_3), 29.1 (CH_3), 32.3 (CH_2), 33.7 (CH_2), 34.9 (CH), 36.3 (CH), 36.3 (CH_2), 38.1 (CH), 38.9 (CH_2), 39.7 (C), 44.3 (CH_2), 52.6 (C), 55.0 (C), 123.6 (CH), 125.8 (CH), 126.1 (CH), 126.6 (CH), 142.8 (C), 143.6 (C).

IR (neat): $\tilde{\nu}$ /cm^{-1} = 2908, 2856, 1480, 1440, 1367, 1345, 1173, 1138, 1104, 1084, 1050, 1023, 920, 745, 715, 663, 637, 561, 536, 497.

HRMS: m/z = 282.2218 ($[M+H]^+$; calculated for $C_{20}H_{28}N^+$ m/z =282.2216).

2.7.4 Synthesis of nitroxyl derivative 8

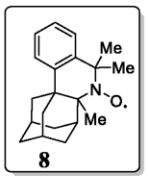

8

A mixture of amine **7** (140 mg, 1 eq., 0.50 mmol) and $Na_2WO_4 \cdot 2H_2O$ (82 mg, 0.5 eq., 0.25 mmol) in MeOH (1.5 mL) was stirred at room temperature for 45 min. Urea hydrogen peroxide (187 mg, 4.0 eq., 1.99 mmol) was added at 22 °C. After stirring for 3.25 h, the reaction mixture was quenched with saturated $NaHCO_3$ solution (50 mL, *aq.*). The mixture was extracted with CH_2Cl_2 (2x 30 mL) and the organic layer was dried over Na_2SO_4 (anhydrous) and concentrated *in vacuo*. The crude material was purified *via* flash column chromatography on silica gel (mobile phase: 10% EtOAc in cHex.) to give the desired product as an orange solid in a yield of 76 % (112 mg, 0.38 mmol).

m.p. (cryst. from EtOAc): 118.1-119.9 °C

IR (neat): $\tilde{\nu}$ /cm^{-1} =2923, 2897, 1492, 1444, 1371, 1361, 1350, 1254, 1179, 1108, 1090, 1052, 1040, 1023, 754, 584, 549, 584, 549, 508.

HRMS: m/z = 319.1914 ([M+Na]$^+$; calculated for $C_{20}H_{26}NONa^{\bullet+}$ m/z = 319.1907)

2.8 NMR spectra of compounds 5-7

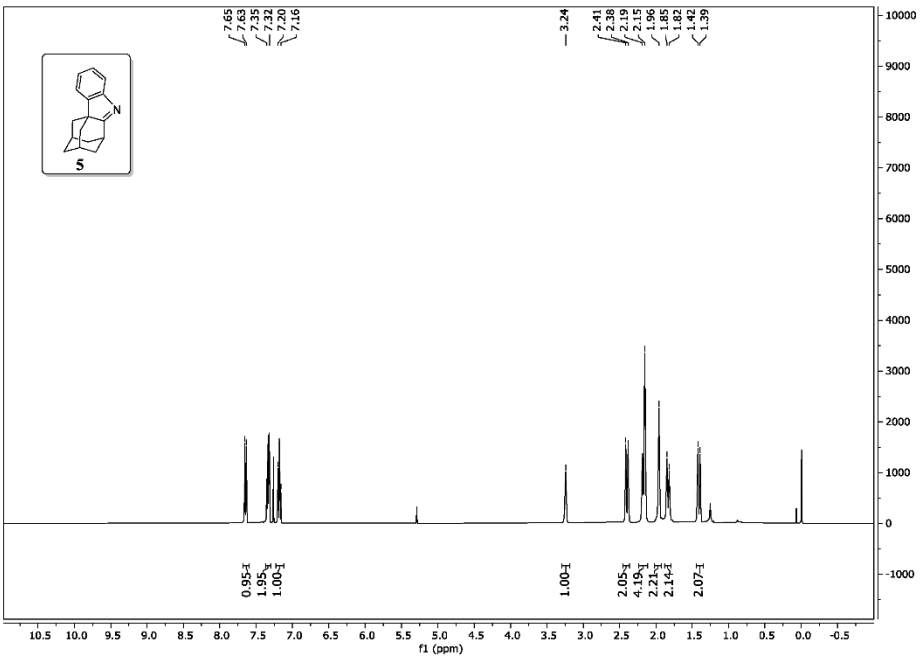
7.65
7.63
7.35
7.32
7.20
7.16
3.24
2.41
2.38
2.19
2.15
1.96
1.85
1.82
1.42
1.39
5
0.95
1.95
1.00
1.00
2.05
4.19
2.21
2.14
2.07
f1 (ppm)

S128

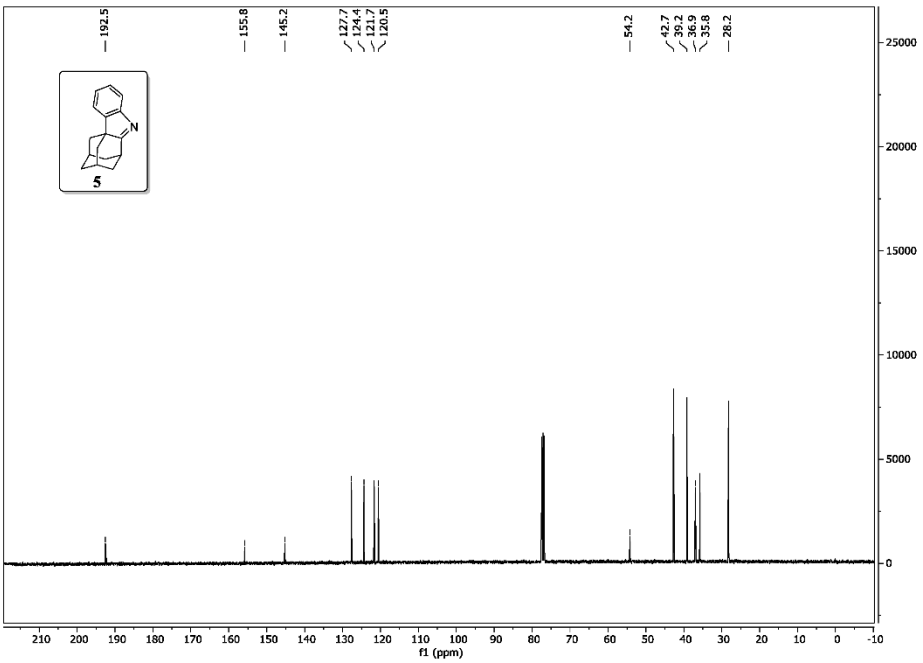
192.5
155.8
145.2
127.7
124.4
121.7
120.5
54.2
42.7
39.2
36.9
35.8
28.2
5
f1 (ppm)

S129

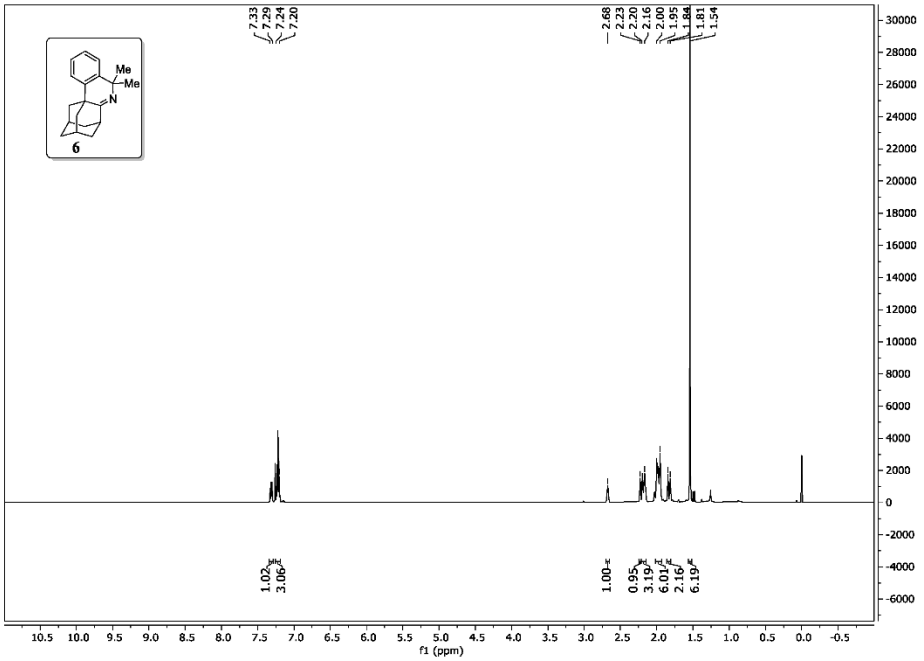
7.33
7.29
7.24
7.20
2.68
2.23
2.20
2.16
2.00
1.95
1.84
1.81
1.54
Me
Me
N
6
1.02
3.06
1.00
0.95
3.19
6.01
2.16
6.19
f1 (ppm)

S130

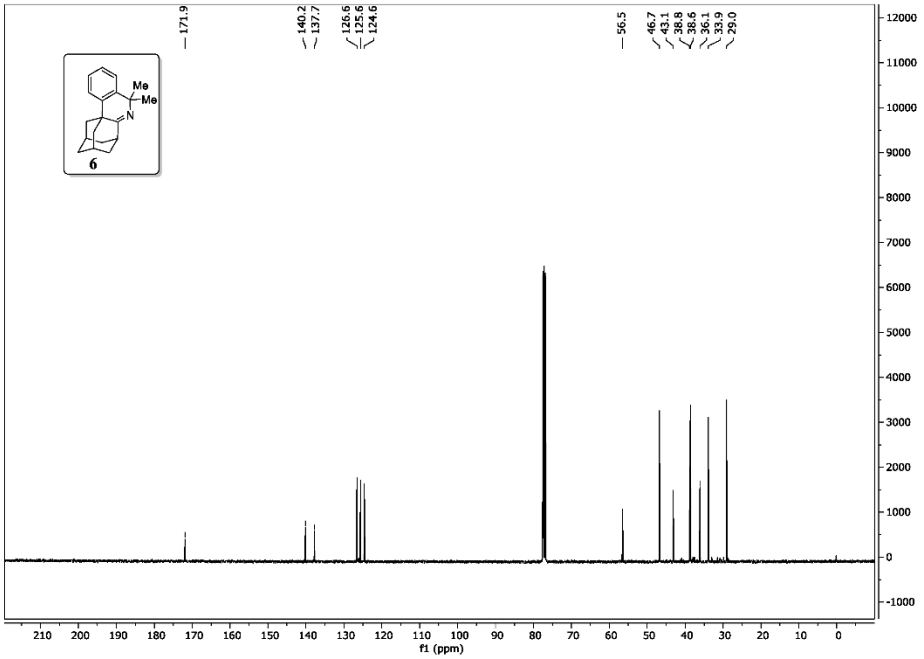
171.9
140.2
137.7
126.6
125.6
124.6
56.5
46.7
43.1
38.8
38.6
36.1
33.9
29.0
Me
Me
N
6
f1 (ppm)

S131

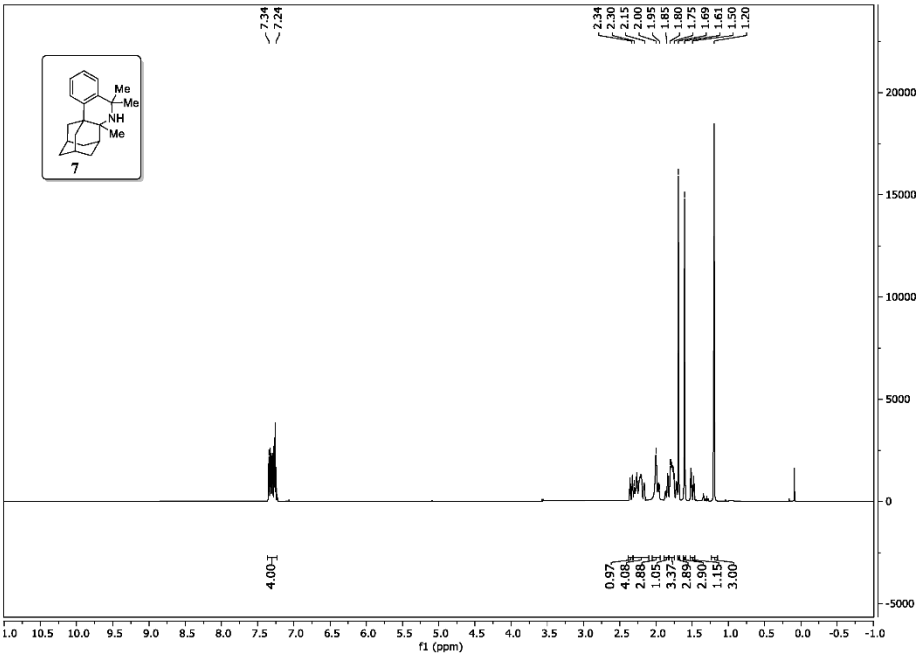
7.34
7.24
2.34
2.30
2.15
2.00
1.95
1.85
1.80
1.75
1.69
1.61
1.50
1.20
Me
Me
NH
Me
7
4.00
0.97
4.08
2.88
1.05
3.37
2.89
2.90
1.15
3.00
f1 (ppm)

S132

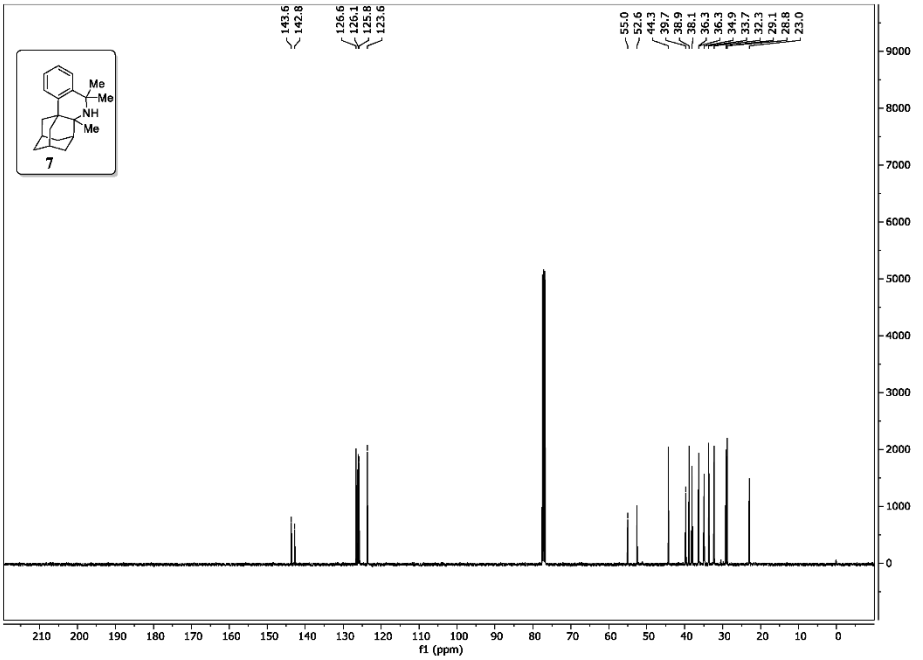
143.6
142.8
126.6
126.1
125.8
123.6
55.0
52.6
44.3
39.7
38.9
38.1
36.3
34.9
33.7
32.3
29.1
28.8
23.0
Me
Me
NH
Me
7
f1 (ppm)

S133

2.9 Synthesis compounds **12-16**

2.9.1 Synthesis of precursor 12

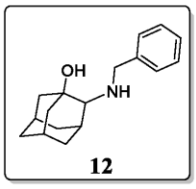

12

1-Amino-adamantan-2-ol[3] (850 mg, 1. eq., 5.1 mmol) was dissolved in DMF (5 mL) and K_2CO_3 (1550 mg, 2.2 eq., 11.2 mmol) and benzyl bromide (670 µL, 1.1 eq., 5.6 mmol) were added and the mixture was heated to 80 °C overnight. The reaction was quenched with water and extracted with EtOAc (2x). The combined organic phases were washed with brine, dried over Na_2SO_4 (anhydrous), filtered and the solvent was removed *in vacuo*. Flash column chromatography on silica gel (mobile phase: 20% EtOAc in *n*-hexane) to give a white solid in a yield of 50% (650 mg, 2.5 mmol).

R_f (silica gel; Et_2O:*n*-hexane 5:95): 0.3.

m.p. (cryst. from EtOAc): 77.0-78.0 °C.

^{1}H NMR (400 MHz, $CDCl_3$): δ/ppm = 1.45-1.69 (m, 7H), 1.73-1.85 (m, 3H), 2.01 (m, 1H), 2.10 (m, 1H), 2.21 (m, 1H), 2.63 (m, 1H), 3.68 (d, *J* = 12.9 Hz, 1H), 3.92 (d, *J* = 12.9 Hz, 1H), 7.26 (m, 1H), 7.31-7.37 (m, 4H).

^{13}C NMR (101 MHz, $CDCl_3$): δ/ppm = 29.7 (CH), 30.1 (CH_2), 30.5 (CH), 31.5 (CH), 36.6 (CH_2), 37.2 (CH_2), 40.4 (CH_2), 44.1 (CH_2), 52.0 (CH_2), 66.8 (CH), 68.5 (C), 127.2 (CH), 128.3 (2CH), 128.6 (2CH), 140.8 (C).

IR (neat): $\tilde{\nu}$ /cm^{-1} = 3252, 2911, 2849, 1494, 1451, 1355, 1298, 1221, 1114, 1087, 1070, 1028, 978, 960, 936, 909, 882, 789, 753, 734, 695, 670, 607, 559, 471.

HRMS: m/z = 258.1853 ([M+H]$^+$; calculated for $C_{17}H_{24}NO^+$ m/z = 258.1852).

[3]Synthesis according to literature procedure: J. J. Rohde, M. A. Pliushchev, B. K. Sorensen, D. Wodka, Q. Shuai, J. Wang, S. Fung, K. M. Monzon, W. J. Chiou, L. Pan, X. Deng, L. E. Chovan, A. Ramaiya, M. Mullally, R. F. Henry, D. F. Stolarik, H. M. Imade, K. C. Marsh, D. W. A. Beno, T. A. Fey, B. A. Droz, M. E. Brune, H. S. Camp, H. L. Sham, E. U. Frevert, P. B. Jacobson, J. T. Link, *J. Med. Chem.,* 2007, **50**, 149-164.

2.9.2 Synthesis of precursor 13

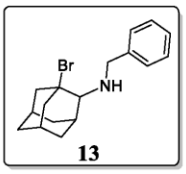

13

1-Bromo-2-amino adamantane[4] (580 mg, 1. eq., 2.5 mmol) was dissolved in dry THF (5 mL) and K_2CO_3 (517 mg, 1.5 eq., 3.8 mmol) and benzyl bromide (643 mg, 1.5 eq., 3.8 mmol) were added and the reaction mixture was heated to 50 °C overnight. The reaction was quenched with water and extracted with EtOAc (2x 50 mL). The combined organic phases were dried over Na_2SO_4 (anhydrous), filtered and the solvent was removed *in vacuo*. Flash column chromatography on silica gel (mobile phase: *n*-hexane/ether/trimethylamine 10/1/0.1) gave a clear liquid in a yield of 27% (215 mg, 0.7 mmol).

R$_f$ (silica gel; MeOH (1% NH_3 *aq.*):CH_2CL_2 1:99): 0.8.

^{1}H NMR (400 MHz, CD_2Cl_2): δ/ppm = 1.42 (m, 1H), 1.73-1.77 (m, 3H), 1.86 (m, 1H), 2.01-2.09 (m, 4H), 2.22- 2.25 (m, 2H), 2.41-2.51 (m, 2H), 2.82 (m, 1H), 3.04 (m, 1H), 3.71 (d, *J* = 13.1 Hz, 1H), 3.87 (d, *J* = 13.1 Hz, 1H), 7.23-7.40 (m, 5H).

^{13}C NMR (101 MHz, $CDCl_3$): δ/ppm = 29.5 (CH_2), 33.3 (CH), 33.4 (CH), 34.6 (CH), 36.5 (CH_2), 36.5 (CH_2), 44.0 (CH_2), 50.6 (CH_2), 51.9 (CH_2), 68.4 (CH), 76.0 (C), 127.3 (CH), 128.7 (2CH), 128.8 (2CH), 141.6 (C).

IR (neat): $\tilde{\nu}$ /cm^{-1} =3027, 2910, 2852, 1698, 1602, 1495, 1450, 1354, 1289, 1215, 1126, 1023, 982, 963, 942, 907, 811, 777, 736, 697, 662, 603, 494, 464.

HRMS: m/z = 322.0990 ([M+H]$^+$; calculated for $C_{17}H_{23}BrN^+$ m/z =322.0988).

[4]Synthesis according to literature procedure: R. Hrdina, M. Larrosa, C. Logemann *J. Org. Chem.,* 2017, **82**, 4891-4899.

2.9.3 Synthesis of precursor 14_s

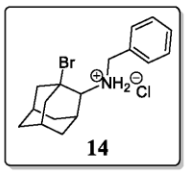

14

Compound **13** was solved in dry diethylether, and HCl in diethylether was added dropwise until precipitation was completed. The resulting solid was washed with diethylether and dried *in vacuo* to yield compound **14** in quantitative yield.

^{1}H NMR (400 MHz, CD_2Cl_2): δ/ppm = 1.49 (m, 1H), 1.64 (m, 1H), 1.72 (m, 1H), 1.80 (m, 1H), 1.99 (m, 1H), 2.15- 2.25 (m, 3H), 2.41-2.47 (m, 2H), 2.66 (m, 1H), 3.24 (m, 1H), 3.33 (m, 1H), 4.40 (m, 1H), 4.80 (m, 1H), 7.41-7.43 (m, 3H), 7.80-7.82 (m, 2H), 9.27 (m, 1H), 10.68 (m, 1H).

^{13}C NMR (101 MHz, CD_2Cl_2): δ/ppm = 29.16 (CH_2), 31.55 (2CH), 33.74 (CH), 35.14 (CH_2), 35.69 (CH_2), 43.19 (CH_2), 50.02 (CH_2), 50.44 (CH_2), 64.68 (C), 65.84 (CH), 129.02 (2CH), 129.25 (CH), 130.57 (C), 130.80 (2CH).

2.9.1 Synthesis of heterocycle 15

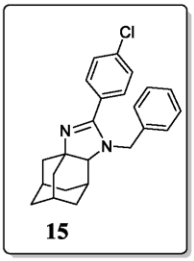

15

Under inert atmosphere, iminium salt $\mathbf{1e_s}$ (130 mg, 1 eq., 0.3 mmol) and 4-chlorobenzonitrile (183 mg, 4 eq., 1.4 mmol) were dissolved in dry 1,2-dichlorobenzene (1 mL). The mixture was heated to 140 °C overnight, cooled to room temperature, diluted with EtOAc (10 mL), washed with 2M NaOH (*aq.*), water and brine, dried over Na_2SO_4 (anhydrous), filtered and evaporated *in vacuo*. The crude residue was purified *via* flash column chromatography on silica gel (mobile phase: 5% MeOH (1% NH_3 (*aq.*)) in CH_2Cl_2) and further purified *via* semi-preparative HPLC (column C18H, mobile phase 85% acetonitrile, 15% TBME, 0.05% TEA, t_r = 4.9 min, flow 0.3 CV/min) to give **15** as a white solid in a yield of 12% (15 mg, 0.04 mmol).

R_f (silica gel; EtOAc:*n*-hexane 2:3): 0.1.

m.p. (cryst. from CH_2Cl_2): 138.0-140.2 °C.

^{1}H NMR (400 MHz, $CDCl_3$): δ/ppm = 1.45 (m, 1H), 1.59-1.71 (m, 6H), 1.86 (m, 1H), 1.99 (m, 3H), 2.12 (m, 1H), 2.24 (m, 1H), 3.02 (m, 1H), 4.03 (d, *J* = 16.0 Hz, 1H), 4.55 (d, *J* = 16.0 Hz, 1H), 7.24 (m, 1H), 7.28 (m, 1H), 7.30-7.36 (m, 5H), 7.51-7.53 (m, 2H).

^{13}C NMR (101 MHz, CD_2Cl_2): δ/ppm = 28.1 (CH), 30.2 (CH), 30.3 (CH), 30.8 (CH_2), 36.8 (CH_2), 37.3 (CH_2), 38.8 (CH_2), 42.1 (CH_2), 52.5 (CH_2), 63.7 (C), 74.8 (CH), 127.5 (2CH), 127.6 (CH), 128.6 (2CH), 128.9 (2CH), 129.3 (2CH), 130.6 (C), 136.1 (C), 138.0 (C), 167.6 (C).

IR (neat): $\tilde{\nu}$ /cm^{-1} = 2912, 2851, 1657, 1601, 1583, 1552, 1489, 1450, 1406, 1359, 1324, 11309, 1256, 1176, 1130, 1093, 1014, 980, 908, 841, 808, 732, 719, 696, 630, 606, 572, 544, 498, 471, 460, 433.

HRMS: m/z = 377.1781 ($[M+H]^+$; calculated for $C_{24}H_{26}ClN_2^+$ m/z = 377.1779)

2.9.1 Synthesis of heterocycle 16 using published method

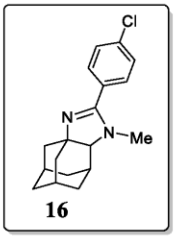

16

Under inert atmosphere, adamantane-*N*-methyl-oxazolidinone[4] (104 mg, 1 eq., 0.5 mmol) and 4-chlorobenzonitrile (274 mg, 4 eq., 2.0 mmol) were dissolved in dry 1,2-dichlorobenzene (0.5 mL) and triflic acid (220 µL, 5 eq, 375 mg, 2.5 mmol) was added. The mixture was heated to 140 °C overnight, cooled to room temperature, diluted with EtOAc (10 mL), washed with 2M NaOH (*aq.*), water and brine, dried over Na_2SO_4 (anhydrous), filtered and evaporated *in vacuo*. The crude residue was purified *via* flash column chromatography on silica gel (mobile phase: 5% MeOH in CH_2CL_2.) to give the desired product as an off-white solid in 13% yield (20 mg, 0.07 mmol).

Rf (silica gel; EtOAc:*n*-hexane 2:3): 0.1.

m.p. (cryst. from CH_2Cl_2): 159.8-161.4 °C

^{1}H NMR (400 MHz, CD_2Cl_2): δ/ppm = 1.55 (m, 2H), 1.65-1.70 (m, 4H), 1.80-1.88 (m, 3H), 1.95 (m, 1H), 2.13-2.18 (m, 2H), 2.28 (m, 2H), 2.65 (s, 3H), 2.74 (m, 1H), 7.37-7.39 (m, 2H), 7.44-7.47 (m, 2H).

^{13}C NMR (101 MHz, CD_2Cl_2): δ/ppm = 28.1 (CH), 29.9 (CH), 30.4 (CH_2), 30.5 (CH), 34.6 (CH), 36.8 (CH_2), 37.0 (CH_2), 38.6 (CH_2), 42.1 (CH_2), 63.6 (C), 75.7 (CH), 128.4 (CH), 129.3 (CH), 131.6 (C), 135.1 (C), 167.4 (C).

IR (neat): $\tilde{\nu}$ /cm^{-1} = 2906, 2846, 1650, 1600, 1577, 1547, 1522, 1487, 1452, 1397, 1345, 1323, 1306, 1257, 1229, 1193, 1154, 1121, 1086, 1073, 1040, 1006, 925, 894, 846, 833, 805, 788, 760, 738, 717, 696, 631, 604, 574, 549, 502, 485, 468, 430.

HRMS: m/z = 301.1469 ($[M+H]^+$; calculated for $C_{18}H_{22}ClN_2^+$ m/z = 301.1466)

[4]Synthesis in accordance to literature procedure: R. Hrdina, M. Larrosa, C. Logemann, *J. Org. Chem,*. 2017, **82**, 4891-4899.

2.10 NMR spectra of compounds **12-16**

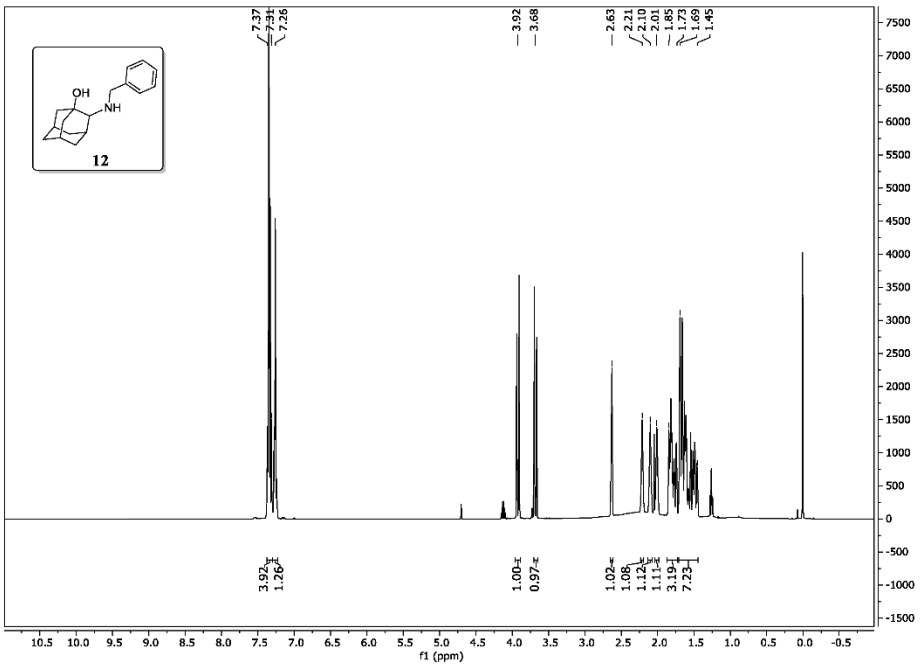
7.37
7.31
7.26
3.92
3.68
2.63
2.21
2.10
2.01
1.95
1.73
1.69
1.45
OH
NH
12
3.92
1.26
1.00
0.97
1.02
1.08
1.12
1.11
3.19
7.23
f1 (ppm)

S140

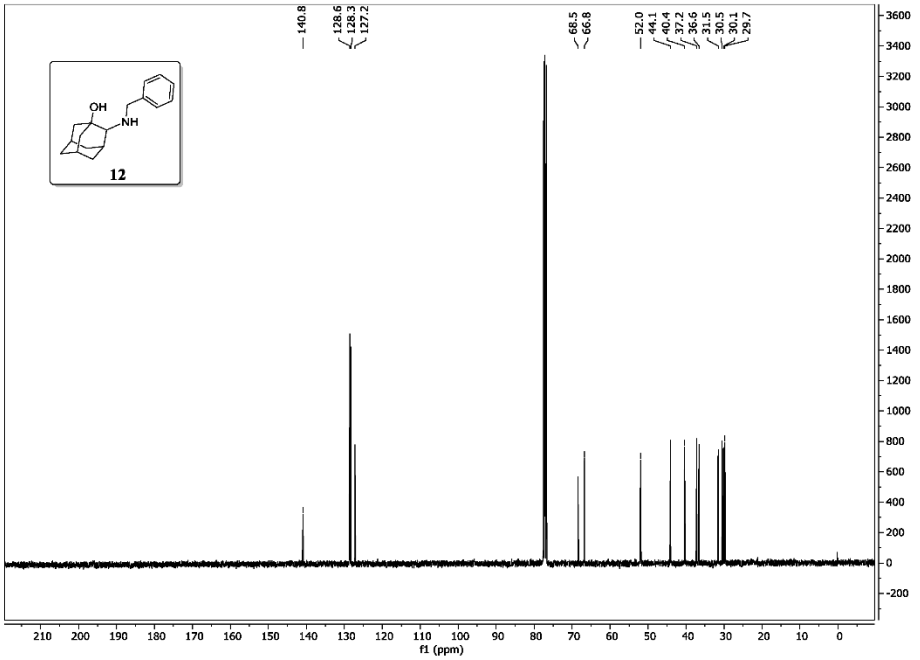
140.8
128.6
128.3
127.2
68.5
66.8
52.0
44.1
40.4
37.2
36.6
31.5
30.5
30.1
29.7
OH
NH
12
f1 (ppm)

S141

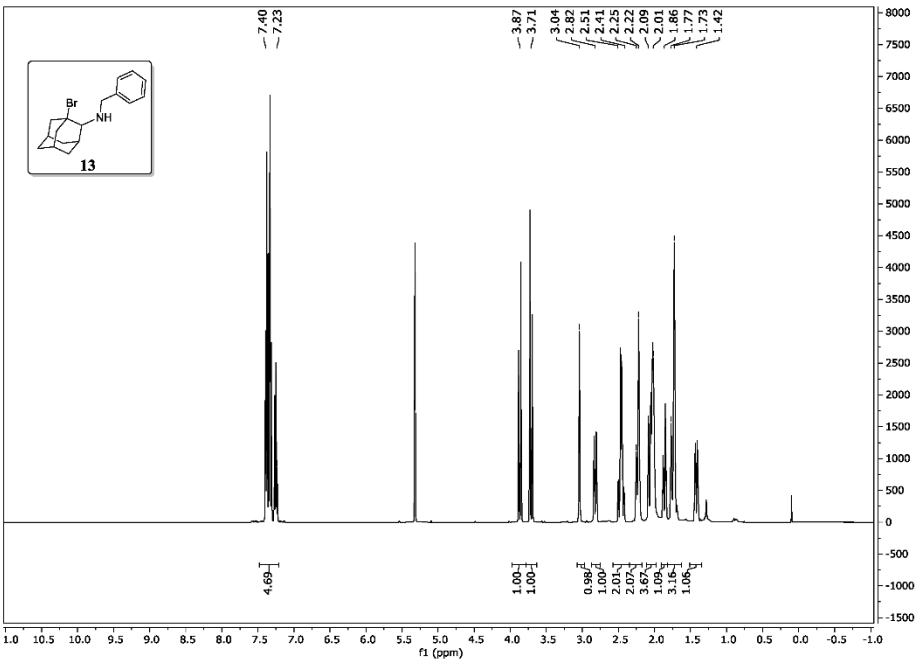
7.40
7.23
3.87
3.71
3.04
2.82
2.51
2.41
2.25
2.22
2.09
2.01
1.86
1.77
1.73
1.42
Br
NH
13
4.69
1.00
1.00
0.98
1.00
2.01
2.07
3.67
1.09
3.16
1.06
f1 (ppm)

S142

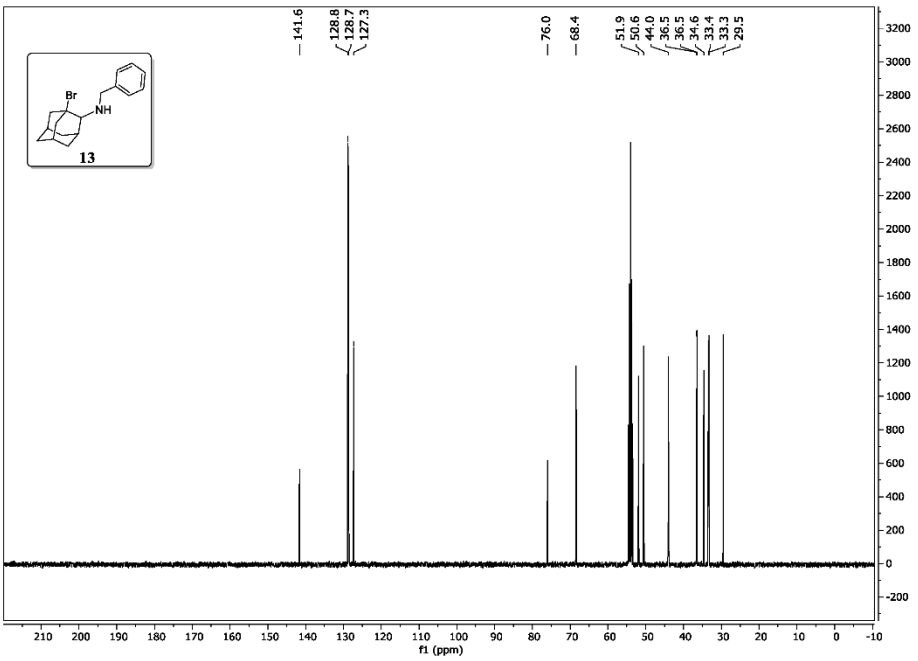
141.6
128.8
128.7
127.3
76.0
68.4
51.9
50.6
44.0
36.5
36.5
34.6
33.4
33.3
29.5
Br
NH
13
f1 (ppm)

S143

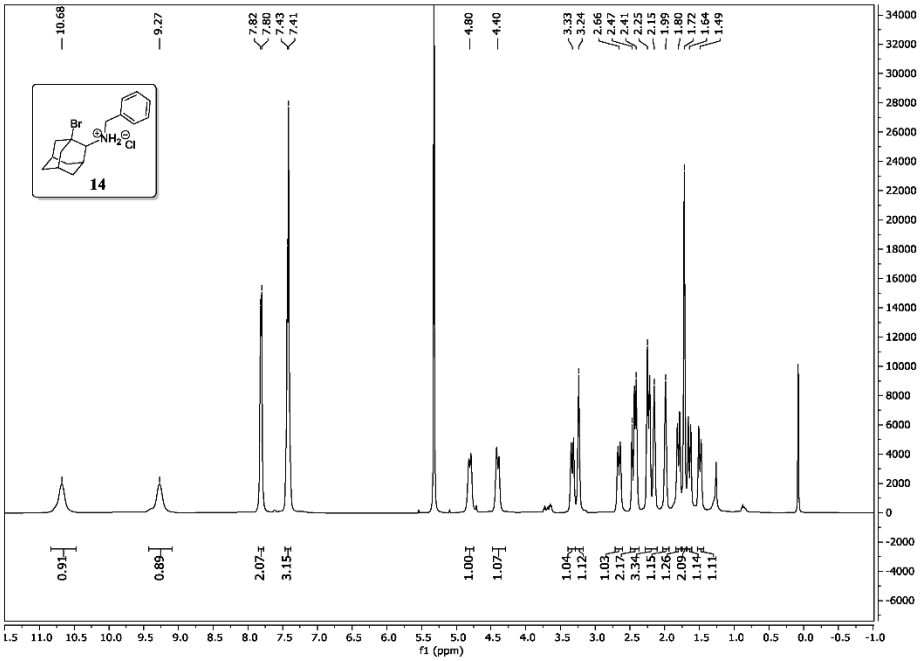
10.68
9.27
7.82
7.80
7.43
7.41
4.80
4.40
3.33
3.24
2.66
2.47
2.41
2.25
2.15
1.99
1.80
1.72
1.64
1.49
Br
NH2
Cl
14
0.91
0.89
2.07
3.15
1.00
1.07
1.04
1.12
1.03
2.17
3.34
1.15
1.26
2.09
1.14
1.11
f1 (ppm)

S144

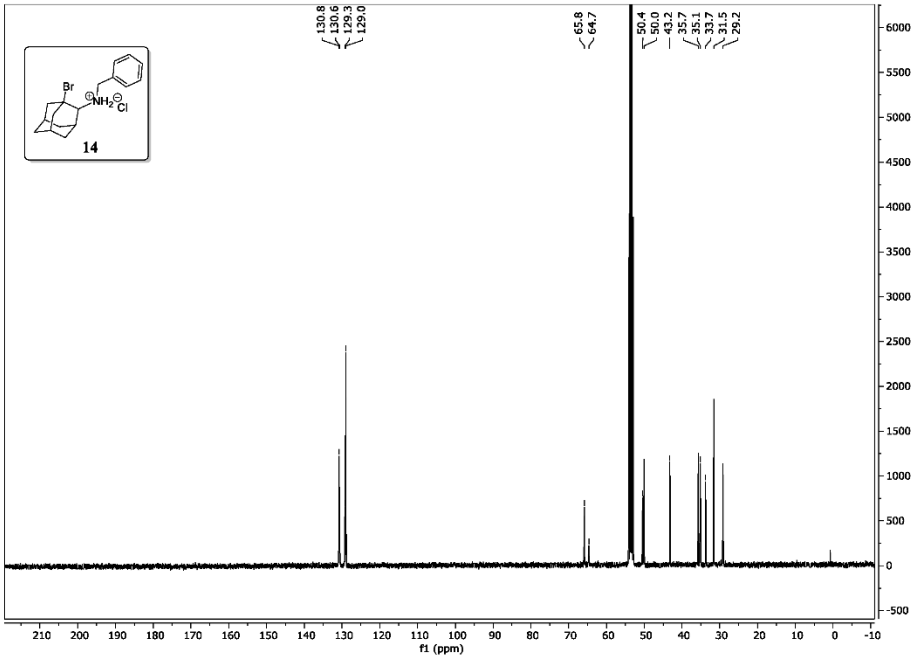
130.8
130.6
129.3
129.0
65.8
64.7
50.4
50.0
49.2
35.7
35.1
33.7
31.5
29.2
Br
NH2
Cl
14
f1 (ppm)

S145

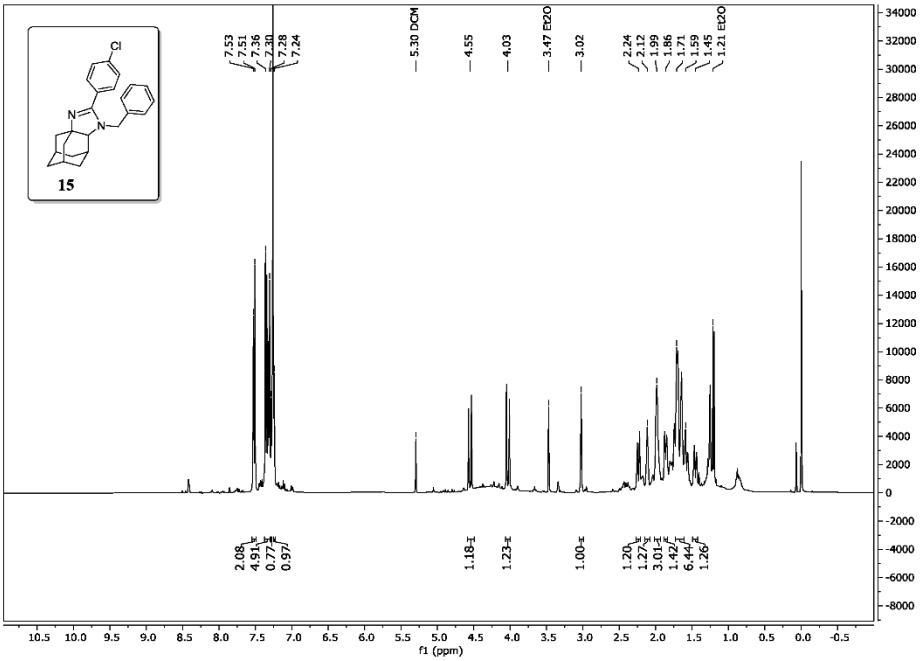
15
7.53
7.51
7.36
7.30
7.28
7.24
5.30 DCM
4.55
4.03
3.47 Et2O
3.02
2.24
2.12
1.99
1.86
1.71
1.59
1.45
1.21 Et2O
2.08
4.91
0.77
0.97
1.18
1.23
1.00
1.20
1.27
3.01
1.42
6.44
1.26
f1 (ppm)

S146

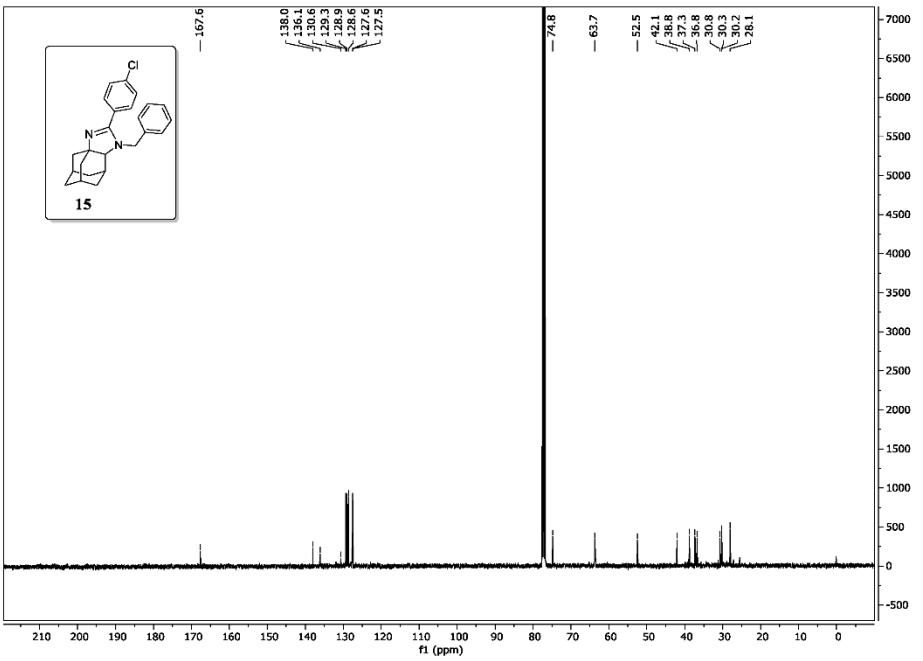
15
167.6
138.0
136.1
130.6
129.3
128.9
128.6
127.6
127.5
74.8
63.7
52.5
42.1
38.8
37.3
36.8
30.8
30.3
30.2
28.1
f1 (ppm)

S147

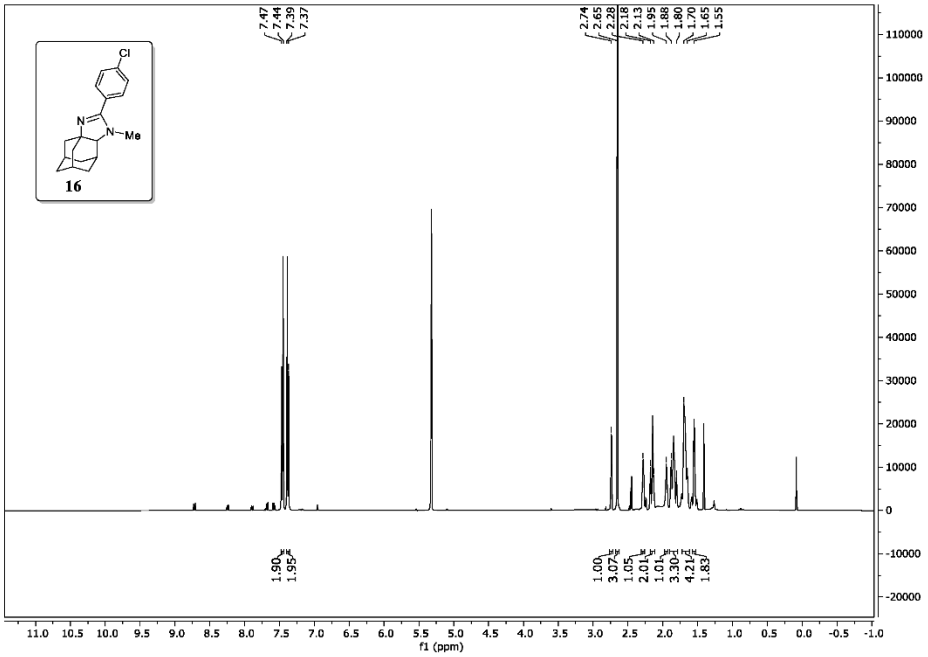
7.47
7.44
7.39
7.37
2.74
2.65
2.28
2.18
2.13
1.95
1.88
1.80
1.70
1.65
1.55
Cl
N
N
Me
16
1.90
1.95
1.00
3.07
1.05
2.01
1.01
3.30
4.21
1.83
f1 (ppm)

S148

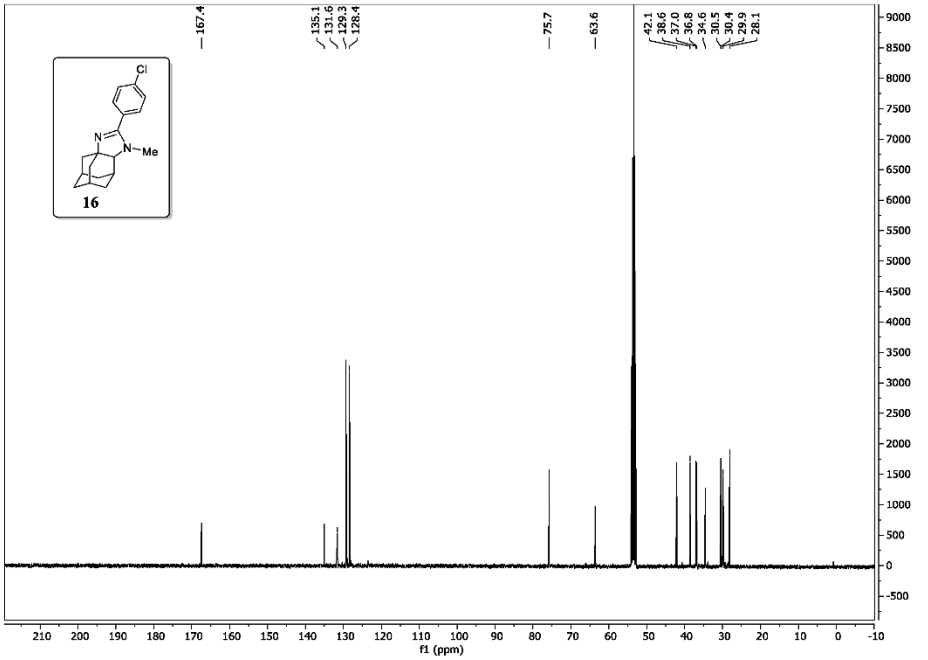
167.4
135.1
131.6
129.3
128.4
75.7
63.6
42.1
38.6
37.0
36.8
34.6
30.5
30.4
29.9
28.1
Cl
N
N
Me
16
f1 (ppm)

S149

3. Mechanistic experiments

3.1 Synthesis experiments

3.1.1 Separated Friedel-Crafts alkylation

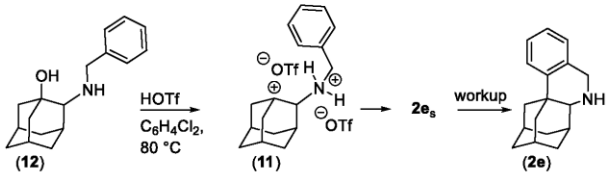

Compound **12** (70 mg, 1. eq., 0.27 mmol) was dissolved in dry 1,2- dichlorobenzene (600 µL) and triflic acid (48 µL, 2 eq., 0.54 mmol) was added. The reaction mixture was heated to 80 °C overnight. The reaction was quenched with 2M NaOH (10 mL, *aq*.) and extracted with EtOAc (2x 10 mL). The combined organic phases were washed with water and brine, dried over Na_2SO_4 (anhydrous), filtered and the solvent was removed *in vacuo* to give the crude residue as a turbid oil. ^{1}H NMR spectrum of crude reaction mixture showed a ratio of starting material **12** (SM) to product **2e** (P) of 1:2.

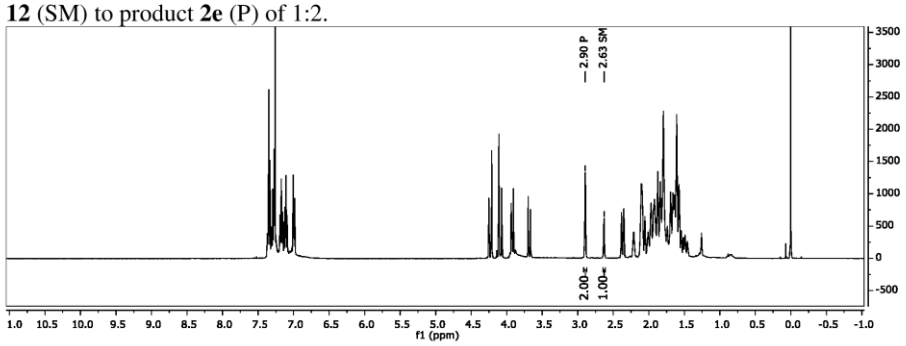

3.1.2 Thermal reactions of $1e_s$ with and without catalyst

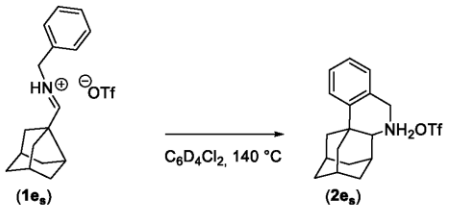

Iminium salt (80 mg, 1 eq., 0.21 mmol) was dissolved in deuterated dichlorobenzene (600 µL) inside a screw-cap NMR tube, flushed with nitrogen and the baseline measurement (^{1}H NMR) was taken. The sample was heated to 140 °C overnight, removed from heating and the next ^{1}H NMR spectrum was measured. Triflic acid (9 µL, 0.5 eq., 0.10 mmol) was added, the tube was flushed with nitrogen again, and heated to 140 °C. After 3 hours the sample was removed from the heating, a ^{1}H NMR spectrum was measured, and the sample was reheated overnight.

Before heating

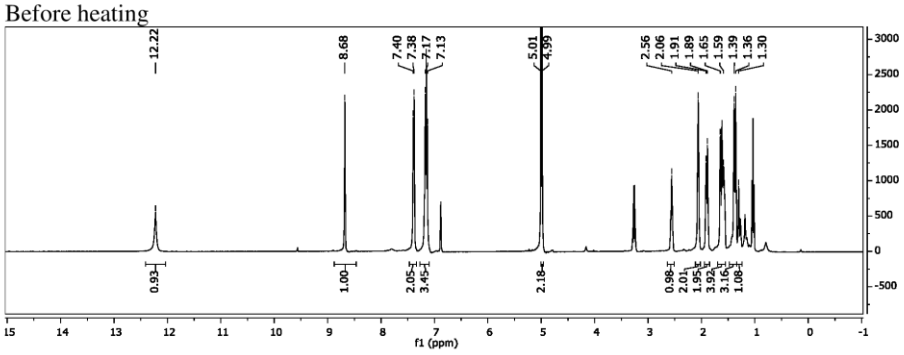

Overnight

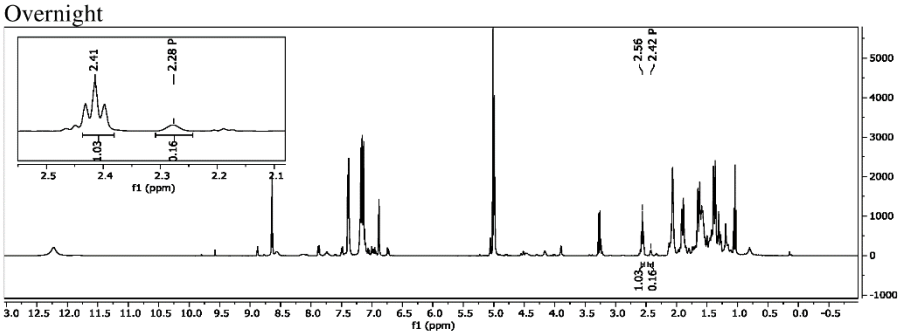

After acid addition 3 h

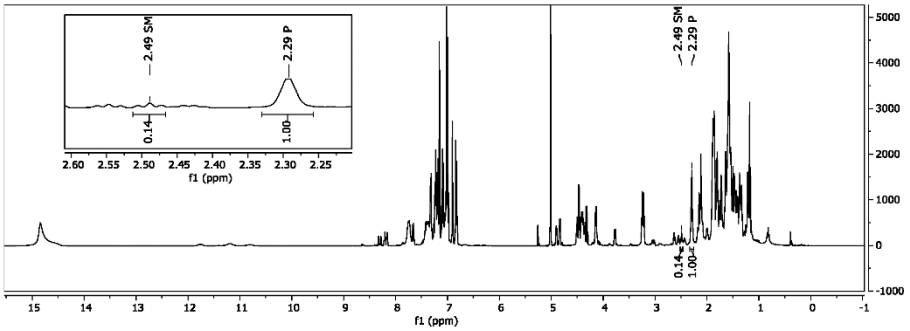

After acid addition overnight

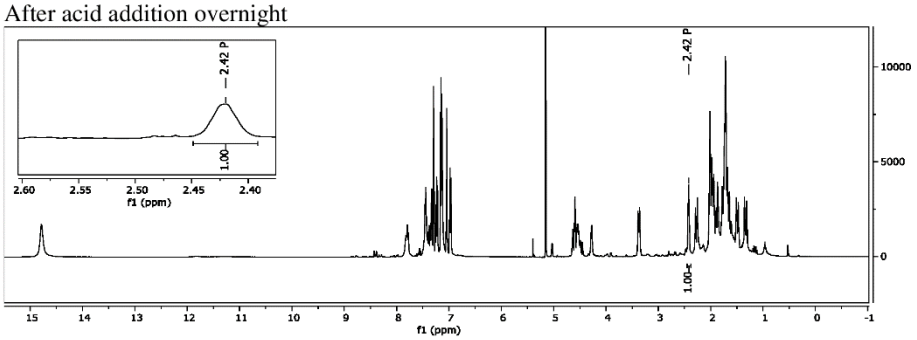

3.1.3 Thermal reaction of $3a_S$ with nitrile 17 towards 16

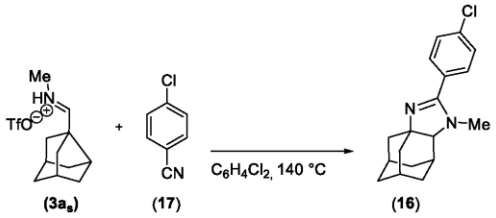

Under inert atmosphere, iminum salt **3a$_S$** (157 mg, 1 eq., 0.5 mmol) and 4-chlorobenzonitrile (274 mg, 4 eq., 2.0 mmol) were dissolved in dry 1,2-dichlorobenzene (0.5 mL). The mixture was heated to 140 °C overnight, cooled to room temperature, diluted with EtOAc (10 mL), washed with 2M NaOH (*aq.*), water and brine, dried over Na_2SO_4 (anhydrous), filtered and evaporated *in vacuo*. The crude residue was analysed *via* ^{1}H NMR, and comparison with the pure target compound (**16**) showed it to be the main compound in the mixture (yield >90%).

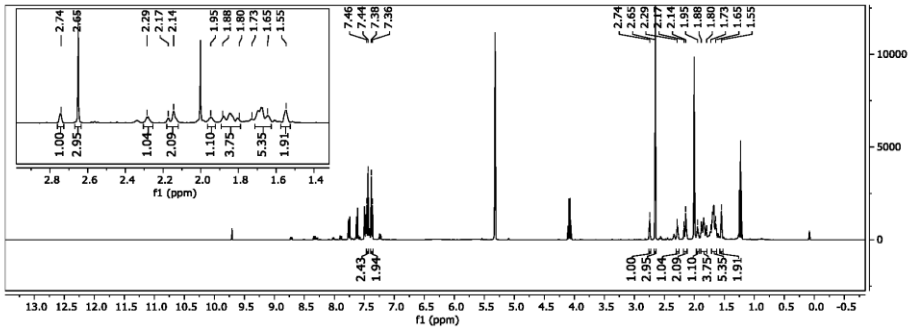

3.1.4 Thermal reaction of $1e_s$ with nitrile 17 towards 15

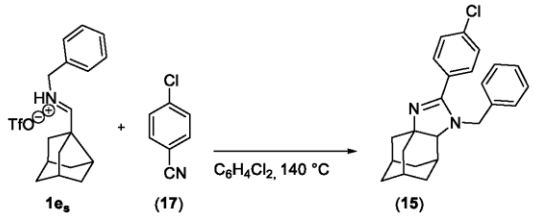

Under inert atmosphere, iminium salt **2e**$_s$ (130 mg, 1 eq., 0.3 mmol) and 4-chlorobenzonitrile (183 mg, 4 eq., 1.4 mmol) were dissolved in dry 1,2-dichlorobenzene (1 mL). The mixture was heated to 140 °C overnight, cooled to room temperature, diluted with EtOAc (10 mL), washed with 2M NaOH (*aq.*), water and brine, dried over Na_2SO_4 (anhydrous), filtered and evaporated *in vacuo*. The crude residue was analysed *via* ^{1}H NMR spectrometry, and comparison with the pure target compound showed heterocycle **15** in a mixture with Friedel-Crafts product **2e** in a ratio of 1:1.7.

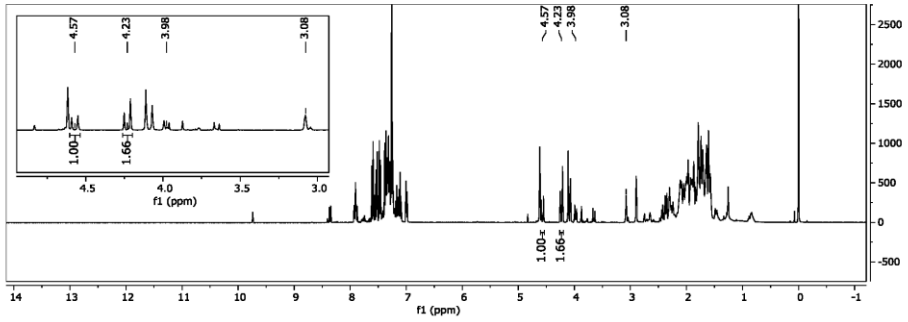

3.1.5 Kinetic models

The description of model I is depicted in Figure 4. In this case the role of the catalyst is the protonation of the intermediate **10**. The rearrangement is a reversible non-catalysed thermal reaction, described using estimated kinetic constants $k_1 = 1.0e^{-4}\ s^{-1}$ and $k_2 = 7.7e^{9}\ s^{-1}$. The following reaction is a diffusion controlled irreversible protonation of intermediate **10** described using estimated kinetic constant $k_3 = 9.7e^{10}\ s^{-1}$. The last reaction is an irreversible Friedel-Crafts reaction described using estimated kinetic constant $k_4 = 3.4e^{-2}\ s^{-1}$.

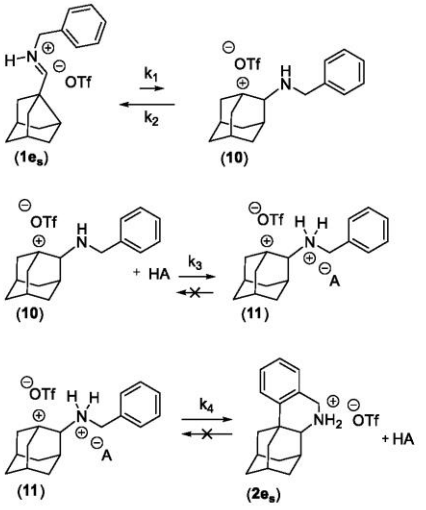

$$\frac{d(\mathbf{1e_s})}{dt} = -k_1 * (\mathbf{1e_s}) + k_2 * (\mathbf{10})$$

$$\frac{d(\mathbf{10})}{dt} = k_1 * (\mathbf{1e_s}) - k_2 * (\mathbf{10}) - k_3 * (\mathbf{10}) * (HA)$$

$$\frac{d(HA)}{dt} = -k_3 * (\mathbf{10}) * (HA) + k_4 * (\mathbf{11})$$

$$\frac{d(\mathbf{11})}{dt} = k_3 * (\mathbf{10}) * (HA) - k_4 * (\mathbf{11})$$

$$\frac{d(\mathbf{2e_s})}{dt} = k_4 * (\mathbf{11})$$

Fig. 4. Description of model I and its system of rate equations.

The kinetic constants were chosen according to estimated Gibbs free energy of the individual reactions in the cascade at 140 °C with pre-exponential factor of the Eyring equation supposed to be 1. Rearrangement reaction ([1,2]-alkyl shift) $\Delta G = 31.9$ kcal/mol, inverse reaction $\Delta G = 5.8$ kcal/mol, barrier free protonation diffusion controlled at 140 °C ($k_3 = 9.7e^{10}\ s^{-1}$), Friedel-Crafts reaction $\Delta G = 25.3$ kcal/mol.

Solutions of the differential rate equations were calculated by Octave 5.2.0 for 5, 20 and 50 mol% catalyst loading (Fig. 5)

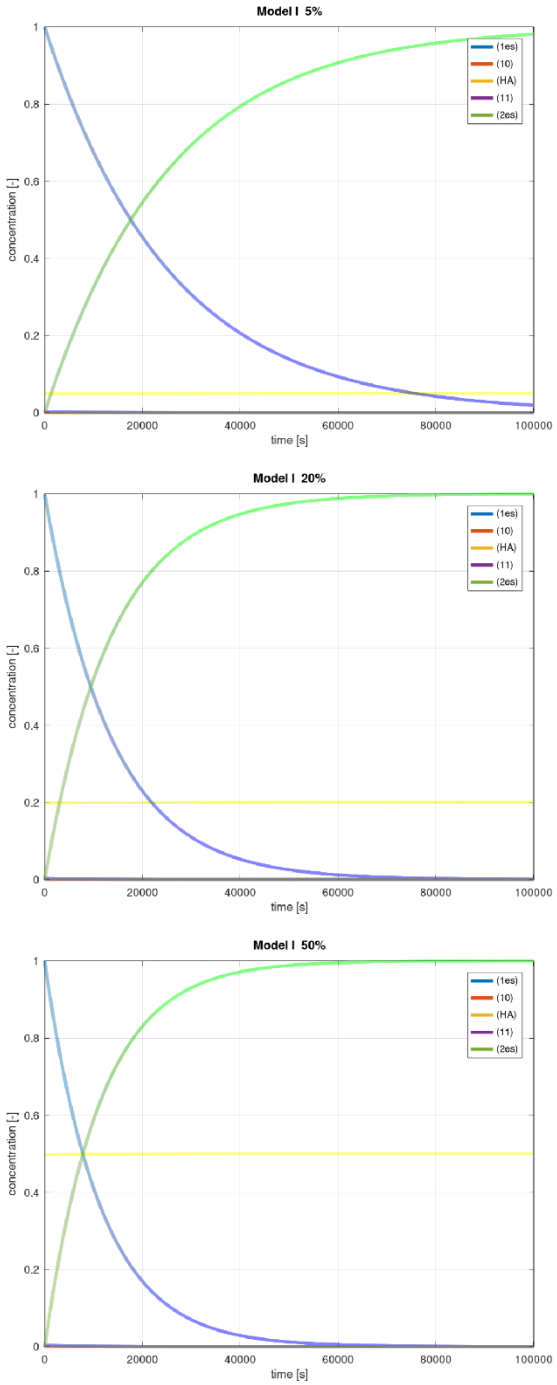

Fig. 5 Solutions of differential rate equations of model I by Octave 5.2.0 for 5, 20 and 50 mol% catalyst loading.

The description of model II is shown in Figure 6. The role of the catalyst is the activation of starting material **1e**$_s$. In this case we assume that the rearrangement is an irreversible catalysed reaction, described by estimated kinetic constant $k_1 = 7.7e^{-4}\ s^{-1}$. Followed by a Friedel-Crafts reaction described by estimated kinetic constant $k_4 = 4.7e^{-2}\ s^{-1}$.

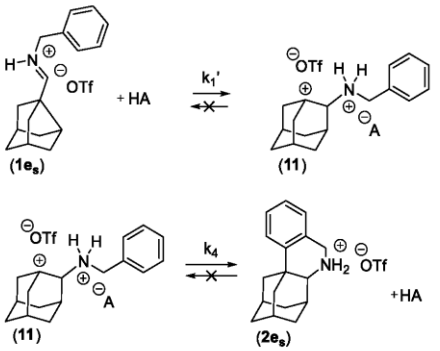

$$\frac{d(\mathbf{1e_s})}{dt} = -k_1' * (\mathbf{1e_s}) * (HA)$$

$$\frac{d(HA)}{dt} = -k_1' * (\mathbf{1e_s}) * (HA) + k_4 * (\mathbf{11})$$

$$\frac{d(\mathbf{11})}{dt} = k_1' * (\mathbf{1e_s}) * (HA) - k_4 * (\mathbf{11})$$

$$\frac{d(\mathbf{2e_s})}{dt} = k_4 * (\mathbf{11})$$

Fig. 6 Description of model II and its system of rate equations.

The kinetic constants were chosen according to estimated Gibbs free energy of the individual reactions in the cascade at 140 °C with pre-exponential factor of the Eyring equation supposed to be 1. Rearrangement reaction ([1,2]-alkyl shift) ΔG = 30.3 kcal/mol, Friedel-Crafts reaction ΔG= 25.1 kcal/mol.

Solutions of the differential rate equations were calculated by Octave 5.2.0 for 5, 20 and 50 mol% catalyst loading (Fig. 7)

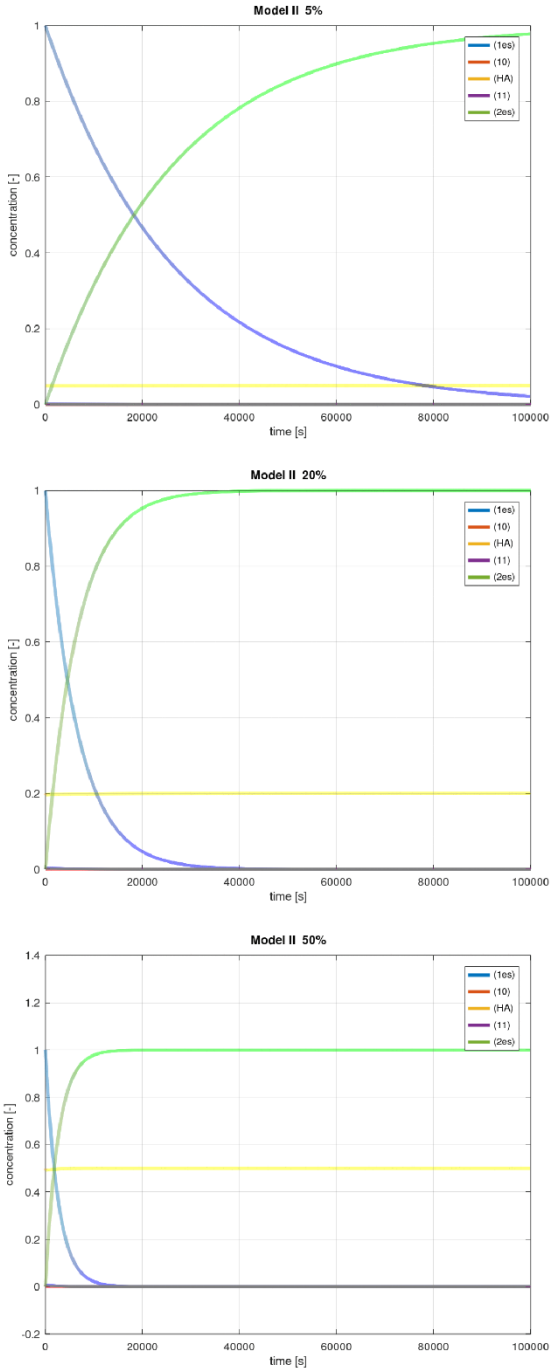

Fig. 7 Solutions of differential rate equations of model II by Octave 5.2.0 for 5, 20 and 50mol% catalyst loading.

3.1.6 Kinetic experiment with 5 mol% catalyst loading

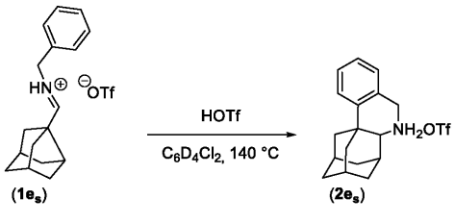

Iminium salt **1e**$_S$ (350 mg, 1 eq., 0.90 mmol) was dissolved in deuterated dichlorobenzene (2.2 mL) and triflic acid (7 mg, 0.05 eq., 0.04 mmol) was added. The mixture was stirred until homogeneous and divided into six NMR tubes under nitrogen, closed and heated to 140 °C. Every half hour, one sample was removed, cooled down to room temperature and analysed *via* ^{1}H NMR spectrometry.

30 min

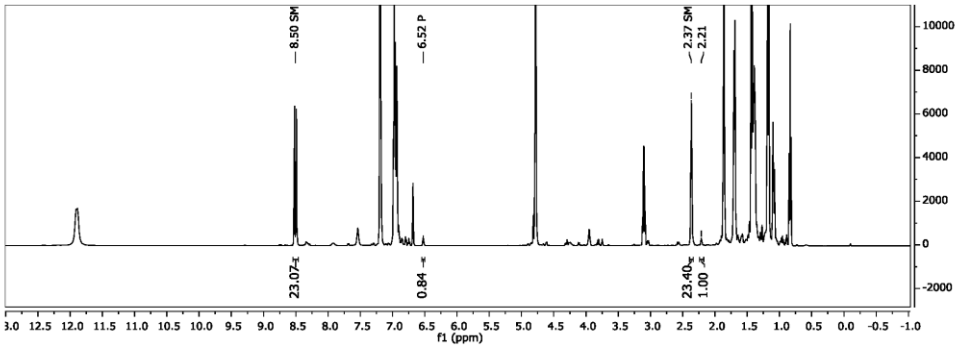

60 min

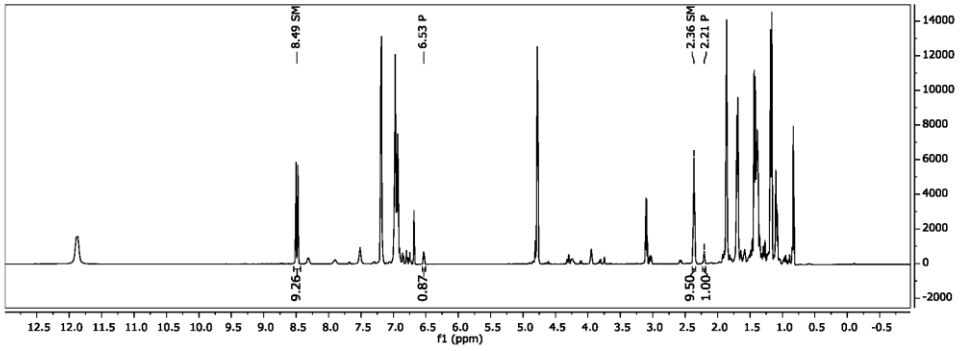

90 min

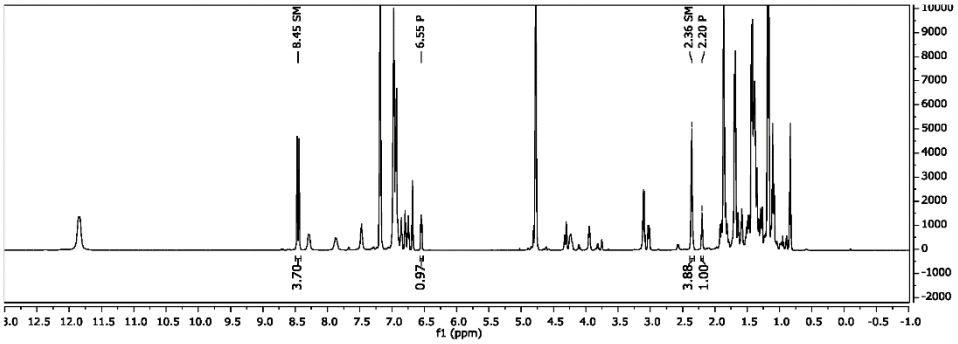

Kinetic constants of both models were fitted separately for 5 mol% of catalyst loading and the change was evaluated in case of 20 and 50 mol% of the catalyst.

Table 2. Calibration of model I and model II for 5% catalyst loading.

Time /min	Experimental	Model I	Model II
30	4%	7%	6%
60	10%	13%	13%
90	20%	19%	18%

3.1.7 Kinetic experiment with 20 mol% catalyst loading

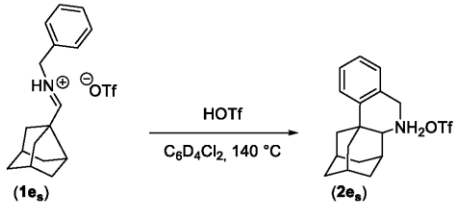

Iminium salt **1e**$_S$ (250 mg, 1 eq., 0.64 mmol) was dissolved in deuterated dichlorobenzene (1.6 mL) and triflic acid (11 µL, 0.20 eq., 0.13 mmol) was added. The mixture was stirred until homogeneous and divided into four NMR tubes under nitrogen, closed and heated to 140 °C. Every half hour one NMR tube was removed, cooled down to room temperature and analysed *via* ^{1}H NMR spectrometry.

30 min

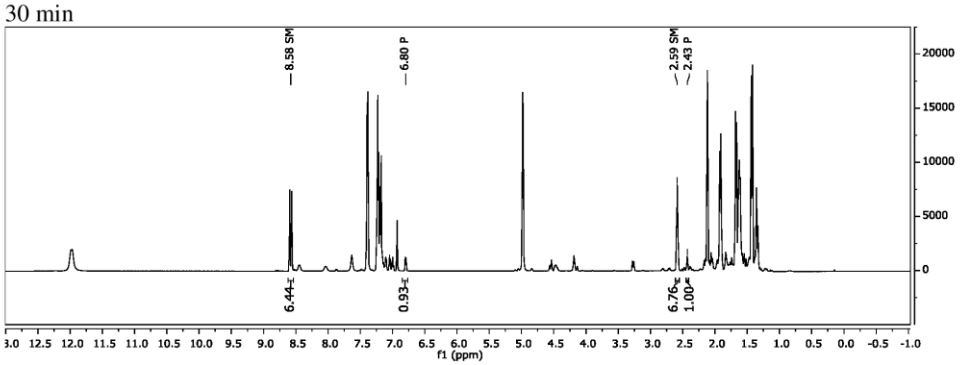

60 min

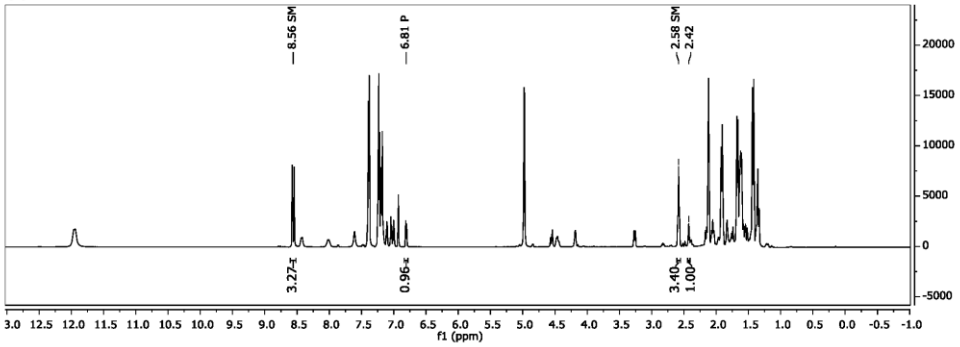

90 min

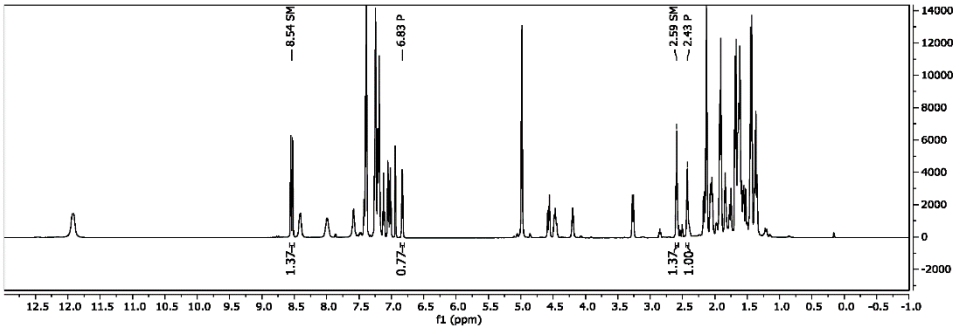

Table 3. Comparison of experimental values to model I and model II for 20 mol% catalyst loadings.

Time /min	Experimental	Model I	Model II
30	13%	13%	25%
60	22%	23%	43%
90	42%	33%	56%

According to the values in table 3 we came to conclusion, that model I describes the real system better than the model II.

3.1.8 Kinetic experiment with 50 mol% catalyst loading

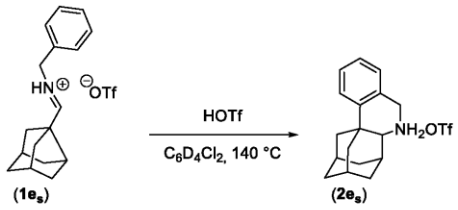

Iminium salt **1e**$_s$ (80 mg, 1 eq., 0.21 mmol) was dissolved in deuterated dichlorobenzene (0.5 mL), triflic acid (9 µL, 0.5 eq., 0.10 mmol) was added and the reaction mixture was heated to 140 °C for exact 30 min. After cooling down to room temperature the mixture was analysed *via* ^{1}H NMR spectrometry.

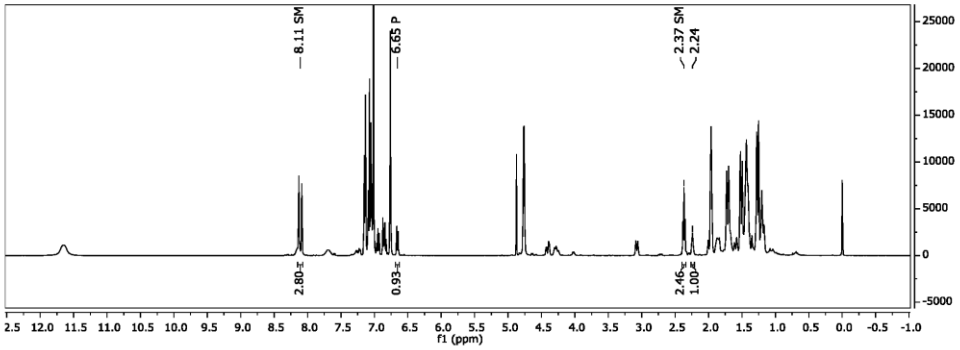

Table 4. Comparison of experimental to calculated conversion at 50% catalyst loading for both models.

Time /min	Experimental	Model I	Model II
30	29%	16%	51%

In the case of 50 mol% of the TfOH the polarity of the system is significantly changed, which may explain the increase in the overall speed of the reaction cascade.

3.1.9 Dilution experiments

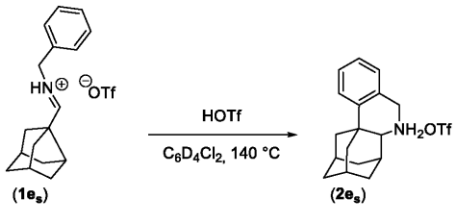

Iminium salt **1e**$_s$ (80 mg, 1 eq., 0.21 mmol) was dissolved in deuterated dichlorobenzene (0.5 mL) and triflic acid (9 µL, 0.5 eq., 0.10 mmol) was added. The mixture was stirred until homogeneous. 0.25 mL were transferred into a second Schlenk tube and further diluted with deuterated dichlorobenzene (0.25 mL). Both reaction vessels were heated to 140 °C for exact 30 min and then ^{1}H NMR spectra of reaction mixtures were directly measured at room temperature. The found conversion to **2e**$_s$ is 26% (0.2 M exp.) and 29% (0.4M exp.).

This experiment indicates as well that the role of the catalyst is not the activation of the starting material 1e$_s$.

c= 0.2M

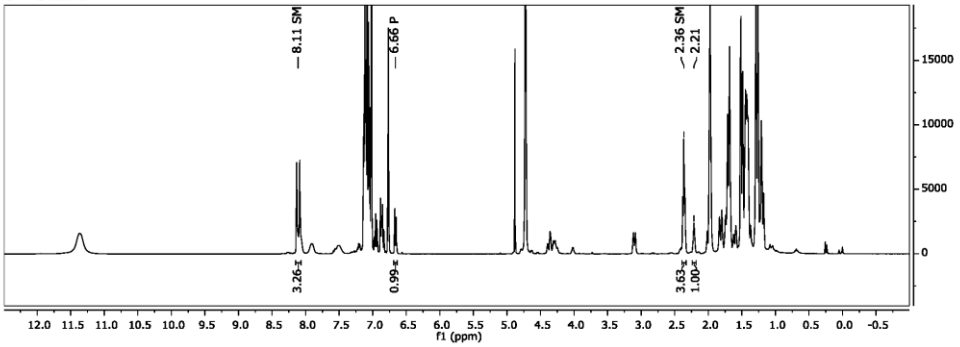

c= 0.4M

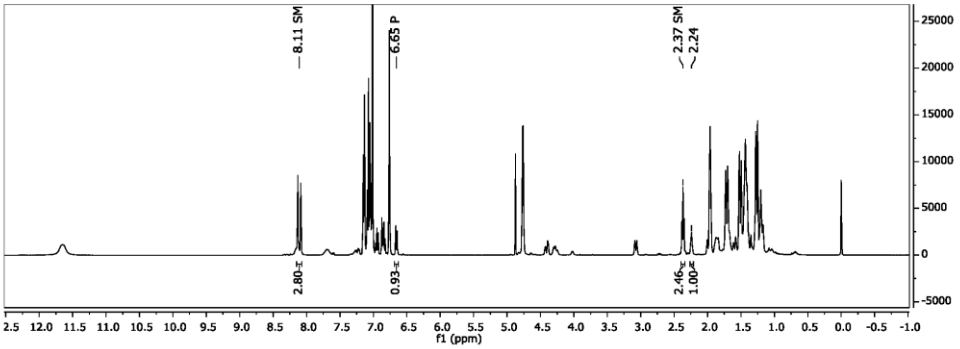

3.1.10 Formation of intermediate 10 from precursor 13 and rearrangement to $1e_S$

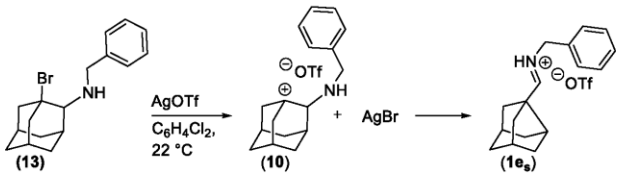

Precursor **13** (32 mg, 1.0 eq., 0.1 mmol) was dissolved in dry 1,2-dichlorobenzene (1 mL) and silver triflate (26 mg, 1.0 eq., 0.1 mmol) was added while stirring. Immediate precipitation of a white solid was observed. After 30 min, the mixture was filtered, washed with dichloromethane, the solvent was evaporated *in vacuo* and the resulting crude residue was measured in deuterated 1,4-dichlorobenzene. ^{1}H NMR spectra comparison of pure compounds showed the targeted iminium species (**$1e_S$**) and noradamantane aldehyde (**9**), its hydrolysis product.

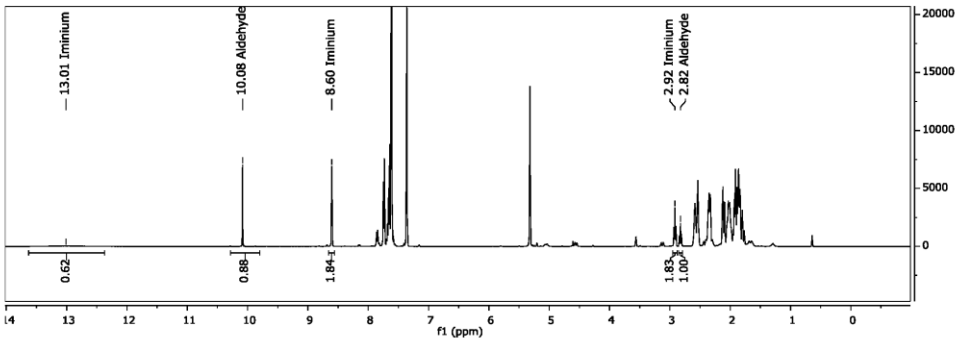

HRMS: m/z = 240.1751 ([M+H]$^+$; calculated for $C_{17}H_{22}rN^+$ m/z =240.1747).

3.1.11 Formation of intermediate 11 from precursor 14 and no rearrangement to $1e_s$

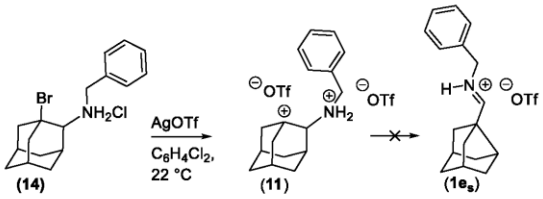

Precursor **14** (35 mg, 1.0 eq., 0.1 mmol) was dissolved in dry 1,2-dichlorobenzene (1 mL) and silver triflate (51 mg, 2.0 eq., 0.2 mmol) was added while stirring. Immediate precipitation of a white solid was observed. After 30 min, the mixture was filtered, washed with dichloromethane, the solvent was evaporated *in vacuo* and the resulting crude residue was measured in deuterated 1,4-dichlorobenzene. ^{1}H NMR and HRMS analysis showed no formation of target compound.

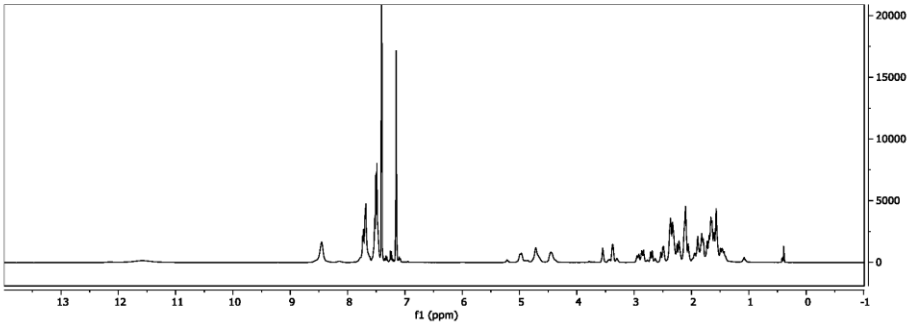

3.2 DFT analysis

3.2.1 Geometric Structures and Electronic energies (Hartree) (10^{+})

1 1

6	0.879227000	-0.876693000	-0.050178000
1	0.899087000	-1.951336000	-0.286749000
6	1.688134000	-0.111186000	-1.010340000
6	1.845350000	-0.666611000	1.251206000
1	1.341703000	-1.209804000	2.055256000
6	3.223744000	-1.269118000	0.953126000
1	3.144829000	-2.339224000	0.743455000
1	3.858742000	-1.172431000	1.838687000
6	2.907908000	-0.733818000	-1.512877000
1	3.344970000	-0.214112000	-2.364687000
1	2.809844000	-1.799597000	-1.715876000
6	3.867794000	-0.530211000	-0.226739000
1	4.832014000	-0.964178000	-0.497844000
6	3.979091000	0.974822000	0.047946000
1	4.642717000	1.142067000	0.901998000
1	4.432047000	1.491452000	-0.802659000
6	1.635484000	1.336341000	-0.946494000
1	0.648270000	1.725035000	-0.709331000
1	2.095827000	1.839358000	-1.795229000
6	1.940476000	0.835095000	1.548746000

1	0.954308000	1.252079000	1.754839000
1	2.548128000	0.987336000	2.446331000
6	2.593303000	1.550617000	0.361957000
1	2.627434000	2.631694000	0.509248000
7	-0.434871000	-0.336423000	0.202063000
1	-0.770468000	-0.634233000	1.113386000
6	-1.433778000	-0.716436000	-0.825955000
1	-1.146513000	-0.221942000	-1.762476000
1	-1.419525000	-1.799210000	-1.019299000
6	-2.819859000	-0.292613000	-0.409297000
6	-3.175245000	1.061101000	-0.388952000
6	-3.762259000	-1.246684000	-0.016567000
6	-4.447775000	1.450976000	0.014125000
1	-2.455260000	1.811642000	-0.698198000
6	-5.038039000	-0.857855000	0.388105000
1	-3.503027000	-2.300517000	-0.036692000
6	-5.381678000	0.491015000	0.404528000
1	-4.715620000	2.501110000	0.018456000
1	-5.762142000	-1.607579000	0.684398000
1	-6.374542000	0.794884000	0.714502000

E[B3LYP] = -715.405891

ZPVE[B3LYP] = 0.355764

($1e_S^+$)

1 1

6	-2.845643000	-1.301614000	-0.710307000
1	-2.565233000	-2.323988000	-0.441291000
1	-3.158519000	-1.294804000	-1.755857000
6	-1.675617000	-0.284589000	-0.442634000
6	-3.894103000	-0.760698000	0.277308000
1	-4.764207000	-1.415853000	0.350149000
6	-3.049897000	-0.721428000	1.563405000
1	-2.764122000	-1.733641000	1.864427000
1	-3.555755000	-0.255334000	2.410444000
6	-1.836477000	0.112637000	1.092970000
1	-0.951029000	-0.045812000	1.715168000
6	-2.269662000	1.595736000	1.045437000
1	-2.837126000	1.878819000	1.933391000
1	-1.414265000	2.273339000	0.968763000
6	-2.063363000	1.021070000	-1.229260000
1	-2.454243000	0.795659000	-2.223027000
1	-1.210830000	1.697424000	-1.338871000
6	-4.317779000	0.674595000	-0.130362000
1	-4.859153000	0.644274000	-1.081112000
1	-5.012170000	1.074790000	0.613957000
6	-3.093130000	1.618403000	-0.254495000
1	-3.405144000	2.621248000	-0.552162000
6	-0.396475000	-0.823580000	-0.920148000

1	-0.315638000	-1.086875000	-1.974641000
7	0.659977000	-1.022479000	-0.212820000
6	1.973204000	-1.542149000	-0.691142000
1	1.894201000	-1.654805000	-1.773157000
1	2.101096000	-2.532278000	-0.248538000
6	3.092539000	-0.615586000	-0.287209000
6	3.852374000	-0.889774000	0.853826000
6	3.369548000	0.528817000	-1.043209000
6	4.875286000	-0.025973000	1.237989000
1	3.660045000	-1.786966000	1.433799000
6	4.392838000	1.389095000	-0.659235000
1	2.798715000	0.741413000	-1.941819000
6	5.144133000	1.113182000	0.482970000
1	5.466909000	-0.248293000	2.117758000
1	4.611183000	2.267888000	-1.253915000
1	5.944625000	1.781121000	0.777697000
1	0.624160000	-0.768850000	0.773149000

E[B3LYP] = -715.446810

ZPVE[B3LYP] = 0.357217

(10-H)

0 1

6	0.898823000	-0.769367000	0.263834000
1	0.857365000	-1.863171000	0.426703000
6	1.584357000	-0.525460000	-1.105007000
6	1.787794000	-0.160876000	1.373641000
1	1.299312000	-0.321740000	2.343465000
6	3.156881000	-0.869890000	1.368387000
1	3.030317000	-1.941200000	1.563041000
1	3.782368000	-0.471151000	2.175176000
6	2.952897000	-1.237612000	-1.107285000
1	3.434664000	-1.109177000	-2.083168000
1	2.819682000	-2.315734000	-0.958522000
6	3.846199000	-0.655738000	0.005983000
1	4.817216000	-1.162892000	0.001923000
6	4.046744000	0.854646000	-0.234619000
1	4.696299000	1.275511000	0.542073000
1	4.550967000	1.017847000	-1.194423000
6	1.785695000	0.984566000	-1.339554000
1	0.817130000	1.490877000	-1.347149000
1	2.249198000	1.146581000	-2.319823000
6	1.992025000	1.349951000	1.136328000
1	1.030475000	1.869409000	1.158495000
1	2.607533000	1.767409000	1.941975000
6	2.679443000	1.568011000	-0.226649000

1	2.823919000	2.640600000	-0.396169000
7	-0.451404000	-0.197331000	0.321218000
1	-0.736136000	-0.127635000	1.294511000
6	-1.469624000	-0.960236000	-0.402300000
1	-1.230674000	-0.922104000	-1.471369000
1	-1.469377000	-2.029900000	-0.127032000
6	-2.859539000	-0.396682000	-0.188865000
6	-3.088854000	0.983556000	-0.231966000
6	-3.944944000	-1.247746000	0.035047000
6	-4.372157000	1.495206000	-0.061092000
1	-2.249431000	1.649745000	-0.391494000
6	-5.231661000	-0.738168000	0.201753000
1	-3.781537000	-2.319997000	0.081013000
6	-5.449176000	0.636204000	0.154259000
1	-4.532948000	2.567294000	-0.096902000
1	-6.061272000	-1.414849000	0.375078000
1	-6.448297000	1.035813000	0.287623000
1	0.963637000	-0.942412000	-1.904928000

E[B3LYP] = -716.281240

ZPVE[B3LYP] = 0.368608

(Ad-H)

0 1

6	-1.010613000	1.237658000	-0.784996000
1	-2.098920000	1.206348000	-0.914127000
1	-0.663945000	2.176966000	-1.231743000
6	-0.358008000	0.037872000	-1.502425000
1	-0.611773000	0.064652000	-2.567850000
6	-0.654731000	1.202566000	0.715687000
1	-1.118967000	2.055176000	1.223414000
6	-1.173401000	-0.112440000	1.333743000
1	-2.264532000	-0.166674000	1.241354000
1	-0.942932000	-0.140699000	2.405267000
6	-0.877819000	-1.274470000	-0.879757000
1	-0.436065000	-2.135761000	-1.394632000
1	-1.963894000	-1.348195000	-1.010444000
6	-0.521586000	-1.315284000	0.620693000
1	-0.891485000	-2.247835000	1.060879000
6	1.010485000	-1.237824000	0.784754000
1	1.277803000	-1.285679000	1.846972000
1	1.484704000	-2.098232000	0.298047000
6	1.173731000	0.112468000	-1.333481000
1	1.557815000	1.032558000	-1.789543000
1	1.650805000	-0.724988000	-1.856103000
6	0.877612000	1.274629000	0.879719000
1	1.256839000	2.214395000	0.461294000

1	1.142441000	1.270101000	1.943636000
6	1.534254000	0.074805000	0.165989000
1	2.622182000	0.127887000	0.283650000

E[B3LYP] = -390.610843

ZPVE[B3LYP] = 0.242494

(Ad^{+})

1 1

6	0.000000000	1.439525000	1.127069000
1	0.898683000	1.944423000	1.478115000
1	-0.898683000	1.944423000	1.478115000
6	0.000000000	0.000000000	1.342380000
6	0.000000000	1.449001000	-0.502379000
1	0.000000000	2.503647000	-0.783865000
6	1.267461000	0.731769000	-0.982882000
1	2.164077000	1.249431000	-0.631686000
1	1.305617000	0.753798000	-2.076290000
6	1.246665000	-0.719763000	1.127069000
1	1.234578000	-1.750494000	1.478115000
1	2.133262000	-0.193929000	1.478115000
6	1.254872000	-0.724501000	-0.502379000
1	2.168222000	-1.251823000	-0.783865000
6	0.000000000	-1.463538000	-0.982882000
1	0.000000000	-1.507597000	-2.076290000

1	0.000000000	-2.498861000	-0.631686000
6	-1.246665000	-0.719763000	1.127069000
1	-2.133262000	-0.193929000	1.478115000
1	-1.234578000	-1.750494000	1.478115000
6	-1.267461000	0.731769000	-0.982882000
1	-2.164077000	1.249431000	-0.631686000
1	-1.305617000	0.753798000	-2.076290000
6	-1.254872000	-0.724501000	-0.502379000
1	-2.168222000	-1.251823000	-0.783865000

E[B3LYP] = -389.728733

ZPVE[B3LYP] = 0.229976

3.3 Isodesmic equation

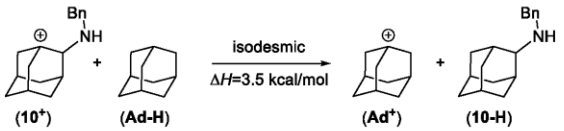

Scheme 6 An isodesmic equation to assess the contribution of the benzylamino group on the stabilisation of positive charge in the molecule (**10**$^{+}$). Structures were optimized using DFT method B3LYP/6-311G-(d,p).

4. Crystallographic data collection and refinement details

Diffraction data for all samples were collected at low temperatures (100K) using φ- and ω-scans on a BRUKER D8 Venture System equipped with dual IμS microfocus sources, a PHOTON100 detector and an OXFORD CRYOSYSTEMS 700 low temperature system. Mo-K_α radiation with a wavelength of 0.71073 Å, Cu-K_α radiation with a wavelength of 1.54178 Å and a collimating Quazar multilayer mirror were used.

Semi-empirical absorption corrections from equivalents were applied using SADABS.[5] The structures were solved by direct methods using SHELXT[6] and refined against F^2 on all data by full-matrix least squares using SHELXL.[7] All non-hydrogen atoms were refined anisotropically and C-H hydrogen atoms were positioned at geometrically calculated positions and refined using a riding model. The isotropic displacement parameters of all hydrogen atoms were fixed to 1.2x or 1.5x (CH_3 hydrogens) the U_{eq} value of the atoms they are linked to. All crystallographic data were deposited with the Cambridge Crystallographic Database as 2000166 and 2000167 and can be obtained free of charge.[8]

4.1 Compound **5**

The structure of **5** was solved in the orthorhombic space group $P2_12_12_1$. The asymmetric unit contains two independent molecules of **5**. Determination of the absolute structure proved to be challenging because of the low hetero atom count. The Parsons parameter indicated correct assignment of the absolute structure and this was confirmed using statistical analysis of Bijvoet pairs, which also showed to indication for racemic twinning.[9]

Table 5. Crystal data and structure refinement for **5**.

CCDC No	2000166	
Empirical formula	$C_{16}H_{17}N$	
Formula weight	223.30	
Temperature	100(2) K	
Wavelength	1.54178 Å	
Crystal system	Orthorhombic	
Space group	$P2_12_12_1$	
Unit cell dimensions	a = 7.2231(2) Å	α= 90°.
	b = 14.5123(4) Å	β= 90°.
	c = 22.3944(6) Å	γ = 90°.
Volume	2347.47(11) Å^3	
Z	8	
Density (calculated)	1.264 Mg/m^3	
Absorption coefficient	0.553 mm^{-1}	
F(000)	960	
Crystal size	0.567 x 0.255 x 0.199 mm^3	
Theta range for data collection	3.629 to 77.310°.	
Index ranges	$-9 \le h \le 9$, $-18 \le k \le 18$, $-28 \le l \le 28$	
Reflections collected	58893	
Independent reflections	4974 [R(int) = 0.0505]	
Completeness to theta = 67.679°	100.0 %	
Absorption correction	Semi-empirical from equivalents	
Refinement method	Full-matrix least-squares on F^2	
Data / restraints / parameters	4974 / 0 / 308	
Goodness-of-fit on F^2	1.041	
Final R indices [I>2σ(I)]	R_1 = 0.0318, wR_2 = 0.0806	
R indices (all data)	R_1 = 0.0331, wR_2 = 0.0818	
Absolute structure parameter	-0.12(14)	
Extinction coefficient	0.0019(3)	
Largest diff. peak and hole	0.223 and -0.203 e.Å^{-3}	

Table6. Atomic coordinates (x 10^4) and equivalent isotropic displacement parameters ($Å^2$x 10^3) for **5**. U(eq) is defined as one third of the trace of the orthogonalized U^{ij} tensor.

	x	y	z	U(eq)
N(1)	7815(2)	5544(1)	4220(1)	18(1)
C(1)	6947(2)	4989(1)	4571(1)	16(1)
C(2)	7601(2)	4987(1)	5216(1)	15(1)
C(3)	5925(2)	5237(1)	5613(1)	18(1)
C(4)	4354(2)	4542(1)	5500(1)	20(1)
C(5)	3763(2)	4580(1)	4841(1)	21(1)
C(6)	5418(2)	4337(1)	4431(1)	18(1)
C(7)	8268(2)	4003(1)	5367(1)	17(1)
C(8)	6691(2)	3319(1)	5249(1)	19(1)
C(9)	5034(2)	3566(1)	5647(1)	22(1)
C(10)	6124(2)	3362(1)	4589(1)	20(1)
C(11)	9096(2)	5698(1)	5180(1)	16(1)
C(12)	10289(2)	6067(1)	5600(1)	19(1)
C(13)	11541(2)	6748(1)	5420(1)	22(1)
C(14)	11616(2)	7033(1)	4827(1)	22(1)
C(15)	10426(2)	6657(1)	4401(1)	20(1)
C(16)	9167(2)	5996(1)	4584(1)	17(1)
N(21)	3435(2)	2688(1)	3486(1)	18(1)
C(21)	4330(2)	2244(1)	3081(1)	16(1)
C(22)	3761(2)	2431(1)	2443(1)	16(1)
C(23)	5477(2)	2772(1)	2097(1)	20(1)
C(24)	7013(2)	2041(1)	2144(1)	21(1)
C(25)	7550(2)	1898(1)	2802(1)	21(1)
C(26)	5848(2)	1556(1)	3160(1)	19(1)
C(27)	3074(2)	1508(1)	2177(1)	20(1)
C(28)	4634(2)	790(1)	2224(1)	22(1)
C(29)	6328(2)	1132(1)	1876(1)	24(1)
C(30)	5166(2)	640(1)	2882(1)	22(1)
C(31)	2268(2)	3136(1)	2551(1)	17(1)
C(32)	1125(2)	3633(1)	2173(1)	21(1)
C(33)	-147(3)	4247(1)	2425(1)	22(1)
C(34)	-272(2)	4354(1)	3041(1)	22(1)
C(35)	874(2)	3855(1)	3424(1)	21(1)
C(36)	2135(2)	3250(1)	3170(1)	17(1)

Table 7. Bond lengths [Å] and angles [°] for **5**.

N(1)-C(1)	1.289(2)	C(15)-H(15)	0.9500
N(1)-C(16)	1.430(2)	N(21)-C(21)	1.286(2)
C(1)-C(6)	1.487(2)	N(21)-C(36)	1.432(2)
C(1)-C(2)	1.519(2)	C(21)-C(26)	1.494(2)
C(2)-C(11)	1.496(2)	C(21)-C(22)	1.511(2)
C(2)-C(7)	1.545(2)	C(22)-C(31)	1.505(2)
C(2)-C(3)	1.546(2)	C(22)-C(23)	1.544(2)
C(3)-C(4)	1.539(2)	C(22)-C(27)	1.548(2)
C(3)-H(3A)	0.9900	C(23)-C(24)	1.539(2)
C(3)-H(3AB)	0.9900	C(23)-H(23A)	0.9900
C(4)-C(9)	1.535(2)	C(23)-H(23B)	0.9900
C(4)-C(5)	1.538(2)	C(24)-C(29)	1.532(2)
C(4)-H(4)	1.0000	C(24)-C(25)	1.537(2)
C(5)-C(6)	1.548(2)	C(24)-H(24)	1.0000
C(5)-H(5A)	0.9900	C(25)-C(26)	1.549(2)
C(5)-H(5AB)	0.9900	C(25)-H(25A)	0.9900
C(6)-C(10)	1.546(2)	C(25)-H(25B)	0.9900
C(6)-H(6)	1.0000	C(26)-C(30)	1.549(2)
C(7)-C(8)	1.534(2)	C(26)-H(26)	1.0000
C(7)-H(7A)	0.9900	C(27)-C(28)	1.538(2)
C(7)-H(7AB)	0.9900	C(27)-H(27A)	0.9900
C(8)-C(9)	1.535(2)	C(27)-H(27B)	0.9900
C(8)-C(10)	1.536(2)	C(28)-C(29)	1.533(2)
C(8)-H(8)	1.0000	C(28)-C(30)	1.538(2)
C(9)-H(9A)	0.9900	C(28)-H(28)	1.0000
C(9)-H(9AB)	0.9900	C(29)-H(29A)	0.9900
C(10)-H(10A)	0.9900	C(29)-H(29B)	0.9900
C(10)-H(10B)	0.9900	C(30)-H(30A)	0.9900
C(11)-C(12)	1.384(2)	C(30)-H(30B)	0.9900
C(11)-C(16)	1.404(2)	C(31)-C(32)	1.385(2)
C(12)-C(13)	1.398(2)	C(31)-C(36)	1.400(2)
C(12)-H(12)	0.9500	C(32)-C(33)	1.398(2)
C(13)-C(14)	1.394(3)	C(32)-H(32)	0.9500
C(13)-H(13)	0.9500	C(33)-C(34)	1.393(2)
C(14)-C(15)	1.395(3)	C(33)-H(33)	0.9500
C(14)-H(14)	0.9500	C(34)-C(35)	1.394(2)
C(15)-C(16)	1.383(2)	C(34)-H(34)	0.9500

C(35)-C(36)	1.387(2)	C(2)-C(7)-H(7A)	109.8
C(35)-H(35)	0.9500	C(8)-C(7)-H(7AB)	109.8
		C(2)-C(7)-H(7AB)	109.8
C(1)-N(1)-C(16)	105.80(13)	H(7A)-C(7)-H(7AB)	108.3
N(1)-C(1)-C(6)	129.07(15)	C(7)-C(8)-C(9)	109.13(13)
N(1)-C(1)-C(2)	115.41(14)	C(7)-C(8)-C(10)	109.70(13)
C(6)-C(1)-C(2)	115.51(13)	C(9)-C(8)-C(10)	110.00(13)
C(11)-C(2)-C(1)	99.93(12)	C(7)-C(8)-H(8)	109.3
C(11)-C(2)-C(7)	115.11(13)	C(9)-C(8)-H(8)	109.3
C(1)-C(2)-C(7)	107.88(12)	C(10)-C(8)-H(8)	109.3
C(11)-C(2)-C(3)	115.73(13)	C(4)-C(9)-C(8)	109.91(13)
C(1)-C(2)-C(3)	107.62(12)	C(4)-C(9)-H(9A)	109.7
C(7)-C(2)-C(3)	109.61(13)	C(8)-C(9)-H(9A)	109.7
C(4)-C(3)-C(2)	109.18(13)	C(4)-C(9)-H(9AB)	109.7
C(4)-C(3)-H(3A)	109.8	C(8)-C(9)-H(9AB)	109.7
C(2)-C(3)-H(3A)	109.8	H(9A)-C(9)-H(9AB)	108.2
C(4)-C(3)-H(3AB)	109.8	C(8)-C(10)-C(6)	110.21(13)
C(2)-C(3)-H(3AB)	109.8	C(8)-C(10)-H(10A)	109.6
H(3A)-C(3)-H(3AB)	108.3	C(6)-C(10)-H(10A)	109.6
C(9)-C(4)-C(5)	109.19(14)	C(8)-C(10)-H(10B)	109.6
C(9)-C(4)-C(3)	109.52(13)	C(6)-C(10)-H(10B)	109.6
C(5)-C(4)-C(3)	109.79(13)	H(10A)-C(10)-H(10B)	108.1
C(9)-C(4)-H(4)	109.4	C(12)-C(11)-C(16)	120.35(15)
C(5)-C(4)-H(4)	109.4	C(12)-C(11)-C(2)	132.82(15)
C(3)-C(4)-H(4)	109.4	C(16)-C(11)-C(2)	106.83(13)
C(4)-C(5)-C(6)	110.25(13)	C(11)-C(12)-C(13)	118.67(15)
C(4)-C(5)-H(5A)	109.6	C(11)-C(12)-H(12)	120.7
C(6)-C(5)-H(5A)	109.6	C(13)-C(12)-H(12)	120.7
C(4)-C(5)-H(5AB)	109.6	C(14)-C(13)-C(12)	120.65(16)
C(6)-C(5)-H(5AB)	109.6	C(14)-C(13)-H(13)	119.7
H(5A)-C(5)-H(5AB)	108.1	C(12)-C(13)-H(13)	119.7
C(1)-C(6)-C(10)	106.79(13)	C(13)-C(14)-C(15)	120.79(16)
C(1)-C(6)-C(5)	107.66(13)	C(13)-C(14)-H(14)	119.6
C(10)-C(6)-C(5)	109.15(14)	C(15)-C(14)-H(14)	119.6
C(1)-C(6)-H(6)	111.0	C(16)-C(15)-C(14)	118.29(15)
C(10)-C(6)-H(6)	111.0	C(16)-C(15)-H(15)	120.9
C(5)-C(6)-H(6)	111.0	C(14)-C(15)-H(15)	120.9
C(8)-C(7)-C(2)	109.20(12)	C(15)-C(16)-C(11)	121.23(15)
C(8)-C(7)-H(7A)	109.8	C(15)-C(16)-N(1)	126.74(15)

C(11)-C(16)-N(1)	112.02(14)	C(22)-C(27)-H(27B)	109.9
C(21)-N(21)-C(36)	105.45(13)	H(27A)-C(27)-H(27B)	108.3
N(21)-C(21)-C(26)	128.32(14)	C(29)-C(28)-C(27)	109.31(14)
N(21)-C(21)-C(22)	116.11(14)	C(29)-C(28)-C(30)	109.48(14)
C(26)-C(21)-C(22)	115.57(13)	C(27)-C(28)-C(30)	110.18(14)
C(31)-C(22)-C(21)	99.55(12)	C(29)-C(28)-H(28)	109.3
C(31)-C(22)-C(23)	115.96(13)	C(27)-C(28)-H(28)	109.3
C(21)-C(22)-C(23)	108.29(13)	C(30)-C(28)-H(28)	109.3
C(31)-C(22)-C(27)	114.84(13)	C(24)-C(29)-C(28)	109.66(14)
C(21)-C(22)-C(27)	107.23(13)	C(24)-C(29)-H(29A)	109.7
C(23)-C(22)-C(27)	109.93(13)	C(28)-C(29)-H(29A)	109.7
C(24)-C(23)-C(22)	108.82(13)	C(24)-C(29)-H(29B)	109.7
C(24)-C(23)-H(23A)	109.9	C(28)-C(29)-H(29B)	109.7
C(22)-C(23)-H(23A)	109.9	H(29A)-C(29)-H(29B)	108.2
C(24)-C(23)-H(23B)	109.9	C(28)-C(30)-C(26)	110.01(14)
C(22)-C(23)-H(23B)	109.9	C(28)-C(30)-H(30A)	109.7
H(23A)-C(23)-H(23B)	108.3	C(26)-C(30)-H(30A)	109.7
C(29)-C(24)-C(25)	109.97(14)	C(28)-C(30)-H(30B)	109.7
C(29)-C(24)-C(23)	109.50(14)	C(26)-C(30)-H(30B)	109.7
C(25)-C(24)-C(23)	109.97(14)	H(30A)-C(30)-H(30B)	108.2
C(29)-C(24)-H(24)	109.1	C(32)-C(31)-C(36)	120.14(15)
C(25)-C(24)-H(24)	109.1	C(32)-C(31)-C(22)	133.11(15)
C(23)-C(24)-H(24)	109.1	C(36)-C(31)-C(22)	106.75(14)
C(24)-C(25)-C(26)	109.79(13)	C(31)-C(32)-C(33)	118.55(15)
C(24)-C(25)-H(25A)	109.7	C(31)-C(32)-H(32)	120.7
C(26)-C(25)-H(25A)	109.7	C(33)-C(32)-H(32)	120.7
C(24)-C(25)-H(25B)	109.7	C(34)-C(33)-C(32)	120.87(16)
C(26)-C(25)-H(25B)	109.7	C(34)-C(33)-H(33)	119.6
H(25A)-C(25)-H(25B)	108.2	C(32)-C(33)-H(33)	119.6
C(21)-C(26)-C(30)	107.08(14)	C(33)-C(34)-C(35)	120.87(16)
C(21)-C(26)-C(25)	107.89(13)	C(33)-C(34)-H(34)	119.6
C(30)-C(26)-C(25)	108.65(13)	C(35)-C(34)-H(34)	119.6
C(21)-C(26)-H(26)	111.0	C(36)-C(35)-C(34)	117.82(15)
C(30)-C(26)-H(26)	111.0	C(36)-C(35)-H(35)	121.1
C(25)-C(26)-H(26)	111.0	C(34)-C(35)-H(35)	121.1
C(28)-C(27)-C(22)	108.98(13)	C(35)-C(36)-C(31)	121.75(15)
C(28)-C(27)-H(27A)	109.9	C(35)-C(36)-N(21)	126.12(15)
C(22)-C(27)-H(27A)	109.9	C(31)-C(36)-N(21)	112.13(14)
C(28)-C(27)-H(27B)	109.9		

Table 8. Anisotropic displacement parameters ($Å^2 x\ 10^3$) for **5**. The anisotropic displacement factor exponent takes the form: $-2p^2[\ h^2\ a^{*2}U^{11} + ...\ + 2\ h\ k\ a^*\ b^*\ U^{12}\ ]$

	U^{11}	U^{22}	U^{33}	U^{23}	U^{13}	U^{12}
N(1)	19(1)	20(1)	16(1)	1(1)	0(1)	2(1)
C(1)	17(1)	16(1)	14(1)	-1(1)	-1(1)	3(1)
C(2)	16(1)	16(1)	13(1)	0(1)	-1(1)	-1(1)
C(3)	18(1)	19(1)	18(1)	-1(1)	1(1)	0(1)
C(4)	16(1)	22(1)	22(1)	1(1)	4(1)	-1(1)
C(5)	15(1)	22(1)	27(1)	1(1)	-3(1)	1(1)
C(6)	19(1)	19(1)	17(1)	0(1)	-4(1)	0(1)
C(7)	16(1)	17(1)	18(1)	1(1)	-2(1)	0(1)
C(8)	18(1)	16(1)	22(1)	4(1)	-2(1)	0(1)
C(9)	20(1)	23(1)	24(1)	4(1)	1(1)	-4(1)
C(10)	19(1)	18(1)	22(1)	-2(1)	-4(1)	-1(1)
C(11)	15(1)	15(1)	17(1)	0(1)	2(1)	1(1)
C(12)	20(1)	18(1)	18(1)	-2(1)	0(1)	2(1)
C(13)	19(1)	20(1)	28(1)	-5(1)	-2(1)	-1(1)
C(14)	19(1)	17(1)	31(1)	2(1)	4(1)	-2(1)
C(15)	19(1)	19(1)	23(1)	4(1)	6(1)	2(1)
C(16)	17(1)	16(1)	17(1)	1(1)	2(1)	3(1)
N(21)	18(1)	21(1)	16(1)	0(1)	-1(1)	-1(1)
C(21)	15(1)	17(1)	15(1)	1(1)	-1(1)	-3(1)
C(22)	17(1)	18(1)	13(1)	-1(1)	-1(1)	-1(1)
C(23)	21(1)	23(1)	17(1)	2(1)	2(1)	-1(1)
C(24)	17(1)	28(1)	19(1)	0(1)	5(1)	-2(1)
C(25)	15(1)	26(1)	22(1)	-2(1)	-1(1)	-1(1)
C(26)	18(1)	22(1)	17(1)	2(1)	-2(1)	2(1)
C(27)	17(1)	23(1)	21(1)	-5(1)	-1(1)	-1(1)
C(28)	19(1)	20(1)	26(1)	-7(1)	0(1)	-1(1)
C(29)	22(1)	28(1)	22(1)	-6(1)	2(1)	4(1)
C(30)	20(1)	19(1)	28(1)	1(1)	2(1)	2(1)
C(31)	16(1)	17(1)	16(1)	-2(1)	-1(1)	-2(1)
C(32)	22(1)	23(1)	16(1)	0(1)	-3(1)	-1(1)
C(33)	21(1)	21(1)	25(1)	2(1)	-4(1)	1(1)
C(34)	19(1)	20(1)	27(1)	-4(1)	1(1)	0(1)
C(35)	21(1)	23(1)	18(1)	-4(1)	0(1)	-1(1)
C(36)	17(1)	18(1)	17(1)	-1(1)	-1(1)	-2(1)

Table 9. Hydrogen coordinates (x 10^4) and isotropic displacement parameters (Å^{2}x 10^3) for **5**.

	x	y	z	U(eq)
H(3A)	6291	5221	6039	22
H(3AB)	5494	5868	5518	22
H(4)	3272	4697	5760	24
H(5A)	3308	5207	4744	26
H(5AB)	2740	4139	4771	26
H(6)	5060	4377	4000	22
H(7A)	9353	3843	5117	20
H(7AB)	8646	3971	5791	20
H(8)	7120	2681	5347	22
H(9A)	4020	3118	5581	27
H(9AB)	5404	3533	6072	27
H(10A)	5137	2904	4510	24
H(10B)	7201	3207	4334	24
H(12)	10257	5863	6003	22
H(13)	12348	7018	5706	26
H(14)	12488	7489	4710	27
H(15)	10478	6849	3996	24
H(23A)	5153	2875	1672	24
H(23B)	5915	3363	2267	24
H(24)	8124	2255	1917	26
H(25A)	8001	2485	2973	25
H(25B)	8561	1439	2830	25
H(26)	6161	1475	3591	23
H(27A)	1970	1291	2398	24
H(27B)	2723	1596	1753	24
H(28)	4200	194	2049	26
H(29A)	7325	664	1895	28
H(29B)	5993	1225	1451	28
H(30A)	6157	170	2909	27
H(30B)	4079	411	3107	27
H(32)	1203	3558	1753	25
H(33)	-937	4595	2172	27
H(34)	-1150	4772	3203	27
H(35)	794	3927	3845	25

4.2 Compound **8**

The structure of **8** was solved in the monoclinic space group *C*2/*c*. The asymmetric unit contains one molecule of **8.**

Table 10. Crystal data and structure refinement for **8**.

CCDC No	20000167	
Empirical formula	C_{20} H_{26} N O	
Formula weight	296.42	
Temperature	100(2) K	
Wavelength	0.71073 Å	
Crystal system	Monoclinic	
Space group	*C*2/*c*	
Unit cell dimensions	a = 27.1498(9) Å	α= 90°.
	b = 10.3031(3) Å	β= 91.1403(16)°.
	c = 11.3085(4) Å	γ = 90°.
Volume	3162.67(18) Å^3	
Z	8	
Density (calculated)	1.245 Mg/m^3	
Absorption coefficient	0.075 mm^{-1}	
F(000)	1288	
Crystal size	0.331 x 0.125 x 0.048 mm^3	
Theta range for data collection	2.114 to 31.505°.	
Index ranges	$-39 \le h \le 39$, $-15 \le k \le 15$, $-16 \le l \le 16$	
Reflections collected	63246	
Independent reflections	5274 [R(int) = 0.0578]	
Completeness to theta = 25.242°	100.0 %	
Absorption correction	Semi-empirical from equivalents	
Refinement method	Full-matrix least-squares on F^2	
Data / restraints / parameters	5274 / 0 / 203	
Goodness-of-fit on F^2	1.039	
Final R indices [I>2σ(I)]	R_1 = 0.0460, wR_2 = 0.1193	
R indices (all data)	R_1 = 0.0607, wR_2 = 0.1303	
Extinction coefficient	0.0024(4)	
Largest diff. peak and hole	0.393 and -0.259 e.Å^{-3}	

Table 11. Atomic coordinates (x 10^4) and equivalent isotropic displacement parameters ($Å^2$x 10^3) for **8**. U(eq) is defined as one third of the trace of the orthogonalized U^{ij} tensor.

	x	y	z	U(eq)
O(1)	2990(1)	8403(1)	2780(1)	22(1)
N(1)	3244(1)	7418(1)	3129(1)	15(1)
C(1)	3001(1)	6126(1)	2998(1)	14(1)
C(2)	2537(1)	6143(1)	3759(1)	19(1)
C(3)	2845(1)	5948(1)	1686(1)	20(1)
C(4)	3347(1)	5034(1)	3390(1)	14(1)
C(5)	3176(1)	3762(1)	3247(1)	17(1)
C(6)	3472(1)	2705(1)	3533(1)	18(1)
C(7)	3952(1)	2911(1)	3939(1)	19(1)
C(8)	4121(1)	4170(1)	4114(1)	18(1)
C(9)	3822(1)	5247(1)	3870(1)	14(1)
C(10)	3990(1)	7276(1)	1983(1)	20(1)
C(11)	3789(1)	7570(1)	3217(1)	14(1)
C(12)	3982(1)	6619(1)	4182(1)	13(1)
C(13)	3754(1)	6978(1)	5392(1)	16(1)
C(14)	3882(1)	8375(1)	5742(1)	18(1)
C(15)	3680(1)	9301(1)	4787(1)	18(1)
C(16)	3911(1)	8978(1)	3595(1)	16(1)
C(17)	4473(1)	9133(1)	3726(1)	21(1)
C(18)	4673(1)	8193(1)	4669(1)	21(1)
C(19)	4544(1)	6785(1)	4329(1)	19(1)
C(20)	4442(1)	8519(1)	5860(1)	23(1)

Table 12. Bond lengths [Å] and angles [°] for **8**.

O(1)-N(1)	1.2860(10)	C(15)-C(16)	1.5347(14)
N(1)-C(11)	1.4892(12)	C(15)-H(15A)	0.9900
N(1)-C(1)	1.4931(12)	C(15)-H(15B)	0.9900
C(1)-C(4)	1.5256(13)	C(16)-C(17)	1.5389(14)
C(1)-C(2)	1.5406(14)	C(16)-H(16)	1.0000
C(1)-C(3)	1.5450(13)	C(17)-C(18)	1.5317(16)
C(2)-H(2A)	0.9800	C(17)-H(17A)	0.9900
C(2)-H(2B)	0.9800	C(17)-H(17B)	0.9900
C(2)-H(2C)	0.9800	C(18)-C(20)	1.5343(16)
C(3)-H(3A)	0.9800	C(18)-C(19)	1.5394(15)
C(3)-H(3B)	0.9800	C(18)-H(18)	1.0000
C(3)-H(3C)	0.9800	C(19)-H(19A)	0.9900
C(4)-C(5)	1.3982(13)	C(19)-H(19B)	0.9900
C(4)-C(9)	1.4065(13)	C(20)-H(20A)	0.9900
C(5)-C(6)	1.3878(14)	C(20)-H(20B)	0.9900
C(5)-H(5)	0.9500		
C(6)-C(7)	1.3898(14)	O(1)-N(1)-C(11)	117.74(8)
C(6)-H(6)	0.9500	O(1)-N(1)-C(1)	116.02(7)
C(7)-C(8)	1.3891(14)	C(11)-N(1)-C(1)	122.55(7)
C(7)-H(7)	0.9500	N(1)-C(1)-C(4)	111.09(7)
C(8)-C(9)	1.4000(13)	N(1)-C(1)-C(2)	107.45(8)
C(8)-H(8)	0.9500	C(4)-C(1)-C(2)	110.57(8)
C(9)-C(12)	1.5185(13)	N(1)-C(1)-C(3)	108.29(8)
C(10)-C(11)	1.5380(13)	C(4)-C(1)-C(3)	110.32(8)
C(10)-H(10A)	0.9800	C(2)-C(1)-C(3)	109.03(8)
C(10)-H(10B)	0.9800	C(1)-C(2)-H(2A)	109.5
C(10)-H(10C)	0.9800	C(1)-C(2)-H(2B)	109.5
C(11)-C(16)	1.5463(13)	H(2A)-C(2)-H(2B)	109.5
C(11)-C(12)	1.5503(13)	C(1)-C(2)-H(2C)	109.5
C(12)-C(19)	1.5405(13)	H(2A)-C(2)-H(2C)	109.5
C(12)-C(13)	1.5578(13)	H(2B)-C(2)-H(2C)	109.5
C(13)-C(14)	1.5307(14)	C(1)-C(3)-H(3A)	109.5
C(13)-H(13A)	0.9900	C(1)-C(3)-H(3B)	109.5
C(13)-H(13B)	0.9900	H(3A)-C(3)-H(3B)	109.5
C(14)-C(20)	1.5315(15)	C(1)-C(3)-H(3C)	109.5
C(14)-C(15)	1.5337(15)	H(3A)-C(3)-H(3C)	109.5
C(14)-H(14)	1.0000	H(3B)-C(3)-H(3C)	109.5

C(5)-C(4)-C(9)	119.37(8)	C(14)-C(13)-H(13B)	109.40
C(5)-C(4)-C(1)	117.16(8)	C(12)-C(13)-H(13B)	109.40
C(9)-C(4)-C(1)	123.47(8)	H(13A)-C(13)-H(13B)	108.00
C(6)-C(5)-C(4)	121.29(9)	C(13)-C(14)-C(20)	109.43(9)
C(6)-C(5)-H(5)	119.40	C(13)-C(14)-C(15)	109.08(8)
C(4)-C(5)-H(5)	119.40	C(20)-C(14)-C(15)	110.04(8)
C(5)-C(6)-C(7)	119.47(9)	C(13)-C(14)-H(14)	109.40
C(5)-C(6)-H(6)	120.30	C(20)-C(14)-H(14)	109.40
C(7)-C(6)-H(6)	120.30	C(15)-C(14)-H(14)	109.40
C(8)-C(7)-C(6)	119.67(9)	C(14)-C(15)-C(16)	109.68(8)
C(8)-C(7)-H(7)	120.20	C(14)-C(15)-H(15A)	109.70
C(6)-C(7)-H(7)	120.20	C(16)-C(15)-H(15A)	109.70
C(7)-C(8)-C(9)	121.54(9)	C(14)-C(15)-H(15B)	109.70
C(7)-C(8)-H(8)	119.20	C(16)-C(15)-H(15B)	109.70
C(9)-C(8)-H(8)	119.20	H(15A)-C(15)-H(15B)	108.20
C(8)-C(9)-C(4)	118.46(9)	C(15)-C(16)-C(17)	108.34(8)
C(8)-C(9)-C(12)	121.93(8)	C(15)-C(16)-C(11)	110.93(8)
C(4)-C(9)-C(12)	119.49(8)	C(17)-C(16)-C(11)	109.23(8)
C(11)-C(10)-H(10A)	109.50	C(15)-C(16)-H(16)	109.40
C(11)-C(10)-H(10B)	109.50	C(17)-C(16)-H(16)	109.40
H(10A)-C(10)-H(10B)	109.50	C(11)-C(16)-H(16)	109.40
C(11)-C(10)-H(10C)	109.50	C(18)-C(17)-C(16)	109.86(8)
H(10A)-C(10)-H(10C)	109.50	C(18)-C(17)-H(17A)	109.70
H(10B)-C(10)-H(10C)	109.50	C(16)-C(17)-H(17A)	109.70
N(1)-C(11)-C(10)	106.70(8)	C(18)-C(17)-H(17B)	109.70
N(1)-C(11)-C(16)	108.86(8)	C(16)-C(17)-H(17B)	109.70
C(10)-C(11)-C(16)	111.02(8)	H(17A)-C(17)-H(17B)	108.20
N(1)-C(11)-C(12)	107.59(7)	C(17)-C(18)-C(20)	109.11(9)
C(10)-C(11)-C(12)	113.14(8)	C(17)-C(18)-C(19)	110.22(8)
C(16)-C(11)-C(12)	109.37(7)	C(20)-C(18)-C(19)	109.31(9)
C(9)-C(12)-C(19)	114.11(8)	C(17)-C(18)-H(18)	109.40
C(9)-C(12)-C(11)	109.49(7)	C(20)-C(18)-H(18)	109.40
C(19)-C(12)-C(11)	109.02(8)	C(19)-C(18)-H(18)	109.40
C(9)-C(12)-C(13)	107.90(7)	C(18)-C(19)-C(12)	110.60(8)
C(19)-C(12)-C(13)	106.77(7)	C(18)-C(19)-H(19A)	109.50
C(11)-C(12)-C(13)	109.44(7)	C(12)-C(19)-H(19A)	109.50
C(14)-C(13)-C(12)	111.04(8)	C(18)-C(19)-H(19B)	109.50
C(14)-C(13)-H(13A)	109.40	C(12)-C(19)-H(19B)	109.50
C(12)-C(13)-H(13A)	109.40	H(19A)-C(19)-H(19B)	108.10

C(14)-C(20)-C(18)	108.93(8)
C(14)-C(20)-H(20A)	109.90
C(18)-C(20)-H(20A)	109.90
C(14)-C(20)-H(20B)	109.90
C(18)-C(20)-H(20B)	109.90
H(20A)-C(20)-H(20B)	108.30

Table 13. Anisotropic displacement parameters ($Å^2 x\ 10^3$) for **8**. The anisotropic displacement factor exponent takes the form: $-2p^2[\ h^2\ a^{*2}U^{11} + ...\ + 2\ h\ k\ a^*\ b^*\ U^{12}\ ]$

	U^{11}	U^{22}	U^{33}	U^{23}	U^{13}	U^{12}
O(1)	22(1)	14(1)	31(1)	3(1)	-6(1)	4(1)
N(1)	14(1)	12(1)	17(1)	0(1)	-2(1)	2(1)
C(1)	15(1)	13(1)	16(1)	-1(1)	-2(1)	0(1)
C(2)	15(1)	18(1)	23(1)	-2(1)	1(1)	1(1)
C(3)	22(1)	20(1)	17(1)	-1(1)	-6(1)	1(1)
C(4)	15(1)	13(1)	13(1)	-1(1)	0(1)	1(1)
C(5)	18(1)	15(1)	17(1)	-2(1)	-2(1)	-1(1)
C(6)	23(1)	13(1)	18(1)	-1(1)	0(1)	0(1)
C(7)	22(1)	15(1)	19(1)	1(1)	-1(1)	4(1)
C(8)	18(1)	17(1)	18(1)	1(1)	-3(1)	2(1)
C(9)	15(1)	13(1)	13(1)	0(1)	0(1)	0(1)
C(10)	24(1)	21(1)	15(1)	1(1)	4(1)	0(1)
C(11)	14(1)	14(1)	14(1)	1(1)	1(1)	0(1)
C(12)	13(1)	13(1)	14(1)	0(1)	-1(1)	0(1)
C(13)	19(1)	15(1)	14(1)	-1(1)	0(1)	-3(1)
C(14)	23(1)	17(1)	16(1)	-3(1)	2(1)	-3(1)
C(15)	21(1)	13(1)	21(1)	-2(1)	3(1)	-2(1)
C(16)	19(1)	12(1)	18(1)	1(1)	2(1)	-2(1)
C(17)	18(1)	18(1)	26(1)	-1(1)	5(1)	-4(1)
C(18)	15(1)	21(1)	27(1)	-3(1)	-2(1)	-4(1)
C(19)	15(1)	18(1)	23(1)	-2(1)	-2(1)	0(1)
C(20)	24(1)	21(1)	22(1)	-4(1)	-5(1)	-5(1)

Table14. Hydrogen coordinates (x 10^4) and isotropic displacement parameters ($Å^2$x 10^3) for **8**.

	x	y	z	U(eq)
H(2A)	2328	6881	3528	28
H(2B)	2634	6225	4595	28
H(2C)	2353	5334	3639	28
H(3A)	2666	6721	1411	30
H(3B)	2630	5186	1607	30
H(3C)	3138	5824	1209	30
H(5)	2851	3619	2947	20
H(6)	3347	1847	3452	22
H(7)	4163	2194	4096	22
H(8)	4448	4303	4405	21
H(10A)	3924	6366	1782	30
H(10B)	4346	7434	1983	30
H(10C)	3827	7839	1397	30
H(13A)	3392	6879	5337	19
H(13B)	3881	6377	6009	19
H(14)	3729	8584	6515	22
H(15A)	3758	10209	5008	22
H(15B)	3317	9213	4721	22
H(16)	3783	9594	2978	20
H(17A)	4629	8950	2960	25
H(17B)	4554	10036	3957	25
H(18)	5039	8288	4739	25
H(19A)	4670	6188	4951	22
H(19B)	4705	6559	3579	22
H(20A)	4572	7924	6480	27
H(20B)	4527	9419	6093	27

References

[5] L. Krause, R. Herbst-Irmer, G. M. Sheldrick, D. J. Stalke, *Appl. Cryst.,* 2015, **48**, 3–10.

[6, 7] G. M. Sheldrick, *Acta Cryst. A,* 2015, **71**, 3–8.

[8] https://www.ccdc.cam.ac.uk/structures/

[9] R. W. W. Hooft, L. H. Straver, A. L. Spek, *J. Appl. Cryst,.* 2008, **41**, 96-103.

3 Synthesis of Noradamantane Derivatives by Ring-Contraction of the Adamantane Framework

3.1 Abstract

We describe a triflic acid promoted cascade reaction of adamantane derivatives consisting of a decarboxylation of *N*-methyl protected cyclic carbamates and subsequent intramolecular nucleophilic 1,2-alkyl shift to generate ring contracted iminium triflates. This reaction expands the family of similar transformations, such as *Wagner-Meerwein-, Demjanov-Tiffeneau-, Meinwald-* or (semi-)pinacol-rearrangement. It allows the preparation of noradamantane derivatives in a few steps, starting from simple hydroxy-substituted adamantane precursors.

Published as: B. Zonker, J. Becker and R. Hrdina, *Org. Biomol. Chem.* **2021**, *19*, 4027-4031.

Organic & Biomolecular Chemistry

ROYAL SOCIETY OF CHEMISTRY

COMMUNICATION

View Article Online
View Journal | View Issue

Cite this: *Org. Biomol. Chem.*, 2021, **19**, 4027

Received 10th March 2021,
Accepted 8th April 2021

DOI: 10.1039/d1ob00471a

rsc.li/obc

Synthesis of noradamantane derivatives by ring-contraction of the adamantane framework†

Benjamin Zonker, [a] Jonathan Becker[b] and Radim Hrdina *[c]

We describe a triflic acid promoted cascade reaction of adamantane derivatives consisting of a decarboxylation of *N*-methyl protected cyclic carbamates and a subsequent intramolecular nucleophilic 1,2-alkyl shift to generate ring contracted iminium triflates. This reaction expands the family of similar transformations, such as Wagner–Meerwein-, Demjanov–Tiffeneau-, Meinwald- or (semi-) pinacol-rearrangement. It allows the preparation of noradamantane derivatives in a few steps, starting from simple hydroxy-substituted adamantane precursors.

Adamantane derivatives belong to a distinct class of aliphatic bridgehead compounds, whose properties and reactivity have been extensively studied.[1] Building blocks with the adamantane framework are frequently used for the development of drugs,[2] homogeneous and heterogeneous catalysts[3] and polymers[4] and for other applications, wherever enhanced lipophilicity, conformational rigidity or bulk is required.[5]

The methylene-contracted noradamantane cage delivers comparable properties but induces different geometries than adamantane congeners.[6] Fig. 1 shows examples of biologically active compounds containing the adamantane or noradamantane scaffold, *e.g.* a 11β-HSD1 inhibitor[7] or Rolofylline®,[8] an adenosine A1 receptor antagonist. Simple adamantane amines, such as amantadine and its derivatives, are known for their anti-influenza A activity for over 50 years.[2c,9] However, over the years, some influenza viruses have developed resistances against these known M2 ion channel inhibitors,[10] so that development of the next generation of anti-influenza substrates can be regarded as an issue of high importance. According to a recent study, similar compounds containing an annulated aza-heterocycle exhibit comparable activity and might thus be regarded as suitable candidates for flu treatment.[11] All compounds shown in Fig. 1 are accessible from the corresponding noradamantane precursors. However, the availability of substituted noradamantane derivatives is rather limited. So far, only two methods have been developed for the construction of the noradamantane framework (Fig. 2), which start from adamantan-2-ones[12] and 1,3-dihydroxy-adamantane derivatives,[13] respectively.

Recently, we have developed a simple approach for the preparation of heterocycles bearing the adamantane scaffold starting from noradamantane carbaldehyde.[14]

The limited access to the starting materials prompted us to find a new access to noradamantanes using readily available or easily accessible hydroxy-precursors. Our approach is based on a Brønsted acid-promoted cascade reaction,[15] starting from *N*-methylated cyclic carbamates. These compounds are prepared in two steps according to well-known literature procedures,[16] followed by *N*-methylation (see Fig. 3, top line).

The herein described ring-contraction reaction is a cascade process, starting with a decarboxylation event induced by

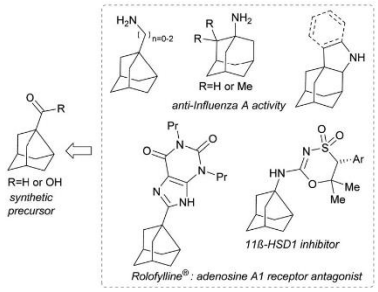

Fig. 1 Biologically active compounds previously prepared from noradamantane carboxylic acid or noradamantane carbaldehyde.

[a]*Institute of Organic Chemistry, Justus-Liebig University, Heinrich-Buff-Ring 17, 35392 Giessen, Germany*
[b]*Institute of Inorganic and Analytical Chemistry, Justus-Liebig University, Heinrich-Buff-Ring 17, 35392 Giessen, Germany*
[c]*Department of Organic Chemistry, Faculty of Science, Charles University in Prague, Hlavova 8, 128 40 Praha, Czech Republic. E-mail: hrdina@natur.cuni.cz*

†Electronic supplementary information (ESI) available. CCDC 2063017. For ESI and crystallographic data in CIF or other electronic format see DOI: 10.1039/d1ob00471a

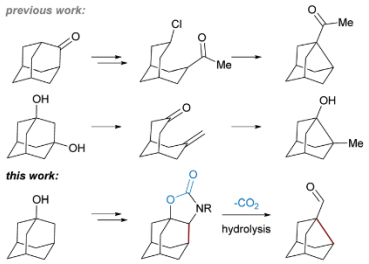

Fig. 2 Construction of the noradamantane framework.

triflic acid and a subsequent intramolecular nucleophilic 1,2-alkyl shift. The resulting methyl-iminium triflic salts are stable under these conditions and do not undergo further transformations. In the following reaction, the methyl-iminium group is hydrolysed to the corresponding carbonyl (Fig. 2). Noradamantane carbaldehydes – our main target – are useful precursors for further transformations as demonstrated in our previous work and by others.[9d,14,17] This new reaction expands the family of transformations such as Wagner–Meerwein-,[18] Demjanov–Tiffeneau-,[19] Meinwald-[20] or (semi-)pinacol-rearrangements.[21]

N-Methylated carbamate **4a** was chosen as a model substrate for the optimization of the reaction conditions (Table 1). No reaction was observed at temperatures below 100 °C (entries 1–3). Performing the reaction in 1,2-dichlorobenzene at 140 °C afforded 91% of the desired product **5a** after 17 h, while the reaction was much faster in 1,2,4-trichlorobenzene with 93% conversion within 3 h (entries 4 and 5). Decreasing the temperature to 120 °C resulted in significantly lower conversion (entry 6). No product was observed in high boiling polar solvents like dimethylacetamide even after a long reaction time (entry 10). Lower amounts of triflic acid resulted in

Table 1 Optimization of reaction conditions for the rearrangement of *N*-substituted carbamates **3a** or **4a** to iminium salts **5a**

	R	Brønsted acid (equiv.)	Solvent	Temp.	Conversion in %[a,b]
1	Me	TfOH (2)	CH_2Cl_2	23 °C	0
2	Me	TfOH (2)	CH_2Cl_2	40 °C	0
3	Me	TfOH (2)	$C_6H_4Cl_2$	110 °C	50
4	Me	TfOH (2)	$C_6H_4Cl_2$	140 °C	91
5	**Me**	**TfOH (2)**	**$C_6H_3Cl_3$**	**140 °C**	**93**[c]
6	Me	TfOH (2)	$C_6H_3Cl_3$	120 °C	30[c]
7	Me	TfOH (2)	$C_6H_3Cl_3$	120 °C	92
8	Me	*p*-TsOH (2)	$C_6H_4Cl_2$	140 °C	0
9	Me	TFA (2)	$C_6H_4Cl_2$	140 °C	0
10	Me	TfOH (2)	DMAC	140 °C	0
11	Me	TfOH (1.2)	$C_6H_3Cl_3$	120 °C	25
12	Me	TfOH (1)/Al(OTf)$_3$ (1)	$C_6H_3Cl_3$	120 °C	30
13	Me	Al(TfO)$_3$ (2)	$C_6H_3Cl_3$	140 °C	n.d.
14	H	TfOH (2)	$C_6H_3Cl_3$	120 °C	n.d.

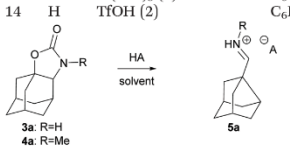

[a] Conversion of the starting material **3a** or **4a** measured by ^{1}H-NMR spectroscopy. [b] Reaction time 17 h. [c] Reaction time 3 h.

long reaction times (entry 11). Weaker Brønsted acids (*i.e.* trifluoroacetic acid or *p*-toluene sulfonic acid) did not decarboxylate the starting material (entries 8 and 9). The Lewis acid Al(OTf)$_3$ had no effect on the reaction, neither when used as an additive nor when used as the sole promoter (entries 12 and 13). Using the unprotected carbamate **3a** led to the formation of unidentified side products (entry 14). The protection of the carbamate seems necessary to prevent subsequent reactions of the generated iminium salt.

The optimised reaction conditions were then applied to more adamantane-based *N*-Me-carbamates in order to explore the scope of the reaction (alterations of the conditions are

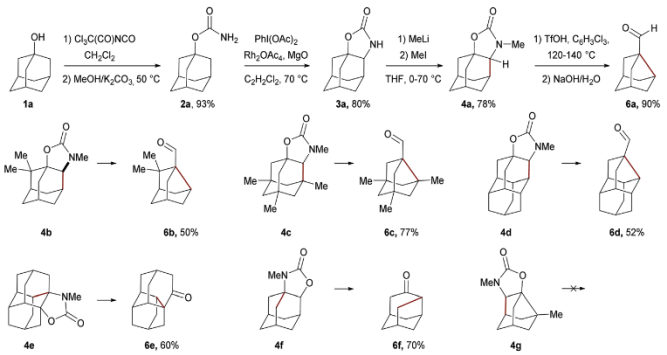

Fig. 3 Scope of the new transformation. Yields of isolated products **6** are stated.

noted in the ESI†). The results are presented in Fig. 3. Generally, the desired carbonyl compounds **6a–f** were obtained in moderate to good yields. Compound **6b** is a selected example of 2,2′-bis alkyl noradamantane derivatives accessible *via* our method. Interestingly, the starting material **3b** was prepared from **2b** as a single regioisomer. Trimethylated noradamantyl carbaldehyde **6c** was synthesized in a good yield from commercially available 3,5,7-trimethyl-1-adamantanol. Nordiamantane carbaldehyde **6d** (diamantane analogue of noradamantane carbaldehyde) was prepared in 52% yield. Diamantane derived ketone **6e**, a newly described hydrocarbon cage and analogue of protoadamantanone,[22] was obtained in 60% yield. The rearrangement of carbamate **4f** provides a new route to protoadamantanone **6f**. In these two cases, the nitrogen atom of the carbamate moiety is connected to a tertiary carbon and thus the sequence of reactions results in the formation of a ketone. Compound **4g** does not undergo further ring-contraction even at elevated temperature (>170 °C). We assume the difference in reactivity is due to the lower stability of the 3-noradamantyl carbocation (which would be the result of the decarboxylation of compound **4g**) compared to the stability of 1-adamantyl carbocation.[2,3] Ring-contraction of frameworks other than adamantane can occur if the intermediate carbocation is stable enough to allow the decarboxylation reaction to proceed.

Contracting the diamantane cage twice towards C_{12}-bis-carbaldehyde **11** (Scheme 1) turned out to be a challenging goal. 4,9-Diamantanediol **8** was synthesized from diamantane (**7**) to be used as the starting material. The strategy had to be changed since the solubility of diamantane bis-carbamate in organic solvents typically used in the oxidation step (*i.e.* nitrene insertion) is very low. The corresponding azide derivative (**9**) proved to be a more suitable starting material for the nitrene insertion step. The thermally induced insertion reaction proceeded quantitatively to afford the desired cyclic bis-carbamate (**10**) as a statistical mixture of six isomers. This cyclic carbamate was not purified due to its low solubility and was directly *N*-methylated. The resulting mixture of isomers of *N*-methylated diamantane bis-carbamates was subjected to the next reaction. The double rearrangement to give bis-carbaldehyde **11** proceeded in a relatively low yield of 10% but provides a single chiral (racemic mixture) regioisomer.

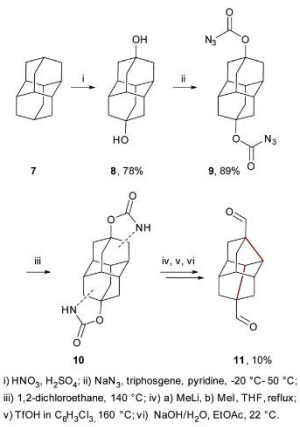

Scheme 1 Synthesis of bis-carbaldehyde **11** from diamantane **7**.

The formation of the more strained second (achiral) isomer[24] was not observed (as evidenced by NMR). This is the first time this C_{12}-cage isomer was isolated and fully described. It is difficult to increase the yield of this reaction, since it requires extremely non-polar solvents to proceed, which interferes with the solubility of the intermediate salt.

The proposed mechanism of the cascade reaction consists of a triflic acid promoted decarboxylation, generating intermediate **12a**, which undergoes a 1,2-alkyl shift to give the iminium salt **5a** as a final product (Fig. 4A).

The decarboxylation event is the rate-limiting step in the proposed sequence. Our previous results show that the rearrangement of the intermediate **12** to the thermodynamically more stable iminium salt occurs instantaneously at room temperature (Fig. 4B).[14] The calculated difference in thermodynamic stability of cation $\mathbf{5}^+$ and intermediate $\mathbf{12}^+$ is $\Delta H_{(rel)} = 22.0$ kcal mol^{-1} (Fig. 4C).

For long-term storage, carboxylic acids are preferable to aldehydes due to their higher stability. Moreover, as shown in Fig. 1, they are versatile building blocks for further syntheses.

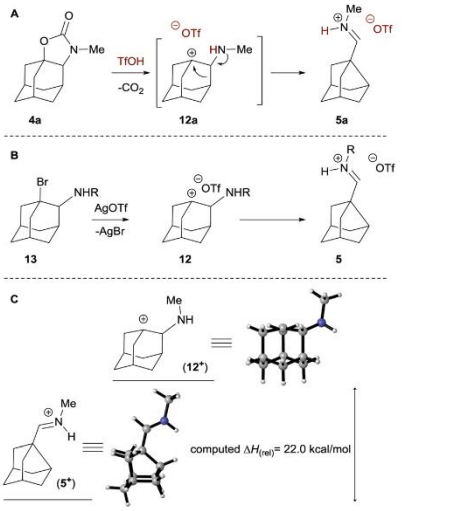

Fig. 4 (A) Mechanistic hypothesis of the new method. (B) Investigations shown in our previously published article.[14] (C) Relative stability of intermediate $\mathbf{12}^+$ *versus* target structure $\mathbf{5}^+$ using the DFT method B3LYP/6-311++G(2d,2p).

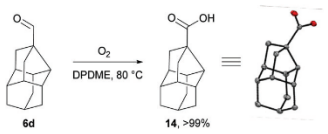

Scheme 2 Oxidation of nordiamantane carbaldehyde **6d** to carboxylic acid **14**; X-ray analysis structure of **14** is shown.

Nordiamantane derivative **6d** was oxidized to afford the corresponding acid **14** as an example. The reaction proceeded quantitatively using oxygen as the oxidant and dipropylene glycol dimethylether as a solvent.[25] The structure of the resulting nordiamantane carboxylic acid **14** was confirmed by X-ray crystallography (Scheme 2).

To conclude, we have developed a new pathway to noradamantane derivatives by decarboxylative ring-contraction of adamantane-based *N*-methyl carbamates. This method allows the preparation of known compounds and building blocks, namely noradamantane carbaldehyde and protoadamantanone, and provides access to new compounds, including diamantane-derived hydrocarbon cages.

Conflicts of interest

There are no conflicts to declare.

Acknowledgements

This work was supported by the DFG (HR 97/1-1). The authors would like to thank members of the Institute of Organic Chemistry JLU Giessen for their generous and continuous support, Lukas Ochmann for synthetic discussions, Dr Heike Hausmann for NMR experiments, Dr Artur Mardyukov for DFT analyses and Prof. Pavel Kočovský for manuscript proofreading.

Notes and references

1 (*a*) R. C. Fort and P. v. R. Schleyer, *Chem. Rev.*, 1964, **64**, 277–300; (*b*) R. Yasue and K. Yoshida, *Adv. Synth. Catal.*, 2021, **363**, 1662–1671.
2 (*a*) T. P. Stockdale and C. M. Williams, *Chem. Soc. Rev.*, 2015, **44**, 7737–7763; (*b*) L. Wanka, K. Iqbal and P. R. Schreiner, *Chem. Rev.*, 2013, **113**, 3516–3604; (*c*) E. De Clercq, *Nat. Rev. Drug Discovery*, 2006, **5**, 1015–1025; (*d*) R. Hrdina, F. M. Metz, M. Larrosa, J. P. Berndt, Y. Y. Zhygadlo, S. Becker and J. Becker, *Eur. J. Org. Chem.*, 2015, 6231–6236; (*e*) C. Tzitzoglaki, K. McGuire, P. Lagarias, A. Konstantinidi, A. Hoffmann, N. A. Fokina, C. Ma, I. P. Papanastasiou, P. R. Schreiner, S. Vázquez, M. Schmidtke, J. Wang, D. D. Busath and A. Kolocouris, *ACS Chem. Biol.*, 2020, **15**, 2331–2337; (*f*) L. C. Watkins, W. F. DeGrado and G. A. Voth, *J. Am. Chem. Soc.*, 2020, **142**, 17425–17433; (*g*) M. Côté, J. Misasi, T. Ren, A. Bruchez, K. Lee, C. M. Filone, L. Hensley, Q. Li, D. Ory, K. Chandran and J. Cunningham, *Nature*, 2011, **477**, 344–348; (*h*) V. V. Bakhonsky, A. A. Pashenko, J. Becker, H. Hausmann, H. J. De Groot, H. S. Overkleeft, A. A. Fokin and P. R. Schreiner, *Dalton Trans.*, 2020, **49**, 14009–14016; (*i*) J. Müller, R. A. Kirschner, J. P. Berndt, T. Wulsdorf, A. Metz, R. Hrdina, P. R. Schreiner, A. Geyer and G. Klebe, *ChemMedChem*, 2019, **14**, 663–672.
3 (*a*) K. A. Agnew-Francis and C. M. Williams, *Adv. Synth. Catal.*, 2016, **358**, 675–700; (*b*) J.-P. Berndt, Y. Radchenko, J. Becker, C. Logemann, D. R. Bhandari, R. Hrdina and P. R. Schreiner, *Chem. Sci.*, 2019, **10**, 3324–3329.
4 H. Nasrallah and J.-C. Hierso, *Chem. Mater.*, 2018, **31**, 619–642.
5 A. Štimac, M. Šekutor, K. Mlinarić-Majerski, L. Frkanec and R. Frkanec, *Molecules*, 2017, **22**, 297.
6 N. Moorthy, V. Poongavanam and V. Pratheepa, *Mini-Rev. Med. Chem.*, 2014, **14**, 819–830.
7 Th. Boehme, K. Ritter, C. Engel, S. Guessregen, T. Haack and G. Tschank, WO2012120050, 2012.
8 A. G. Moore, S. R. Schow, R. T. Lum, M. G. Nelson and C. R. Melville, *Synthesis*, 1999, 1123–1126.
9 (*a*) M. Lipsitch, J. B. Plotkin, L. Simonsen and B. Bloom, *Science*, 2012, **336**, 1529–1531; (*b*) W. L. Davies, R. R. Grunert, R. F. Haff, J. W. McGahen, E. M. Neumayer, M. Paulshock, J. C. Watts, T. R. Wood, E. C. Hermann and C. E. Hoffmann, *Science*, 1964, **144**, 862–863; (*c*) P. Camps, M. D. Duque, S. Vázquez, L. Naesens, E. De Clercq, F. X. Sureda, M. López-Querol, A. Camins, M. Pallàs, S. R. Prathalingam, J. M. Kelly, V. Romerof, D. Ivorra and D. Cortés, *Bioorg. Med. Chem.*, 2008, **16**, 9925–9936; (*d*) E. Torres, R. Fernandez, S. Miquet, M. Font-Bardia, E. Vanderlinden, L. Naesens and S. Vazquez, *ACS Med. Chem. Lett.*, 2012, **3**, 1065–1069.
10 (*a*) V. Pardali, E. Giannakopoulou, A. Konstantinidi, A. Kolocouris and G. Zoidis, *Croat. Chem. Acta*, 2019, **92**, 211–228; (*b*) M. Hussain, H. D. Galvin, T. Y. Haw, A. N. Nutsford and M. Husain, *Infect. Drug Resist.*, 2017, **10**, 121.
11 G. Zoidis, N. Kolocouris, L. Naesens and E. De Clercq, *Bioorg. Med. Chem.*, 2009, **17**, 1534–1541.
12 J. Janjatovic and Z. Majerski, *J. Org. Chem.*, 1980, **45**, 4892–4898.
13 M. Eakin, J. Martin and W. Parker, *Chem. Commun.*, 1965, 206–206.
14 B. Zonker, E. Duman, H. Hausmann, J. Becker and R. Hrdina, *Org. Biomol. Chem.*, 2020, **18**, 4941–4945.
15 C. Grondal, M. Jeanty and D. Enders, *Nat. Chem.*, 2010, **2**, 167–178.
16 R. Hrdina, M. Larrosa and C. Logemann, *J. Org. Chem.*, 2017, **82**, 4891–4899.
17 K. i. Takeuchi, I. Kitagawa, F. Akiyama, T. Shibata, M. Kato and K. Okamoto, *Synthesis*, 1987, 612–615.

18 (*a*) F. Romanov-Michailidis, L. Guénée and A. Alexakis, *Angew. Chem., Int. Ed.*, 2013, **52**, 9266–9270; (*b*) D. J. Cram, *J. Am. Chem. Soc.*, 1949, **71**, 3863–3870; (*c*) Z. Pakulski, P. Cmoch, A. Korda, R. Luboradzki, K. Gwardiak and R. Karczewski, *J. Org. Chem.*, 2021, **86**, 1084–1095; (*d*) V. A. Shadrikova, E. V. Golovin, V. B. Rybakov and Y. N. Klimochkin, *Chem. Heterocycl. Compd.*, 2020, **56**, 898–908; (*e*) H. A. Sharma, K. M. Mennie, E. E. Kwan and E. N. Jacobsen, *J. Am. Chem. Soc.*, 2020, **142**, 16090–16096; (*f*) Y.-Y. Liu, Z. Ao, G.-M. Xue, X.-B. Wang, J.-G. Luo and L.-Y. Kong, *Org. Lett.*, 2018, **20**, 7953–7956.

19 S. M. Kohlbacher, V.-S. Ionasz, L. Ielo and V. Pace, *Monatsh. Chem.*, 2019, 1–9.

20 (*a*) D. Ma, C.-B. Miao and J. Sun, *J. Am. Chem. Soc.*, 2019, **141**, 13783–13787; (*b*) R. Hrdina, C. E. Müller, R. C. Wende, K. M. Lippert, M. Benassi, B. Spengler and P. R. Schreiner, *J. Am. Chem. Soc.*, 2011, **133**, 7624–7627.

21 B. Wang and Y. Q. Tu, *Acc. Chem. Res.*, 2011, **44**, 1207–1222.

22 N. Kolocouris, G. Zoidis and C. Fytas, *Synlett*, 2007, 1063–1066.

23 J.-L. M. Abboud, M. Herreros, R. Notario, J. S. Lomas, J. Mareda, P. Müller and J.-C. Rossier, *J. Org. Chem.*, 1999, **64**, 6401–6410.

24 A. de Meijere, C. H. Lee, M. A. Kuznetsov, D. V. Gusev, S. I. Kozhushkov, A. A. Fokin and P. R. Schreiner, *Chem. – Eur. J.*, 2005, **11**, 6175–6184.

25 K.-J. Liu, Y.-L. Fu, L.-Y. Xie, C. Wu, W.-B. He, S. Peng, Z. Wang, W.-H. Bao, Z. Cao, X. Xu and W.-M. He, *ACS Sustainable Chem. Eng.*, 2018, **6**, 4916–4921.

Electronic Supplementary Material (ESI) for Organic & Biomolecular Chemistry.

Supporting Information

Synthesis of Noradamantane Derivatives by Ring-Contraction of the Adamantane Framework

Benjamin Zonker,[a] Jonathan Becker[b] and Radim Hrdina*[c]

1. General information

NMR spectra were recorded on 200, 400 or 600 MHz machine at RT (25 °C) unless otherwise stated. ^{1}H-NMR chemical shifts are given in ppm relative to Me_4Si with the solvent resonance used as the internal standard ($CDCl_3$ δ = 7.26 ppm). ^{13}C-NMR (60, 101 or 150 MHz) chemical shifts are given in ppm relative to Me_4Si with the solvent resonance used as the internal standard ($CDCl_3$ = 77.16 ppm). IR spectra were recorded using an ATR sampler and are reported in wave numbers (cm^{-1}). Melting points (m.p.) were measured in open capillary tubes and are uncorrected. All reactions involving air sensitive compounds were carried out under dry and inert atmosphere (N_2 or argon) by means of an inert gas/vacuum double manifold line and standard Schlenk techniques. Flash column chromatography was performed with silicagel 60 as stationary phase. High resolution mass spectra were recorded with Brucker Micro TOF LC.

2. Experimental procedures

2.1 Preparation of starting materials

2.1.1 General procedure A: Carbamate Synthesis

Under inert atmosphere, corresponding alcohol (1 eq., 5 mmol) is dissolved in CH_2Cl_2 (25 mL), cooled to 0 °C and treated with trichloroacetylisocyanate (1.3 eq., 6 mmol). The reaction mixture is stirred at room temperature for 3 hours and concentrated *in vacuo*. The residue is dissolved in MeOH (10 mL), treated with a saturated potassium carbonate solution (*aq.*, 15 mL) and stirred at 50°C overnight. The MeOH is removed *in vacuo* and the precipitate is filtered and washed with water. If the compound is not solid after MeOH evaporation, the aqueous phase is extracted with EtOAc (3x), washed with brine, dried over Na_2SO_4 (anhydrous), filtered and the solvent is evaporated *in vacuo*. The crude product is purified by flash column chromatography (mobile phase: hexanes/EtOAc).

2.1.2 General procedure B: Nitrene Insertion

Under inert atmosphere, the corresponding carbamate (1.0 eq., 2 mmol), iodobenzene I,I-diacetate (1.3 eq., 2.6 mmol), $Rh_2(OAc)_4$ (5-10 mol%, 0.01 mol), and MgO (2.5 eq., 5.0 mmol) are suspended in dry 1,2-dichloroethane (12 mL) and the reaction mixture is heated to 70 °C overnight. After the reaction mixture is cooled down to room temperature, it is filtered through a pad of silica gel and washed with a hexane/EtOAc 1:1 mixture to separate the product from the dirhodium catalyst and salts. The solvents are evaporated *in vacuo*, and the crude product is purified by flash column chromatography on silica gel (mobile phase: hexanes/EtOAc).

2.1.3 General procedure C: *N*-Methylation of Cyclic Carbamates

Under inert atmosphere, the corresponding oxazolidinone (1.0 eq., 2 mmol) is dissolved in dry THF (4 mL) and cooled to -20°C. Methyl lithium (1.05 eq., 2.1 mmol) is added dropwise. After stirring for 30 min, methyl iodide (2eq., 4 mmol) is added and the mixture is heated to reflux overnight. The solvents are evaporated *in vacuo*, and the crude product is purified by flash column chromatography on silica gel (mobile phase: hexanes/EtOAc).

2.1.4 Compound 4a

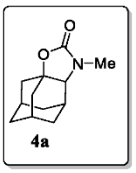

Compound **4a** was synthesized from adamantane annulated 1,3-oxazolidinone[1] according to *general procedure C* to give the desired product as a white solid in a yield of 76% (7.40 g, 40 mmol).

R_f (silica gel; EtOAc:*n*-hexane 2:3): 0.3.

m.p. (cryst. from $CDCl_3$): 71.1-72.6 °C.

^{1}H NMR (400 MHz, $CDCl_3$): δ/ppm = 1.61-1.84 (m, 7H), 1.94-2.09 (m, 4H), 2.27 (m, 2H), 2.78 (s, 3H), 3.28 (m, 1H).

^{13}C NMR (101 MHz, $CDCl_3$): δ/ppm = 29.3 (CH_3), 29.3 (CH), 29.5 (CH_2), 30.3 (CH), 31.3 (CH), 36.2 (CH_2), 36.3 (CH_2), 37.9 (CH_2), 40.0 (CH_2), 68.3 (CH), 77.9 (C), 160.7 (C).

IR (neat): $\tilde{\nu}$ /cm^{-1} = 2916, 2861, 1746, 1472, 1450, 1421, 1405, 1358, 1331, 1307, 1292, 1272, 1183, 1155, 1138, 1100, 1075, 1045, 1024, 990, 962, 901, 856, 828, 817, 774, 672, 648, 546, 515, 441.

HRMS: m/z = 208.1330 ([M+H]$^+$; calculated for $C_{12}H_{18}NO_2^+$ m/z =208.1332).

[1]R. Hrdina, M. Larrosa, C. Logemann, *J. Org. Chem*., 2017, **82**, 4891-4899.

2.1.5 Compound 2b

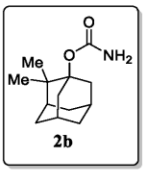

Compound **2b** was synthesized from 2,2-dimethyl adamantan-1-ol[2] following *general procedure A* to give a white solid in a yield of 75% (1.02 g, 5 mmol).

Rf (silica gel; EtOAc:*n*-hexane 2:3): 0.4.

m.p. (cryst. from $CDCl_3$): 106.4-107.8 °C.

^{1}H NMR (400 MHz, $CDCl_3$): δ/ppm = 1.08 (s, 6H), 1.42-1.46 (m, 2H), 1.56-1.59 (m, 3H), 2.02-2.06 (m, 2H), 2.11-2.15 (m, 4H), 2.60-2.65 (m, 2H), 4.37 (bs, 2H).

^{13}C NMR (101 MHz, $CDCl_3$): δ/ppm = 23.4 ($2CH_3$), 31.4(2CH), 32.6 ($2CH_2$), 35.8 ($2CH_2$), 37.9 (CH_2), 40.6 (C), 41.8 (CH), 83.9 (C).

IR (neat): $\tilde{\nu}$ /cm^{-1} = 3492, 3307, 3242, 2980, 2909, 2886, 1702, 1596, 1466, 1360, 1345, 1281, 1142, 1113, 1051, 950, 926, 898, 842, 817, 780, 757, 696, 652, 594.

HRMS: m/z = 246.1464 ([M+Na]$^+$; calculated for $C_{13}H_{21}NO_2Na^+$ m/z = 246.1464).

[2]E. Torres, R. Fernandez, S. Miquet, M. Font-Bardia, E. Vanderlinden, L. Naesens and S. Vazquez, *ACS Med. Chem. Lett.*, 2012, **3**, 1065–1069.

2.1.6 Compound 3b

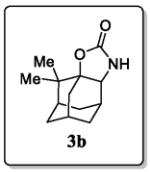

Compound **3b** was synthesized from compound **2b** following *general procedure B* to give the desired product as a clear oil in a yield of 77% (374 mg, 1.7 mmol,) as a single diastereomer.

R$_f$ (silica gel; EtOAc:*n*-hexane 1:4): 0.1.

^{1}H NMR (400 MHz, $CDCl_3$): δ/ppm = 1.15 (s, 3H), 1.18 (s, 3H), 1.44-1.56 (m, 2H), 1.60-1.65 (m, 2H), 1.83 (m, 1H), 1.95-2.05 (m, 4H), 2.13 (m, 1H), 2.26 (m, 1H), 4.10 (m, 1H), 5.67 (s, 1H).

^{13}C NMR (101 MHz, $CDCl_3$): δ/ppm = 22.7 (CH_3), 22.8 (CH_3), 29.4 (CH), 30.7 (CH_2), 31.9 (CH), 32.1 (CH_2), 32.1 (CH_2), 33.1 (CH_2), 41.3 (C), 58.7 (CH).

IR (neat): $\tilde{\nu}$ /cm^{-1} = 3288, 2920, 1738, 1634, 1462, 1401, 1321, 1285, 1247, 1196, 1143, 1098, 1082, 1047, 992, 951, 924, 898, 851, 785, 772, 727, 645, 622, 553, 522.

HRMS: m/z = 244.1304 ([M+Na]$^+$; calculated for $C_{13}H_{19}NO_2Na^+$ m/z = 244.1308).

2.1.7 Compound 4b

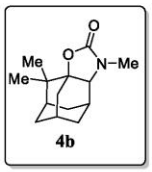

Compound **4b** was synthesized from compound **3b** according to *general procedure C* to give the desired product as a white solid in a yield of 94% (210 mg, 0.9 mmol).

R_f (silica gel; EtOAc:*n*-hexane 2:3): 0.3.

m.p. (cryst. from $CDCl_3$): 76.6-77.4 °C.

^{1}H NMR (400 MHz, $CDCl_3$): δ/ppm = 1.14 (s, 3H), 1.20 (s, 3H), 1.47-1.60 (m, 2H), 1.66-1.71 (m, 3H), 1.87 (m, 1H), 1.99-2.08 (m, 3H), 2.15 (m, 1H), 2.25 (m, 1H), 2.79 (s, 3H), 3.71 (m, 1H).

^{13}C NMR (101 MHz, $CDCl_3$): δ/ppm = 22.6 (CH_3), 22.9 (CH_3), 29.5 (CH), 29.5 (CH), 31.1 (CH), 31.1 (CH_2), 32.2 (CH_2), 32.9 (CH_2), 33.1 (CH_2), 39.6 (C), 41.6 (CH_3), 63.1 (CH), 82.2 (C), 160.6 (C).

IR (neat): $\tilde{\nu}$ /cm^{-1} = 2989, 2921, 2880, 2862, 1748, 1479, 1453, 1423, 1396, 1362, 1346, 1324, 1303, 1268, 1246, 1199, 1162, 1148, 1129, 1101, 1089, 1070, 1045, 1030, 1013, 987, 948, 929, 849, 798, 763, 675, 649, 608, 524.

HRMS: m/z = 236.1642 ([M+H]$^+$; calculated for $C_{14}H_{22}NO_2^+$ m/z = 236.1645).

2.1.8 Compound 2c

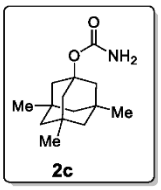

2c

Compound **2c** was synthesized from 3,5,7-trimethyl adamantan-1-ol[4] according to *general procedure A* to give the desired product as a white solid in a yield of 90% (1.10 g, 4.6 mmol).

R_f (silica gel; EtOAc:*n*-hexane 2:3): 0.3.

m.p. (cryst. from $CDCl_3$): 126.3-128.0 °C.

^{1}H NMR (400 MHz, $CDCl_3$): δ/ppm = 0.88 (s, 9H), 1.01-1.04 (m, 3H), 1.13-1.16 (m, 3H), 1.69 (m, 6H), 4.38 (bs, 2H).

^{13}C NMR (101 MHz, $CDCl_3$): δ/ppm = 29.6 ($3CH_3$), 34.1 (3C), 46.7 ($3CH_2$), 49.9 ($3CH_2$), 81.6 (C), 155.9 (C).

IR (neat): $\tilde{\nu}$ /cm^{-1} = 3281, 2945, 2920, 2897, 2862, 2837, 1715, 1605, 1526, 1454, 1373, 1353, 1334, 1254, 1225, 1205, 1049, 1031, 1001, 922, 845, 781, 745, 667, 643, 551, 486.

HRMS: m/z = 260.1616 ([M+Na]$^+$; calculated for $C_{14}H_{23}NO_2Na^+$ m/z =260.1621).

[4]Y. N. Klimochkin,., A. V. Yudashkin, E. O. Zhilkina, E. A. Ivleva, I. K. Moiseev, and Y. F. Oshis, *Russ. J. Org. Chem.*, 2017, **53**, 971-76.

2.1.9 Compound 3c

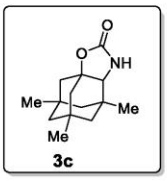

3c

Compound **3c** was synthesized from compound **2c** following *general procedure B* to give the desired product as a white solid in a yield of 95% (707 mg, 3.0 mmol).

R_f (silica gel; EtOAc:*n*-hexane 1:4): 0.1.

m.p. (cryst. from $CDCl_3$): 210.5-211.8 °C.

^{1}H NMR (400 MHz, $CDCl_3$): δ/ppm = 0.91-0.92 (m, 6H), 0.95 (s, 3H), 1.01 (m, 1H), 1.09-1.21 (m, 3H), 1.26 (m, 1H), 1.38-1.48 (m, 2H), 1.69-1.78 (m, 3H), 3.20 (s, 1H), 5.01 (m, 1H).

^{13}C NMR (101 MHz, $CDCl_3$): δ/ppm = 25.7 (CH_3), 29.0 (CH_3), 29.3 (CH_3), 33.1 (C), 34.9 (C), 35.7 (C), 42.7 (CH_2), 42.8 (CH_2), 45.4 (CH_2), 50.2 (CH_2), 50.8 (CH_2), 67.9 (CH), 82.7 (C), 161.1 (C).

IR (neat): $\tilde{\nu}$ /cm^{-1} = 3251, 2951, 2900, 2867, 2840, 1742, 1455, 1404, 1377, 1356, 1331, 1314, 1296, 1281, 1255, 1223, 1200, 1183, 1135, 1081, 1019, 993, 985, 957, 942, 923, 854, 839, 802, 775, 706, 683, 595, 562, 539, 527, 498, 482, 471, 446.

HRMS: m/z = 258.1466 ([M+Na]$^+$; calculated for $C_{14}H_{21}NO_2Na^+$ m/z = 258.1465).

2.1.10 Compound 4c

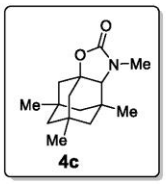

4c

Compound **4c** was synthesized from compound **3c** according to *general procedure C* to give the desired product as a white solid in a yield of 96% (213 mg, 0.9 mmol).

R_f (silica gel; EtOAc:*n*-hexane 2:3): 0.4.

m.p. (cryst. from $CDCl_3$): 110.2-111.0 °C.

^{1}H NMR (400 MHz, $CDCl_3$): δ/ppm = 0.90 (s, 3H), 0.94 (s, 3H), 1.05-1.21 (m, 7H), 1.30-1.43 (m, 3H), 1.61-1.72 (m, 3H), 2.89 (m, 4H).

^{13}C NMR (101 MHz, $CDCl_3$): δ/ppm = 26.5 (CH_3), 29.0 (CH_3), 29.3 (CH_3), 32.6 (CH), 32.9 (C), 35.1 (C), 36.1 (C), 43.6 (CH_2), 43.6 (CH_2), 45.1 (CH_2), 50.0 (CH_2), 52.2 (CH_2), 72.1 (CH_3), 79.5 (C), 161.2 (C).

IR (neat): $\tilde{\nu}$ /cm^{-1} = 2950, 2897, 2865, 2837, 1741, 1453, 1411, 1375, 1343, 1308, 1261, 1209, 1188, 1139, 1120, 1093, 1080, 1031, 1012, 995, 982, 940, 919, 902, 851, 803, 773, 704, 671, 598, 561, 431, 497, 482, 444.

HRMS: m/z = 250.1805 ([M+H]$^+$; calculated for $C_{15}H_{24}NO_2^+$ m/z = 250.1802).

2.1.11 Compound 4d

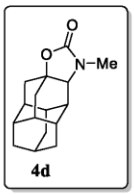

4d

Compound **4d** was synthesized from diamantane annulated 1,3-oxazolidinone[5] according to *general procedure C* to give the desired product as a white solid in a yield of 95% (250 mg, 1 mmol).

R_f (silica gel; EtOAc:*n*-hexane 1:4): 0.1.

m.p. (cryst. from $CDCl_3$): 166.6-167.5 °C.

^{1}H NMR (400 MHz, $CDCl_3$): δ/ppm = 1.73-1.83 (m, 9H), 1.86-1.97 (m, 4H), 2.01-2.06 (m, 2H), 2.13 (m, 2H), 2.79 (s, 3H), 3.22 (m, 1H).

^{13}C NMR (101 MHz, $CDCl_3$): δ/ppm = 25.9 (CH_3), 29.4 (CH), 31.0 (CH), 36.0 (CH_2), 36.7 (CH), 36.8 (CH_2), 37.1 (CH), 37.3 (CH_2), 38.1 (CH_2), 38.3 (CH), 39.1 (CH), 40.0 (CH_2), 40.5 (CH), 69.2 (CH), 77.5 (C), 160.9 (C).

IR (neat): $\tilde{\nu}$ /cm^{-1} = 2879, 1738, 1462, 1427, 1375, 1352, 1334, 1303, 1269, 1258, 1244, 1190, 1127, 1069, 1050, 1039, 1006, 947, 908, 846, 797, 775, 763, 722, 689, 659, 620, 559, 540, 469.

HRMS: m/z = 260.1643 ([M+H]$^+$; calculated for $C_{16}H_{22}NO_2^+$ m/z =260.1645).

[5]B. Zonker, E. Duman, H. Hausmann, J. Becker, R. Hrdina., *Org Biomol. Chem.*, 2020, **18**, 4941-4945.

2.1.12 Compound 2e

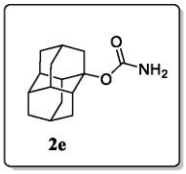

2e

Compound **2e** was synthesized from diamantan-1-ol[6] according to *general procedure A* to give the desired product as a white solid in a yield of 87% (680 mg, 2.8 mmol).

R_f (silica gel; EtOAc:*n*-hexane 2:3): 0.2.

m.p. (cryst. from EtOAc): 162.6.-163.9 °C.

^{1}H NMR (400 MHz, $CDCl_3$): δ/ppm = 1.43-1.48 (m, 2H), 1.56-1.60 (m, 2H), 1.66-1.76 (m, 6H), 1.97-1.98 (m, 2H), 2.03-2.09 (m, 3H), 2.15-2.16 (m, 2H), 2.30 (m, 2H), 4.47 (bs, 2H).

^{13}C NMR (101 MHz, $CDCl_3$): δ/ppm = 25.1 (CH), 30.3 (CH), 32.8 ($2CH_2$), 36.8 (CH), 37.3 ($2CH_2$), 38.1 (CH_2), 40.3 (2CH), 40.4 (2CH), 40.9 (CH_2), 83.0 (C), 156.0 (C).

IR (neat): $\tilde{\nu}$ /cm^{-1} = 3426, 3219, 2901, 2872, 2850, 1716, 1688, 1667, 1606, 1460, 1440, 1372, 1341, 1321, 1297, 1137, 1079, 1041, 1023, 991, 981, 953, 905, 847, 814, 782, 6763, 722, 606, 566, 481, 435.

HRMS: m/z =270.1465 ([M+Na]$^+$; calculated for $C_{15}H_{21}NO_2Na^+$ m/z =270.1465).

[6]Andrey A. Fokin , B. A. Tkachenko, P. A. Gunchenko, D. V. Gusev, P. R. Schreiner , *Chem. Eur. J.*, 2005, **11**, 7091-7101.

2.1.13 Compound 3e

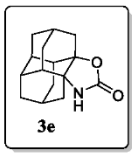

3e

Compound **3e** was synthesized from compound **2e** according to *general procedure B* to give the desired product as a white solid in a yield of 83% (510 mg, 2.1 mmol) as a single regiomer.

R_f (silica gel; EtOAc*:n*-hexane 2:3): 0.2.

m.p. (cryst. from $CDCl_3$): >250 °C

^{1}H NMR (400 MHz, $CDCl_3$): δ/ppm = 1.47-1.69 (m, 8H), 1.89-2.11 (m, 8H), 2.23-2.28 (m, 2H), 5.17 (bs 1H).

^{13}C NMR (101 MHz, $CDCl_3$): δ/ppm = 27.8 (CH), 29.0 (CH), 31.3 (CH_2), 31.5 (CH_2), 36.8 (CH_2), 37.0 (CH_2), 39.4 (CH_2), 39.7 (CH), 39.7 (CH), 40.1 (CH), 41.3 (CH), 42.3 (CH_2), 60.4 (CH), 83.4 (C), 161.5 (C).

IR (neat): $\tilde{\nu}$ /cm^{-1} = 3227, 2918, 2855, 1740, 1634, 1460, 1439, 1337, 1273, 1218, 1188, 1118, 1108, 1063, 1052, 1008, 948, 932, 920, 892, 853, 827, 807, 777, 700, 684, 663, 624, 546, 516, 485, 465.

HRMS: m/z = 246.1491 ([M+H]$^+$; calculated for $C_{15}H_{20}NO_2^+$ m/z =246.1489).

2.1.14 Compound 4e

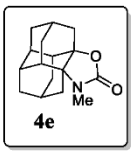

4e

Compound **4e** was synthesized from compound **3e** according to *general procedure C* to give the desired product as a white solid in a yield of 93% (165 mg, 1.4 mmol).

R_f (silica gel; EtOAc:*n*-hexane 2:3): 0.3.

m.p. (cryst. from $CDCl_3$): 114.2-115.0 °C.

^{1}H NMR (400 MHz, $CDCl_3$): δ/ppm = 1.52-1.77 (m, 9H), 1.85 (m, 1H), 1.93 (m, 1H), 2.01-2.10 (m, 5H), 2.15 (m, 1H), 2.25 (m, 1H), 2.69 (s, 3H).

^{13}C NMR (101 MHz, $CDCl_3$): δ/ppm = 25.6 (CH_3), 27.3 (CH), 28.9 (CH), 31.6 (CH_2), 31.7 (CH_2), 36.9 (CH_2), 37.0 (CH_2), 37.5 (CH_2), 38.9 (CH), 39.6 (CH_2), 39.6 2(CH), 41.5 (CH), 62.3 (C), 81.3 (C), 160.1 (C).

IR (neat): $\tilde{\nu}$ /cm^{-1} = 2914, 2851, 1733, 1460, 1483, 1424, 1380, 1346, 1323, 1294, 1283, 1252, 1223, 1123, 1074, 1063, 1034, 1020, 1003, 944, 919, 813, 772, 685, 667, 646, 634, 520, 485, 470.

HRMS: m/z = 260.1642 ([M+H]$^+$; calculated for $C_{16}H_{22}NO_2^+$ m/z =260.1645).

2.1.15 Compound 4f

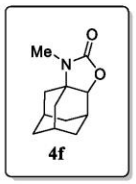

Compound **4f** was synthesized from corresponding oxazolidinone[7] according to *general procedure C* to give the desired product as a white solid in a yield of 34%[8] (177 mg, 0.9 mmol).

R_f (silica gel; EtOAc:*n*-hexane 2:3): 0.3.

m.p. (cryst. from $CDCl_3$): 105.4-106.7 °C.

^{1}H NMR (400 MHz, $CDCl_3$): δ/ppm = 1.56-1.78 (m, 6H), 1.82-1.94 (m, 4H), 2.07 (m, 1H), 2.18 (m, 1H), 2.42 (m, 1H), 2.69 (s, 3H), 3.98.

^{13}C NMR (101 MHz, $CDCl_3$): δ/ppm = 26.1 (CH_3), 27.7 (CH), 29.6 (CH), 30.0 (CH_2), 30.2 (CH), 35.1(CH_2), 36.1(CH_2), 36.6(CH_2), 38.4(CH_2), 58.8 (C), 83.8(CH), 160.0 (C).

IR (neat): $\tilde{\nu}$ /cm^{-1} = 2922, 2903, 2857, 1740, 1456, 1423, 1383, 1362, 1334, 1319, 1301, 1267, 1246, 1122, 1081, 1067, 1050, 1017, 997, 965, 928, 856, 811, 772, 756, 690, 673, 617, 548, 511, 465, 441.

HRMS: m/z = 208.1333 ([M+H]$^+$; calculated for $C_{12}H_{18}NO_2^+$ m/z =208.1332).

[7]R, Hrdina, M. Larrosa, C. Logemann, *J. O. Chem*., 2017, **82**, 4891-4899.
[8]starting material recovered.

2.1.16 Compound 2g

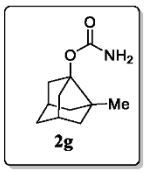

2g

Compound **2g** was synthesized from 7-methyl-noradamantan-3-ol[9] according to *general procedure A* to give the desired product as a white solid in a yield of 84% (530 mg, 2.7 mmol).

R_f (silica gel; EtOAc:*n*-hexane 2:3): 0.4.

m.p. (cryst. from $CDCl_3$): 109.0-110.9 °C.

^{1}H NMR (400 MHz, $CDCl_3$): δ/ppm = 1.05 (s, 3H), 1.48-1.68 (m, 6H), 1.92-1.96 (m, 2H), 2.23-2.26 (m, 2H), 2.39-2.43 (m, 2H), 4.50 (bs, 2H).

^{13}C NMR (101 MHz, $CDCl_3$): δ/ppm = 22.0 (CH_3), 33.6 (CH_2), 35.9 (CH), 46.1 (C), 48.6 ($2CH_2$), 50.3($2CH_2$), 89.6 (C), 156.5 (C).

IR (neat): $\tilde{\nu}$ /cm^{-1} = 3482, 3322, 3254, 3182, 2934, 2865, 1694, 1594, 1459, 1366, 1324, 1305, 1262, 1221, 1170, 1121, 1045, 963, 934, 901, 866, 783, 705, 638, 607, 495.

HRMS: m/z = 218.1150 ([M+Na]$^+$; calculated for $C_{13}H_{19}NO_2Na^+$ m/z = 218.1151).

[9]M. Takefumi, O. Muraoka, S. Atarashi, and T. Horita, *Chem. Pharm. Bull.*, 1979, **27**, 222-29.

2.1.17 Compound 3g

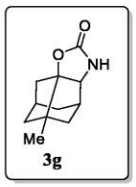

3g

Compound **3g** was synthesized from compound **2g** according to *general procedure B* to give the desired product as an off-white solid in a yield of 81% (200 mg, 1.0 mmol) as a single diastereomer.

R_f (silica gel; EtOAc:*n*-hexane 2:3): 0.2.

m.p. (cryst. from $CDCl_3$): 107.5-109.2 °C.

^{1}H NMR (400 MHz, $CDCl_3$): δ/ppm = 1.05 (s, 3H), 1.51-1.76 (m, 5H), 1.98 (m, 1H), 2.11-2.18 (m, 2H), 2.30-2.40 (m, 5H), 3.79 (m, 1H), 5.31 (bs, 1H).

^{13}C NMR (101 MHz, $CDCl_3$): 21.6 (CH_3), 33.1 (CH_2), 35.1 (CH), 39.5 (CH), 43.9 (CH_2), 45.3 (C), 45.5 (CH_2), 49.9 (CH_2), 71.3 (CH), 92.4 (C), 160.5 (C).

IR (neat): $\tilde{\nu}$ /cm^{-1} = 3280, 2948, 2928, 2864, 1761, 1731, 1479, 1455, 1374, 1324, 1305, 1269, 1257, 1218, 1192, 1169, 1149, 1124, 1112, 1089, 1074, 1018, 970, 954, 931, 916, 790, 768, 757, 689, 659, 627, 590, 534, 511, 494, 444.

HRMS: m/z = 216.0997 ([M+Na]$^+$; calculated for $C_{11}H_{15}NO_2Na^+$ m/z = 216.0995).

2.1.18 Compound 4g

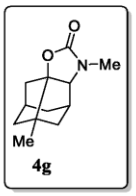

4g

Compound **4g** was synthesized from compound **3g** according to *general procedure C* to give the desired product as a white solid in a yield of 96% (155 mg, 0.8 mmol).

R_f (silica gel; EtOAc:*n*-hexane 3:7): 0.2.

m.p. (cryst. from $CDCl_3$): 74.8-75.6 °C.

^{1}H NMR (400 MHz, $CDCl_3$): δ/ppm = 1.02 (s, 3H), 1.51-1.67 (m, 4H), 1.74-1.84 (m, 2H), 1.91-1.94 (m, 1H), 2.14-2.18 (m, 1H), 2.32 (m, 1H), 2.41 (m, 1H), 2.72 (s, 3H), 3.48 (m, 1H).

^{13}C NMR (101 MHz, $CDCl_3$): δ/ppm = 21.6 (CH_3), 28.5 (CH_3), 32.9 (CH_2), 35.2 (CH), 37.8 (CH), 43.6 (CH_2), 45.2 (C), 45.3 (CH_2), 49.8 (CH_2), 75.6 (CH), 89.3 (C), 159.5 (C).

IR (neat): $\tilde{\nu}$ /cm^{-1} = 2947, 2919, 2862, 1742, 1475, 1459, 1426, 1391, 1331, 1285, 1260, 1228, 1207, 1166, 1112, 1077, 1038, 1016, 995, 956, 910, 848, 785, 766, 756, 699, 663, 640, 598, 533, 511, 484, 442.

HRMS: m/z = 208.1333 ([M+H]$^+$; calculated for $C_{12}H_{18}NO_2^+$ m/z = 208.1332).

2.1.19 Compound 9

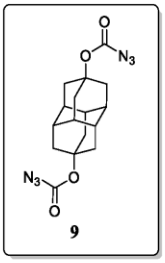

At -20 °C, 4,9-diamantanediol (1 eq., 220 mg, 1 mmol)[10] and sodium azide (4 eq., 260 mg, 4 mmol) in pyridine (10 mL) were treated with triphosgene (1 eq., 297 mg, 1 mmol) in 2 ml methylene chloride. The reaction mixture was allowed to warm to room temperature and subsequently heated to 50 °C for 6 hours. The reaction was quenched with water and extracted with EtOAc (2x). The combined organic phases were dried over Na_2SO_4 (anhydrous), filtered and the solvents were evaporated *in vacuo*. The crude product was washed with hexane to remove non-polar impurities and used without further purification.

Yield: 89% (320 mg, 0.89 mmol).

^{1}H NMR (400 MHz, $CDCl_3$): δ/ppm = 1.74 (s, 6H), 1.99 (s, 6H), 2.15 (s, 6H).

^{13}C NMR (101 MHz, $CDCl_3$): δ/ppm = 38.6 (6CH), 40.0 (6CH_2), 82.8 (C), 155.5 (C).

IR (neat): $\tilde{\nu}$ /cm^{-1} = 3572, 3306, 2895, 2172, 2131, 1716, 1616, 1585, 1525, 1443, 1349, 1291, 1259, 1217, 1195, 1135, 1106, 1073, 1049, 1001, 977, 951, 926, 823, 779, 753, 718, 665, 651, 487, 437.

HRMS: m/z = 381.1280 ([M+Na]$^+$; calculated for $C_{16}H_{18}N_6O_4Na^+$ m/z = 381.1282).

[10]M. A. Gunawan, O. Moncea, D. Poinsot, M. Keskes, B. Domenichini, O. Heintz, R. Chassagnon, F. Herbst, R. M. Carlson, J. E. Dahl, *Adv. Funct. Mater.*, 2018, **28**, 1705786. |

2.1.20 Compound 10

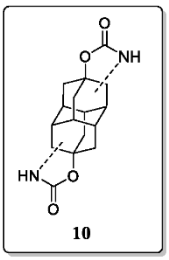

10

Compound **9** (100 mg, 0.28 mmol) was dissolved in 1,2-dichloroethane (10 mL) and heated to 130 °C for 24 hours. The solvent was evaporated *in vacuo* and the crude mixture of six isomers was used in the next step without further purification.

^{1}H NMR (400 MHz, CD_3OD): δ/ppm = 1.80-2.42 (m, 14H), 3.70 (m, 2H), 4.67 (m, 2H).

HRMS: m/z = 325.1160 ([M+Na]$^+$; calculated for $C_{16}H_{18}N_2O_4Na^+$ m/z = 325.1159).

2.1.21 Compound 15

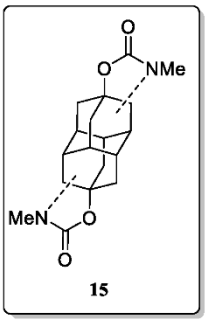

15

Compound **15** was synthesized from compound 10 according to *general procedure C*. The crude mixture was purified by flash column chromatography on silica gel (mobile phase: EtOAc) to isolate the product as a mixture of six isomers.

^{1}H NMR (400 MHz, $CDCl_3$): δ/ppm = 1.75-2.26 (m, 16H), 2.78-2.81 (m, 6H), 3.30-3.36 (m, 2H).

HRMS: m/z = 353.1473 ([M+Na]$^+$; calculated for $C_{18}H_{22}N_2O_4Na^+$ m/z = 353.1472).

2.2 NMR spectra of starting materials

2.2.1 Compound 4a

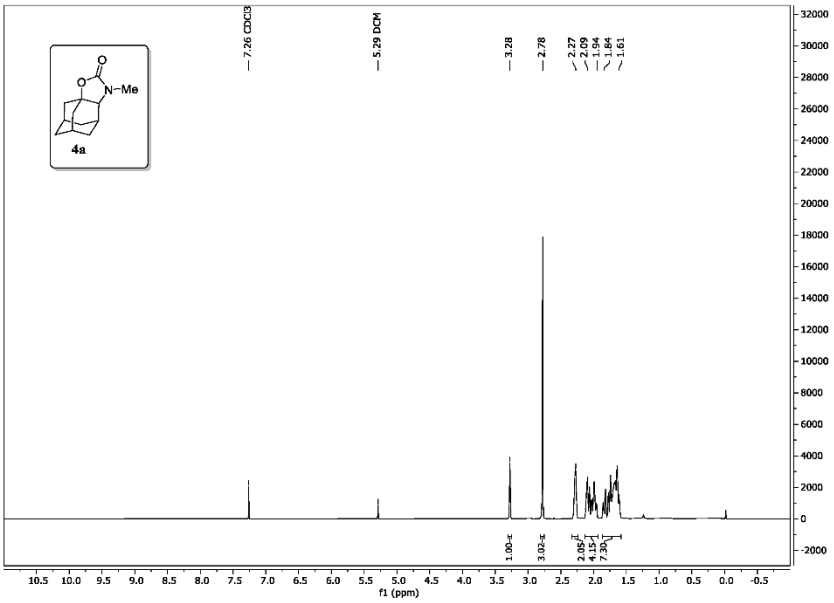

S21

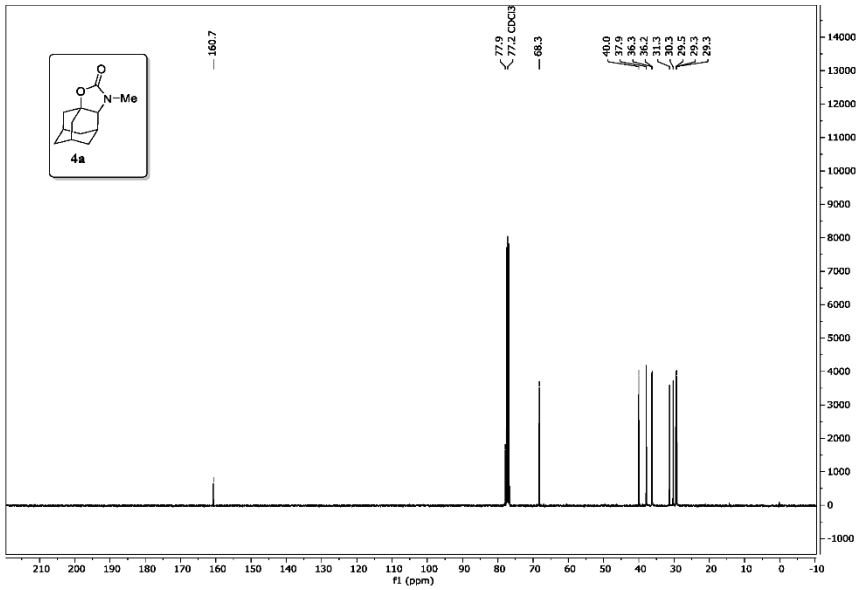

S22

2.2.2 Compound 2b

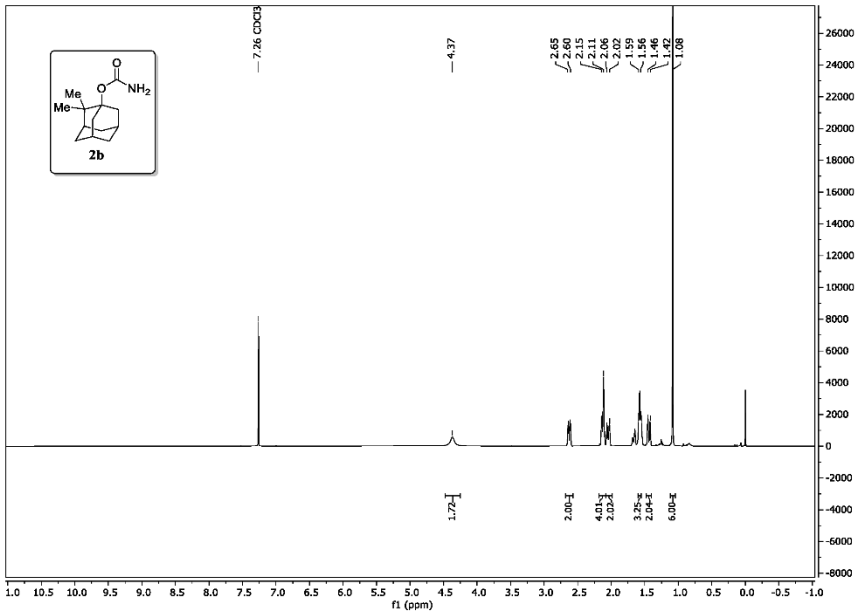

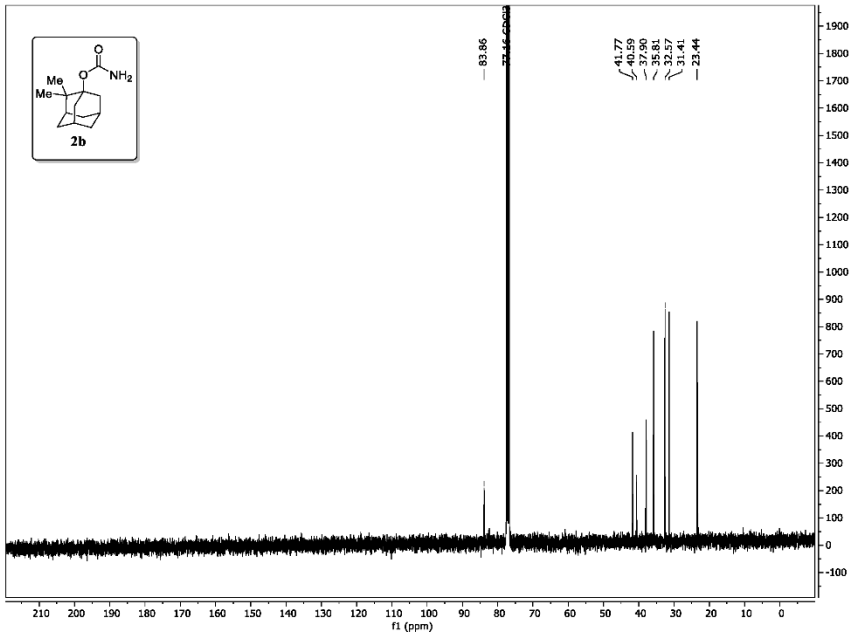

2.2.3 Compound 3b

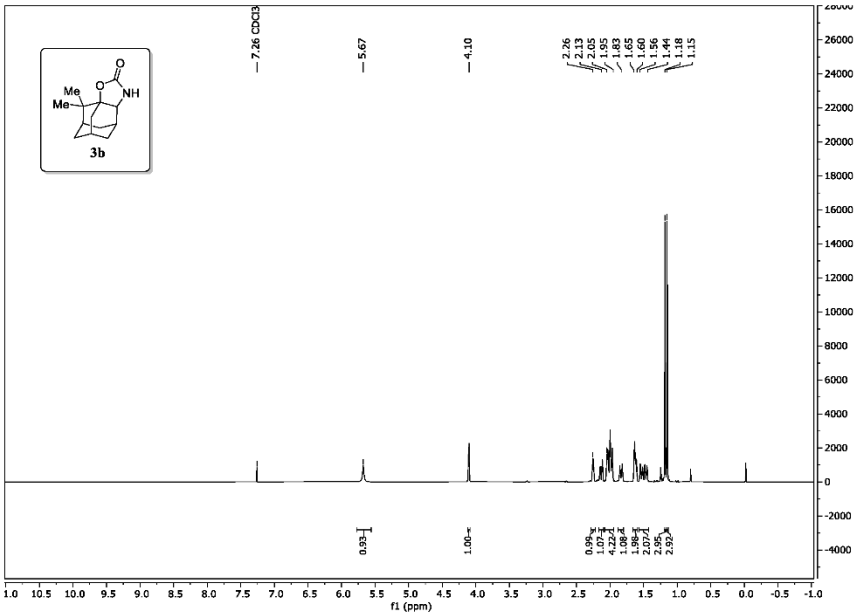

S25

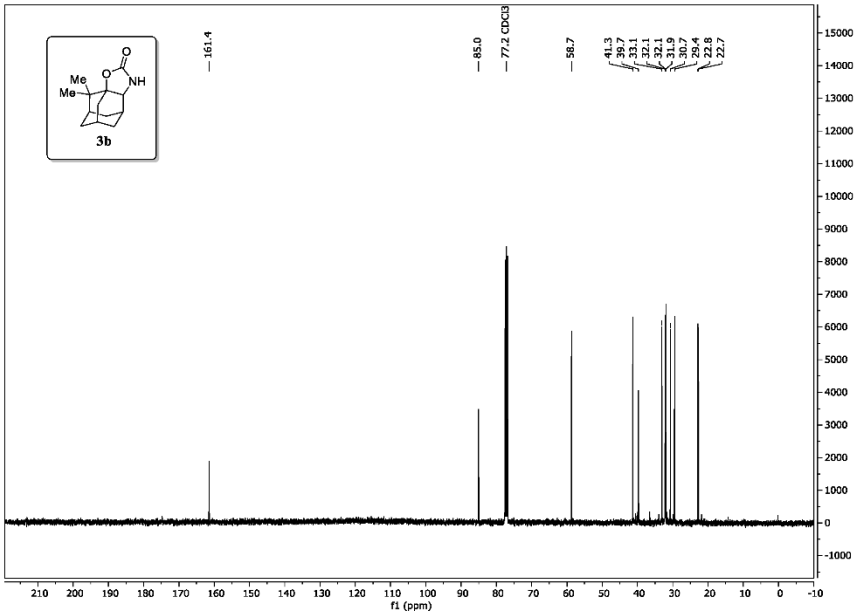

S26

2.2.4 Compound 4b

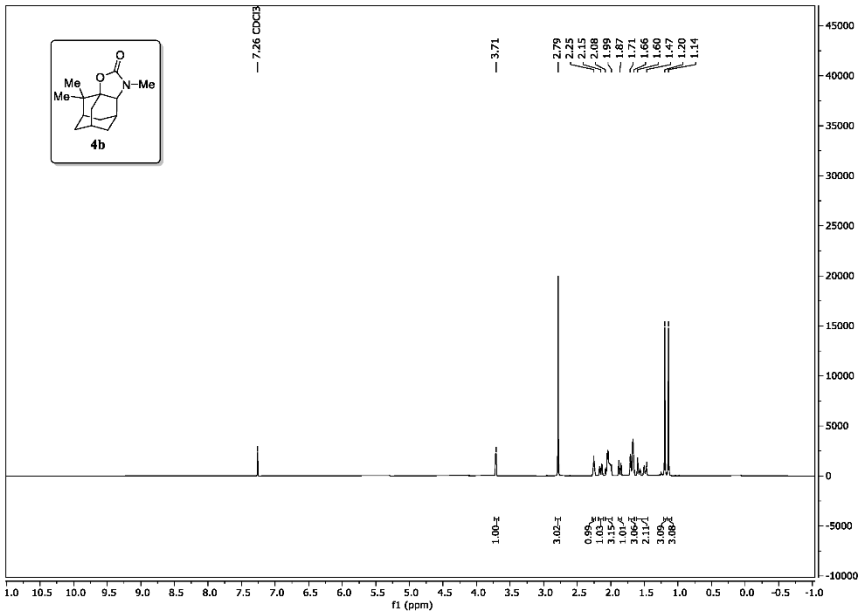

S27

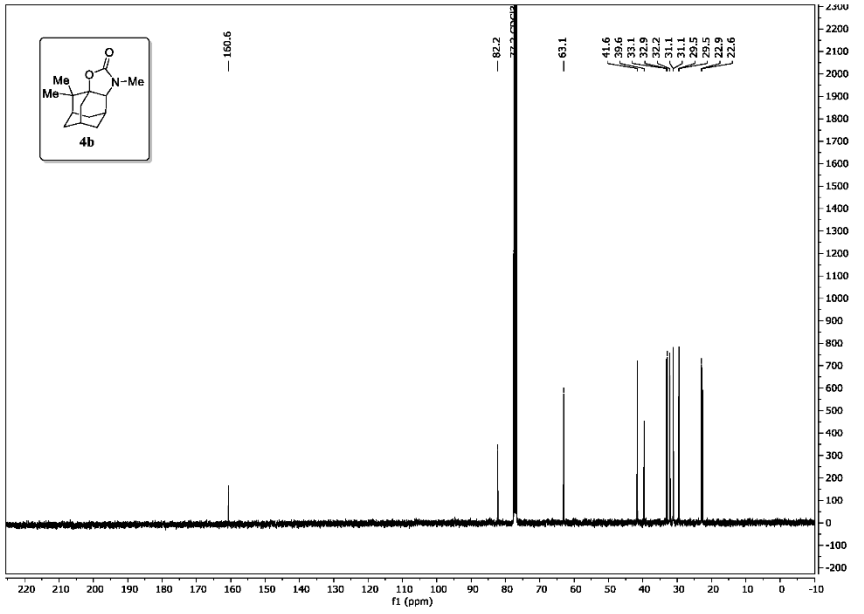

S28

2.2.5 Compound 2c

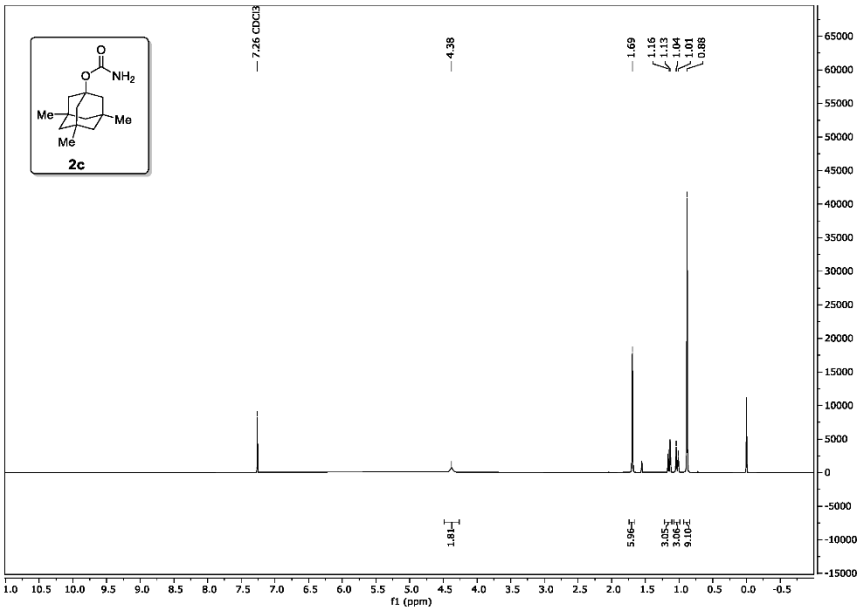

S29

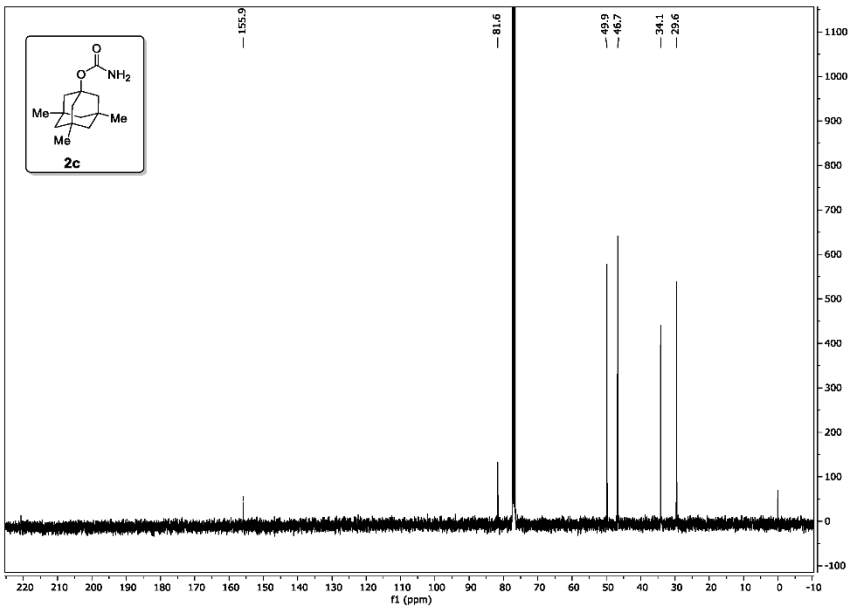

S30

2.2.6 Compound 3c

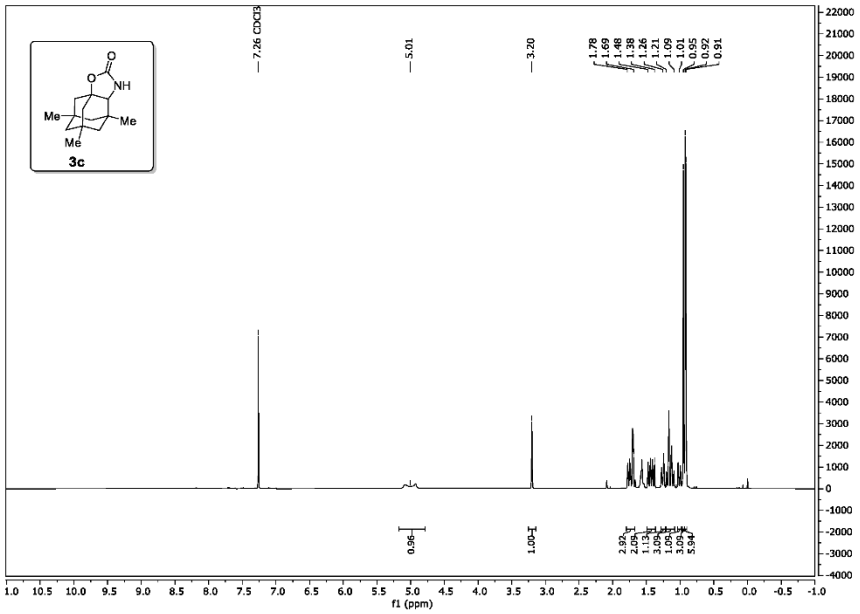

S31

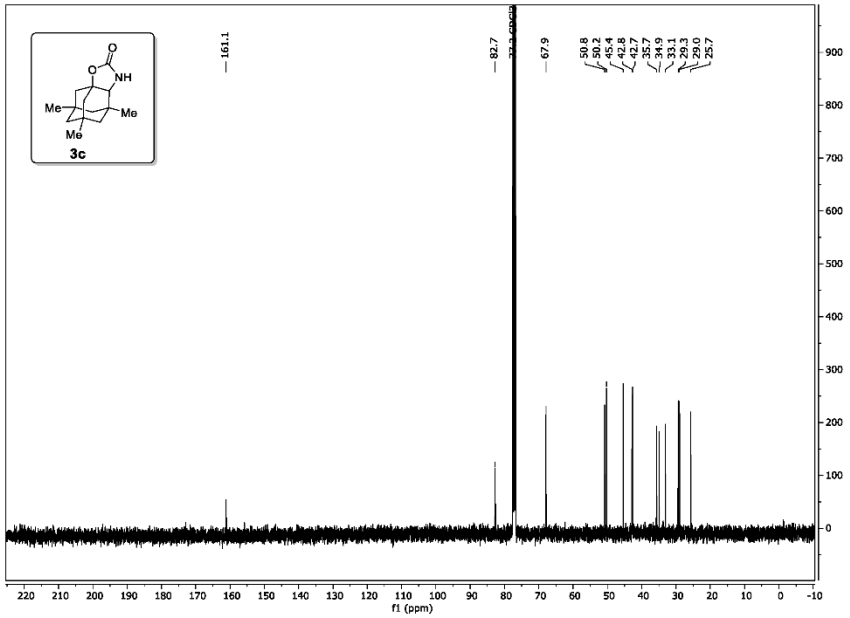

S32

2.2.7 Compound 4c

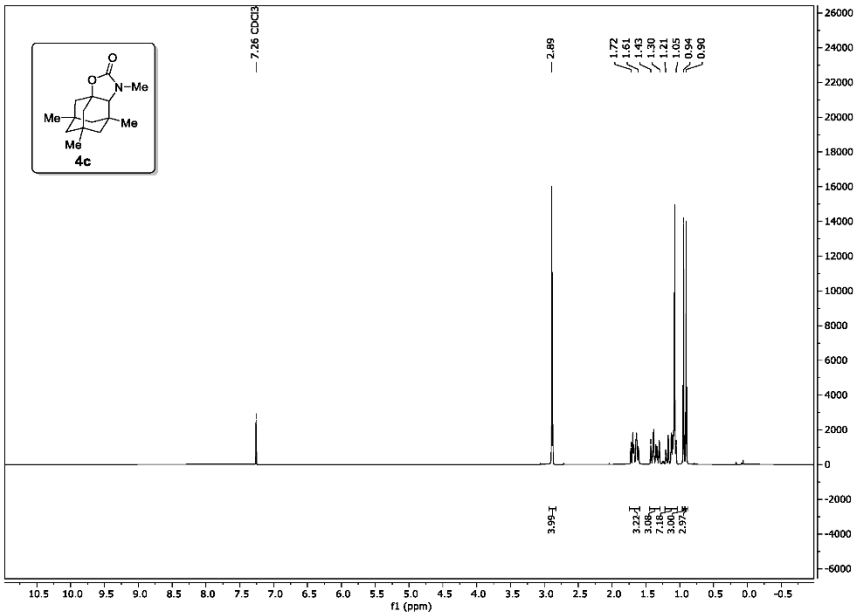

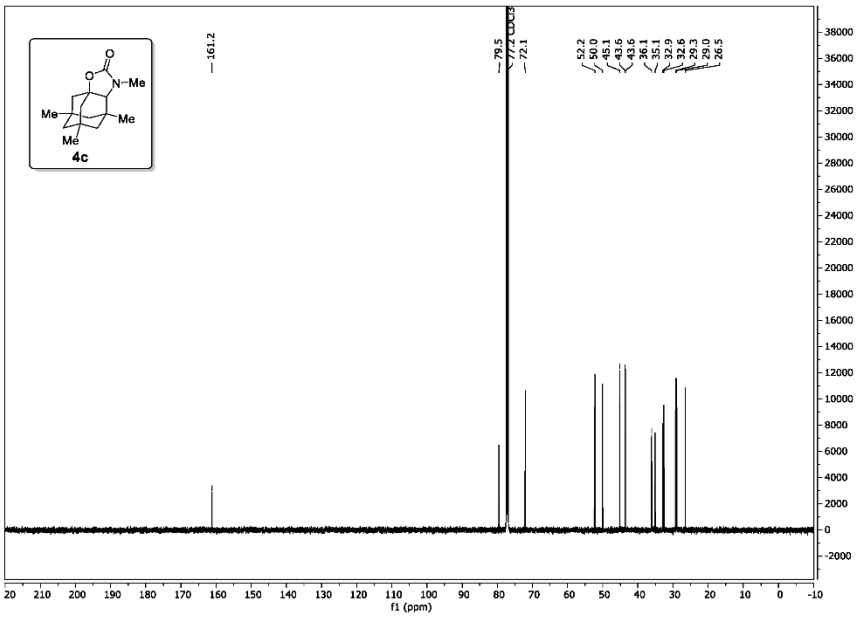

2.2.8 Compound 4d

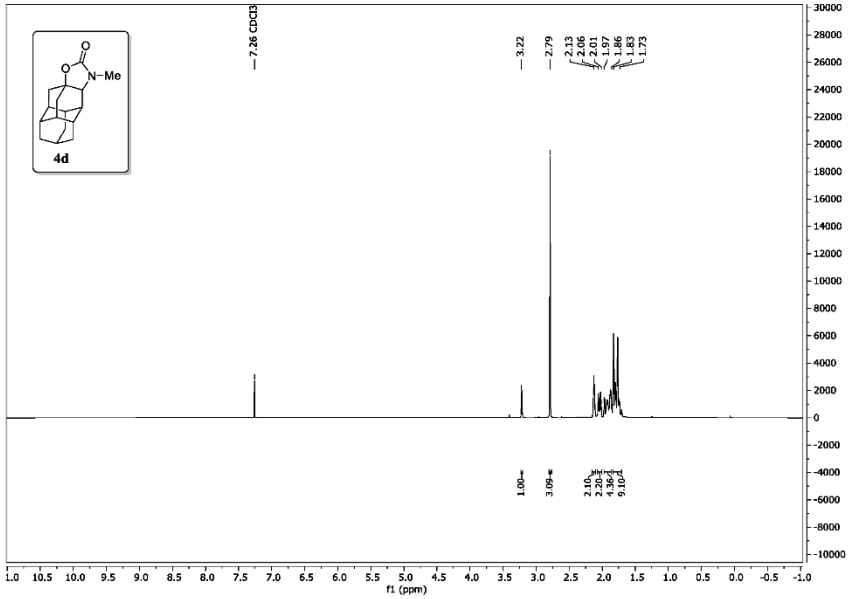

S35

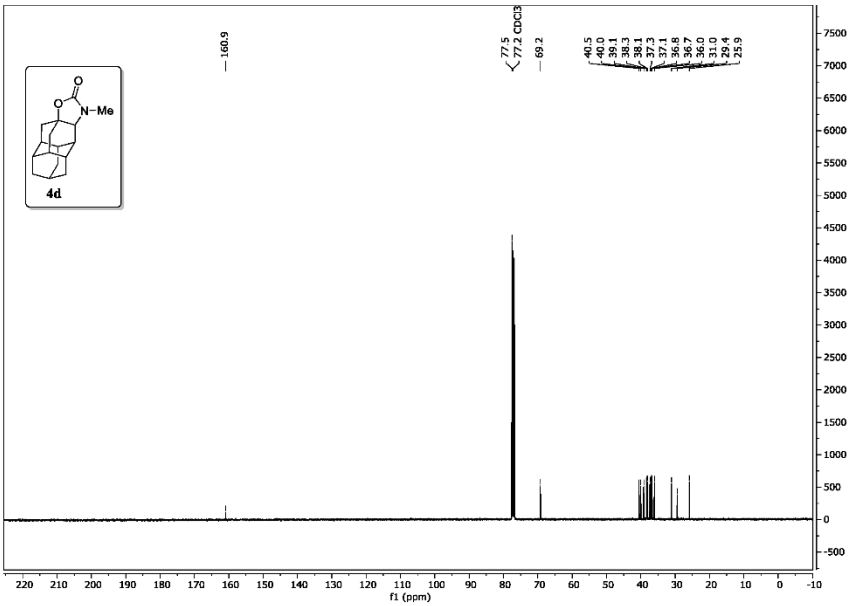

S36

2.2.9 Compound 2e

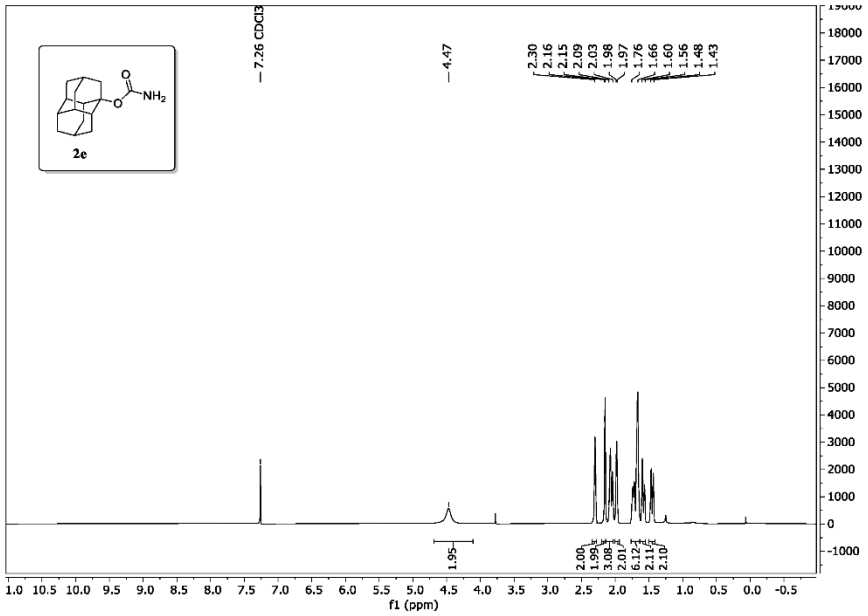

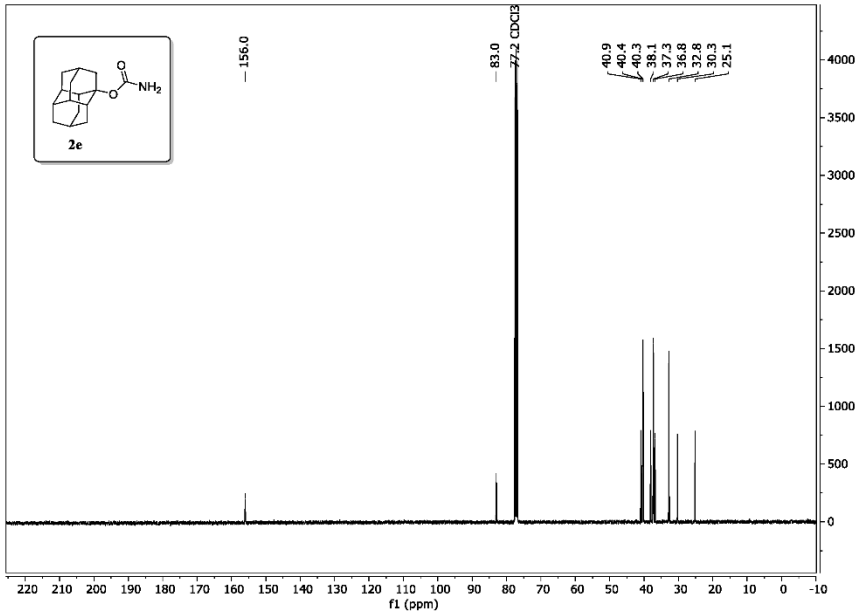

2.2.10 Compound 3e

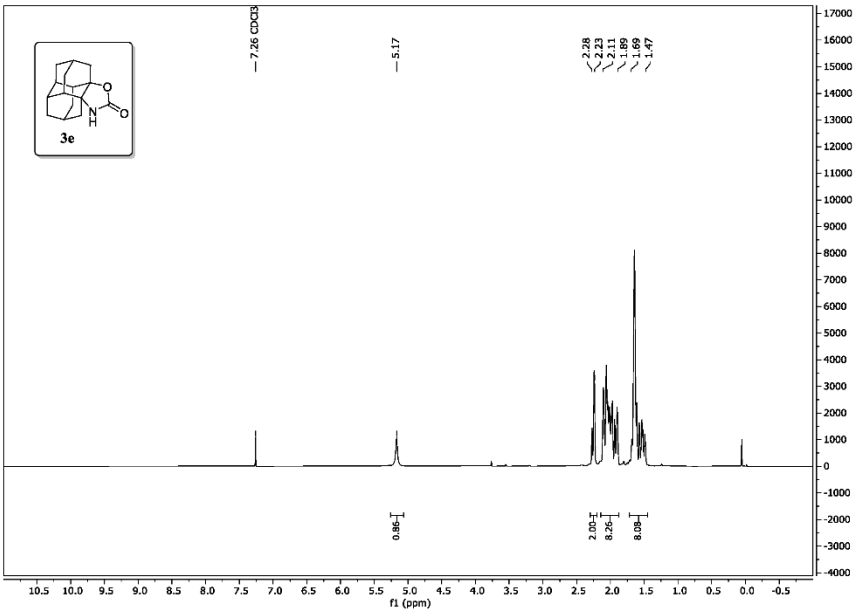

S39

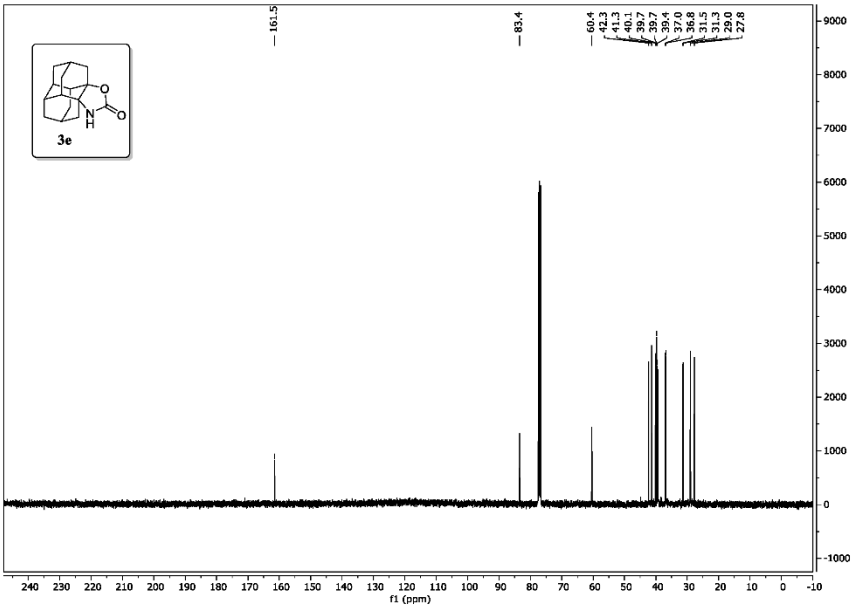

S40

2.2.11 Compound 4e

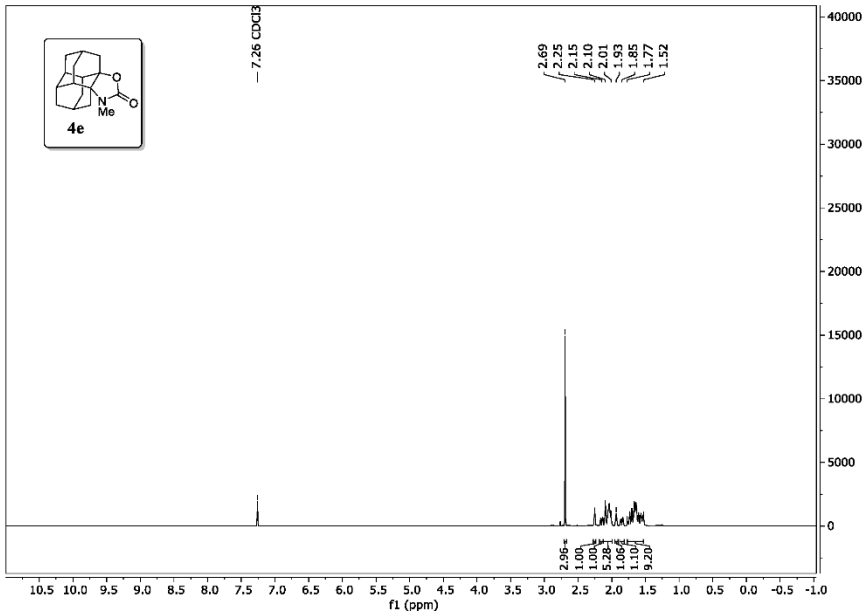

S41

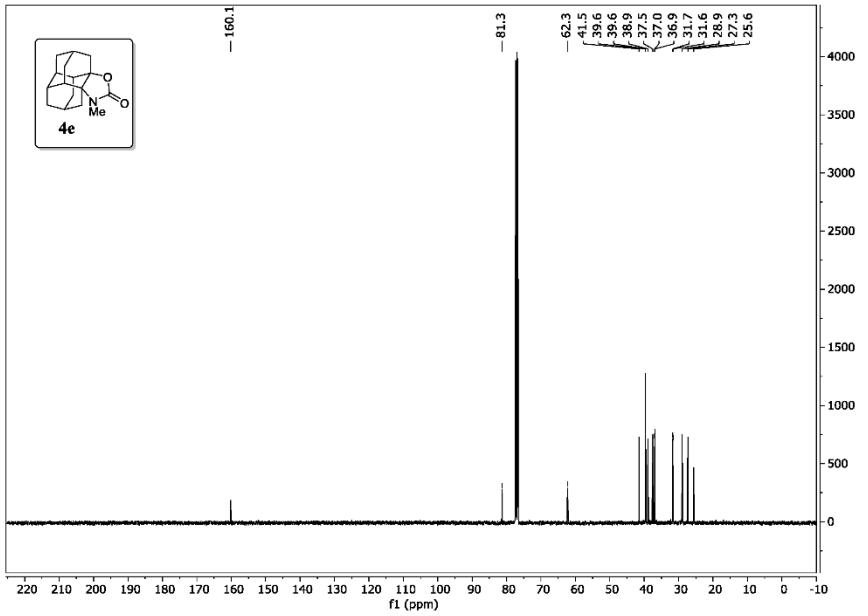

S42

2.2.12 Compound 4f

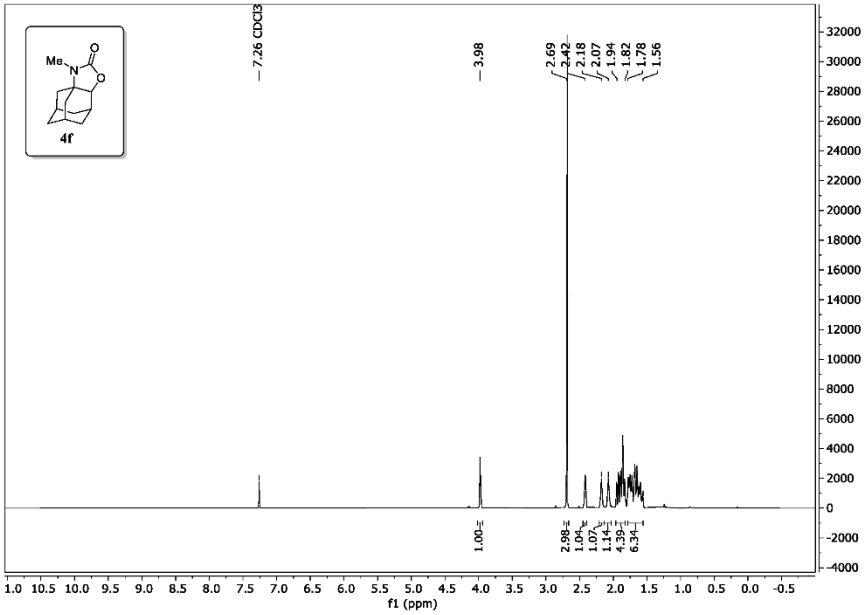

S43

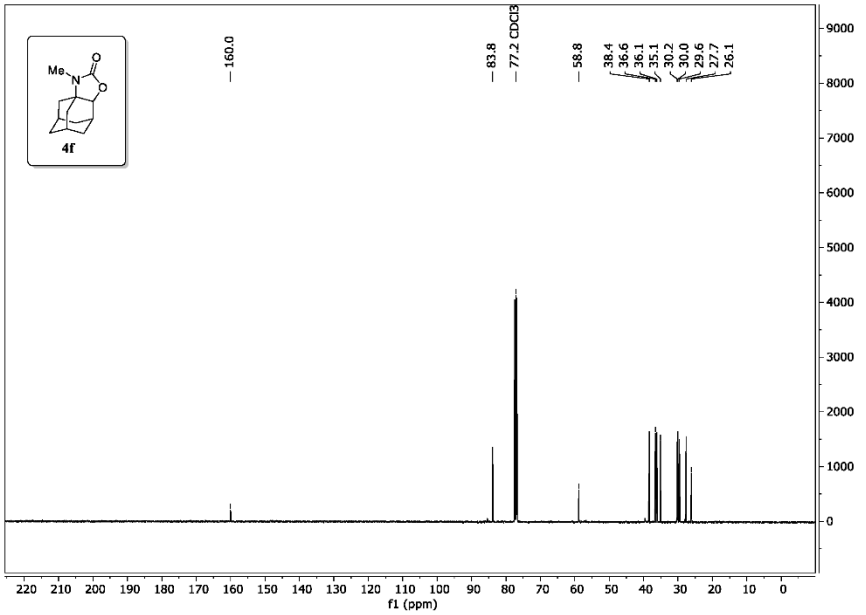

S44

2.2.13 Compound 2g

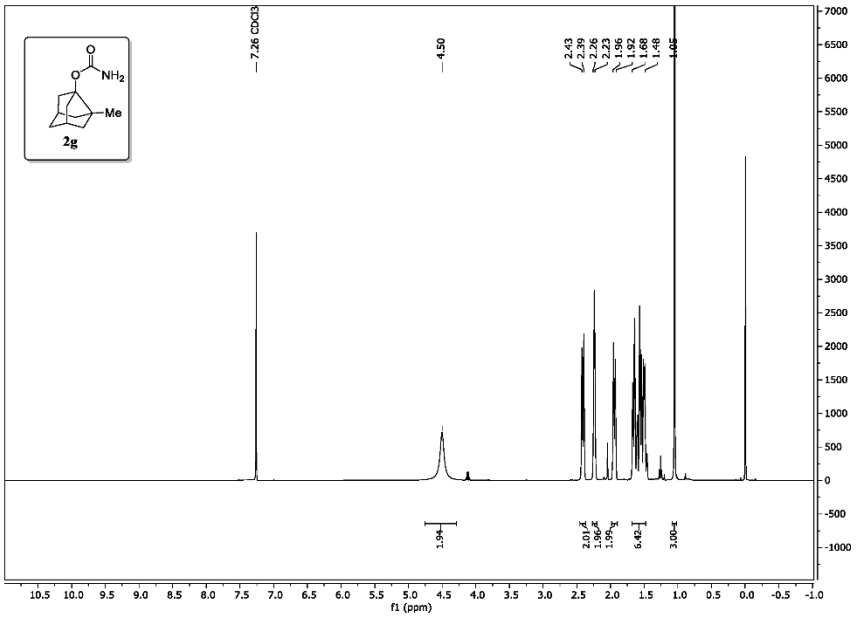

S45

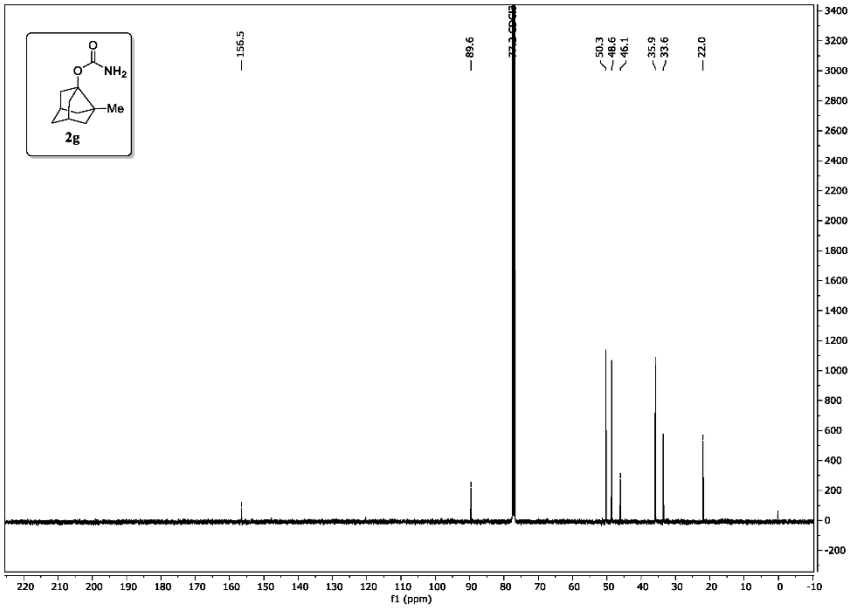

S46

2.2.14 Compound 3g

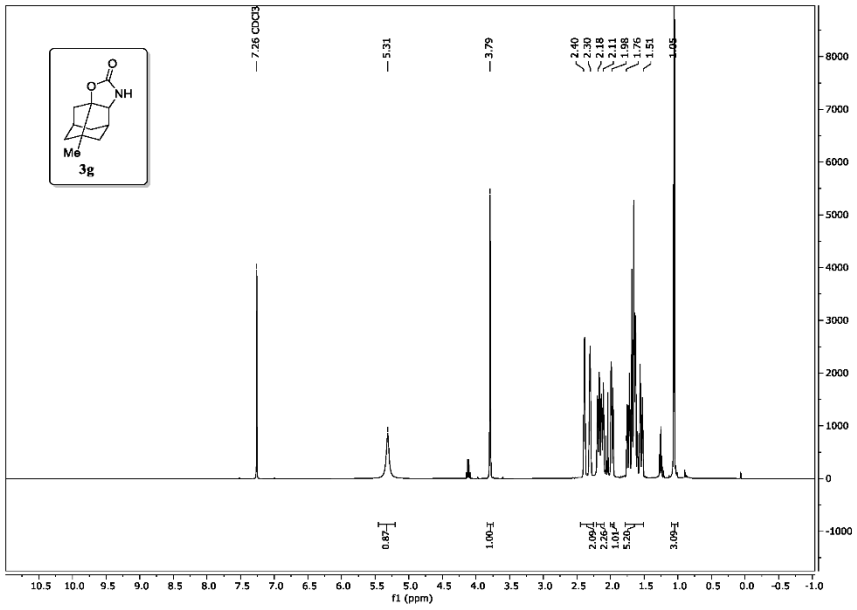

S47

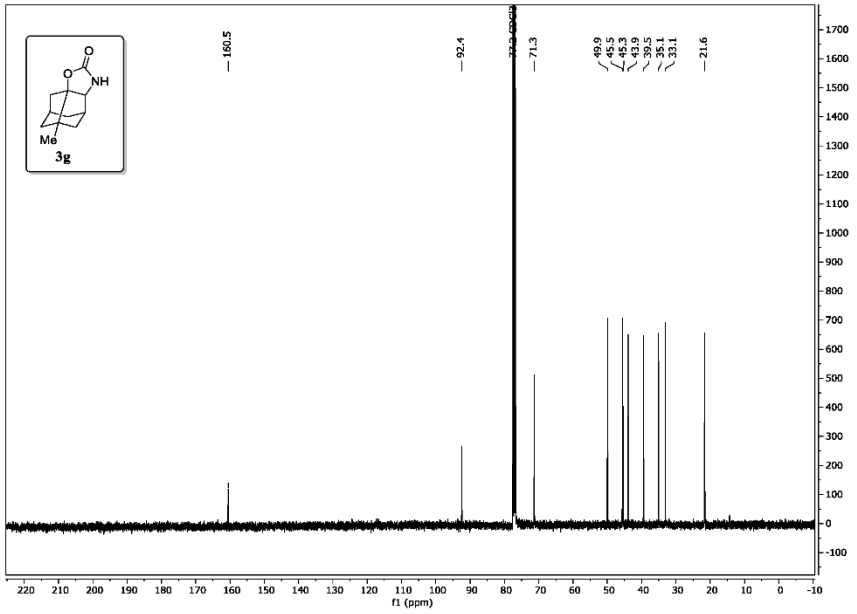

S48

2.2.15 Compound 4g

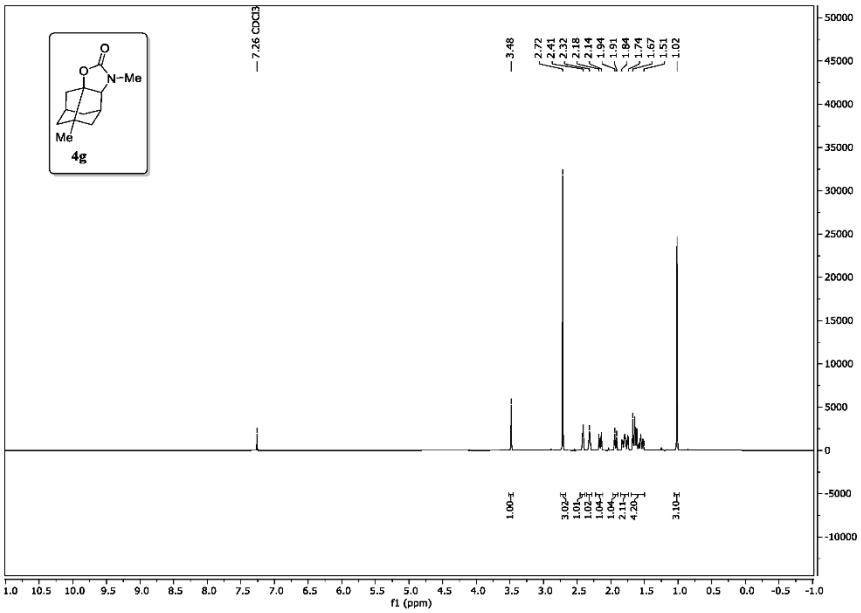

S49

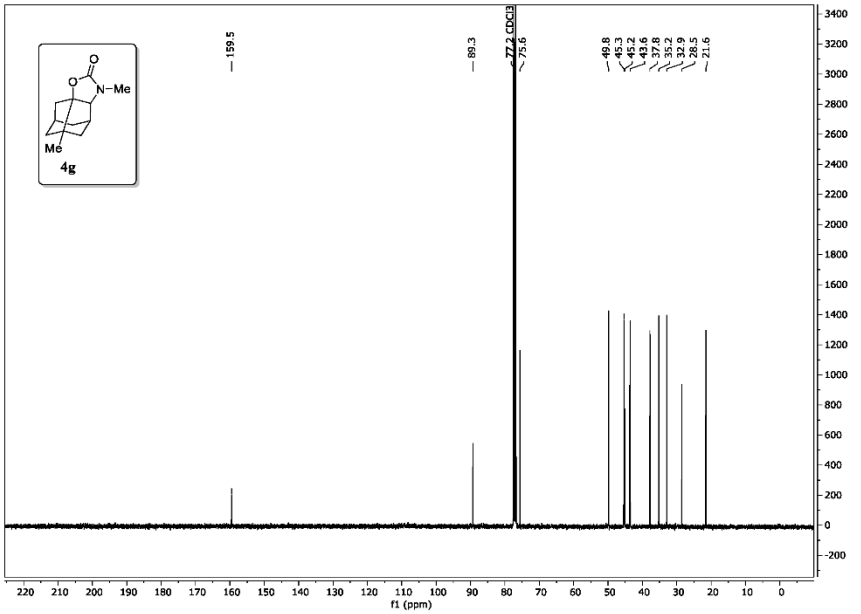

S50

2.2.16 Compound 9

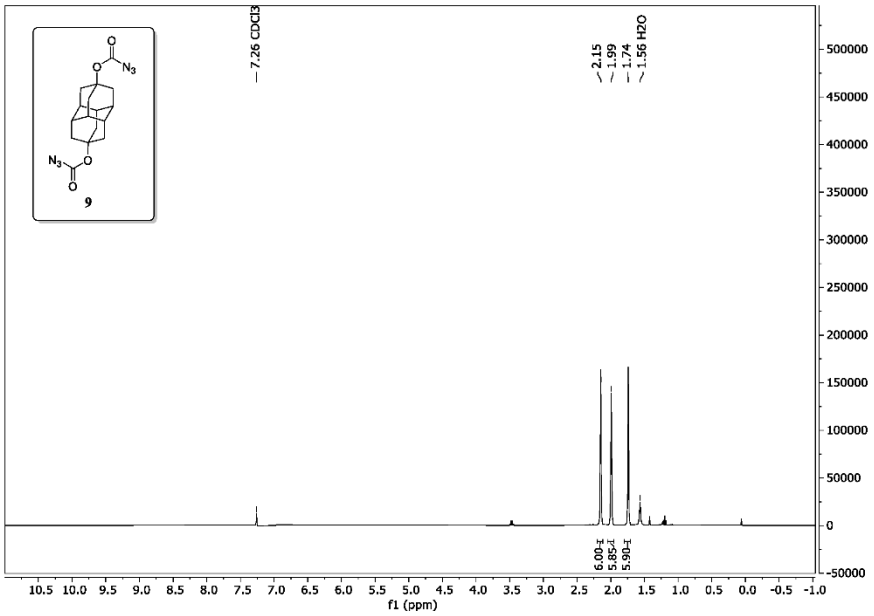

S51

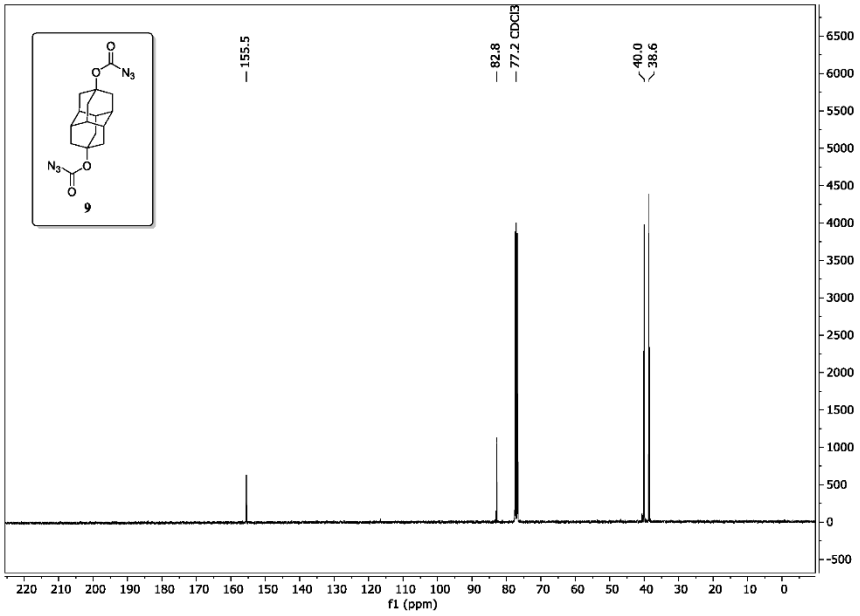

S52

2.2.17 Compound 10

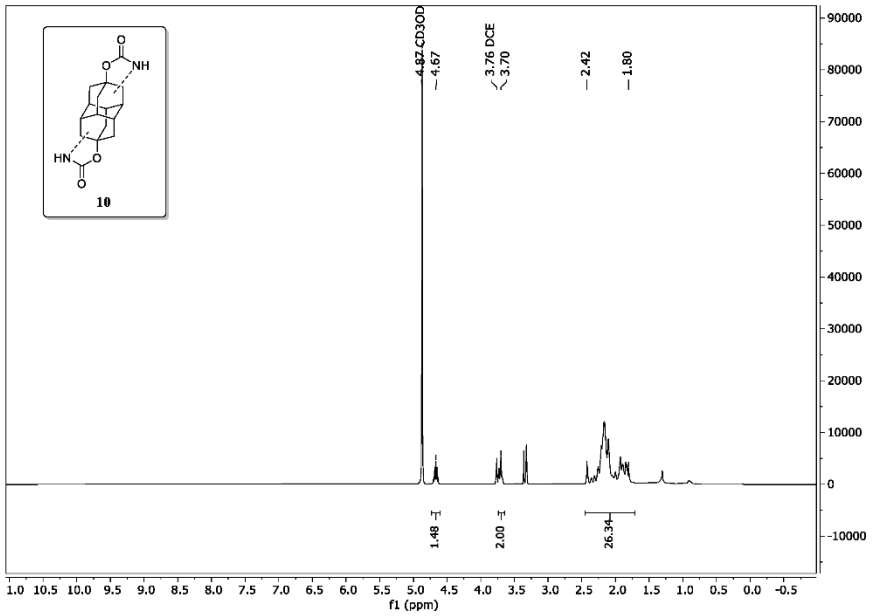

S53

2.2.18 Compound 15

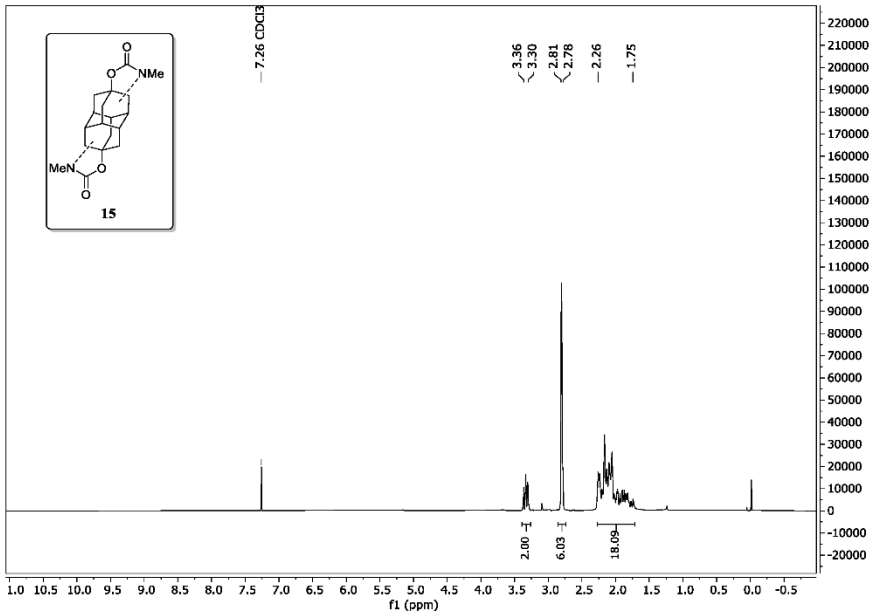

S54

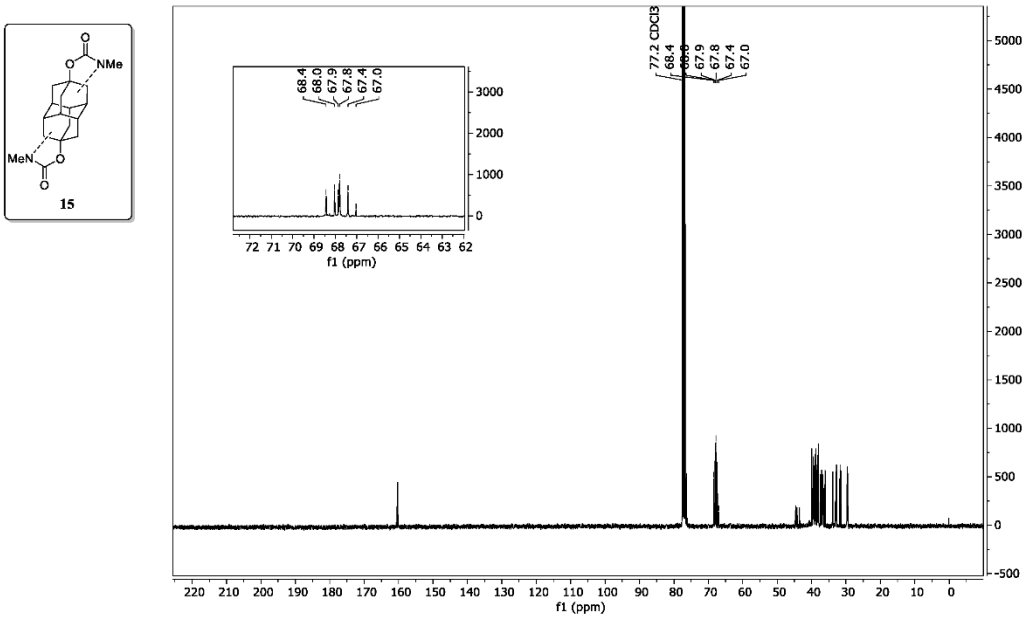
15
77.2 CDCl3
68.4
68.0
67.9
67.8
67.4
67.0
f1 (ppm)

2.3 Syntheses and description of aldehydes **6a-f** and **11**

2.3.1 Optimization of reaction conditions

Table 1 shows the result of the reaction optimization. Under inert atmosphere, 1.0 equivalent of substrate **3a** or **4a** was dissolved and stated equivalents of corresponding Brønsted acid and or additive were added. The reaction vessel was transferred into a preheated oil bath at the given temperature and stirred for the given time. After cooling down, the reaction mixture was transferred in a round bottom flask with CH_2Cl_2 and evaporated *in vacuo*. The crude residue was analysed *via* ^{1}H NMR analysis.

Table 1. Screening of Brønsted/Lewis acids, additives and reaction conditions

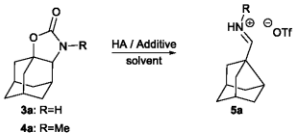

3a: R=H
4a: R=Me

5a

Entry	R	Brønsted acid (equiv.)	Additive (equiv.)	Solvent	Temperature	time	Conversion in %[a]
1	Me	TfOH (2)		CH_2Cl_2	23 °C	17 h	0
2	Me	TfOH (2)		CH_2Cl_2	40 °C	17 h	0
3	Me	TfOH (2)		$C_6H_4Cl_2$	110 °C	17 h	50
4	Me	TfOH (2)		$C_6H_4Cl_2$	140 °C	17 h	91
5	**Me**	**TfOH** (2)		**$C_6H_3Cl_3$**	**140 °C**	**3 h**	**93**
6	Me	TfOH (2)		$C_6H_3Cl_3$	120 °C	3 h	30
7	**Me**	**TfOH** (2)		**$C_6H_3Cl_3$**	**120 °C**	**17 h**	**92**
8	Me	*p*-TsOH (2)		$C_6H_4Cl_2$	140 °C	17 h	0
9	Me	TFA (2)		$C_6H_4Cl_2$	140 °C	17 h	0
10	Me	TfOH (2)		$CH_3CON(CH_3)_2$	140 °C	17 h	0
11	Me	TfOH (1.2)		$C_6H_3Cl_3$	120 °C	17 h	25
12	Me	TfOH (1)	$Al(OTf)_3$ (1)	$C_6H_3Cl_3$	120 °C	17 h	30
13	Me		$Al(OTf)_3$ (2)	$C_6H_3Cl_3$	140 °C	17 h	*n.d.*
14	H	TfOH (2)		$C_6H_3Cl_3$	120 °C	17 h	*n.d.*

2.3.2 General procedure D: Acidic Rearrangement and Hydrolysis

Under inert atmosphere, corresponding *N*-methyl carbamate (1.0 eq.) is dissolved in dry 1,2,4-trichlorobenzene (2.5 mL/ mmol) and treated with triflic acid (2.0 eq.). The reaction mixture is heated to the specified temperature and heated for the given time. After the reaction vessel is cooled to room temperature the solvent is evaporated from CH_2Cl_2, EtOAc and n-hexane *in vacuo* to remove as much of the high-boiling solvent as possible. For hydrolysis, the residue is dissolved in EtOAc (15mL/mmol; degassed), treated with NaOH (2M, *aq*., 15mL/mmol; degassed) and stirred at room temperature overnight in the dark. The two phases are separated, the aqueous phase is extracted with EtOAc, the combined organic phases are washed with water and brine, dried over Na_2SO_4 (anhydrous), filtered and the solvent is evaporated *in vacuo*. If necessary, the crude mixture is purified by silica filtration in 1-5% EtOAc in hexanes.

2.3.3 Compound 6a

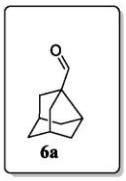

Compound **6a** was synthesized rom compound **4a** according to *general procedure D* (140 °C, 3h) to give the desired product as an off-white solid in a yield of 90% (130 mg, 0.9 mmol).

^{1}H NMR (400 MHz, $CDCl_3$): δ/ppm = 1.58-1.71 (m, 8H), 1.98-2.04 (m, 2H), 2.33-2.35 (m, 2H), 2.57 (m, 1H), 9.72 (s, 1H).

Spectrum in accordance with literature: B. Zonker, E. Duman, H. Hausmann, J. Becker, R. Hrdina., *Org Biomol. Chem.*, 2020, **18**, 4941-4945.

2.3.4 Compound 6b

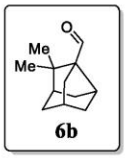

Compound **6b** was synthesized from compound **4b** according to *general procedure D* (120 °C, 18h) to give a white solid in a yield of 50% (45 mg, 0.3 mmol).

R$_f$ (silica gel; EtOAc:*n*-hexane 4:96): 0.4.

^{1}H NMR (400 MHz, $CDCl_3$): δ/ppm = 1.04 (s, 3H), 1.19 (s, 3H), 1.41-1.50 (m, 3H), 1.66 (m, 3H), 1.89 (m, 1H), 2.15-2.26 (m, 3H), 2.75 (m, 1H), 9.84 (s, 1H).

^{13}C NMR (101 MHz, $CDCl_3$): δ/ppm = 22.7 (CH_3), 27.2 (CH_3), 32.1 (CH_2), 36.2 (CH), 37.0 (CH_2), 40.2 (CH_2), 40.2 (CH), 44.4 (CH_2), 47.5 (C), 47.7 (CH), 65.3 (C), 206.1 (CH).

IR (neat): $\tilde{\nu}$ /cm^{-1} = 2920, 2871, 1687, 1551, 1456, 1409, 1385, 1366, 1294, 1255, 1233, 1204, 1179 1140, 1088, 1067, 1042, 943, 846, 815, 744, 569, 514, 454.

HRMS: m/z = 177.1282 ([M-H]$^-$; calculated for $C_{12}H_{17}O^-$ m/z = 177.1285).

2.3.5 Compound 6c

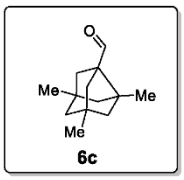

6c

Compound **6c** was synthesized from compound **4c** according to *general procedure D* (120 °C, 20h) to give an off-white solid in a yield of 77% (101 mg, 0.5 mmol).

R_f (silica gel; EtOAc:*n*-hexane 4:96): 0.4.

^{1}H NMR (400 MHz, $CDCl_3$): δ/ppm = 1.02 (s, 6H), 1.08 (s, 3H), 1.19-1.24 (m, 2H), 1.34-1.38 (m, 2H), 1.40 (m, 2H), 1.44-1.47 (m, 2H), 1.96-1.99 (m, 2H), 9.63(s, 1H).

^{13}C NMR (101 MHz, $CDCl_3$): δ/ppm = 22.8 (CH_3), 24.5 ($2CH_3$), 41.1 (2C), 48.9 (CH_2), 49.5 ($2CH_2$), 52.9 (C), 57.0 ($2CH_2$), 62.2 (C), 206.9 (CH).

IR (neat): $\tilde{\nu}$ /cm^{-1} = 2947, 2924, 2865, 1798, 1714, 1457, 1376, 1329, 1278, 1231, 1206, 1173, 1146, 1067, 1026, 991, 970, 732, 635, 527.

HRMS: m/z = 193.1589 ([M+H]$^+$; calculated for $C13H_{21}O^+$ m/z = 193.1587).

2.3.6 Compound 6d

Compound **6d** was synthesized from compound **4d** according to *general procedure D* (140 °C, 3h) to give a white solid in a yield of 52% (81 mg, 0.4 mmol).

R$_f$ (silica gel; EtOAc*:n*-hexane 1:9): 0.2.

m.p. (cryst. from $CDCl_3$): 165.0-166.0 °C.

^{1}H NMR (400 MHz, $CDCl_3$): δ/ppm = 1.57-1.60 (m, 2H), 1.72 (m, 2H), 1.80-1.84 (m, 4H), 1.90-1.93 (m, 4H), 1.98-2.02 (m, 2H), 2.07 (m, 2H), 2.39 (m, 1H), 9.73 (s, 1H).

^{13}C NMR (101 MHz, $CDCl_3$): δ/ppm = 25.0 (CH), 33.8 ($2CH_2$), 35.1 (CH_2), 36.1 (CH), 42.3 (2CH), 42.8 ($2CH_2$), 45.8 (2CH), 46.0 (CH), 62.6 (C), 205.6 (CH).

IR (neat): $\tilde{\nu}$ /cm^{-1} = 293, 2848, 2690, 1804, 1722, 1686, 1470, 1460, 1441, 1418, 1320, 1287, 1261, 1186, 1171, 1075, 1053, 1029, 996, 950, 933, 844, 820, 804, 752, 737, 634, 565, 533, 490, 448.

HRMS: m/z = 201.1287 ([M-H]$^-$; calculated for $C_{14}H_{17}^-$ m/z = 201.1285).

2.3.7 Compound 6e

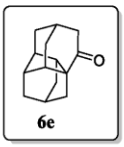

Compound **6e** was synthesized from compound **4e** according to *general procedure D* (120 °C, 21h) to give a white solid in a yield of 60% (70 mg, 0.4 mmol).

R_f (silica gel; EtOAc:*n*-hexane 1:9): 0.2.

m.p. (cryst. from Et_2O): 124.8-125.6 °C

^{1}H NMR (400 MHz, $CDCl_3$): δ/ppm = 1.44 (m, 1H), 1.51-1.66 (m, 6H), 1.70-1.80 (m, 1H), 2.00 (m, 1H), 2.08-2.10 (m, 2H), 2.20 (m, 1H), 2.26-2.33 (m, 3H), 2.42 (m, 1H), 2.56 (m, 1H).

^{13}C NMR (101 MHz, $CDCl_3$): δ/ppm = 30.4 (CH), 33.9 (CH_2), 37.0 (CH_2), 37.1 (CH), 37.9 (CH_2), 40.9 ($2CH_2$), 45.9 (CH_2), 47.6 (CH), 50.3 (CH), 53.0 (CH), 53.8 (CH), 62.3 (C), 214.6 (C).

IR (neat): $\tilde{\nu}$ /cm^{-1} = 2904, 2858, 1706, 1438, 1407, 1333, 1310, 1282, 1248, 1226, 1173, 1117, 1056, 1028, 1011, 982, 945, 921, 877, 836, 788, 772, 746, 696, 654, 600, 493, 475, 458.

HRMS: m/z = 225.1253 ([M+Na]$^+$; calculated for $C_{14}H_{18}ONa^+$ m/z = 225.1250).

2.3.8 Compound 6f

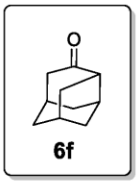

Compound **6f** was synthesized from compound **4f** according to *general procedure D* (120 °C, 19h) to give a white solid in a yield of 70% (71 mg, 0.5 mmol).

^{1}H NMR (400 MHz, $CDCl_3$): δ/ppm = 1.53 (m, 1H), 1.61-1.81 (m, 5H), 1.91-1.98 (m, 2H), 2.23-2.32 (m, 2H), 2.41 (m, 1H), 2.51-2.63 (m, 2H), 2.73 (m, 1H).

Spectrum in accordance with literature: Z. Majerski, Z.Hamersak, *Org. Synth.* 1979, **59**, 147-153.

2.3.9 Compound 11

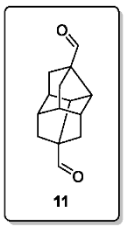

11

Compound **11** was synthesized from compound **15** according to *general procedure D* (4. eq. TfOH, 160 °C, 48h) to give a white solid in a yield of 10% (21 mg, 0.1 mmol) as a racemic isomer. Formation of the second achiral isomer was not detected.

R_f (silica gel; EtOAc:n-hexane 1:1) 0.4.

^{1}H NMR (400 MHz, $CDCl_3$): δ/ppm = 1.59-1.61 (m, 2H), 1.92-1.95 (m, 2H), 2.07-2.12 (m, 2H), 2.18-2.22 (m, 4H), 2.46-2.48 (m, 2H), 2.75-2.79 (m, 2H), 9.71 (s, 2H).

^{13}C NMR (101 MHz, $CDCl_3$): δ/ppm = 40.3 ($2CH_2$), 41.9 ($2CH_2$), 43.0 (2CH), 51.4 (2CH), 55.7 (2CH), 59.4 (C), 203.9 (C).

IR (neat): $\tilde{\nu}$ /cm^{-1} = 2922, 2858, 2702, 1712, 1464, 1389, 1325, 1246, 1184, 1074, 811, 723.

HRMS: m/z = 217.1225 ($[M+Na]^+$; calculated for $C_{14}H_{16}O_2Na^+$ m/z = 217.1223).

2.4 NMR spectra of aldehydes **6a-f** and **11**

2.4.1 Compound 6a

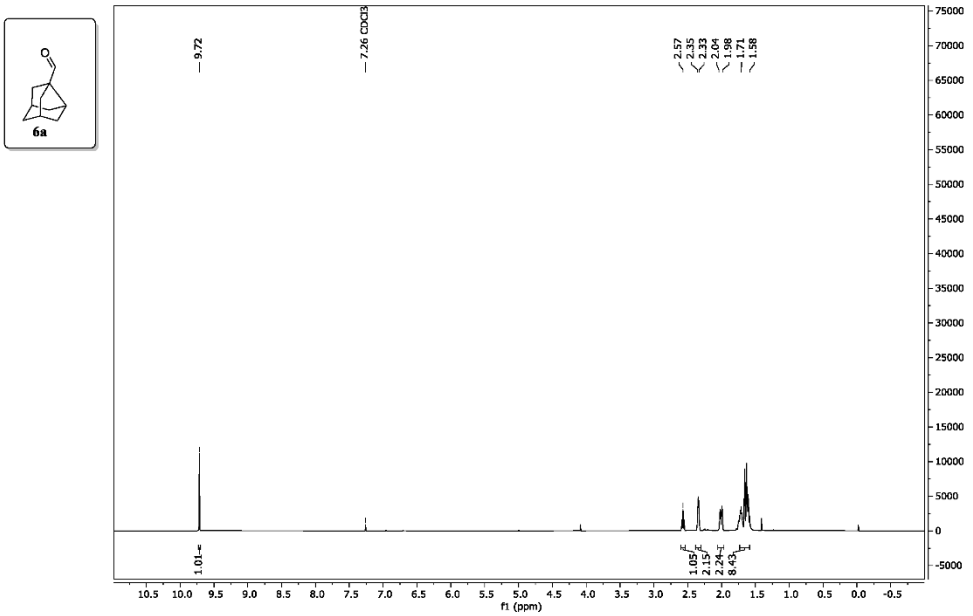

2.4.2 Compound 6b

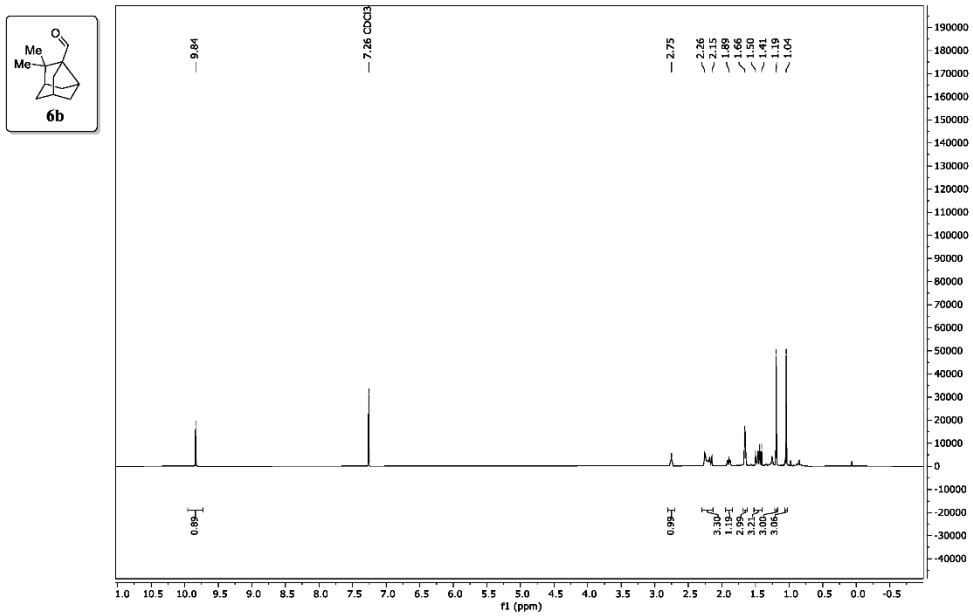

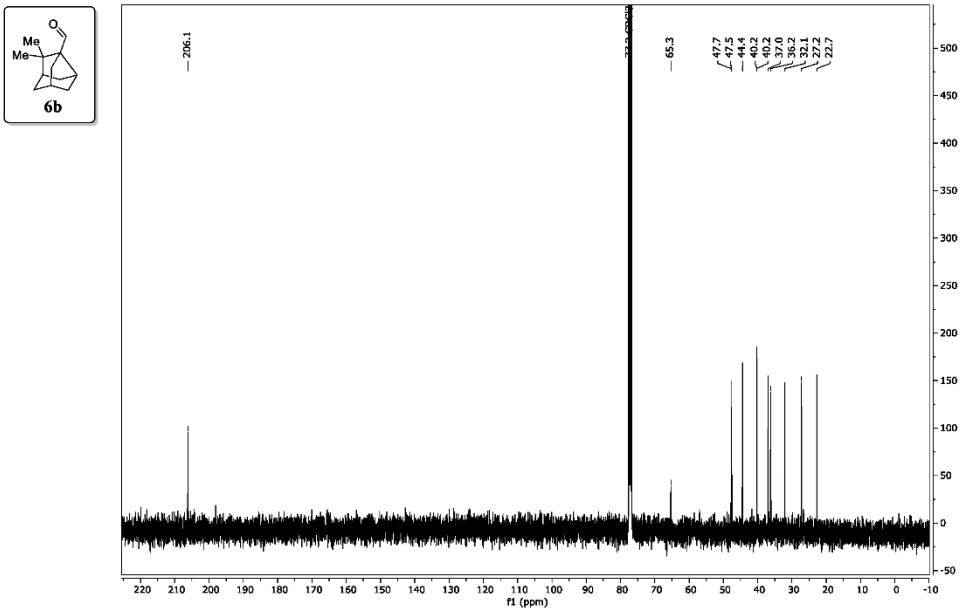

S65

2.4.3 Compound 6c

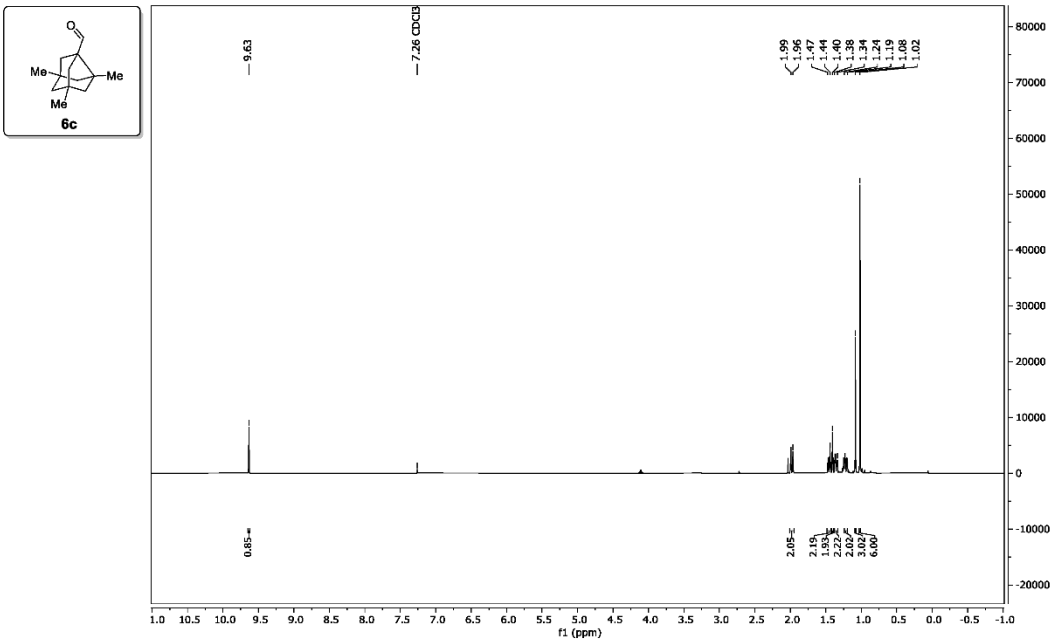

S66

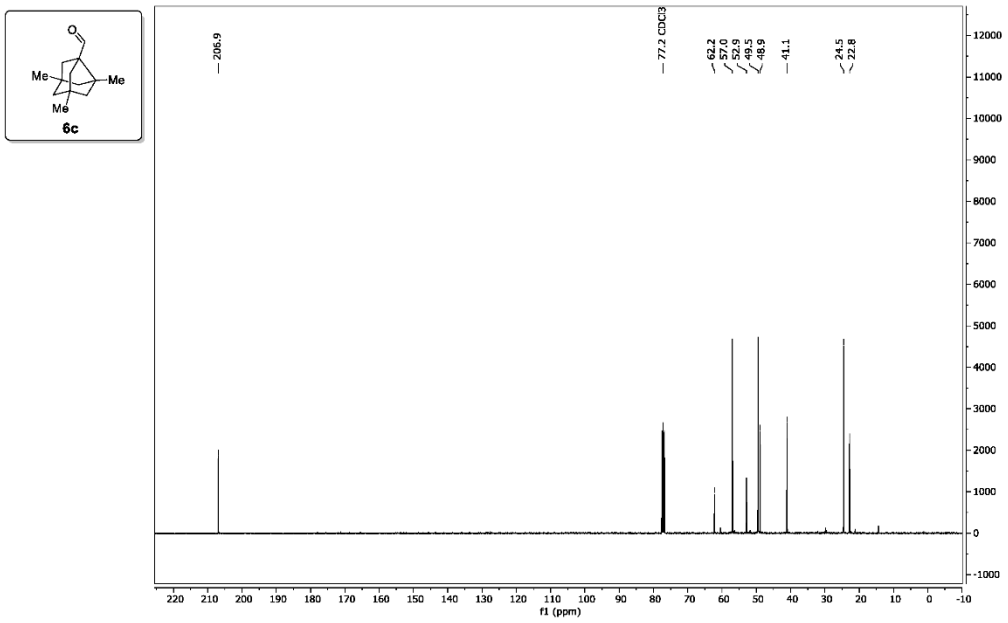

S67

2.4.4 Compound 6d

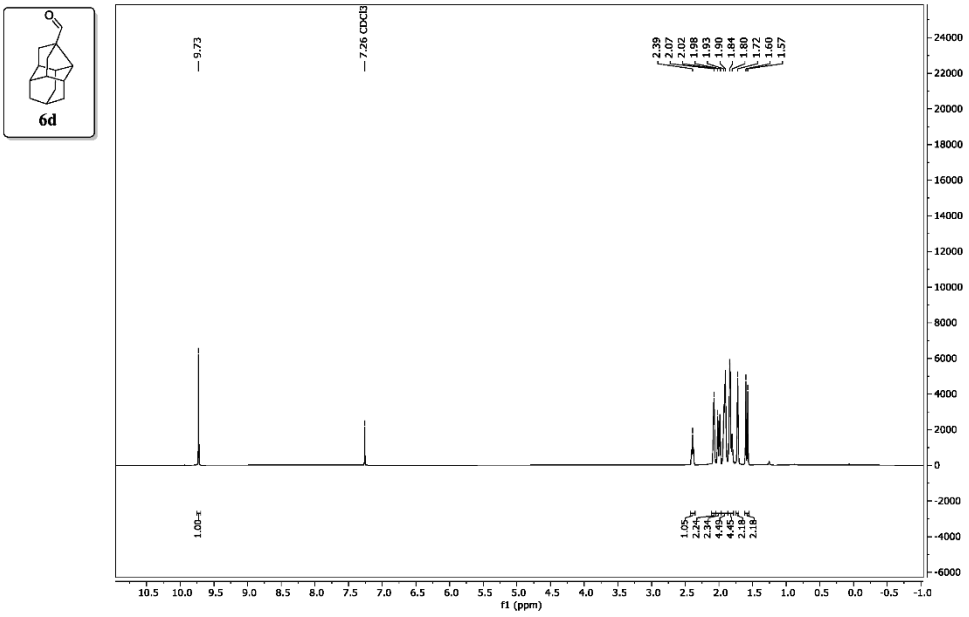

S68

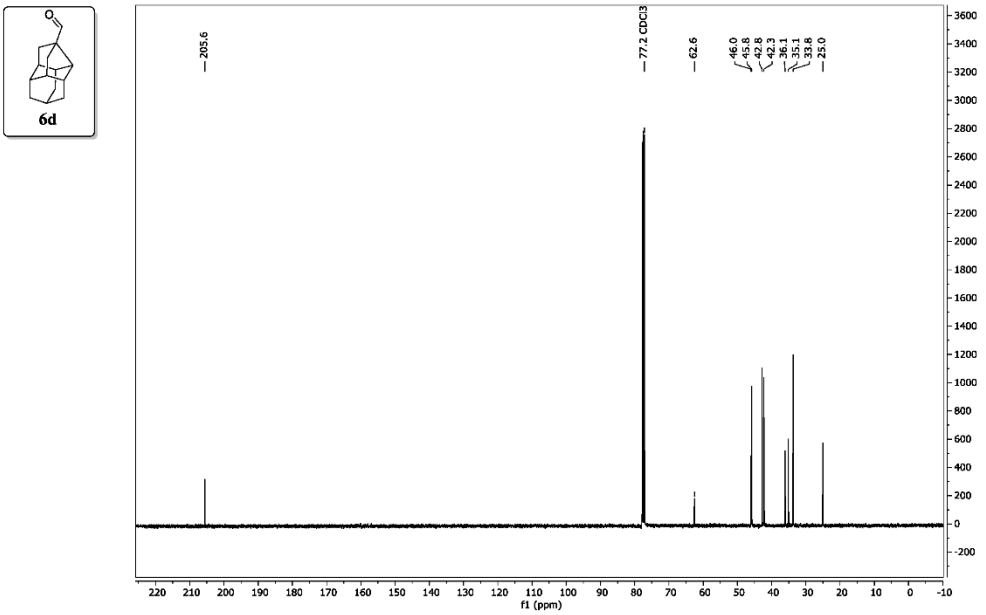

S69

2.4.5 Compound 6e

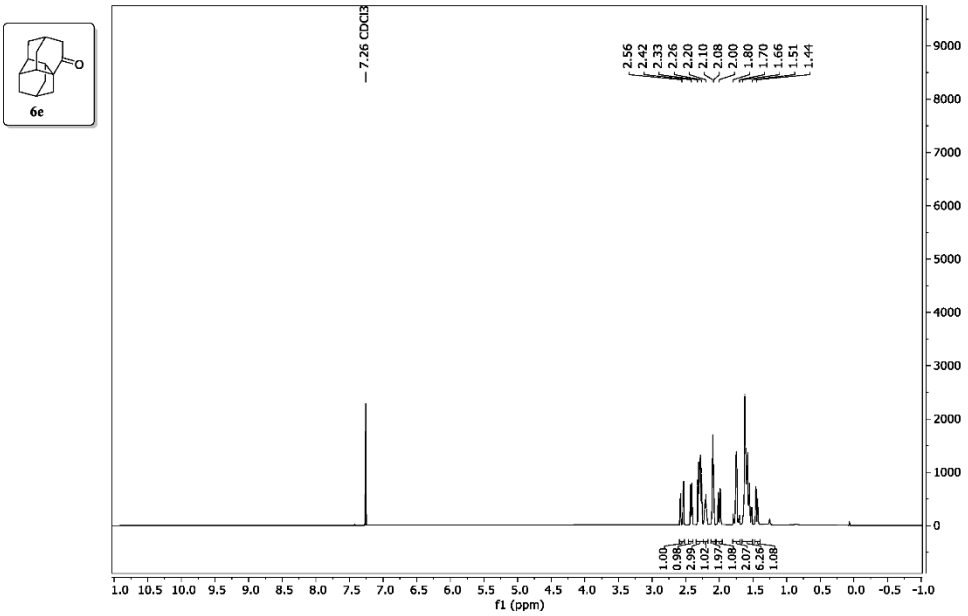

S70

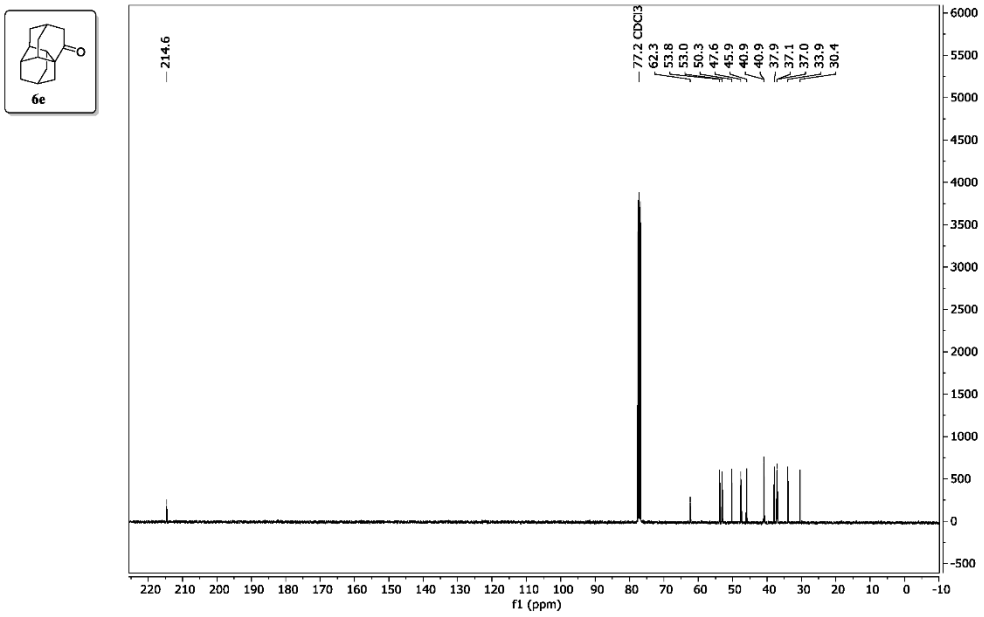

S71

2.4.6 Compound 6f

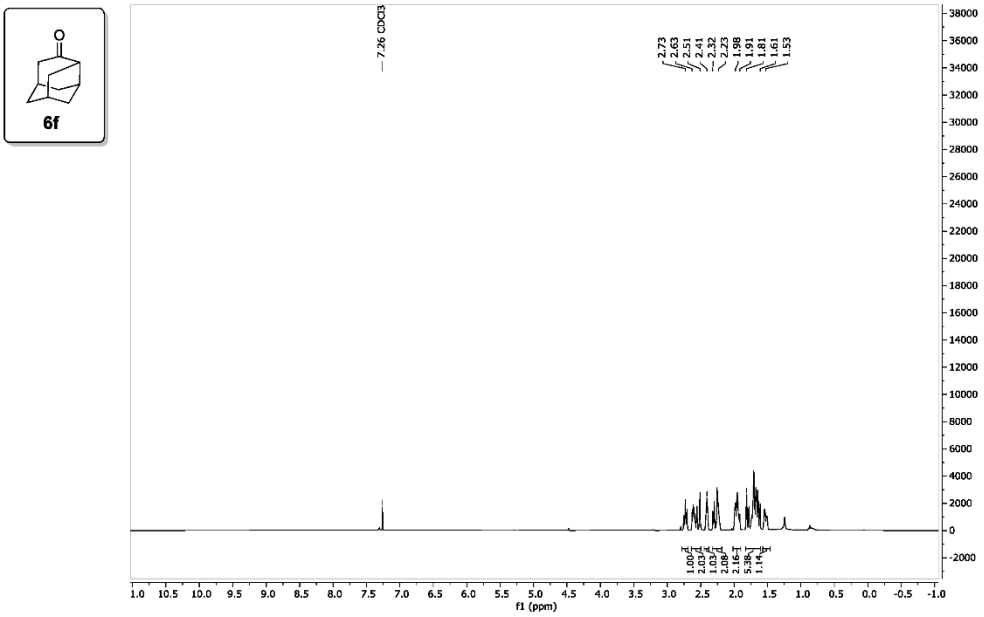

S72

2.4.7 Compound 11

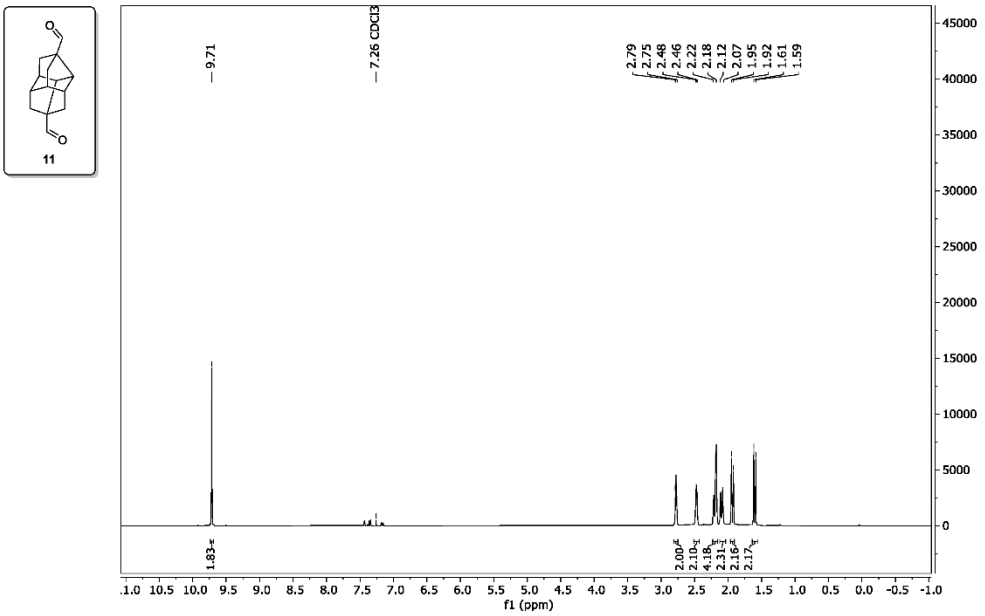

S73

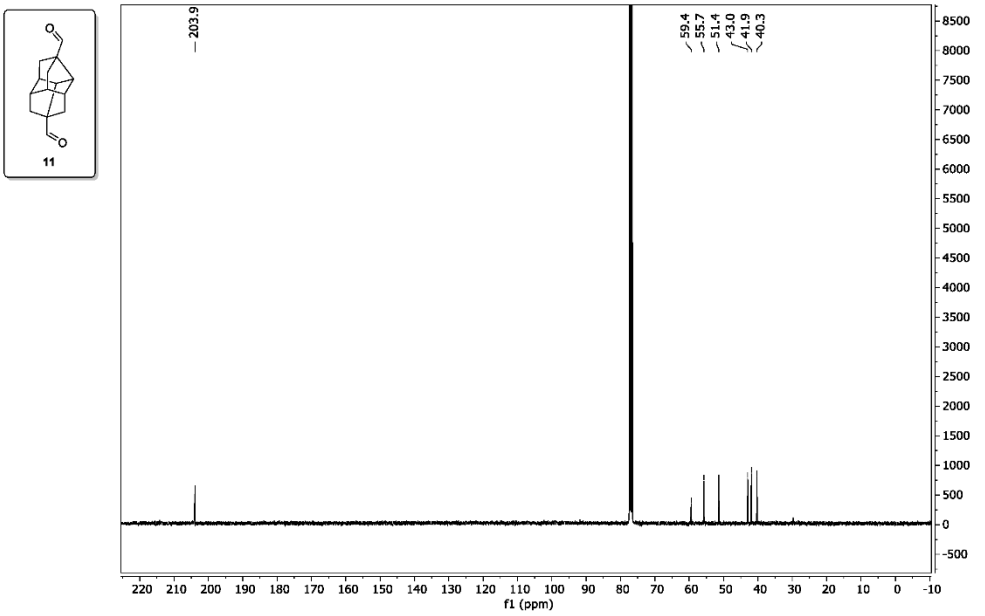

S74

2.5 Postfunctionalization

2.5.1 Compound 14

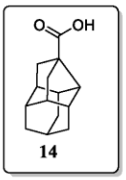

14

A solution of aldehyde **6d** (40 mg, 0.2 mmol) in DPDME (8 eq.) was heated to 80 °C overnight while connected to an oxygen balloon. The solvent was evaporated to give the clean desired compound as a white solid in a yield of 99% (45 mg, 0.2 mmol).

R_f (silica gel; MeOH:CH_2Cl_2 1:99): 0.2.

m.p. (cryst. from $CDCl_3$): 177.7-178.6 °C.

^{1}H NMR (400 MHz, $CDCl_3$): δ/ppm = 1.69-1.83 (m, 8H), 1.87-1.91 (m, 2H), 2.02-2.08 (m, 6H), 2.50 (m, 1H), 10.22 (bs, 1H).

^{13}C NMR (101 MHz, $CDCl_3$): δ/ppm = 24.8 (CH), 33.4 ($2CH_2$), 34.7 (CH_2), 35.0 (CH), 41.8 (2CH), 45.5 (2CH), 45.6 ($2CH_2$), 48.1 (CH), 55.1 (C), 182.5 (C).

IR (neat): $\tilde{\nu}$ /cm^{-1} = 2903, 2880, 2596, 1834, 1682, 1470, 1418, 1320, 1287, 1261, 1215, 1194, 1088, 1056, 997, 986, 953, 935, 857, 845, 821, 753, 738, 634, 567, 534, 490, 448.

HRMS: m/z = 241.1198 ([M+Na]$^+$; calculated for $C_{14}H_{18}O_2Na^+$ m/z = 241.1199).

2.6 NMR spectra of acid **14**

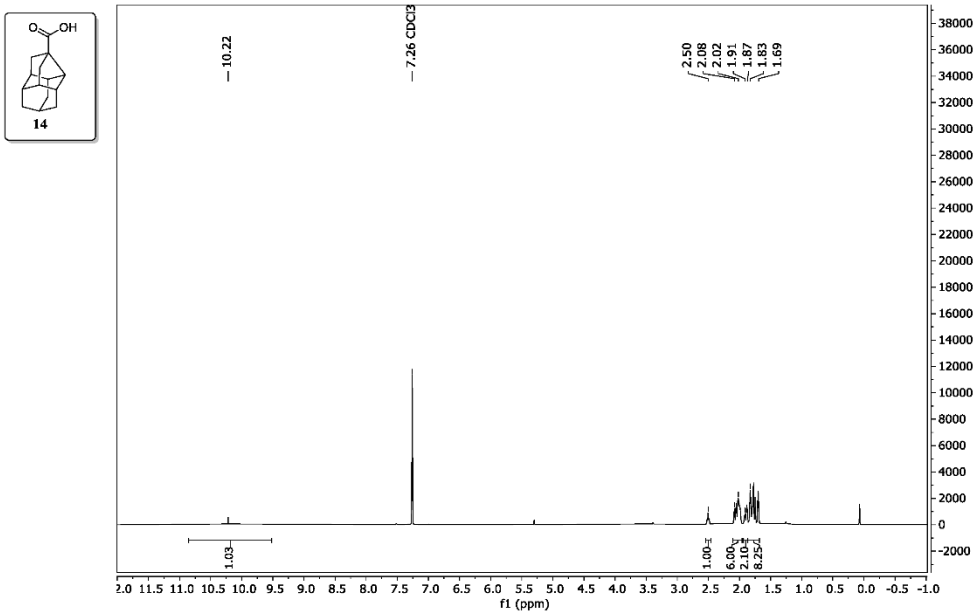

S76

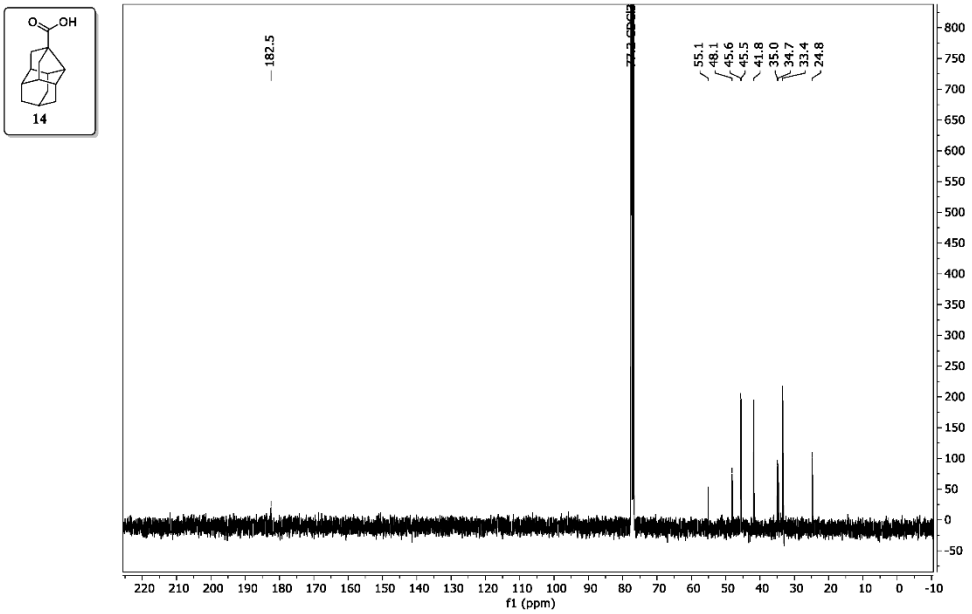

S77

3. DFT analysis of cations 12^+ and 5^+

3.1 Geometric Structures and Electronic energies (Hartree)

Cation 12^+

1 1

6	1.094749000	0.380585000	0.509932000
1	1.293275000	1.283414000	1.100637000
6	0.283602000	0.695249000	-0.673942000
6	-0.041118000	-0.465942000	1.319907000
1	0.450242000	-0.762402000	2.247284000
6	-1.241562000	0.443930000	1.595294000
1	-0.948081000	1.303536000	2.198609000
1	-1.982851000	-0.104872000	2.178365000
6	-0.732444000	1.728896000	-0.535234000
1	-1.149154000	2.059890000	-1.482348000
1	-0.420565000	2.575774000	0.069583000
6	-1.861340000	0.897858000	0.270045000
1	-2.688701000	1.587869000	0.426499000
6	-2.272198000	-0.296189000	-0.596106000
1	-3.051095000	-0.865953000	-0.085632000
1	-2.703073000	0.040671000	-1.539562000
6	0.071206000	-0.343668000	-1.656156000
1	0.931184000	-0.985840000	-1.811095000
1	-0.369196000	0.002348000	-2.586112000
6	-0.441142000	-1.678220000	0.472760000
1	0.415792000	-2.320172000	0.281633000

1	-1.170367000	-2.275585000	1.023500000
6	-1.062813000	-1.201104000	-0.840447000
1	-1.304152000	-2.032178000	-1.500931000
7	2.256583000	-0.435008000	0.256184000
1	2.514006000	-0.938360000	1.095552000
6	3.410408000	0.327344000	-0.241074000
1	3.193243000	0.716028000	-1.236851000
1	3.685877000	1.169470000	0.403691000
1	4.263441000	-0.341018000	-0.325984000

Temperature 298.150 Kelvin. Pressure 1.00000 Atm.

Zero-point correction=	0.275387 (Hartree/Particle)
Thermal correction to Energy=	0.285384
Thermal correction to Enthalpy=	0.286328
Thermal correction to Gibbs Free Energy=	0.240980
Sum of electronic and zero-point Energies=	-484.357053
Sum of electronic and thermal Energies=	-484.347056
Sum of electronic and thermal Enthalpies=	-484.346112
Sum of electronic and thermal Free Energies=	-484.391459

Cation 5^{+}

1 1

6	-0.398146000	-1.251957000	-1.021040000
1	0.169124000	-2.165383000	-0.837942000
1	-0.506921000	-1.124755000	-2.096375000
6	0.277819000	-0.000001000	-0.350354000
6	-1.721086000	-1.281344000	-0.240066000
1	-2.304602000	-2.173319000	-0.461622000
6	-1.180683000	-1.248454000	1.198507000
1	-0.617956000	-2.157583000	1.415945000
1	-1.953778000	-1.149643000	1.957892000
6	-0.274176000	-0.000002000	1.142861000
1	0.487265000	-0.000005000	1.924574000
6	-1.180679000	1.248452000	1.198511000
1	-1.953774000	1.149641000	1.957896000
1	-0.617950000	2.157578000	1.415951000
6	-0.398144000	1.251959000	-1.021037000
1	-0.506921000	1.124758000	-2.096372000
1	0.169128000	2.165383000	-0.837938000
6	-2.540447000	0.000003000	-0.534402000
1	-2.863830000	0.000005000	-1.576909000
1	-3.445532000	0.000002000	0.074413000
6	-1.721084000	1.281346000	-0.240062000
1	-2.304597000	2.173324000	-0.461614000
6	1.719978000	0.000001000	-0.588255000
1	2.068770000	0.000006000	-1.617915000

7	2.640039000	-0.000006000	0.311217000
6	4.089099000	0.000002000	0.074859000
1	4.279467000	0.000014000	-0.993751000
1	4.524392000	-0.887641000	0.528674000
1	2.338356000	-0.000010000	1.280746000
1	4.524383000	0.887640000	0.528693000

Temperature 298.150 Kelvin. Pressure 1.00000 Atm.

Zero-point correction= 0.276647 (Hartree/Particle)

Thermal correction to Energy= 0.286892

Thermal correction to Enthalpy= 0.287836

Thermal correction to Gibbs Free Energy= 0.240993

Sum of electronic and zero-point Energies= -484.392153

Sum of electronic and thermal Energies= -484.381908

Sum of electronic and thermal Enthalpies= -484.380964

Sum of electronic and thermal Free Energies= -484.427807

4. Crystallographic data collection and refinement details

Diffraction data were collected at low temperatures (100K) using φ- and ω-scans on a BRUKER D8 Venture system equipped with dual IμS microfocus sources, a PHOTON100 detector and an OXFORD CRYOSYSTEMS 700 low temperature system. Mo-K_α radiation with wavelength 0.71073 Å and a collimating Quazar multilayer mirror were used. The data was corrected for absorption using semi-empirical absorption correction from equivalents using SADABS-2016/2[10] and the structure of 14 was solved in the monoclinic space group $P2_1/n$ by the dual space algorithm implemented in SHELXT2014/5.[11] Refinement was performed against F^2 on all data by full-matrix least squares using SHELXL2018/3.[11]All non-hydrogen atoms were refined anisotropically and C-H hydrogen atoms were positioned at geometrically calculated positions and refined using a riding model. The O-H hydrogen atom was located in the difference map and was set to ideal distance. The isotropic displacement parameters of all hydrogen atoms were fixed to 1.2x or 1.5x (OH hydrogen) the U_{eq} value of the atoms they are linked to. The asymmetric unit contains one molecule of **14** which forms a dimer with its symmetry equivalent *via* hydrogen bonding.

The crystallographic data has been deposited with the Cambridge Crystallographic Data Centre as CCDC No. 2063017 and can be obtained free of charge.[12]

[10] L. Krause, R. Herbst-Irmer, G. M. Sheldrick, D. J. Stalke, *Appl. Cryst.,* 2015, **48**, 3–10.
[11] G. M. Sheldrick, *Acta Cryst. A,* 2015, **71**, 3–8.
[12] https://www.ccdc.cam.ac.uk/structures/

Table S1. Crystal data and structure refinement for **14**.

CCDC No	2063017	
Empirical formula	$C_{14}\ H_{18}\ O_2$	
Formula weight	218.28	
Temperature	100(2) K	
Wavelength	0.71073 Å	
Crystal system	Monoclinic	
Space group	$P2_1/n$	
Unit cell dimensions	a = 6.5170(4) Å	α= 90°.
	b = 10.4112(7) Å	β= 97.934(2)°.
	c = 15.8832(10) Å	γ = 90°.
Volume	1067.36(12) Å^3	
Z	4	
Density (calculated)	1.358 Mg/m^3	
Absorption coefficient	0.089 mm^{-1}	
F(000)	472	
Crystal size	0.240 x 0.146 x 0.056 mm^3	
Theta range for data collection	2.346 to 30.019°.	
Index ranges	$-9 \le h \le 9$, $-14 \le k \le 14$, $-22 \le l \le 22$	
Reflections collected	77056	
Independent reflections	3129 [R(int) = 0.0505]	
Completeness to theta = 25.242°	100.0 %	
Absorption correction	Semi-empirical from equivalents	
Refinement method	Full-matrix least-squares on F^2	
Data / restraints / parameters	3129 / 1 / 148	
Goodness-of-fit on F^2	1.051	
Final R indices [I>2σ(I)]	R1 = 0.0424, wR2 = 0.1069	
R indices (all data)	R1 = 0.0529, wR2 = 0.1145	
Largest diff. peak and hole	0.359 and -0.285 e.Å^{-3}	

Table S2. Atomic coordinates (x 10^4) and equivalent isotropic displacement parameters ($Å^2$x 10^3) for **14**. U(eq) is defined as one third of the trace of the orthogonalized U^{ij} tensor.

	x	y	z	U(eq)
O(1)	4201(1)	5011(1)	5929(1)	17(1)
O(2)	6435(1)	6392(1)	5467(1)	20(1)
C(1)	5356(2)	5948(1)	6048(1)	12(1)
C(2)	5586(2)	6711(1)	6857(1)	12(1)
C(3)	5351(2)	5890(1)	7682(1)	12(1)
C(4)	3474(2)	6502(1)	8029(1)	13(1)
C(5)	3753(2)	7911(1)	7776(1)	14(1)
C(6)	3851(2)	7747(1)	6824(1)	15(1)
C(7)	7645(2)	7444(1)	7076(1)	13(1)
C(8)	7698(2)	7602(1)	8038(1)	12(1)
C(9)	7366(2)	6200(1)	8292(1)	12(1)
C(10)	5834(2)	8397(1)	8267(1)	14(1)
C(11)	5749(2)	8276(1)	9230(1)	16(1)
C(12)	5440(2)	6862(1)	9475(1)	16(1)
C(13)	3426(2)	6336(1)	8982(1)	16(1)
C(14)	7227(2)	6042(1)	9240(1)	15(1)

Table S3. Bond lengths [Å] and angles [°] for **14**.

O(1)-C(1)	1.2309(14)	C(14)-H(14B)	0.9900
O(2)-C(1)	1.3180(13)		
O(2)-H(2)	0.879(14)	C(1)-O(2)-H(2)	108.3(12)
C(1)-C(2)	1.5009(15)	O(1)-C(1)-O(2)	123.01(10)
C(2)-C(7)	1.5421(15)	O(1)-C(1)-C(2)	122.47(10)
C(2)-C(6)	1.5586(15)	O(2)-C(1)-C(2)	114.48(10)
C(2)-C(3)	1.5888(14)	C(1)-C(2)-C(7)	115.82(9)
C(3)-C(4)	1.5472(15)	C(1)-C(2)-C(6)	110.58(9)
C(3)-C(9)	1.5540(15)	C(7)-C(2)-C(6)	105.61(9)
C(3)-H(3)	1.0000	C(1)-C(2)-C(3)	114.39(9)
C(4)-C(13)	1.5280(15)	C(7)-C(2)-C(3)	105.10(8)
C(4)-C(5)	1.5381(16)	C(6)-C(2)-C(3)	104.35(8)
C(4)-H(4)	1.0000	C(4)-C(3)-C(9)	109.53(8)
C(5)-C(6)	1.5316(15)	C(4)-C(3)-C(2)	104.10(8)
C(5)-C(10)	1.5529(16)	C(9)-C(3)-C(2)	103.51(8)
C(5)-H(5)	1.0000	C(4)-C(3)-H(3)	113.0
C(6)-H(6A)	0.9900	C(9)-C(3)-H(3)	113.0
C(6)-H(6AB)	0.9900	C(2)-C(3)-H(3)	113.0
C(7)-C(8)	1.5325(14)	C(13)-C(4)-C(5)	112.70(9)
C(7)-H(7A)	0.9900	C(13)-C(4)-C(3)	115.58(9)
C(7)-H(7AB)	0.9900	C(5)-C(4)-C(3)	99.88(8)
C(8)-C(9)	1.5379(15)	C(13)-C(4)-H(4)	109.4
C(8)-C(10)	1.5546(15)	C(5)-C(4)-H(4)	109.4
C(8)-H(8)	1.0000	C(3)-C(4)-H(4)	109.4
C(9)-C(14)	1.5293(14)	C(6)-C(5)-C(4)	100.04(9)
C(9)-H(9)	1.0000	C(6)-C(5)-C(10)	112.29(9)
C(10)-C(11)	1.5428(15)	C(4)-C(5)-C(10)	107.83(9)
C(10)-H(10)	1.0000	C(6)-C(5)-H(5)	112.0
C(11)-C(12)	1.5434(17)	C(4)-C(5)-H(5)	112.0
C(11)-H(11A)	0.9900	C(10)-C(5)-H(5)	112.0
C(11)-H(11B)	0.9900	C(5)-C(6)-C(2)	99.97(8)
C(12)-C(14)	1.5313(16)	C(5)-C(6)-H(6A)	111.8
C(12)-C(13)	1.5332(16)	C(2)-C(6)-H(6A)	111.8
C(12)-H(12)	1.0000	C(5)-C(6)-H(6AB)	111.8
C(13)-H(13A)	0.9900	C(2)-C(6)-H(6AB)	111.8
C(13)-H(13B)	0.9900	H(6A)-C(6)-H(6AB)	109.5
C(14)-H(14A)	0.9900	C(8)-C(7)-C(2)	100.15(8)

C(8)-C(7)-H(7A)	111.7	C(12)-C(13)-H(13B)	109.8
C(2)-C(7)-H(7A)	111.7	H(13A)-C(13)-H(13B)	108.2
C(8)-C(7)-H(7AB)	111.7	C(9)-C(14)-C(12)	109.33(9)
C(2)-C(7)-H(7AB)	111.7	C(9)-C(14)-H(14A)	109.8
H(7A)-C(7)-H(7AB)	109.5	C(12)-C(14)-H(14A)	109.8
C(7)-C(8)-C(9)	100.12(8)	C(9)-C(14)-H(14B)	109.8
C(7)-C(8)-C(10)	112.35(9)	C(12)-C(14)-H(14B)	109.8
C(9)-C(8)-C(10)	107.52(9)	H(14A)-C(14)-H(14B)	108.3
C(7)-C(8)-H(8)	112.1		
C(9)-C(8)-H(8)	112.1		
C(10)-C(8)-H(8)	112.1		
C(14)-C(9)-C(8)	112.97(9)		
C(14)-C(9)-C(3)	115.55(9)		
C(8)-C(9)-C(3)	99.81(8)		
C(14)-C(9)-H(9)	109.4		
C(8)-C(9)-H(9)	109.4		
C(3)-C(9)-H(9)	109.4		
C(11)-C(10)-C(5)	108.83(9)		
C(11)-C(10)-C(8)	108.97(9)		
C(5)-C(10)-C(8)	111.43(9)		
C(11)-C(10)-H(10)	109.2		
C(5)-C(10)-H(10)	109.2		
C(8)-C(10)-H(10)	109.2		
C(10)-C(11)-C(12)	110.59(9)		
C(10)-C(11)-H(11A)	109.5		
C(12)-C(11)-H(11A)	109.5		
C(10)-C(11)-H(11B)	109.5		
C(12)-C(11)-H(11B)	109.5		
H(11A)-C(11)-H(11B)	108.1		
C(14)-C(12)-C(13)	107.62(9)		
C(14)-C(12)-C(11)	109.88(9)		
C(13)-C(12)-C(11)	110.11(10)		
C(14)-C(12)-H(12)	109.7		
C(13)-C(12)-H(12)	109.7		
C(11)-C(12)-H(12)	109.7		
C(4)-C(13)-C(12)	109.42(9)		
C(4)-C(13)-H(13A)	109.8		
C(12)-C(13)-H(13A)	109.8		
C(4)-C(13)-H(13B)	109.8		

Table S4. Anisotropic displacement parameters ($Å^2 x\ 10^3$) for **14**. The anisotropic displacement factor exponent takes the form: $-2p^2[\ h^2\ a^{*2}U^{11} + ...\ + 2\ h\ k\ a^*\ b^*\ U^{12}\ ]$

	U^{11}	U^{22}	U^{33}	U^{23}	U^{13}	U^{12}
O(1)	21(1)	17(1)	12(1)	-2(1)	3(1)	-5(1)
O(2)	26(1)	22(1)	12(1)	-3(1)	7(1)	-9(1)
C(1)	14(1)	13(1)	10(1)	1(1)	1(1)	1(1)
C(2)	14(1)	11(1)	10(1)	0(1)	2(1)	0(1)
C(3)	14(1)	11(1)	9(1)	0(1)	1(1)	0(1)
C(4)	12(1)	17(1)	11(1)	-1(1)	2(1)	-1(1)
C(5)	14(1)	15(1)	13(1)	-1(1)	2(1)	4(1)
C(6)	16(1)	16(1)	12(1)	1(1)	1(1)	2(1)
C(7)	14(1)	13(1)	12(1)	-1(1)	3(1)	-2(1)
C(8)	13(1)	13(1)	11(1)	-1(1)	1(1)	-2(1)
C(9)	12(1)	13(1)	11(1)	0(1)	1(1)	1(1)
C(10)	18(1)	11(1)	13(1)	-1(1)	3(1)	0(1)
C(11)	19(1)	17(1)	13(1)	-4(1)	3(1)	-1(1)
C(12)	17(1)	19(1)	10(1)	-2(1)	2(1)	-2(1)
C(13)	16(1)	21(1)	12(1)	-1(1)	4(1)	-4(1)
C(14)	17(1)	18(1)	10(1)	1(1)	0(1)	1(1)

Table S5. Hydrogen coordinates (x 10^4) and isotropic displacement parameters ($Å^2$x 10^3) for **14**.

	x	y	z	U(eq)
H(2)	6160(30)	5916(16)	5008(10)	29
H(3)	5167	4952	7562	14
H(4)	2162	6157	7708	16
H(5)	2556	8458	7886	17
H(6A)	4250	8555	6561	18
H(6AB)	2520	7435	6516	18
H(7A)	8838	6936	6936	16
H(7AB)	7612	8285	6782	16
H(8)	9055	7950	8316	15
H(9)	8525	5659	8137	15
H(10)	6030	9320	8123	17
H(11A)	4592	8802	9385	20
H(11B)	7054	8606	9550	20
H(12)	5385	6798	10100	19
H(13A)	3276	5415	9116	20
H(13B)	2226	6804	9152	20
H(14A)	8544	6315	9578	18
H(14B)	6988	5128	9368	18

Table S6. Hydrogen bonds for **14** [Å and °].

D-H...A	d(D-H)	d(H...A)	d(D...A)	<(DHA)
O(2)-H(2)...O(1)#1	0.879(14)	1.762(14)	2.6394(12)	175.4(17)

Symmetry transformations used to generate equivalent atoms:

#1 -x+1,-y+1,-z+1

4 Abbreviations

Ac_2O	acetic anhydride
COF	covalent organic framework
cp.	compare
DMA	dimethylacetamide
e.g.	*exempli gratia*
et al.	*et alia*
Et	ethyl
Et_2O	diethyl ether
etc.	*et cetera*
Hal	halogenide
i.e.	*id est*
M.S.	molecular sieve
*m*CPBA	*meta*-chloroperoxybenzoic acid
Me	methyl
NHC	*N*-heterocyclic carbene
POP	porous organic polymers
*p*TsOH	*para*-toluenesulfonic acid
*t*Bu	*tert*-butyl

5 Acknowledgement

I would like to thank Prof. Dr. Peter Schreiner and Dr. Radim Hrdina for the opportunity to work as a doctoral student at the JLU-Gießen.

Next, I would like to thank the people who accompanied me in that time: Marta, thank you so much for all the help, knowledge, “tips and tricks” and support you gave me during the first years. Vlad, Jan and Jean, for fruitful discussion and helping me to find my way in Gießen. The analytical department for their help, the Chemikalien- and Glasausgabe for their obvious work. Especially Anja, for always having a smile on her face when I entered the room with weird glassblowing-requirements. The Wegner Group for the best coffee in the building! My bachelor student Ediz, and the students from the OC-Praktikum.

To all of you: Thank you, it’s been a pleasure working with you.

Finally, I thank my family for always being there, giving support in a myriad of forms! Most of all I would like to thank my Wife, for more than I could possibly put into words here! I couldn’t have done it without you.